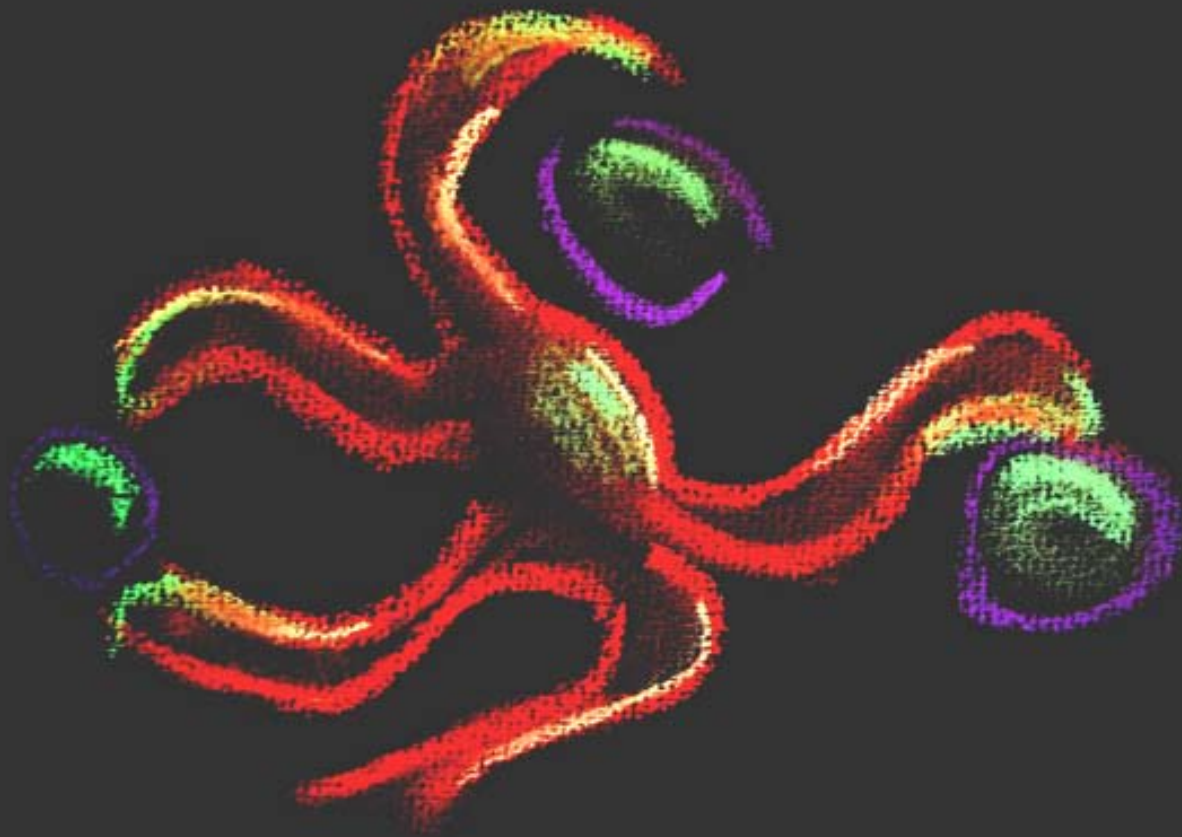


**Maturation of Dendritic
Cells and HIV Transmission
to CD4⁺ T cells**



Immunology Department
Faculty of Medicine
Universidad Aut3noma de Barcelona

**Nuria Izquierdo-Useros
Fundaci3 IrsiCaixa**

Cover & CD design: Clara Morer, 2009.

Cover & CD illustrations: Julia Garcia Prado, 2008.

Bookmark design: Alexis Capera, 2009.

This thesis has been supported by the Agència de Gestió d'Ajuts Universitaris i de Recerca from the Generalitat de Catalunya through a FI scholarship, the Spanish Ministry of Education and Science through grants SAF2004-06991 and SAF2007-64696, the Spanish AIDS network “Red Temática Cooperativa de Investigación en SIDA” (RD06/0006), the Catalan HIV Vaccine Development Program (HIVACAT), and the Fundación para la Investigación y Prevención del Sida en España (FIPSE) through grants 36356/05, 36523/05, and 36621/06.

Fernando Izquierdo, Maria Teresa Useros and Teresa Serrano also supported Nuria's work.

The printing of this thesis was made possible by the financial aid of the UAB.

Universidad Aut3noma de Barcelona

Faculty of Medicine, Department of Cellular Biology,

Physiology and Immunology

Maturation of Dendritic Cells & HIV

Transmission to CD4⁺ T cells

Nuria Izquierdo-Useros

Retrovirology Laboratory

IrsiCaixa Foundation

Hospital Germans Trias i Pujol

2009

Thesis to obtain the PhD degree in Immunology of the

Universidad Aut3noma de Barcelona

Directors: Dr. Javier Mart3nez-Picado & Dr. Juli3 Blanco

Tutor: Dr. Paz Mart3nez Ram3rez

Los Doctores Javier Martínez-Picado y Julià Blanco, investigadores principales en el laboratorio de Retrovirología de la Fundación IrsiCaixa, certifican:

Que el trabajo experimental y la tesis titulada “Maturation of Dendritic Cells & HIV Transmission to CD4⁺ T cells” han sido realizados por Nuria Izquierdo-Userso bajo su dirección y que consideran que son aptos para su lectura y defensa con objeto de optar al título de Doctora en Inmunología por la Universidad Autónoma de Barcelona.

Badalona, 7 de enero de 2009

Dr. Javier Martínez-Picado

Dr. Julià Blanco



La Doctora Paz Martínez Ramírez, coordinadora del programa de Doctorado en Inmunología de la Universidad Autónoma de Barcelona, certifica:

Que el trabajo experimental y la tesis titulada “Maturation of Dendritic Cells & HIV Transmission to CD4⁺ T cells” han sido realizados por Nuria Izquierdo-Userso bajo su tutela y que considera que son aptos para su lectura y defensa con objeto de optar al título de Doctora en Inmunología por la Universidad Autónoma de Barcelona.

Bellaterra, 7 de enero de 2009

Dra. Paz Martínez Ramírez

*I can be the million that
you never made*

A. DiFranco.

Preface

Hace muchos miles de años vivían seis hombre ciegos que pasaban las horas compitiendo entre ellos para ver quién era el más sabio. Un día los hombres no llegaban a un acuerdo sobre la forma exacta de un elefante. Por ello pidieron que les trajeran un hermoso ejemplar ante su presencia. El primero de los sabios se abalanzó sobre el elefante y chocó con el costado del animal.

-Yo os digo que este elefante es igual que una pared de barro secada al sol.

Llegó el turno del segundo de los ciegos, que avanzó con más precaución, con las manos extendidas ante él para no asustarlo. En esta posición en seguida tocó los colmillos.

-¡La forma de este animal es exactamente como la de un par de sables...sin duda!

El tercer ciego empezó a acercarse al elefante lentamente, para tocarlo con cuidado. El animal se giró hacia él y le envolvió la cintura con su trompa.

-Escuchad, este elefante es más bien como...como una larga serpiente.

El cuarto sabio cogió la cola y la examinó de arriba abajo con las manos. No tuvo dudas y exclamó:

-¡Ya lo tengo! Yo os diré cual es la verdadera forma del elefante. Sin duda es como una vieja cuerda.

Al alzar su mano para buscarlo, los dedos del quinto sabio toparon con la oreja del animal y gritó a los demás:

-Ninguno de vosotros ha acertado. El elefante es más bien como un gran abanico plano – y cedió su turno al último de los sabios para que lo comprobara por sí mismo. El sexto ciego pasó por debajo de la barriga del elefante y al buscarlo, agarró con fuerza su gruesa pata.

-¡Lo estoy tocando ahora mismo y os aseguro que el elefante tiene la misma forma que el tronco de una gran palmera!

Abbreviations
Commonly Used

ABS: Antibody binding sites
AIDS: Acquired immunodeficiency syndrome
APCs: Antigen-presenting cells
ASLV: Avian sarcoma and leukemia virus

BDCA: Blood dendritic cell antigen
βMCD: β-methyl-cyclodextrin

CCR5: Chemokine (C-C motif) receptor 5, also known as CD195
CLRs: C-type lectin receptors
CRD: Carbohydrate recognition domain
CXCR4: CXC Chemokine receptor 4, also known as CD184

DAPI: 4,6-diamidino-2-phenylindole
DCs: Dendritic cells
DCIR: Dendritic cell immunoreceptor
DC-SIGN: Dendritic cell specific ICAM-3 grabbing nonintegrin
DNA: Deoxyribonucleic acid

eGFP: Enhanced green fluorescent protein
ELISA: Enzyme-linked immunosorbent assay

FACS: Fluorescence-activated cell sorting
FB1: Fumonisin B1
FBS: Fetal bovine serum
Fc: Fragment crystallizable region of an antibody
FcR: Receptor of the fragment crystallizable of an antibody
Fig: Figure
FITC: Fluorescein isothiocyanate

GALT: Gut-associated lymphoid tissue
GFP: Green fluorescent protein
GM-CSF: Granulocyte-macrophage colony-stimulating factor

HAART: Highly active antiretroviral therapy
HIV: Human immunodeficiency virus
HIV-1: Human immunodeficiency virus type 1
HTLV-1: Human T-lymphotropic virus type 1

iDCs: Immature monocyte-derived dendritic cells

Ig: Immunoglobulin
ICAM: Intercellular adhesion molecule
IL-4: Interleukin-4

LCs: Langerhans cells
LFA-1: Lymphocyte function-associated antigen 1
LPS: Lipopolysaccharides

mAb: Monoclonal antibody
mDCs: Mature monocyte-derived dendritic cells
MDDCs: Monocyte-derived dendritic cells
MHC-I: Class I major histocompatibility complex
MHC-II: Class II major histocompatibility complex
MLV: Murine leukemia virus
MVB: Multivesicular body

NB-DNJ: N-Butyldeoxynojirimycin, Hydrochloride

PAMPs: Pathogen-associated molecular patterns
PBMCs: Peripheral blood mononuclear cells
PBS: Phosphate buffer saline
PE: Phycoerythrin
PerCP: Peridinin chlorophyll protein
PHA: Phytohaemagglutinin
PRRs: Pattern-recognition receptors

RFUs: Relative fluorescent units
RLUs: Relative light units
RNA: Ribonucleic acid

SEM: Standard errors of the means
SIV: Simian immunodeficiency virus

TCID₅₀/ml: 50% tissue culture infective doses per milliliter
TCR: T cell receptor
TLRs: Toll-like receptors
TRITC: Tetramethyl rhodamine isothiocyanate

VLPs: Viral like particles
VSV: Vesicular stomatitis virus

Table of Contents

Are Dendritic Cells Dr. Jekyll during Immune Responses and Mr. Hyde upon HIV Disease Progression?

| | |
|--|-----------|
| I. Dr. Jekyll: The role of dendritic cells in immunity | 5 |
| 1. Innate immunity | 5 |
| 2. Adaptive immunity | 8 |
| 2.1 Exogenous antigen presentation | 8 |
| 2.2 Endogenous antigen presentation | 10 |
| 2.3 Cross-presentation | 11 |
| 2.4 Immunity mediated by exosomes | 13 |
| 3. DC subsets and anatomical location | 17 |
| | |
| II. Dr. Jekyll's potion: The human immunodeficiency virus | 20 |
| 1. HIV collapses our immune system | 23 |
| 2. Viral evasion and the Trojan exosome hypothesis | 25 |
| 2.1 Similarities in host cell lipids and proteins | 27 |
| 2.2 Similarities in protein targeting and vesicle biogenesis | 28 |
| | |
| III. Mr. Hyde: Interactions of HIV-1 with dendritic cells | 31 |
| 1. To be or not to be infected | 31 |
| 1.1 General features of the HIV-1 replication cycle | 33 |
| 1.2 Specific features of the HIV-1 replication cycle in DCs | 33 |
| a) Viral binding | 34 |
| b) DC infection as a selection mechanism for CCR5 tropic viruses | 34 |
| c) DC infection allows for antigen presentation to CD8 ⁺ T cells | 35 |
| 2. DC as Trojan horses: Viral transmission to CD4 ⁺ T cells | 37 |
| 2.1 Viral capture: The role of DC-SIGN | 40 |
| 2.2 DC-SIGN-Independent viral capture mechanisms | 44 |
| 2.3 Intracellular viral trafficking | 45 |
| 2.4 Viral transmission: Infectious synapses and exosomes | 47 |
| 2.5 Role of DC maturation in HIV-1 transmission | 51 |

HYPOTHESIS & OBJECTIVES **55**

MATERIAL & METHODS **59**

| | |
|---|-----------|
| I. Cell culture | 61 |
| 1. Primary cells | 61 |
| 2. Cell lines | 65 |
| II. Immunophenotype | 66 |
| 1. DC-SIGN quantification | 69 |
| III. Plasmids | 71 |
| IV. Transfections and viral stocks | 73 |
| V. Virus binding and capture assays | 74 |
| VI. Viral transmission assays | 77 |
| VII. Exosome generation | 79 |
| VIII. VLP and exosome capture assays | 79 |
| IX. Carboxylated beads assays | 81 |
| X. Capture and transmission followed by microscopy | 81 |
| 1. Electron microscopy | 81 |
| 2. Confocal microscopy and co-localization analysis | 82 |
| 3. Deconvolution microscopy | 83 |
| 4. Epifluorescent microscopy | 84 |
| XI. Capture assays after proteolytic treatments | 84 |
| 1. Confocal microscopy of Pronase-treated mDCs | 85 |
| 2. Confirmation of Pronase activity | 85 |
| XII. Capture of VLPs, HIV and exosomes produced from ceramide-deficient cells | 87 |
| XIII. Characterization of macropinocytic activity and treatment of DCs with β -methyl-cyclodextrin, amantadine and chlorpromazine | 88 |
| XIV. Statistical analysis | 89 |

RESULTS I

91

Maturation of Blood-derived DCs Enhances HIV-1 Capture & Transmission

| | |
|--|-----------|
| I. Results | 94 |
| 1. mDCs capture larger amounts of HIV _{NFN-SX} than iDCs | 94 |
| 2. Enhanced viral transmission of mDCs depends on the amount of virus actively captured | 98 |
| 3. mDC viral capture increases over time, and captured virus has a longer lifespan than in iDCs | 100 |
| 4. Higher viral capture in mDCs than in iDCs can occur independently of DC-SIGN and does not require the viral envelope glycoprotein | 103 |
| 5. Viral stocks produced in different cell lines are also captured with greater ability by mDCs than by iDCs | 106 |
| 6. Greater viral transmission in mature DCs than in immature DCs can occur independently of DC-SIGN | 108 |
| 7. Confirmation of viral capture, turnover and transmission results by microscopy | 110 |
| 8. Mature Myeloid DCs retain HIV _{NFN-SX} and HIV _{Δenv-NL4-3} in a compartment similar to that of mDCs | 114 |
| 9. mDC viral capture is not mediated through pinocytosis and requires cholesterol | 116 |

RESULTS II

121

Capture & Transfer of HIV-1 Particles by Mature DCs Converges with the Exosome Dissemination Pathway

| | |
|--|------------|
| I. Results | 124 |
| 1. Maturation of DCs enhances VLP and exosome capture | 124 |
| 2. Competition experiments suggest that different particles derived from cholesterol-enriched domains use the same entry pathway into mDCs | 128 |
| 3. Mature DCs retain HIV-1, VLPs and exosomes within the same CD81 ⁺ intracellular compartment | 131 |
| 4. Mechanism of VLP and exosome uptake in mDCs is dose-dependent and increases over time, allowing efficient transfer to target CD4 ⁺ T cells | 138 |

RESULTS II

- 5. VLPs, HIV-1 and exosomes enter mDCs through a mechanism resistant to proteolysis 142
- 6. VLP, HIV-1 and exosome capture can be inhibited when particles are produced from ceramide-deficient cells 146

DISCUSSION & FUTURE DIRECTIONS

- I. mDCs *versus* iDCs: Two evil sides for Mr. Hyde 153
- II. mDCs *trans*-infection 156
 - 1. *In vivo* evidence of Mr. Hyde criminal activity 157
 - 2. Viral binding and capture: No sign of DC-SIGN 161
 - 3. Hiding Dr. Jeckyll's evil potion: Intracellular viral trafficking 165
 - 4. Mr. Hyde's murder weapon: The infectious synapse 167
- III. Convergence with the exosome dissemination pathway 170

CONCLUSIONS

BIBLIOGRAPHY

PUBLICATIONS

ACKNOWLEDGMENTS

1.

General Introduction.

Are Dendritic Cells Dr. Jekyll
during immune responses
and Mr. Hyde upon
HIV disease progression?

The best defense is a good offence. This principle seems to govern immunity, the resistance of our organism to infections or pathogen invasions. The immune system integrates and coordinates all the physiological elements that control immunity, including the quick and nonspecific reactions linked to innate immunity and the more sophisticated and specific responses that arise afterwards through adaptive immunity.

In all battlefields, reacting at the right moment and having accurate information on the enemy's strategy provides an advantage that can be crucial to winning the war. Therefore, what triggers the initiation of immune responses in our body and how our immune system determines who the actual enemy is are key aspects in combating infections, including that caused by the human immunodeficiency virus. Until 1973, the year in which dendritic cells were discovered – named after the Greek word for tree (dendreon) due to the branched projections of their membranes (208) – these relevant questions could not be accurately addressed. Back then, dendritic cells were characterized as the most potent and specialized antigen-presenting cells, in charge of

coordinating innate and adaptive immune responses to invading pathogens. Although at first it seemed hard to believe that such an infrequent and rare population of cells could have such a relevant role in the initiation of immunity, three decades later this model remains valid.

Here, we will first review how this preliminary dendritic cell model has evolved, focusing on the general aspects that originate immune responses. However, we will soon see that even an exquisite and precise defense system like the one coordinated by dendritic cells has its weaknesses, allowing the establishment of persistent infections. In particular, we will try to underscore why the human immunodeficiency virus, the etiologic agent of the acquired immunodeficiency syndrome, is still winning the battle against our immune system. Finally, we will focus on the different strategies that this virus has developed to evade the dendritic cells' antiviral activity, facilitating disease progression.

In this thesis we will revisit the plot of an old story: dendritic cells can act as Dr. Jekyll and aid in defending our body against multiple pathogens. However, the human immunodeficiency virus works as the doctor's evil potion, turning our dendritic cells into Mr. Hyde. As a consequence of this functional metamorphosis, dendritic cells contribute to viral dissemination. Changing the end of Robert Louis Stevenson's story, where Dr. Jekyll gives up and we never learn if the cruel and remorseless Mr. Hyde survives, is a key challenge to finally winning the war against the human immunodeficiency virus.

I. Dr. Jekyll:

The role of dendritic cells in immunity

1. Innate immunity

At the primary stage of any infection, our immune system initially relies on the quick but unspecific defenses that constitute innate immunity. Dendritic cells (DCs) form an integral part of this innate immune system, supported by the activity of bone marrow derived non-specific immune cells – such as mast cells, natural killer cells, granulocytes and other phagocytes such as monocytes or macrophages – and various resident tissue cells, including epithelial cells. These innate immune cells respond rapidly to invading microorganisms in the mucosa and other exposed tissues, releasing inflammatory cytokines and initiating antimicrobial activity.

However, what triggers the activation of innate immune cells? Pathogen detection takes place through **pattern-recognition receptors** (PRRs) that distinguish a set of evolutionary conserved hallmarks (Fig. 1A) known as **pathogen-associated molecular patterns** (PAMPs). These surveillance receptors or PRRs consist of nonphagocytic molecules, such as **toll-like receptors** (TLRs) that recognize pathogen hallmarks extracellularly or intracellularly and lead to elaborate signal transduction cascades – reviewed in (162, 229) . Interestingly, TLRs bind to a wide variety of microbial compounds or PAMPs (1, 21, 162, 195), including RNA or DNA from several pathogens and bacterial cell wall components such as lipopolysaccharides (LPS). Surveillance receptors also include molecules that induce endocytosis such as **scavenger receptors** and **C-type lectin receptors** (CLRs). This later family includes DC-SIGN (Dendritic Cell Specific ICAM-3 Grabbing Nonintegrin, or

formally CD209), a CLR extensively discussed in this thesis and depicted in Figure 1B.

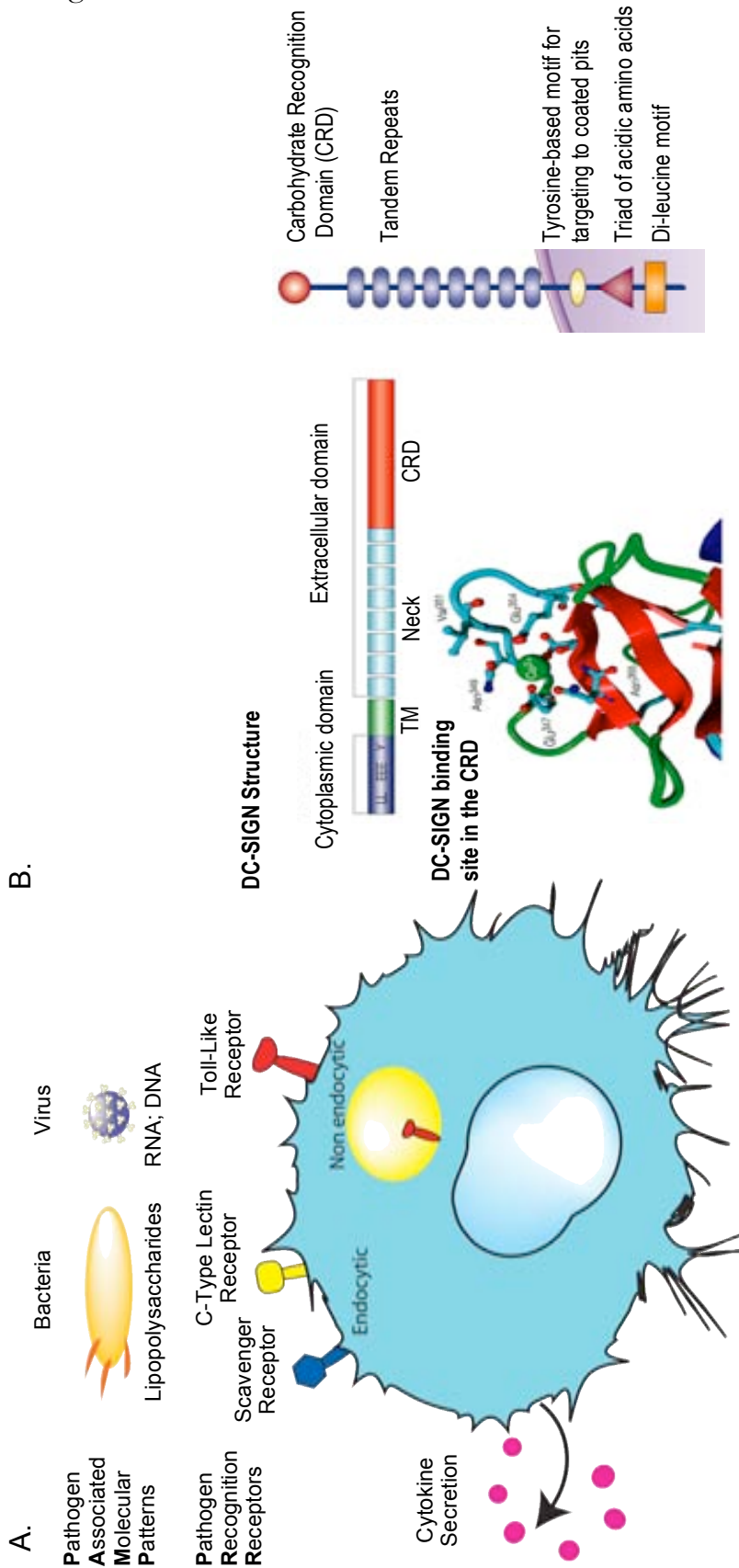


Figure 1. (A) Innate Immunity in DCs. Players in the innate response described in the text. **(B) DC-SIGN Structure.** DC-SIGN is a type II transmembrane protein that contains a short cytoplasmic domain with several intracellular signaling motifs, a neck domain implicated in the oligomerization of this receptor in the cell surface and a C-type lectin terminal domain (CRD) or carbohydrate recognition domain) essential in recognizing mannose and galactose structures: reviewed in (67, 227). Binding of ligands to the carbohydrate recognition domain is calcium dependent and can be blocked with chelant agents. The natural ligands for DC-SIGN are intercellular adhesion molecules 3 and 2 (ICAM-3 and ICAM-2), molecules that contribute to transient DC-T cell attachment and to transmigration of DCs across vascular endothelium, respectively: reviewed in (67). Illustrations in B. are adapted from (67, 227), Nature Reviews Immunology.

Engagement of surveillance receptors to pathogen domains leads to the activation of some of the immune cells (such as DCs, macrophages, or natural killer cells) and some of the resident tissue epithelial cells. This activation triggers the secretion of cytokines and chemokines, as well as the maturation and migration of **antigen-presenting cells** (APCs) such as DCs. Concurrently, this creates an inflammatory environment that allows the establishment of adaptive immunity. Therefore, innate non-clonal responses lead to a conditioning of the immune system for subsequent development of specific adaptive immune responses. The activation of APCs allows a delayed antigen-specific response that can generate clonal expansion of immune cells, thereby providing specific long-lasting immunological memory, which contributes to the fight against microorganisms in later encounters. There is thus a close interaction between the innate and the adaptive immune systems, and DCs orchestrate both types of defense responses to invading pathogens (Fig. 2).

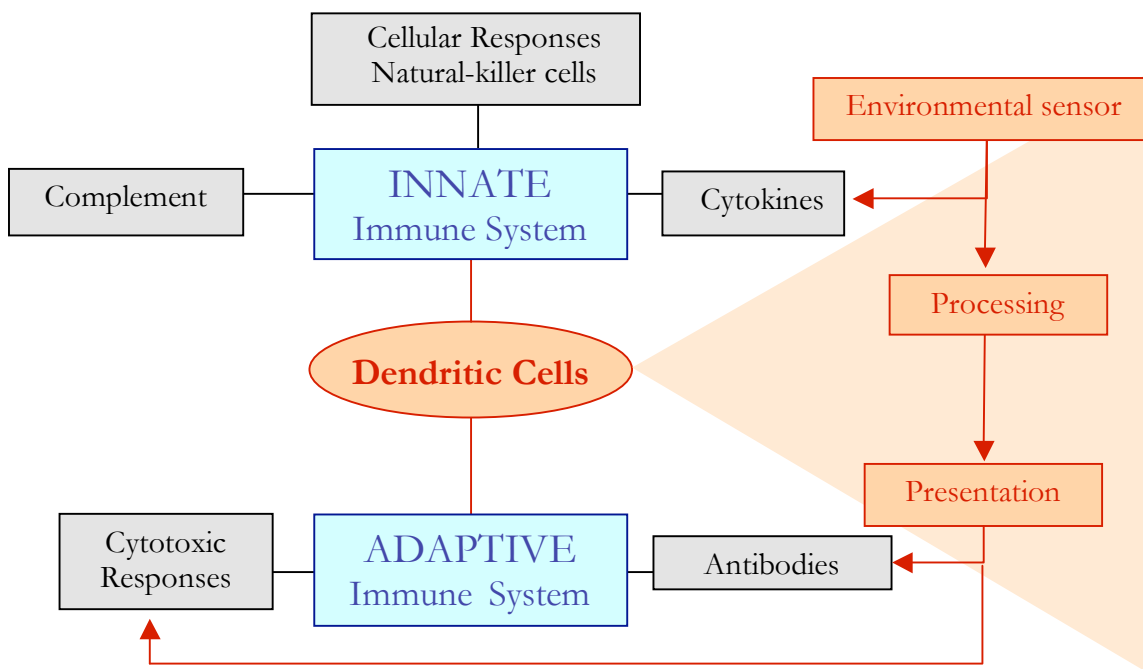


Figure 2. Link between innate and adaptive immune systems (blue) through DC functions (red), leading to distinct immune responses (grey).

2. Adaptive immunity

2.1 Exogenous antigen presentation

As we have seen, DCs scattered throughout the peripheral tissues of the body act like real sentinels and are ready to recognize a wide range of microorganisms. At this stage, DCs display an immature phenotype. When pathogen invasion takes place, immature DCs can capture microorganisms via endocytic surveillance receptors, employing two distinct mechanisms (140):

- **Phagocytosis**, which involves internalization of large size particles, and
- **Pinocytosis**, which requires the ingestion of fluid or solutes via small pinocytic vesicles that can be coated with **clathrin** or dependent on the formation of specific domains in the plasma membrane, termed **lipid rafts**.

Pathogen uptake through any of these mechanisms in immature DCs can result in the classical intracellular lytic pathway that characterizes APC function. Once pathogens reach lysosomes, DCs process them into antigens that interact with class II major histocompatibility complexes (MHC-II). However, these antigens are not efficiently uploaded into MHC-II molecules yet, and are instead retained intracellularly for later presentation (Fig. 3A, left panel).

The signaling through PRRs or the detection of proinflammatory cytokines prompts immature DC activation and migration from the periphery towards the secondary lymphoid organs. This transition is accompanied by a dramatic redistribution of antigen–MHC-II complexes that have now been formed efficiently and redistributed from intracellular compartments to the plasma membrane (Fig. 3A, right panel and B, middle panel). Interestingly,

downregulation of endocytosis begins soon after the receipt of a maturation signal: a feature that has been extensively used as a maturation hallmark, as reviewed in (140, 207, 231). However, clathrin-coated vesicle formation appears to continue, so maturing DCs must not be considered as being completely incapable of endocytosis (140).

On reaching lymph nodes, DCs develop into their mature state, which is not only characterized by high levels of MHC-II expression on the membrane's cell-surface (36) but also by the upregulation of T cell co-stimulatory molecules, such as CD86 and CD83 – reviewed in (140, 206, 207, 231). Overall, maturation regulates antigen processing by lowering the pH of endocytic vacuoles, activating proteolysis, and transporting antigen–MHC-II complexes to the cell surface (207, 217).

In the T cell areas of the lymph nodes, mature DCs present pathogen-derived peptides in association with MHC-II molecules to naïve T helper (Th) lymphocytes or CD4⁺ T cells, which recognize the MHC-II/peptide complex via the T cell receptor or TCR (10, 11). After recognition, and with the appropriate additional interactions mediated by co-stimulatory molecules on the DCs, naïve T lymphocytes become effector CD4⁺ T cells (107). The crosstalk between DCs and CD4⁺ T cells is provided by different adhesion molecules that form a dynamic structure, described as “**the immunological synapse**” (55, 101).

Following the selection of clones, antigen-selected T cells undergo extensive clonal expansion and differentiation to bring about an array of potential helper and cytotoxic activities (207).

This way, CD4⁺ T cells can acquire the capacity to generate powerful cytokines and induce several responses:

- **T helper 1 cells** produce interferon- γ that activates macrophages to resist infection by intracellular microbes (148, 174);
- **T helper 2 cells** secrete interleukin (IL)-4, 5 and 13, stimulating B cells, inducing B cell antibody class-switching and increasing antibody production (197);
- **T helper 17 cells** are polarized by IL-17 secretion, combating extracellular bacilli (207); and
- **T regulatory cells** arise on signaling with IL-10, allowing suppressive functions and thereby maintaining immune system homeostasis and tolerance to self-antigens (207).

Finally, DCs induce the T cell clone to acquire memory, allowing it to persist for prolonged periods and to respond rapidly to repeated exposure to the antigen (8, 218).

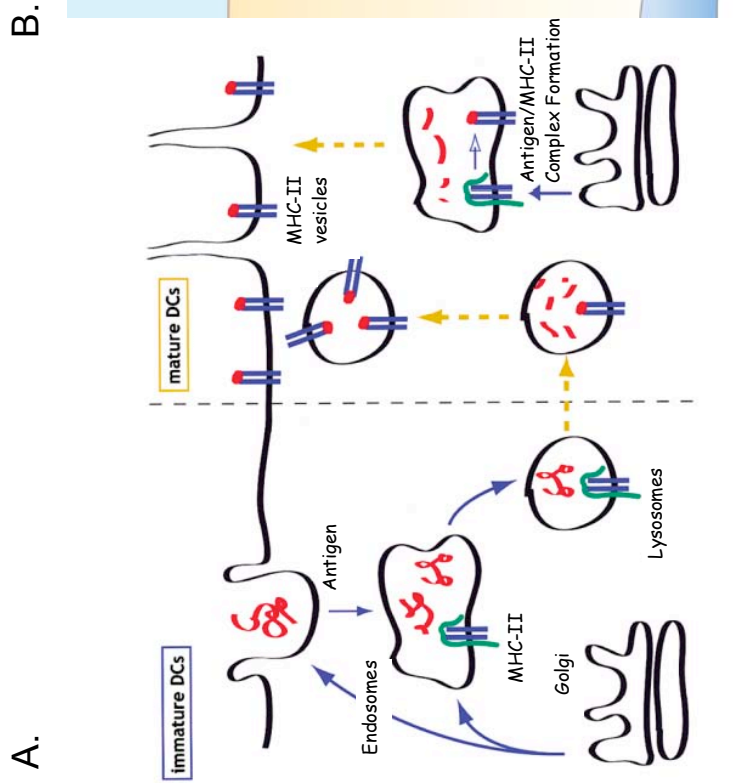
2.2 Endogenous antigen presentation

DCs do not only rely on pathogen capture through PRRs but are also able to present antigens derived from proteins degraded mainly in the cytosol by the proteasome, presenting them to CD8⁺ T cells in MHC class I (MHC-I) molecules, and triggering cytotoxic responses (Fig. 3B, left panel). This pathway allows DCs to constantly present peptides that are derived from endogenous proteins, including for instance viral components synthesized in the cytoplasm after productive infection of the DC.

2.3 Cross-presentation

Interestingly, exogenous and endogenous antigen presentation pathways are not mutually exclusive and mature DCs can also present exogenous antigens to CD8⁺ T cells through the MHC-I endogenous pathway. Following uptake of microorganisms such as virions that do not fuse with the plasma membrane but instead are endocytosed, DCs are able to present processed antigens via MHC-I to elicit CD8⁺ T cell responses (2, 91, 105). During this process, known as **cross-presentation**, non-replicating protein antigens are internalized and somehow gain access to the cytoplasm before being processed by the proteasome for peptide presentation on MHC-I (Fig. 3B, right panel). Critical steps in this degradation mechanism seem to occur in compartments less acidic than lysosomes. Notably, cross-presentation allows DCs to induce CD8⁺ T cell responses not only to non-replicating forms of microbes – such as viruses that do not infect DCs – but also to immune complexes and dying cells (207).

By all these means, DCs provide the necessary link between the pathogen entry locations and the lymph nodes, bringing in and presenting antigens to T cells in secondary lymphoid tissues that would otherwise not be able to respond to the distant invasion.



B.

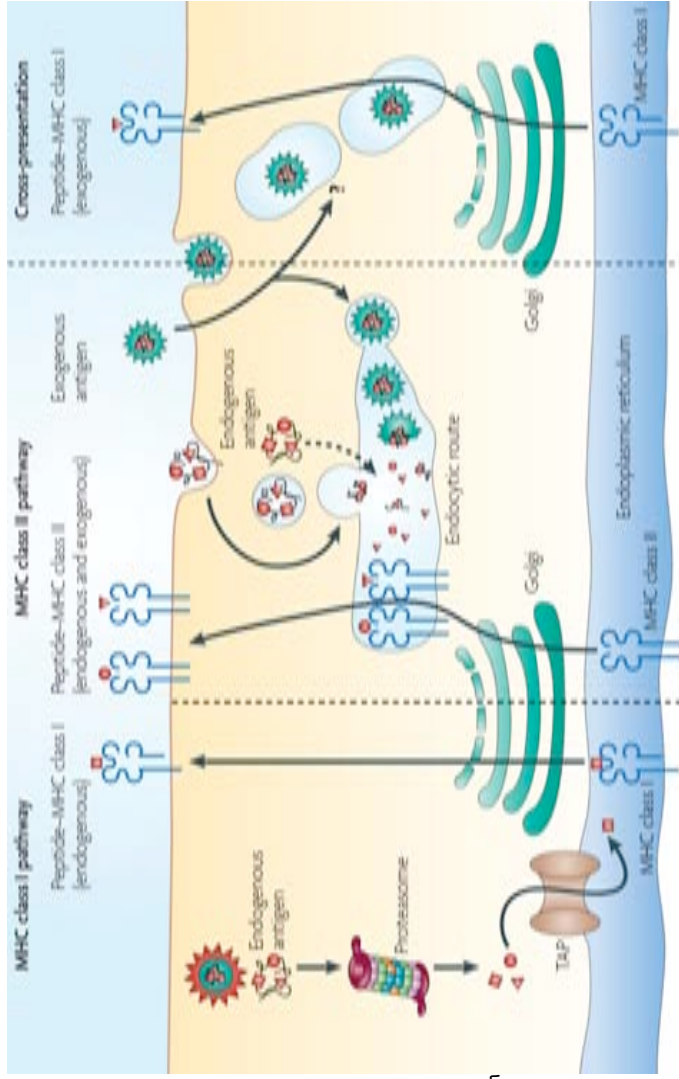
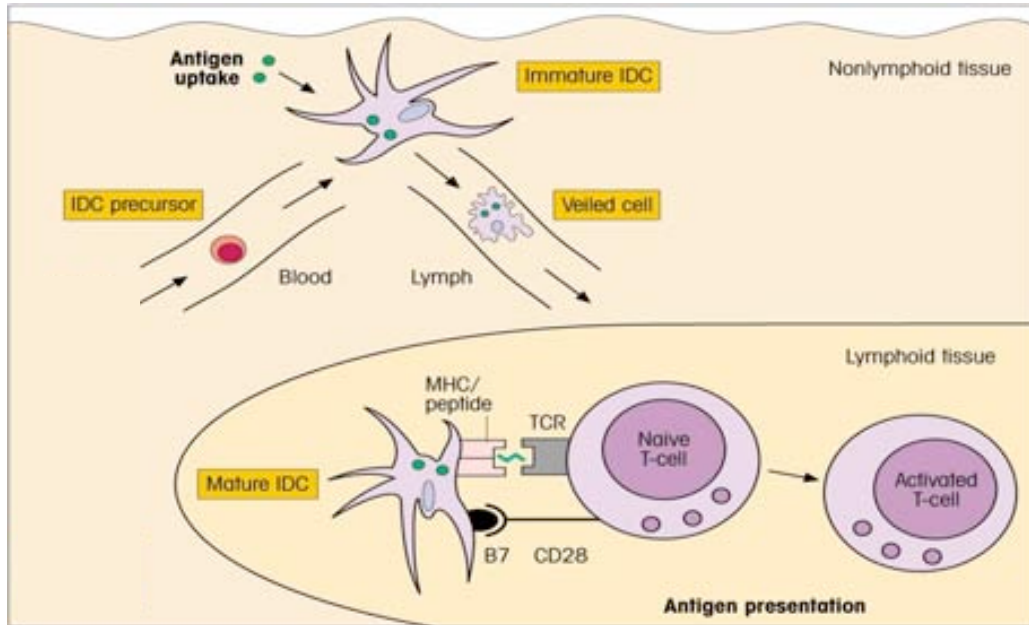


Figure 3. (A) Dendritic Cell maturation induces multiple alterations in the **function and intracellular transport of MHC-II molecules**. Adapted from (140), Cell. **(B)** DCs have functional **MHC class I and class II presentation pathways**. MHC class I molecules present peptides that are derived from proteins degraded mainly in the cytosol, which in most DC types comprise almost exclusively endogenous proteins. MHC class II molecules acquire peptide cargo that is endocytosed from the extracellular environment, and endogenous components, such as plasma membrane proteins, components of the endocytic pathway and cytosolic proteins that access the endosomes by autophagy. DCs have a unique ability to deliver exogenous antigens to the MHC class I (**cross-presentation**) pathway. The bifurcated arrow indicates that the MHC class II and the MHC class I cross-presentation pathways may 'compete' for exogenous antigens, or that the endocytic mechanism involved in the internalization of a given antigen may determine whether it is preferentially delivered to the MHC class II pathway or the MHC class I cross-presentation pathway. TAP, is the transporter associated with antigen processing. Adapted from (231), Nature Reviews Immunology.

2.4 Immunity mediated by exosomes

The current view of DC functionality has immature DCs encountering an antigen in the periphery and carrying it to lymphoid organs, maturing *en route* (Fig. 4). This view is probably too simple to describe the complex DC system *in vivo*. DCs migrating from the periphery may not always be the ones that present the captured antigen in the lymph nodes. Rather, migrating DCs may transfer their captured antigens to other DCs for presentation. The transfer could occur either by the phagocytosis of antigen-loaded DC fragments by another DC (102) or by the release of antigen-bearing vesicles, termed exosomes (214). During periods of pathogen invasion, these exosomes could act as real couriers, transferring vital information on the enemy's plan between the immune cells and strengthening the magnitude of the body's defenses.

Exosomes are small secreted cellular organelles that form within late endocytic compartments called multivesicular bodies (MVB) in macrophages and DCs. These small vesicles are secreted upon fusion of these compartments with the plasma membrane (210, 215). Alternatively, in T cells, exosomes can bud directly at particular cholesterol-enriched microdomains in the plasma membrane (23, 65, 151). Interestingly, although many different cell types can produce exosomes, the available proteomic studies define a subset of cellular proteins that are targeted specifically at most of them (Fig. 5A). Many of the protein families that have been found in DC-derived exosomes (the ones that have been most extensively characterized) have also been described in exosomes produced by other cell types (213). The conserved exosomal proteins include integrins, cell surface peptidases, heat-shock proteins, cytoskeletal proteins, and molecules involved in signal transduction, membrane transport and fusion. They also share glycosphingolipids and tetraspanin proteins that have been previously used as *bona fide* lipid raft markers (23, 244).



14

Figure 4. Classical model of pathogen capture in the periphery by immature DCs that migrate to the lymph nodes, where they present antigens upon cell maturation. Adapted from Roitt's Essential Immunology, Blackwell Publishing Ltd.

Interestingly, aside from proteins potentially involved in exosomal biogenesis and targeting, exosomes contain proteins associated with the immunological function, such as MHC-I and MHC-II (212, 214). The existence of antigen presentation-related molecules in exosomes prompted different groups to examine the immune-stimulatory capacities of these vesicles. It was first observed that B cell-derived exosomes carrying peptide-loaded MHC-II were able to stimulate $CD4^+$ T cells *in vitro* in an antigen-specific manner (178). Studying other APCs, it was later shown that antigen-bearing DC-derived exosomes could indirectly stimulate antigen-specific naïve $CD4^+$ T cell activation *in vivo* (213). Interestingly, exosomes could not induce naïve T cell proliferation *in vitro* unless mature DCs were also present, indicating that exosomes do not overcome the need for a competent APC to stimulate naïve $CD4^+$ T cells. Therefore, at least two distinct cell populations are required for

exosomes to stimulate naïve T cells *in vitro*. One population is needed to produce exosomes bearing an intact antigen or, in the case of DCs, antigen-MHC-II complexes. The other population has to be competent DCs capable of capturing these exosomes and presenting them, either by reprocessing the antigen they contain or by directly presenting the antigen–MHC-II complexes to T lymphocytes. These alternative pathways were characterized when it was observed that the antigen-presenting competent DC population could be devoid of MHC-II molecules and still stimulate CD4⁺ T cells, because MHC-II molecules were already present on the exosomes (213). Therefore, in addition to carrying antigens, exosomes promote the exchange of functional peptide–MHC complexes between DCs. Such a mechanism could increase the number of DCs bearing a particular peptide, thus amplifying the initiation of primary adaptive immune responses (215).

Similar observations have been made by studying exosomes from cultured DCs loaded with tumor-derived peptides on MHC-I that were able to stimulate cytotoxic T lymphocyte-mediated anti-tumor responses *in vivo* (249). Interestingly, tumor cells have also been demonstrated to secrete exosomes carrying tumor antigens, which, after transfer to DCs, also mediate CD8⁺ T-cell-dependent anti-tumor effects (239). Thus, exosomes carrying tumor peptides provide an antigen source for cross-presentation by DCs.

Collectively, these studies have resulted in the idea that exosomes can transfer antigens to DCs and contribute to the initiation of adaptive immune responses (Fig. 5B). Therefore, during pathogen invasion, exosomes can act as real couriers transferring vital information on the enemy's plan between immune cells, strengthening the magnitude of our defenses.

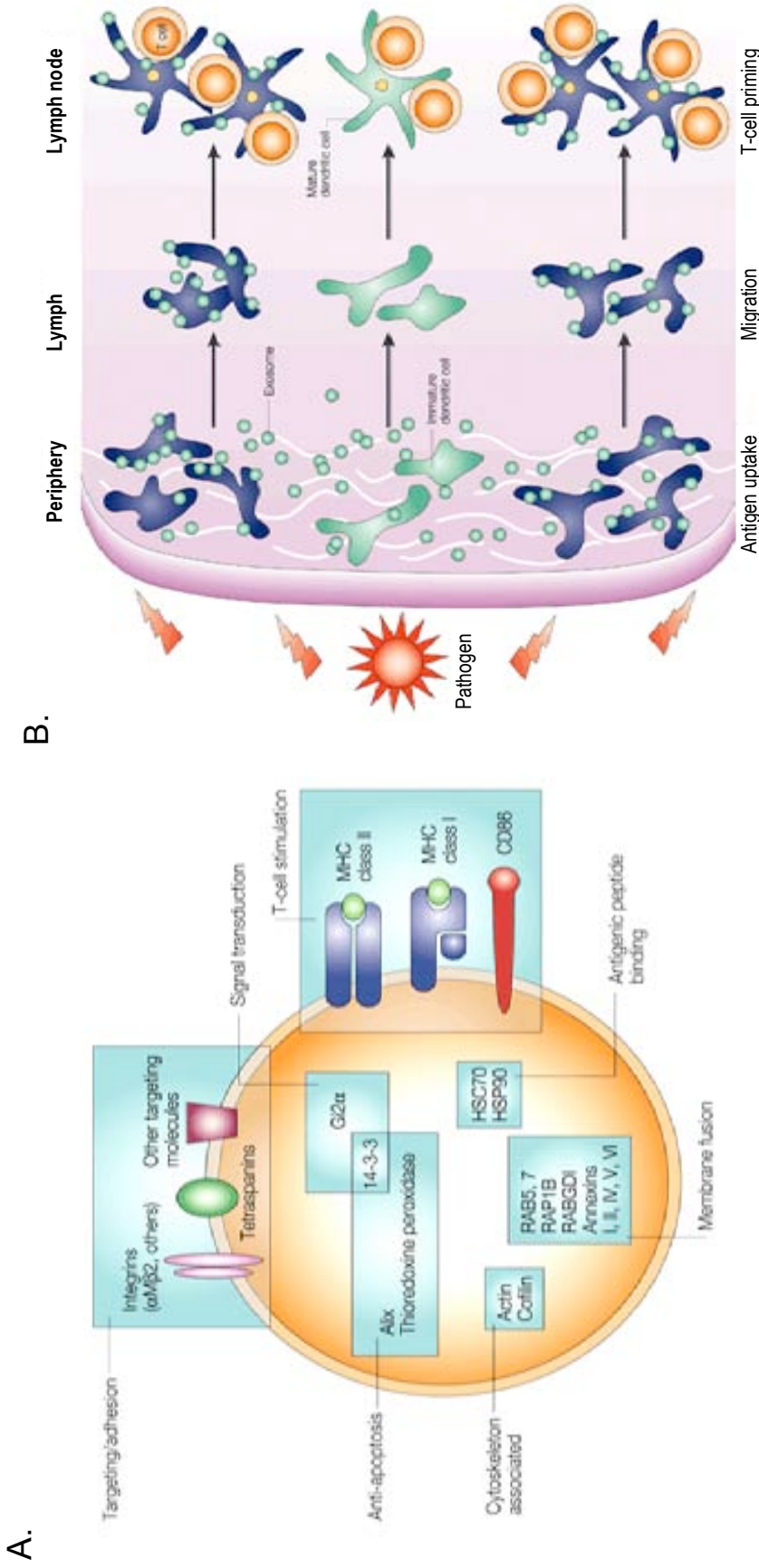


Figure 5. (A) Proposed structure of an exosome as a vesicle that is delimited by a lipid bilayer, which contains cytosol from the producing cell and exposes the extracellular domain of various transmembrane proteins at its surface. The proteins shown here were identified in exosomes from DCs, and are arranged in categories according to their known functions in the cell. **(B) Immunity mediated by exosomes.** After the uptake of incoming pathogens in the periphery, DCs (green) generate peptide–MHC complexes. Some of these complexes could be secreted on exosomes and locally sensitize other DCs (blue) that have not encountered the pathogen directly. As a result of the effects of inflammation, all of these DCs migrate out of the tissue towards the draining lymph nodes. Although maturing DCs seem to secrete fewer exosomes than immature DCs (214), an exchange of exosomes inside the lymph nodes between newly arrived and resident DCs could also take place. Therefore, exosome production would increase the number of DCs that bear the relevant peptide–MHC complexes and thereby amplify the magnitude of the immune responses. Illustrations from (215), Nature Reviews Immunology.

3. DC subsets and anatomical location

One of the most enigmatic features of DC biology is the complexity of the distinct subsets found *in vivo*. Sometimes, DC classifications are so complicated that one would tend to think that there are as many DC subsets as the cells have dendrites. Unlike other immune cells, DCs can have either a myeloid or a lymphoid origin (Fig. 6), although this is still a matter for debate (199, 231). Many studies, especially of the human system, use the terms lymphoid and myeloid to refer to the two main DC categories, but these terms are now considered obsolete (200, 231) and experts prefer to use the plasmacytoid and conventional DC terminology. However, aside from this general classification, DCs can be categorized into several subsets on the basis of their anatomical distribution, immunological function and cell-surface-marker expression.

Plasmacytoid DCs, so named because of the cytologic similarities to antibody producing plasma cells, mainly circulate through the blood and lymphoid tissue, but can be recruited to sites of inflammation and acquire typical DC morphology after activation (72, 124, 131, 183). These cells are phenotypically characterized by the expression of CD123 and the lack of expression of CD11c. In humans, plasmacytoid DCs selectively express the activating fragment crystallizable receptor (FcR), as well as TLR-7 and TLR-9 but no other TLRs (42, 77, 106). When immune complexes containing DNA and RNA are bound and ingested by this cell type, plasmacytoid DCs signal high levels of type I interferons (14, 18), promoting antiviral responses.

Conventional DCs, formerly termed ‘myeloid’, secrete high levels of interleukin-12 (IL-12) and express CD11c. In contrast to plasmacytoid DCs, conventional DCs preferentially express TLR-1, 2, 3 and 8, similarly to monocytes that express TLR-1, 2, 4, 5 and 8 (1, 42, 106, 124, 125). Conventional DCs can be further subdivided on the basis of their allocation

and the expression of certain surface molecules. These DCs include **Langerhans cells**, **dermal DCs** and **interstitial DCs** that are widely distributed throughout the mucosal surfaces. Langerhans cells are located in the epidermis and express langerin (CD207) and DEC-205 (CD205), and induce strong cytotoxic T cell responses. Some DCs in the dermis express DC-SIGN (CD209) and the mannose receptor (CD206), and can activate antibody forming B cells (207). In the circulatory system, at least two different types of conventional DCs can be distinguished on the basis of their expression of blood DC antigens (BDCA), termed **BDCA-1** and **BDCA-3 Myeloid DCs** (56).

Regarding anatomical location, DCs are abundant at body surfaces such as the skin, the pharynx, the upper oesophagus, the vagina, the ectocervix and the anus, and at the so-called internal or mucosal surfaces, such as the respiratory and gastrointestinal systems, where these cells extend their processes through the tight junctions of epithelia (207). DCs are also present in the blood and the lymphoid tissue.

Although DCs are widely distributed, they are also relatively rare and hard to isolate. For instance, DCs are present at very low frequencies in blood, together constituting 0.5–2% of the total peripheral-blood mononuclear cells (124, 182). Owing to the low abundance of DCs *in vivo*, **monocyte-derived DCs** (MDDCs) are commonly used to model the immunological function of DCs. CD14⁺ monocytes cultured with IL-4 and granulocyte-macrophage colony-stimulating factor (GM-CSF) render immature MDDCs with similar characteristics to conventional DCs. This *in vitro* model mimics inflammation and infection, where it is believed that cytokines such as GM-CSF mobilize increased numbers of monocytes that give rise to MDDCs (118). Indeed, during infection it has been shown that monocytes can be recruited to the

dermis and differentiate into dermal DCs that subsequently migrate into the lymph nodes (118). In addition, upon inflammation, monocytes can be recruited directly to the lymph nodes. However, in the noninfectious steady state, monocytes can only give rise to DCs in some non-lymphoid tissues (230), whereas lymphoid tissue DCs emanate from other bone marrow progenitors (123, 200). Overall, the lineage and developmental relationship between the heterogeneous DC subtypes is still a matter of intense debate (5, 183, 199, 200, 231), reflecting a complexity as intricate as DC morphology.

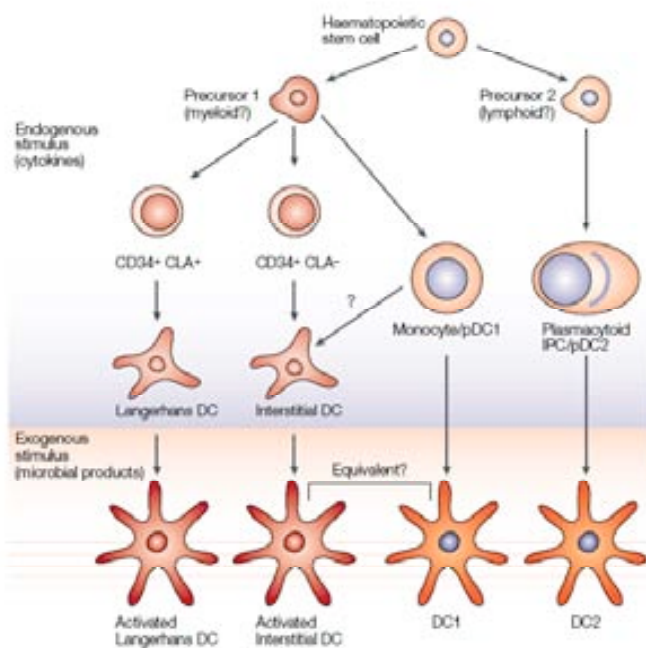


Figure 6. DC development and subtypes. Interstitial DCs, Langerhans cells, monocytes and plasmacytoid cells are generated by distinct precursors (top). Under normal or non-pathologic conditions, these cells are regulated by endogenous stimulus such as cytokines. Upon exogenous stimulus, like the ones generated by HIV infection (bottom), cells activate and give rise to different mature DCs. Figure from (200), *Nature Reviews Immunology*.

II. Dr. Jekyll's potion:

The human immunodeficiency virus

So far we have seen that DCs orchestrate innate and adaptive immune responses to invading pathogens and therefore have a pivotal role during viral infections. However, viruses, including the human immunodeficiency virus (HIV), have evolved different strategies to evade DC antiviral activity. Indeed, like the potion prepared by Dr. Jekyll, HIV can awake the darkest side of our DCs, causing these cells to contribute to viral transmission to new target cells and accelerating disease progression. Intriguingly enough, some of the ingredients of this evil potion allow the virus to escape from all the innate and adaptive responses that DCs coordinate. After more than two decades fighting HIV – the etiologic agent of the **acquired immunodeficiency syndrome** (AIDS) – it is now evident that our immune system has failed to control disease progression. HIV has spread worldwide and is now a pandemic that seriously challenges public health. In 2007, 33 million people were living with HIV-1, and around two million people had died from AIDS (AIDS epidemic update 2007; <http://www.unaids.org>). The situation is particularly critical in many sub-Saharan African countries, where it remains the leading cause of death in the general population. Since our immune defenses are helpless in combating HIV infection, there is an urgent need to find effective pharmaceutical treatments to control this pandemic. This challenge to the scientific community has produced extensive knowledge of several key aspects of the HIV structure and genome (Figs. 7 and 8), allowing the design of various antiviral drugs.

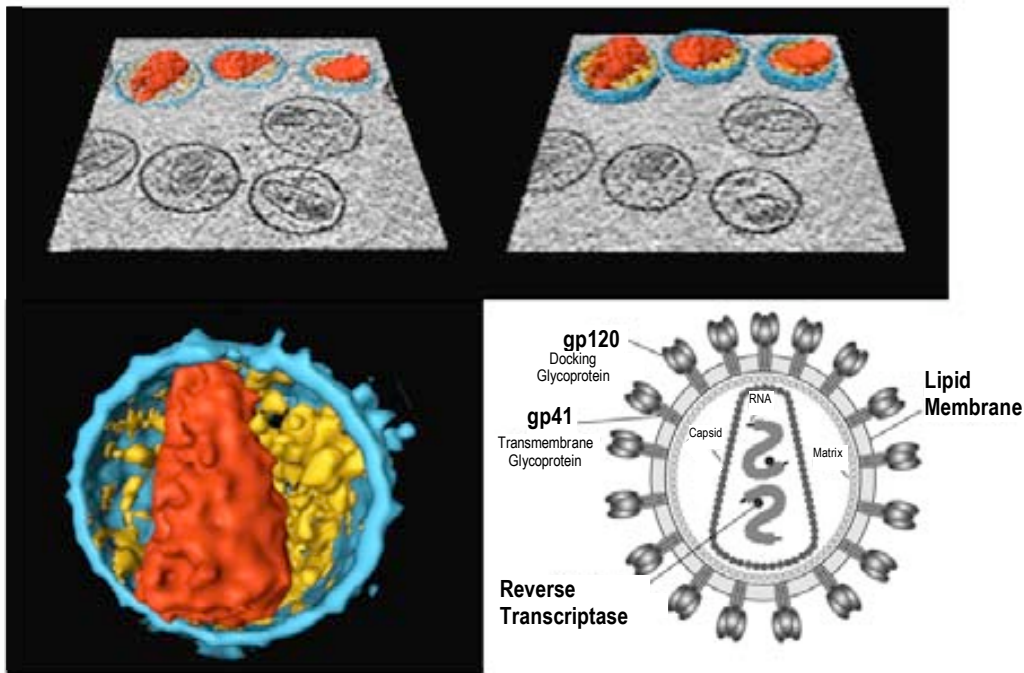


Figure 7. Schematic representation of the structure of HIV reconstructed after analysis of viral cryo-sections. HIV belongs to the Retroviridae family, classified within Group VI of enveloped RNA viruses. It is included in the Lentivirus genus, because it leads to the long-term illness with an extended incubation period known as AIDS (120). HIV is a spherical particle of approximately 90 to 150 nm diameter that integrates two copies of positive single-stranded RNA surrounded by a conical capsid formed by the viral protein p24^{Gag}. Viral RNA is tightly bound to nucleocapsid proteins, p7 and the enzymes needed for the development of the virion such as reverse transcriptase, protease, ribonuclease and integrase. A matrix, composed of the viral protein p17, maintains the integrity of the viral particle. Surrounding the matrix there is an outer membrane, dragged off when a newly synthesized viral particle buds from the host cell. Indeed, HIV buds from particular cholesterol microdomains in the cell plasma membrane (23, 65, 151) unusually enriched in glycosphingolipids, tetraspanin and other human proteins that have been previously used as *bona fide* lipid raft markers (23, 244). Embedded in this membrane are viral envelope glycoproteins containing two distinct parts: a trimer of gp120 projected towards the exterior and a stem consisting of three gp41 molecules that anchor the structure into the viral membrane. This complex enables the virus to attach to and fuse with target cells to initiate the infectious cycle. The HIV cryo-sections are from (27), Cell Press, and the schematic cartoon is from NIAID (<http://www.niaid.nih.gov/factsheets/howhiv.htm>).

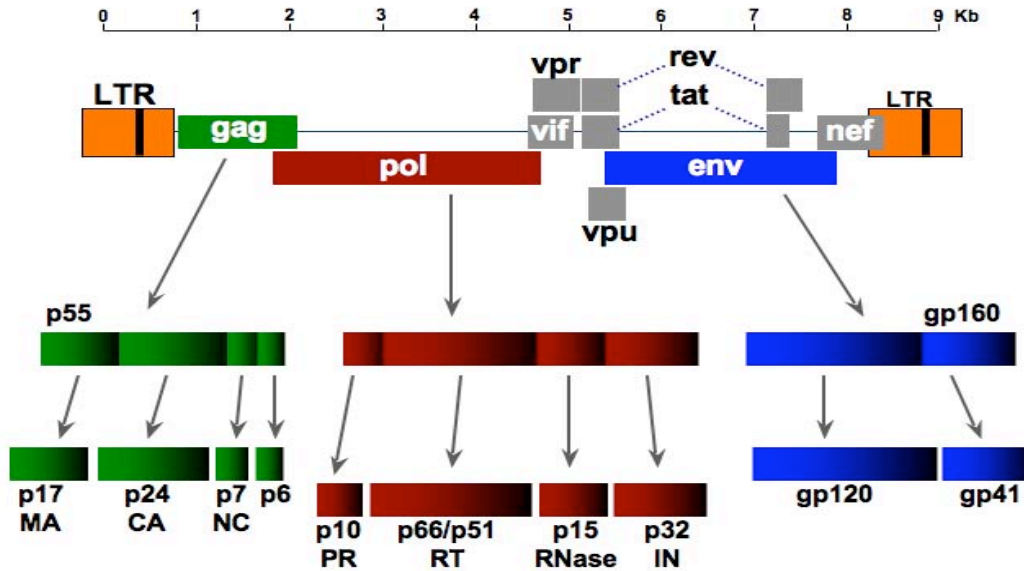


Figure 8. Scheme representing the structure of the HIV genome. The HIV RNA genome has around 10 Kb and codes for nine genes. The products of gag, pol and env contain the information needed to make the structural proteins and viral enzymes for new virus particles. The gene env codes for a gp160 precursor processed to yield the glycoproteins gp120 (external) and gp41 (transmembrane). The gene gag encodes the capsid proteins that are yielded when the precursor p55 is processed by the viral protease to p17 (**MA**trix), p24^{Gag} (**CA**psid), p7 (**NucleoCA**psid) and p6 proteins. The gene pol codes for the viral enzymes **PR**otase, **RT**ranscriptase, **RNaseH** and **IN**tegrase. Tat and rev code for regulatory proteins that modulate transcriptional and posttranscriptional steps of virus gene expression that are essential for viral replication. The four remaining genes, nef, vif, vpr and vpu code for accessory or auxiliary proteins that are not necessary for viral propagation *in vitro*, albeit their relevance *in vivo*. The ends of each strand of RNA are flanked by a long terminal repeat (LTR) that act as a promoter of viral replication and can be triggered by proteins from either HIV or the host cell. This information is posted in the HIV sequence database (<http://www.hiv.lanl.gov/>). Owing to the precise knowledge of the viral genome, different molecular constructs have been designed fused to fluorescent proteins or lacking important genes such as the envelope, allowing the construction of traceable virus or single-cycle replication competent virus.

Although the first anti-HIV drug entered clinical use in 1987, it was not until 1996 that the three-drug highly active antiretroviral therapy (HAART) was implemented (184), leading to a net reduction in mortality and morbidity in developed countries. However, a decade after HAART's introduction, over 6,800 persons become infected with HIV and over 5,700 persons die from AIDS every day, mostly because of inadequate access to HIV prevention and treatment services (AIDS epidemic update 2007; <http://www.unaids.org>). Therefore, HIV has evolved to escape not only our immune system but also all the antiretroviral drugs that have been designed so far.

In any event, how is HIV able to evade HAART and the innate and adaptive responses that DCs coordinate? Many aspects of HIV's biology aid in explaining, at least in part, why our immune system is still losing this fight.

1. HIV collapses our immune system

HIV mainly infects cells from the immune system bearing CD4 molecules and the appropriate coreceptors on their surface (generally CCR5 and CXCR4, determining the viral tropism or virus ability to employ these coreceptors). Although these cell types are mainly CD4⁺ T lymphocytes and macrophages, infection can also affect B lymphocytes, monocytes, natural killer cells and DCs, causing a gradual collapse of the host's defenses leading to opportunistic infections, various types of cancer, and eventual death: reviewed in (119, 184).

The main immunological feature of advanced HIV-mediated disease is a fall in the number of circulating CD4⁺ T cells, and this feature rapidly became the main surrogate marker for HIV-related immunodeficiency. Once the absolute CD4⁺ T cell count falls below a threshold of 200 T cells per mm³ in the peripheral blood, an individual becomes vulnerable to characteristic AIDS-defining opportunistic infections and malignancies, as reviewed in (119, 184).

Until the immune system collapses, four major stages of HIV pathogenesis can be outlined (Fig. 9):

1) **Acute virus infection** lasting up to four weeks after viral transmission. This clinical phase is characterized by viral dispersion throughout the lymphoid organs. CCR5⁺ T cells in lymphatic tissue become the principal site of virus production (69, 160, 161). Interestingly, gut-associated lymphoid tissue (GALT) is also an important site for early HIV replication and severe CD4⁺ T cell depletion, as reviewed in (119). During the establishment of infection, the general features are a dramatic increase of viral RNA in plasma and a partial loss of CD4⁺ T lymphocytes.

2) **Primary or early period** during which high virus production takes place, while HIV antibodies and cytotoxic responses appear. Once the adaptive immune responses control viral replication, CD4⁺ T cell counts are partially recovered.

3) **Persistent asymptomatic period** where the virus is maintained at a steady state set-point, primarily by the immune system. This viral set-point will vary among individuals, probably influenced by different host factors (66).

4) **Symptomatic period** when viral production has reemerged and presages the development of disease. The loss of CD4⁺ T cells reaches a critical threshold and the number of viral RNA copies in plasma increases constantly. During this stage, HIV-1 proviral DNA can be isolated from CXCR4⁺ naïve T cells (157): reviewed in (119). Under these circumstances, opportunistic infections appear and the symptomatic phase known as AIDS leads to death.

Overall, these major stages of HIV pathogenesis clearly denote that by targeting our immune system, HIV is able to gradually destroy our specific antiviral defenses.

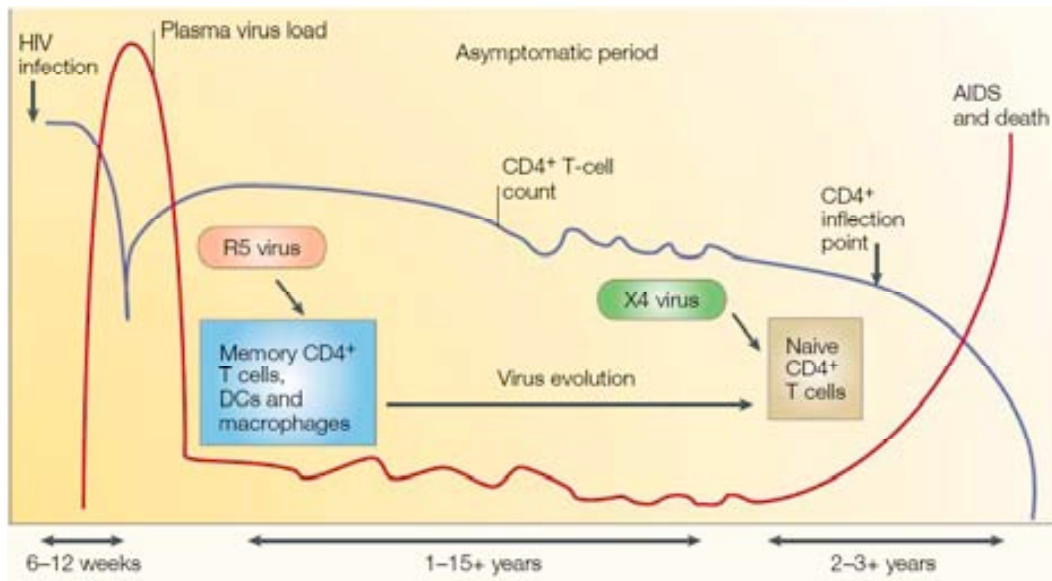


Figure 9. Schematic diagram of the course of an HIV-1 infection. This diagram illustrates the relationship between HIV-1 virus load (red line) and the CD4⁺ T cell count (blue line) over time in a typical case of untreated HIV-1 infection. Illustration from (184), *Nature Reviews Immunology*.

2. Viral evasion and the Trojan exosome hypothesis

In addition to the global collapse prompted by viral targeting of our immune cells, it is worth noting that HIV belongs to the Retroviridae family and replicates through a DNA intermediate employing a reverse transcriptase enzyme. This feature gives the virus another key advantage: viral DNA integrates into the host genome and once incorporated, can remain undetectable to the immune system for prolonged periods. Furthermore, HIV is hypervariable due to its rapid replication rate, high mutation rate, and capacity for recombination, leaving immune responses unable to control evolving viral populations (Fig. 10).

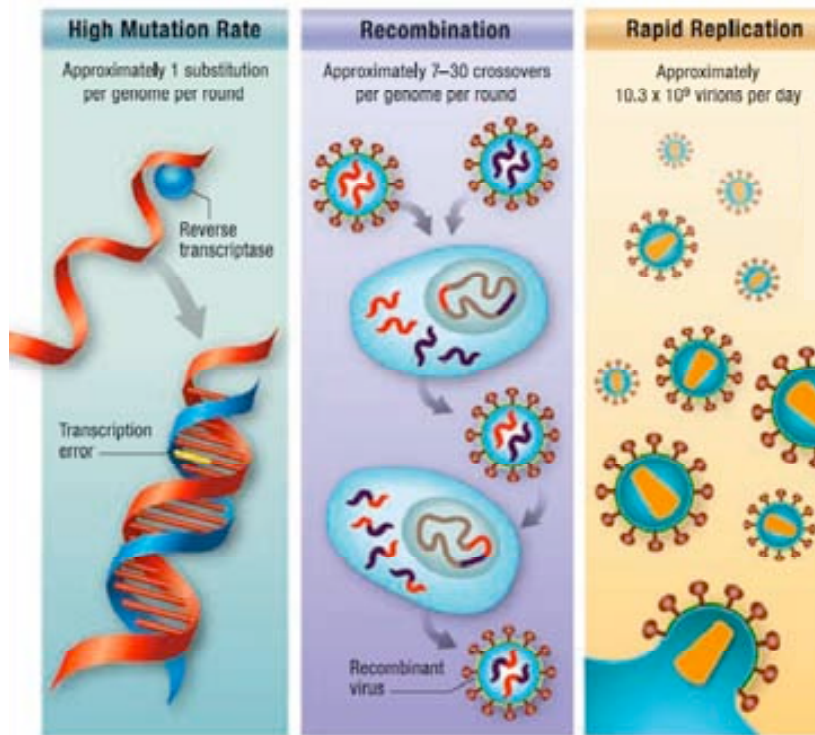


Figure 10. Causes of HIV variability. Illustration from the “AIDS Vaccine Blueprint 2006” edited by the International AIDS Vaccine Initiative.

Interestingly, aside from these well-known HIV features, a new hypothesis with important consequences for viral immune evasion has recently been proposed. This new model states that retroviruses, including HIV, are indeed Trojan exosomes (79). As we have previously seen, many cells synthesize and release small extracellular vesicles or exosomes that can induce immune responses or fuse with the membranes of neighboring cells to complete an intercellular vesicle trafficking pathway (49, 210, 215). The Trojan exosome hypothesis postulates that retroviruses use a preexisting exosome biogenesis pathway for the formation of infectious particles, also exploiting a preexisting exosome uptake pathway for a receptor-independent, envelope-independent mode of transmission (79). By subverting this pathway, HIV can mimic exosomes and escape immune surveillance.

Furthermore, this model provides a mechanistic explanation for many important properties of retroviruses, including the array of host cell molecules that retroviral particles display (7, 61, 87, 93, 135, 156, 158) and the observation of receptor-independent and envelope-independent retroviral infections (40, 159): reviewed in (119). Let us then examine some of the linked features of exosomes and retroviruses that support this hijacker hypothesis, focusing specifically on HIV.

2.1 Similarities in host cell lipids and proteins

The Trojan exosome hypothesis predicts that retroviral particles and exosomes will contain a similar array of host cell lipids and proteins. Retroviruses and exosomes have a shared lipid composition that includes significantly higher levels of cholesterol and glycosphingolipids than the cell plasma membrane (3, 142, 244). Retroviruses and exosomes also share many protein components that are enriched relative to the cell plasma membrane – such as tetraspanins (60) – or membrane proteins present at high levels in these particles as well as the cell surface – such as integrins or MHC proteins (7, 61, 135, 156, 158, 175, 212) – and numerous cytoplasmic proteins such as actin, cyclophilin, tsg101 and heat shock proteins (88, 129, 136, 158, 212, 214). Moreover, side-by-side analyses show identical host cell protein profiles for HIV particles and exosomal preparations (15). Remarkably, these host cell proteins incorporated in retroviruses are not just trace components, as some – such as MHC-II – can exceed the abundance of the envelope glycoproteins (79). Interestingly, the incorporation of these host components facilitates viral evasion, as camouflage aids soldiers to pass unnoticed in the battlefield.

2.2 Similarities in protein targeting and vesicle biogenesis

The Trojan exosome hypothesis also postulates that retrovirus budding can be a manifestation of a normal, cell-encoded exosome biogenesis pathway. Indeed, several lines of evidence suggest a link between the biogenesis and the release of exosomes and retroviruses. In macrophages and DCs, exosome biogenesis can take place by reverse budding into the multivesicular body, an intracellular compartment that can fuse with the plasma membrane, releasing its internal vesicles as exosomes. Analogously, HIV can bud in macrophages into endosomes, releasing viral particles upon fusion with the plasma membrane (20, 177); although these findings have been recently challenged (237). Furthermore, previous studies have demonstrated an association of endocytosed HIV-1 particles with intraluminal vesicle-containing compartments within immature DCs that liberate HIV in association with exosomes (Fig. 11), permitting the infection of CD4⁺ T cells (238).

Nonetheless, as we have previously mentioned, HIV mainly buds from the plasma membrane of CD4⁺ T cells. The Trojan exosome hypothesis suggests that retroviruses should also bud from endosomal patches of the cell surface that are transient entities that form as a consequence of endosome–plasma membrane fusion. Interestingly, both exosomes and HIV can bud at particular microdomains of the T cell plasma membrane that are not distributed evenly across the cell surface but located in focal patches. These structures have been termed endosome-like domains because they are enriched with a variety of endosomal and exosomal proteins and are competent for outward vesicle budding (23, 65).

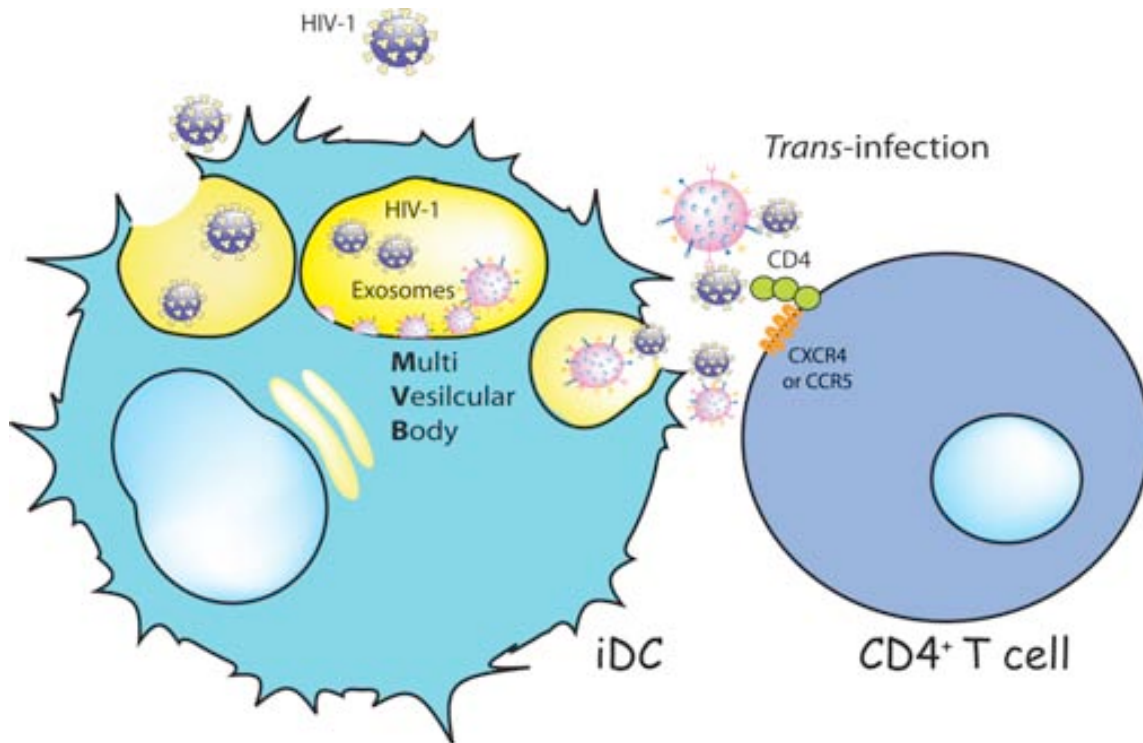


Figure 11. Exosomes and HIV in immature DCs. Endocytosed HIV-1 traffic into intraluminal exosome-containing compartments or multivesicular bodies. Upon recycling of these compartments with the plasma membrane, immature DCs liberate HIV in association with exosomes, allowing infection of interacting CD4⁺ T lymphocytes.

Although several lines of evidence indicate that these endosomal-like domains correspond to the lipid raft structures from which HIV-1, ecotropic murine leukemia virus (MLV) and other retroviruses have been suggested to bud (128, 151), exosome release from lipid rafts remains controversial (116). Either way, like retroviruses, exosomes derived from T and B lymphocytes are enriched in cholesterol, glycosphingolipids and many tetraspanins that are located in lipid rafts (23, 244). Furthermore, from a mechanistic point of view, a recent paper has demonstrated that higher order oligomerization in the plasma membrane targets proteins both into exosomes and HIV virus-like particles (65).

Even though this whole line of thinking is still controversial (45, 216), the proposed exosomal origin of the retrovirus predicts that HIV poses an unsolvable paradox for adaptive immune responses. Even more challenging is that from this perspective, retroviral-based vaccines are unlikely to provide prophylactic protection.

By underscoring the HIV features that contribute to viral escape, we now know some of the most important ingredients of Dr. Jekyll's evil potion. However, we still do not know how the functional transformation of DCs into Mr. Hyde takes place.

III. Mr. Hyde:

Interactions of HIV-1 with dendritic cells

Because immature DCs are located in the mucosal epithelia, they are probably among the earliest targets of HIV infection. Furthermore, upon maturation, their preferential location in the T cell areas of lymphoid organs, where they continuously interact with CD4⁺ T cells – the main targets of HIV – renders these cells one of the principal candidates for contributing to viral spread *in vivo*. These mechanisms are in fact what we have been referring to as the functional metamorphosis of DCs into Mr. Hyde, a complex interplay that is the main topic of this thesis.

In the following sections, we will review the different outcomes of the interaction between DCs and HIV, including the direct productive infection of these cells and the viral transmission mediated by DCs to CD4⁺ T cells. This later mechanism is unique to DCs among all immune cells, and therefore it will be presented in greater detail. As we will emphasize, many efforts have been dedicated to understanding the role of DCs in HIV disease progression, although no evident consensus has been reached yet.

1. To be or not to be infected

Conventional DCs and plasmacytoid DCs are all susceptible to infection with HIV (109, 201): reviewed in (168, 241). However, over the years DC infection *in vivo* has remained controversial, probably because the frequency of HIV-1 infected DCs is often 10 to 100-fold lower than CD4⁺ T cells (139). Indeed, finding productive HIV infection in a rare population of cells that migrate rapidly from epithelial and dermal tissues upon antigen contact is a real challenge. To gain insight into the infection of DCs and Langerhans cells

during viral transmission at mucosal surfaces *in vivo*, Simian Immunodeficiency Virus (SIV) infection of rhesus macaques was studied. Employing this animal model, several investigators were unable to detect SIV⁺ Langerhans cells within mucosal tissue after a couple of days following intravaginal or intraoral inoculation of the virus (205, 248). By contrast, when vaginal tissue was examined only 18 hours after intravaginal exposure, SIV-infected intraepithelial Langerhans cells could easily be found (99), and virus could also be recovered from lymph nodes in a DC associated form. In subsequent studies performed in the gut-associated lymphoid tissue (GALT), where CD4⁺ T cells were present in large numbers, productive infection of T cells was more readily detected than infection of DCs (25, 121).

32

Finally, HIV infection of DCs *in vitro* has also been difficult to detect because HIV-1 replication in DCs is generally less productive than in CD4⁺ T cells or macrophages (81, 209). A number of reasons are presumed to explain this moderate HIV infection of DCs, including the low levels of expression of CD4 and coreceptors, and the rapid and extensive degradation of internalized virus in intracellular compartments (144, 153, 226). Furthermore, DC maturation is associated with a reduced ability to support HIV-1 replication, being 10 to 100-fold less active in mature DCs than in immature DCs (9, 32, 81). Interestingly, this finding correlates with the observation that the levels of the antiviral protein APOBEC3G increase during the DC maturation process (170), allowing the accumulation of a cellular factor that effectively blocks the HIV lifecycle after entry in primary cells (39). Therefore, the expression of host factors that block HIV replication could also account for the restricted DC infection observed.

Although limited, the small proportion of HIV infected DCs could spread newly synthesized virus to T cells in a highly efficient way (126). Indeed,

several lines of evidence suggest that the long-term ability of immature DCs to transfer HIV relies on *de novo* production of viral particles after DC infection (30, 153, 226).

1.1 General features of the HIV-1 replication cycle

Regarding the viral replication cycle (Fig. 12A), HIV follows several common main steps in DCs, CD4⁺ T cells and macrophages. After viral attachment to the cell surface, the HIV envelope glycoproteins interact with the cellular receptor CD4 and another cellular coreceptor, mainly CCR5 or CXCR4. This allows the fusion of the viral membrane with the cellular membrane, the liberation of the viral capsid and the final release of the RNA into the cytoplasm. Viral reverse transcriptase catalyzes the RNA transcription into a complementary DNA strand that is finally copied and translocated into the nucleus as a double-stranded DNA molecule. This DNA is then integrated into the host genome thanks to the integrase activity, where it can remain latent and evade the immune surveillance. Upon cellular activation, HIV regulatory genes are expressed, modulating the latter expression of structural genes. The synthesis of viral polyprotein precursors allows the assembly and budding of immature viral particles that are released into the extracellular milieu. Maturation of viral particles culminates when viral protease processes the incorporated protein precursors into the different viral proteins, allowing the achievement of full viral infectivity, as reviewed in (221).

1.2 Specific features of the HIV-1 replication cycle in DCs

Despite its common features with HIV infection of CD4⁺ T cells and macrophages, DC infection has certain peculiarities. In the following sections we will review some of these characteristics and their implications for HIV pathogenesis.

a) Viral binding

Regarding attachment (Fig. 12B), CLRs that are not expressed in T lymphocytes, like DC-SIGN or DCIR, could play a role during viral binding to the DC surface, facilitating viral interactions with CD4 and allowing fusion (113, 117). However, these findings are challenged in another report (152), leaving this subject open to further debate. Another recent work shows that Syndecan-3, a DC-specific heparan sulfate proteoglycan, captures HIV-1 through its envelope glycoprotein, enhancing direct infection of DCs (48).

b) DC infection as a selection mechanism for CCR5 tropic viruses

DCs are more susceptible to infection by HIV-1 strains that use the CCR5 molecule as a fusion-coreceptor than by those strains that employ the CXCR4 coreceptor (81, 108, 180, 201, 204). This observation is crucial because it could explain the preferential transmission of HIV-1 strains exploiting the CCR5 receptor during primoinfection and the selective amplification of these viral strains during acute and chronic stages of disease progression *in vivo* (44, 194): reviewed in (130). In general, immature DCs tend to express higher surface levels of CCR5 and little or no CXCR4, whereas mature DCs tend to express less CCR5 and higher levels of CXCR4 (110, 188, 246). This could provide a simple explanation for the restriction of CXCR4 tropic HIV replication in immature DCs or Langerhans cells, the gatekeepers of the mucosa that interact with the virus during primary infection. However, other studies detected both CXCR4 and CCR5 expression in immature DCs and Langerhans cells (126, 169). Another possible explanation springs from the fact that the fusion of HIV-using CXCR4 coreceptors in immature DCs is restricted, irrespective of the surface levels of CXCR4 (33, 169). Interestingly, similar observations have been made in mature DCs, where maturation also results in decreased viral

fusion with the plasma membrane (34) and a later inhibition of HIV transcription when viral integration takes place (9). However, the mechanism or mechanisms responsible for CCR5-tropic HIV-1 predominance early in infection remains unknown, and several other plausible hypotheses aside from DC susceptibility to HIV infection should be taken into account.

c) DC infection allows for antigen presentation to CD8⁺ T cells

Finally, we should not forget that infected DCs contribute to antigen presentation. Upon infection, viral proteins that gain access to the cellular cytoplasm or that are being synthesized *de novo* can be processed by the proteasome and presented in MHC-I molecules to CD8⁺ T lymphocytes (144), leading to cytotoxic cellular immune responses (Fig. 12B). This is precisely the pathway that the HIV therapeutic vaccine is trying to enhance, employing DCs pulsed with inactivated virus to stimulate a specific CD8⁺ T response that could aid the immune system of infected patients in controlling viremia, as reviewed in (4).

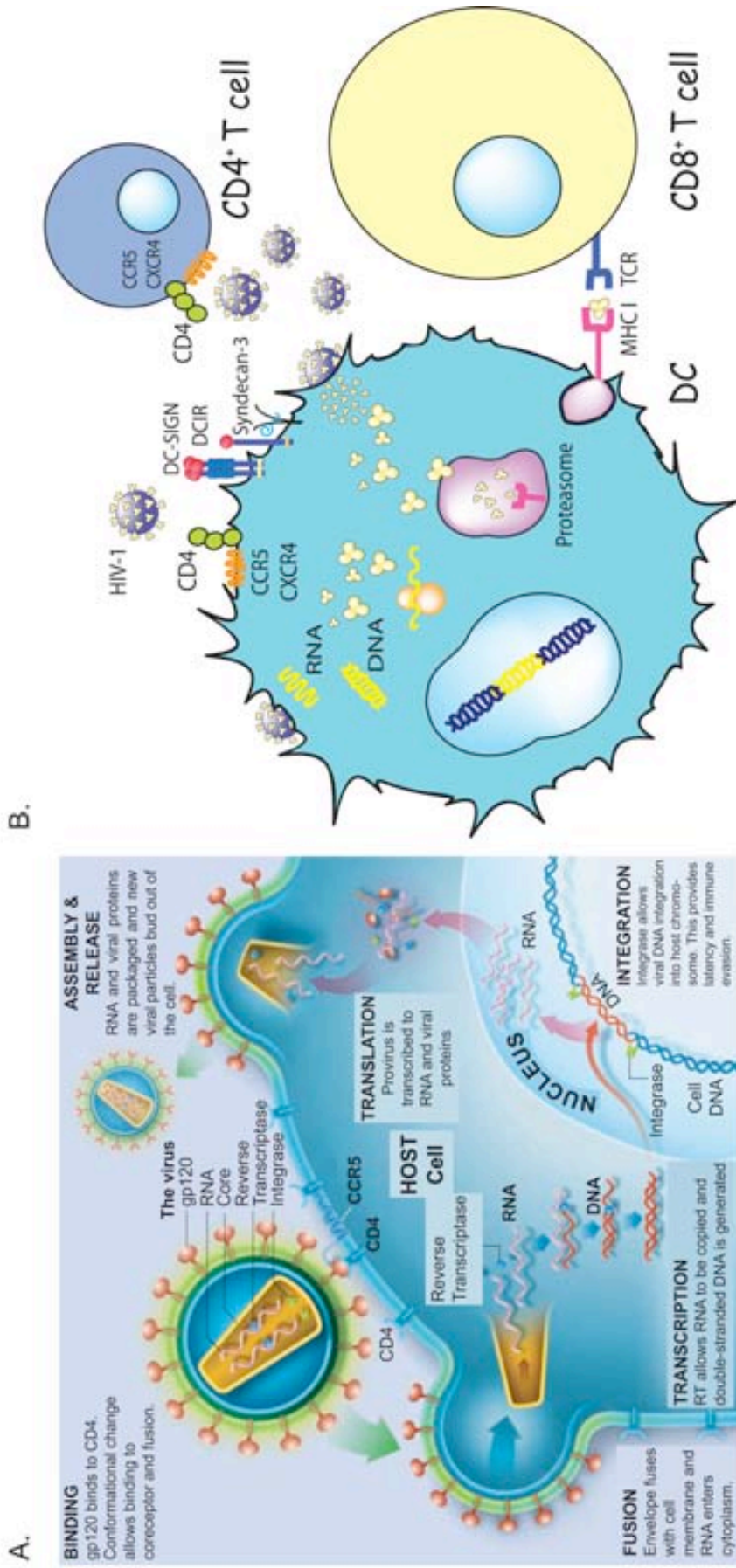


Figure 12. (A) Schematic representation of the **general HIV replication lifecycle** from the “AIDS Vaccine Blueprint 2006” edited by the International AIDS Vaccine Initiative. **(B) HIV infection of a DC.** Viral binding to specific DC attachment factors, fusion, integration of the viral genome, and *de novo* viral production are depicted. Proteasome machinery can degrade viral proteins in the cytoplasm that are then presented to CD8⁺ T cells in MHC-I molecules. Notably, new viral particles released by DCs can infect interacting CD4⁺ T cells.

2. DC as Trojan horses: Viral transmission to CD4⁺ T cells

It has been known for years that DCs exposed to HIV-1 transmit a vigorous cytopathic infection to CD4⁺ T cells (32). Interestingly, DCs do not need to be productively infected to transmit the virus and spread it in an infectious form, contrasting in this with other HIV-1 target cells like CD4⁺ T lymphocytes or macrophages. Indeed, separate pathways mediate the productive infection of DCs and their ability to capture HIV-1 (19). This particular viral capture mechanism involves binding and uptake of HIV-1, traffic of internalized virus and its final release allowing transfer to CD4⁺ T cells (76), a process known as **trans-infection** (Fig. 13). The resemblance of this mechanism to the ruse described in Homer's *Odyssey* is obvious: viruses hide within DCs as the Greek soldiers did within the Trojan horse, gaining access to the city of Troy and taking the defenders by surprise, thus winning the war.

Knowing the antigen-presenting capabilities of immature DCs, one would expect that after HIV interaction with surveillance receptors (PRRs), endocytosed virus would end up in classical lysosomic pathways (Fig. 13), where viral antigens are degraded and presented in MHC-II molecules to CD4⁺ T cells (145). Furthermore, part of the internalized virus could also gain access to the cytoplasm and be processed throughout the proteasome, being finally crosspresented in MHC-I molecules to CD8⁺ T cells (31, 144).

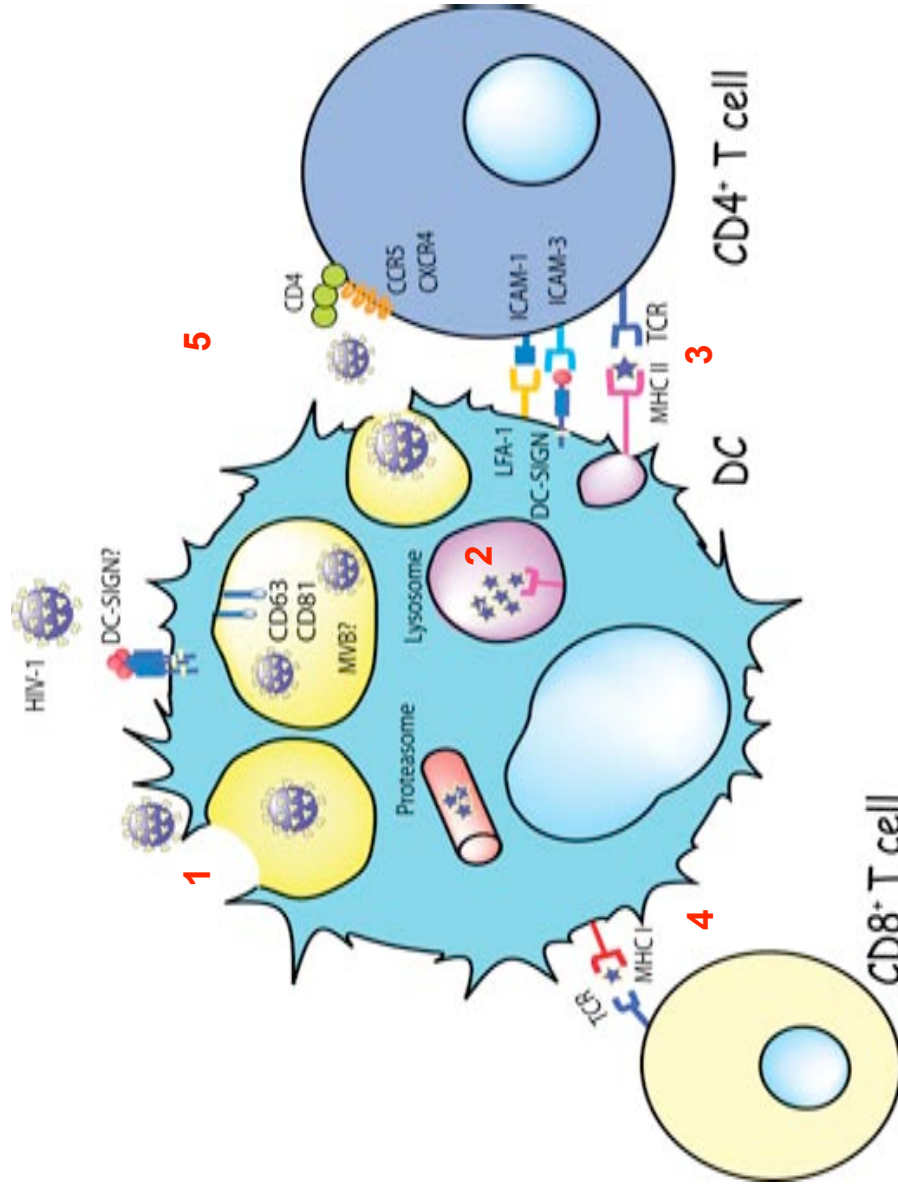
However, in the specific case of HIV interaction with DCs, it has been proposed that part of the internalized virus escapes these degradation routes and its maintained in endosomal acidic compartments, retaining viral infectivity for the long periods required to promote efficient HIV-1 transfer to CD4⁺ T cells (76, 112).

Nevertheless, the mechanisms that mediate the prolonged survival of virions captured by DCs are currently unclear and controversial. Indeed, it is

ironic that professional antigen-presenting cells such as DCs, rich in degradative compartments, are unable to process HIV and instead protect the virions in an infectious form for periods longer than four days (76). A plausible explanation could be that the longer retention of intact viral particles within an intracellular compartment could in fact aid immunological surveillance, allowing DCs to have a source of antigen to present to T cells in the absence of surrounding viral particles. Therefore, this mechanism could be beneficial, although recent works have demonstrated that immature DCs show rapid degradation of captured viral particles, which do not last more than 24 hours before being processed (144, 153, 226). As an alternative, these authors suggest a two-phase mechanism of viral transmission mediated by immature DCs: one restricted to a short period through the *trans*-infection process and a later one due to a long-term transfer of *de novo* viral particles produced after immature DC infection (30, 153, 226).

Figure 13. Antigen presentation and *trans*-infection of a CD4⁺ T cell mediated by a DC.

Viral binding to distinct cellular receptors allows viral endocytosis via a non-fusogenic mechanism (1). The virus is retained in the multivesicular body compartment (MVB), enriched in tetraspanins such as CD81 and CD63. Part of the virus is degraded in the lysosomes (2) and viral antigens are presented via MHC-II to the T cell receptor (TCR) of specific CD4⁺ T cells (3) through the formation of an immunological synapse. This synapse relies on earlier low affinity contacts between LFA-1 and DC-SIGN molecules expressed by DCs with ICAM-1 and 3 counterparts in T cells. If an endocytosed virus gains access to the cytoplasm of the DC, it can be processed by the proteasome and crosspresented via MHC-I to CD8⁺ T cells (4). Viral transmission takes place when part of the virus evades classical degradation pathways. MVB recycles back and fuses with the plasma membrane, allowing the liberation of entrapped virus and the productive infection of DC-interacting CD4⁺ T cells (5), a mechanism known as *trans*-infection. The contact area between an uninfected DC bearing HIV infectious particles and a CD4⁺ T cell is termed the infectious synapse.



2.1 Viral capture: The role of DC-SIGN

Trans-infection has been related to the ability of DC-SIGN expressed in certain subtypes of DCs to tightly bind to the HIV-1 surface envelope glycoprotein gp120 (76). Further studies also suggest that DC-SIGN on B lymphocytes or macrophages could also be implicated in HIV-1 transmission to T lymphocytes (179, 192). The initial identification of DC-SIGN as an HIV receptor permitting *trans*-infection of CD4⁺ T cells led to the “Trojan horse” hypothesis, which relates the preliminary establishment of HIV-1 infection to the ability of immature DCs to capture the virus via DC-SIGN in the peripheral tissue and then migrate to the lymph nodes, where HIV-1 transferred to CD4⁺ T cells could easily start the spread of infection (Fig. 14). However, as we have previously mentioned, several different mechanisms could mediate the establishment of HIV infection *in vivo* (Fig. 15).

DC-SIGN affinity for monomeric gp120 is five times greater than the one displayed by the receptor CD4 (46). That is why it was first suggested that DC-SIGN could efficiently capture low numbers of HIV-1 particles in the periphery, facilitating HIV transport to secondary lymphoid organs that are rich in CD4⁺ T cells, where infection of target cells would take place (76). Although this DC-SIGN high affinity interaction could play a prominent role in situations where the amount of free viral particles is limited, this does not need to be the only physiological setting. Cell-to-cell viral transmission efficiently concentrates viral particles at the site of cellular contacts, increasing considerably the amount of contacting virus (64, 234) and its infectivity (50).

In fact, previous studies have calculated that only ~10% of the infections in the lymphoid tissue are transmitted by cell-free virions and ~90% are transmitted by infected cells (51). In our laboratory, it has been previously shown that cell-free virus preparations containing amounts of p24^{Gag} equivalent

to infected cells failed to transfer HIV antigens to unstimulated primary CD4⁺ T lymphocytes, while p24^{Gag} antigen uptake occurred during cell-to-cell contacts (17).

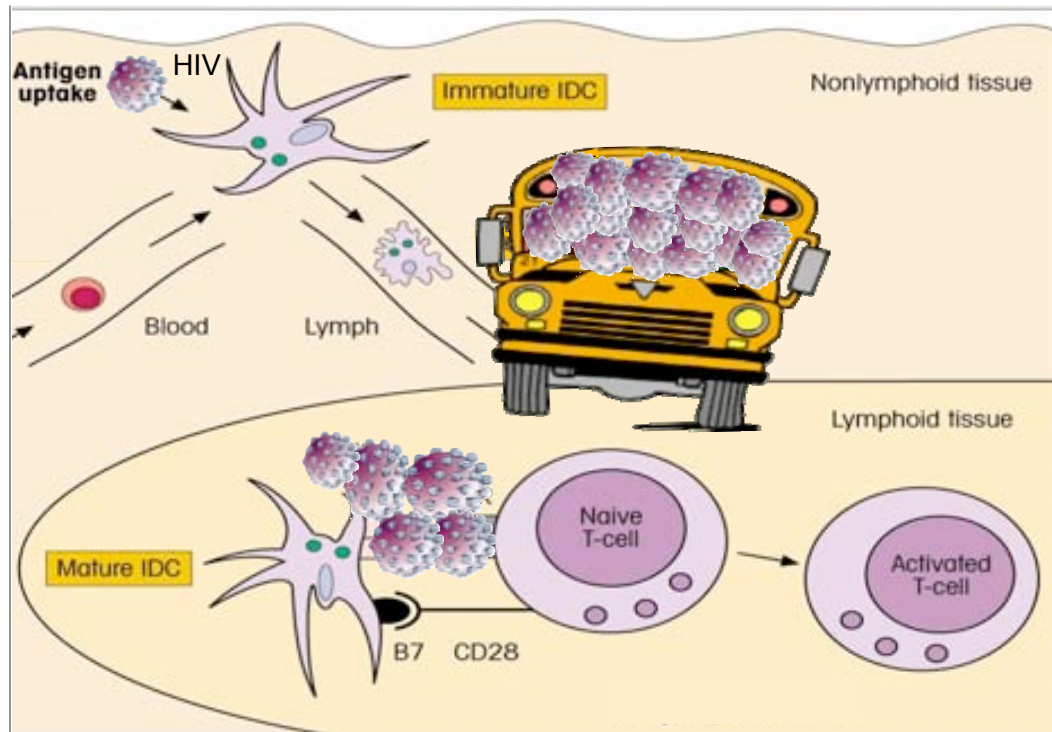


Figure 14. The Trojan horse hypothesis. Immature DCs in the peripheral tissues capture HIV and migrate to secondary lymph nodes, where they end their maturation process and transmit captured virus to susceptible target T cells, allowing the initial spread of viral infection in secondary lymph nodes. Here, the HIV-loaded DC or Trojan horse is represented as a school bus. Modified from Roitt's Essential Immunology, Blackwell Publishing Ltd.

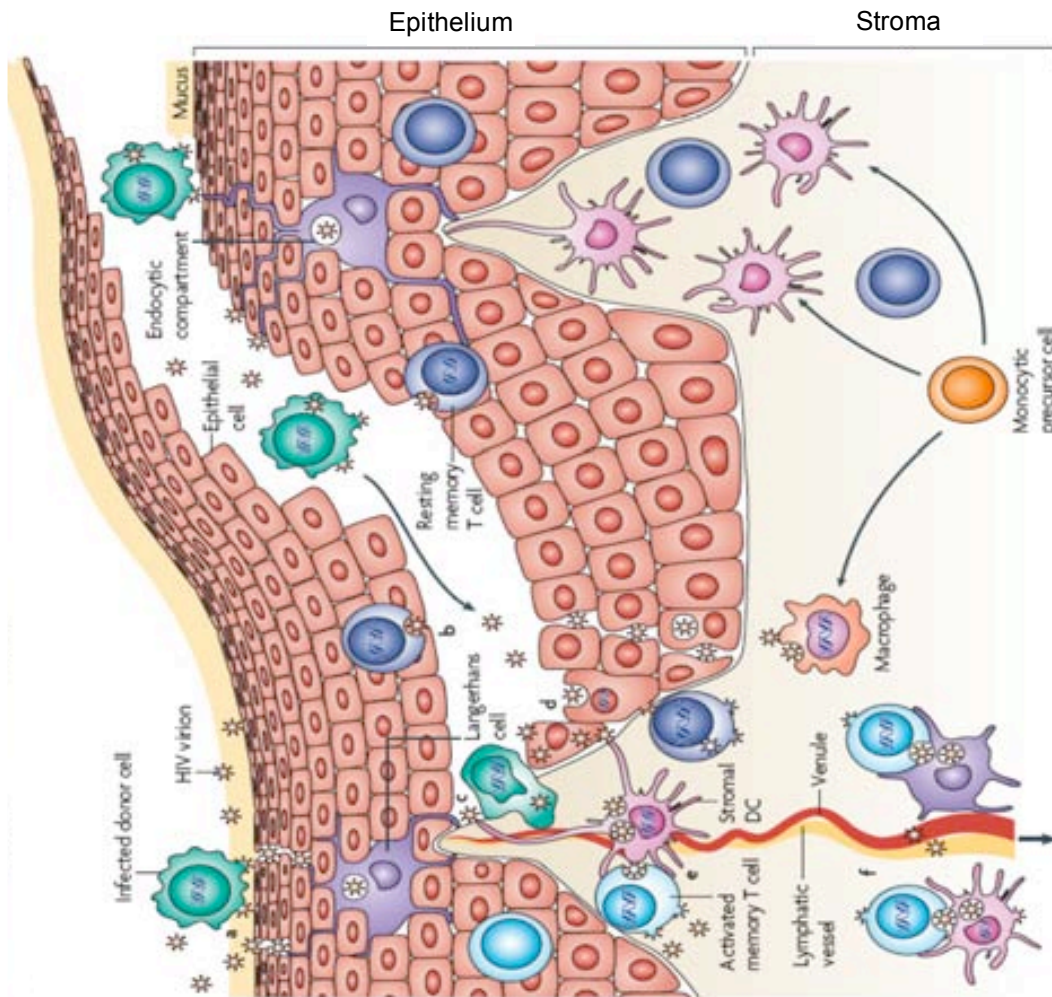
In vivo, primary subepithelial DCs in the gut, cervix, vagina, foreskin, rectum and glans penis express DC-SIGN and are therefore thought to mediate HIV-1 transmission (89, 103, 137, 203). DC-SIGN has also been detected in a rare subset of CD14⁺ cells that represent less than 0.01% in blood and serve as DC precursors (58), and in DCs in lymph nodes and tonsils (59, 127). After

isolation, DC-SIGN⁺ DCs present throughout the whole rectal epithelia have been shown to mediate transmission to CD4⁺ T cells through DC-SIGN, but only when low numbers of infectious viral particles were employed (89). Interestingly, at higher viral inputs, DC-SIGN dependency was lost. Again, DC-SIGN reliance in CD14⁺ blood myeloid cells was only shown at low viral inputs (58). Therefore, as we have previously mentioned, in cell-to-cell viral transmissions, where large amounts of virus are concentrated, the role of DC-SIGN might be dispensable. Another report has shown that migratory cells emigrating from cervical tissue efficiently captured and transmitted HIV-1 infection in *trans* (100). Although the DC-SIGN role was highlighted in this study, antibodies against DC-SIGN could only block 30% of viral transmission to target cells, further stressing that multiple receptors are involved in HIV-1 uptake by conventional DCs.

Finally, it is worth mentioning that DC-SIGN interactions with the gp120 envelope glycoprotein do not distinguish between the tropism of different viruses, allowing equal *trans*-infection of both CCR5 and CXCR4-tropic viruses (76, 81, 84, 126, 172). Thus, this model fails to explain the initial establishment of CCR5 tropic viral strains during primoinfection and adds an additional caveat to the original Trojan horse hypothesis. Furthermore, it has been recently observed that transmission of HIV-1 by immature and mature DCs is significantly higher for CXCR4 than CCR5-tropic viral strains and that DCs preferentially facilitate infection of viral populations with an envelope phenotype found late in disease (228). Hence, these authors hypothesize that this discrimination could contribute to the *in vivo* coreceptor switch and could be responsible for the increase in viral load at later stages of disease progression.

Figure 15. Suggested pathways of HIV invasion in the mucosa. (A)

Free HIV virions or HIV-infected donor cells are trapped in mucus, resulting in penetration of virions into gaps between epithelial cells or secretion of virions by HIV-infected donor cells upon contact with the luminal surface of the mucosa. Virions are then captured and internalized into endocytic compartments by Langerhans cells (LCs) that reside within the epithelium. **(B)** HIV can also fuse with the surface of intraepithelial CD4⁺ T cells, followed by productive infection of these cells. **(C)** Infected donor cells or free virions can migrate along physical abrasions of the epithelium into the mucosal stroma, establishing contacts with stromal DCs, T cells and macrophages. There, infected donor cells or virions can also be taken by the lymphatic or venous system and transported to the lymph nodes or the blood, respectively. **(D)** Virions can transcytose through epithelial cells near or within the basal layer of the squamous epithelium, productively infecting basal epithelial cells, internalizing into endocytic compartments or penetrating between epithelial cells. **(E)** Once in the stroma, virions can productively infect DCs or be internalized into the endocytic compartments and pass from the DCs to CD4⁺ T cells across an infectious synapse. In addition, virions can productively infect resting mucosal CD4⁺ memory T cells and possibly macrophages. **(F)** Productively infected CD4⁺ T cells and stromal DCs or cells harboring virions in endocytic compartments, such as DCs or intraepithelial LCs, can migrate into the submucosa and the draining lymphatic and venous microvessels. Figure from (94), Nature Reviews Immunology.



2.2 DC-SIGN-Independent viral capture mechanisms

Although DC-SIGN has been proposed as the most important HIV-1 attachment factor that concentrates virus particles on the surface of DCs (76, 112), other studies also suggest that HIV-1 binding, uptake and transfer from DCs to CD4⁺ T lymphocytes may involve alternative pathways such as C-type lectin receptors (CLRs) – including mannose receptor, DCIR and trypsin-sensitive CLRs – CD4-independent receptors and glycosphingolipids, such as galactosyl ceramide expressed on the DC surface (22, 82, 86, 113, 132, 223, 225, 240). These studies demonstrate that a single receptor is not responsible for HIV-1 binding to all DC subsets (100, 225) and highlight that additional HIV-1 binding molecules remain to be identified. Furthermore, the relative contribution of these receptors to HIV-1 transmission *in vivo* and their role in different DC subsets is still largely unknown.

Intriguingly, these alternative results have been somehow eclipsed by the initial DC-SIGN findings, although there are several limitations to the preliminary proposed model. For instance, the functional relevance of the high-affinity interaction between HIV-1 and DC-SIGN has been hampered in several studies by the use of monomeric glycoprotein gp120 instead of HIV-1 virions bearing the functional trimeric gp120 protein (76, 98, 112, 202, 223, 225). Furthermore, even when this limited monomeric gp120 model is employed, results obtained in freshly isolated or cultured peripheral blood DCs differed from initial observations in monocyte-derived DCs, as this more physiological set of cells binds gp120 only through CD4 and not through CLRs (223-225). Additionally, blood Myeloid DCs and Langerhans cells do not express DC-SIGN, but can mediate HIV *trans*-infection (63, 82).

Finally, the viral capture and cellular contacts that lead to *trans*-infection of CD4⁺ T cells could also have been initially misinterpreted, because the

presumed “THP-1” monocytic cells used to model DCs in those studies (76, 112, 172, 219) were instead Raji B cells (242). Interestingly, B cell transfectants that express DC-SIGN mediate HIV *trans*-infection as efficiently as DCs, whereas monocyte transfectants do not (242). However, in permissive cell lines, DC-SIGN promotes transfer of HIV infection in a manner that is strictly dependent on DC-SIGN (6, 76, 112, 219) and its level of expression in the cell surface (12, 172). These unambiguous results contrast with studies in primary DCs that have shown a variable contribution of DC-SIGN in the transfer of HIV infection to CD4⁺ T cells (i.e. from a minimal to a significant contribution), perhaps depending on the DCs used, as well as the experimental conditions employed regarding for instance the viral input added.

Overall, these findings reinforce the idea that the cellular environment is an important consideration when examining the transmission of HIV captured by DC-SIGN or other viral attachment factors (241). Collectively, these studies explain why the preliminary results regarding DC-SIGN function in HIV-1 pathogenesis are controversial and need further investigation.

2.3 Intracellular viral trafficking

Regardless the nature of the initial receptors implicated in the viral binding process, once the virus is attached to the surface of the DCs, it is internalized into endosomes or multivesicular bodies – (74, 111) and (Fig. 16A). These structures are endocytic vesicles with a mildly acidic pH that are enriched in tetraspanins, such as CD81, CD82 or CD9, and other related molecules (74).

However, in this field it seems as though every discovery is fraught with controversy. A recent study challenges this internalization view (35), suggesting that cell-surface-bound HIV is the predominant pathway for viral transmission mediated by monocyte-derived DCs (Fig. 16B). In contraposition to the results

obtained by this group, several other publications have reported that HIV associated with DCs at 37°C is protected from trypsin treatment (19, 76, 238) and from Pronase treatment (22, 63, 234). Therefore, the most extended view proposes that the virus is endocytosed and accumulated into a non-conventional, non-lysosomal, endocytic compartment protected from proteolytic treatments. Interestingly, the latest report on this topic reconciles these two models by demonstrating that the intracellular, apparently endocytosed HIV remains fully accessible to surface-applied viral inhibitors and other membrane-impermeable probes (245). These results demonstrate that HIV resides in an invaginated domain within DCs that is both contiguous with the plasma membrane and distinct from classical endocytic vesicles (Fig. 16C).

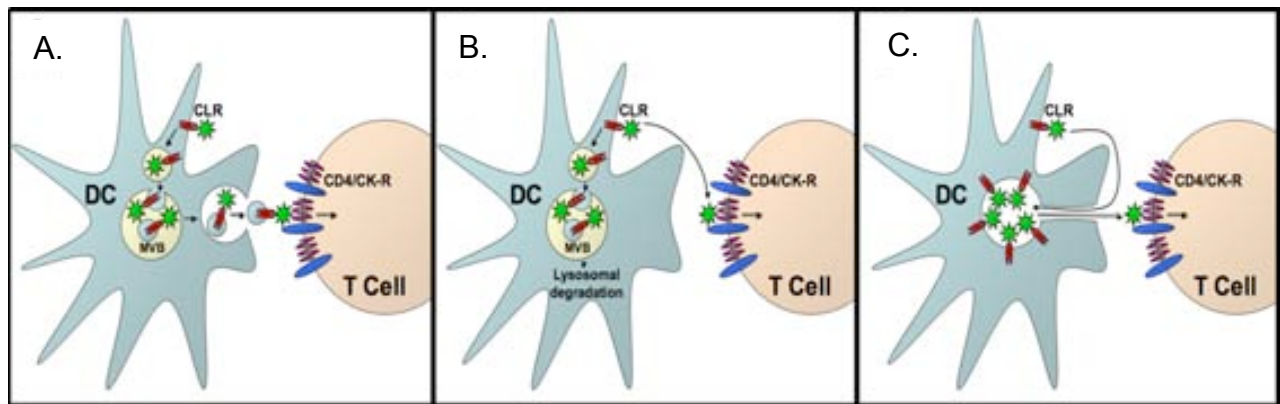


Figure 16. Models of *trans*-infection. (A) MVB/exosomal transfer. HIV is endocytosed and concentrated in a non-degradative late endosome or multivesicular body (MVB). The MVB subsequently fuses with the DC plasma membrane and delivers HIV by exocytosis. **(B) Surface transfer.** Only surface-bound HIV is able to infect CD4⁺ T cells. Internalized HIV is degraded following lysosomal maturation. **(C) Pocket transfer.** HIV is concentrated and internalized in a non-endosomal compartment that remains contiguous with the plasma membrane. HIV remains accessible to the extracellular milieu and individual virions are delivered back to the DC surface prior to transmission. Illustration from (245), Plos Pathogens.

Notably, the location of internalized virions is dramatically different in immature and mature DCs (70). Strikingly, the poorly macropinocytic mature DCs sequester significantly more whole, structurally intact virions into large vesicles deep within the cells, whereas the endocytically active immature DCs not only retain fewer internalized virions, but also locate them closer to the cell periphery (70). Therefore, most of the characterization of multivesicular bodies has been done in mature DCs, where the cellular tetraspanins have been shown to co-localize with endocytosed virus (74). In immature DCs, partial co-localization with transferrin has been identified during the early time points of viral entry (112), but later time points show partial co-localization with tetraspanins as well (238). Overall, the precise intracellular trafficking and localization of internalized HIV within DCs remains to be elucidated.

2.4 Viral transmission: Infectious synapses and exosomes

How is the endocytosed virus released and transferred to CD4⁺ T cells? This is a key issue that still lacks a molecular explanation. Initial *in vitro* studies using monocyte-derived DCs indicated that cell-to-cell contact is required for efficient CD4⁺ T cell infection (220). More recently, studies have revealed that HIV-1 transmission can occur across the **infectious synapse**, a cell-to-cell contact zone between DCs and CD4⁺ T cells that facilitates transmission of HIV-1 by locally concentrating virus and viral receptors (6, 74, 138, 167): also termed “the kiss of death” in our laboratory (Fig. 17). It is worth mentioning that the infectious synapse is formed between an uninfected DC that directs transfer of the captured virus to an uninfected target cell. In contrast, the term “**virological synapse**” normally refers to the interaction between productively infected cells and uninfected target cells (167). The difference between these two mechanisms might be more pronounced than previously expected, given

that the envelope glycoprotein expression on the surface of infected cells increases the number of effective contacts between infected DCs or $CD4^+$ T cells and uninfected target T cells (173, 222).

In the absence of the envelope glycoprotein, the structure of the infectious synapse could have similarities to the immunological synapse, which is formed between mature antigen-presenting cells and T cell conjugates. In both types of synapses, adhesion molecules such as ICAM-1 and 3 have been found to play a relevant role (83, 143).

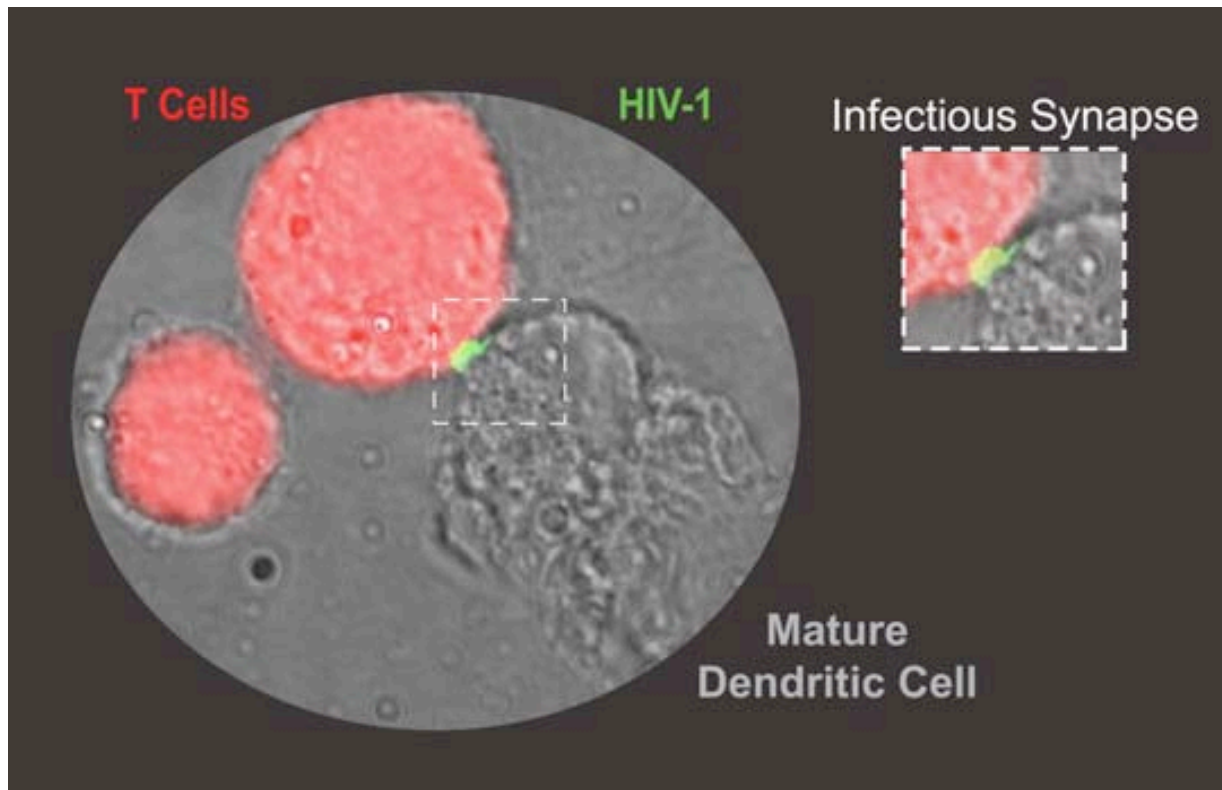


Figure 17. Infectious Synapse; “the kiss of death”. Mature monocyte-derived DC previously pulsed with fluorescently labeled HIV (green) concentrates viral particles at the site of cellular contact with a $CD4^+$ T cell, distinguished by the red staining.

However, the infectious synapse does not need antigen processing or recognition and thus requires less time to be formed. Infectious synapse assembly is probably initiated by a normal cellular process in which DCs form transient contacts with T cells without the requirement for antigen specificity: this is proposed to be a kind of “scanning” by a T cell to enable potential recognition of a cognate peptide presented by the APC (181). T cells approach DCs randomly and make exploratory contacts that last only minutes, enabling DCs to contact thousands of T cells per hour (141). DC–T cell conjugates are formed and virions concentrate at the surface in contact with the T cell, while the HIV-1 receptor CD4 and coreceptors appear to be partially enriched in the T cell at the point of contact with the DC (138). Therefore, receptor recruitment and virus polarization at the synapse site explains, at least in part, why DC transmission of HIV-1 to T cells is such an efficient process (168).

The formation of infectious synapses could explain why *in vivo*, HIV infects antigen-specific CD4⁺ T cells more efficiently than other CD4⁺ T cells (54). HIV-specific naïve CD4⁺ T cells become activated on first encounter with HIV antigens presented by DCs in the lymph node and are in prolonged close proximity to HIV-containing DCs, becoming highly susceptible to HIV infection as they undergo several rounds of division during their initial expansion and differentiation into effector T cells (54). Latter works *in vitro* have demonstrated that HIV-bearing DCs preferentially infect antigen-specific CD4⁺ T cells (126, 145), further supporting this model.

Interestingly, the set of cell-surface molecules that contributes to the infectious synapse and potentially supports the transfer of HIV-1 from DCs to CD4⁺ T cells has not yet been fully identified, although DC-SIGN involvement has been indicated (6). A potential explanation for the role of DC-SIGN in DC–T cell infectious synapse formation has been recently proposed. HIV

binding to DC-SIGN recruits the Rho guanine nucleotide-exchange factor LARG, which increases DC–T cell infectious synapse formation (96). However, the functional relevance of this process remains largely uncharacterized. Finally, tetraspanins, which also participate in antigen presentation and immunological synapse formation, are enriched in the DC–T cell infectious synapse (74).

We should not forget that immature DC-derived exosomes can mediate HIV-1 *trans*-infection (238). This work demonstrates that captured HIV-1 is rapidly internalized into multivesicular bodies, where exosomes are produced by reverse budding (Fig. 11). Intriguingly, some of the endocytosed HIV-1 virions are constitutively released into the extracellular milieu associated with exosomes, allowing delivery of infectious virus to target CD4⁺ T cells.

Overall, *cis* and *trans*-infection mediated by infected or uninfected DCs via virological synapses, infectious synapses or the release of exosomes are likely to contribute to the *in vivo* transfer of HIV from DCs to CD4⁺ T cells. However, clear evidence for any of these described modes of viral transmission from DCs to CD4⁺ T cells *in vivo* is still lacking. Recent experiments performed *ex vivo* in tissue culture models show that HIV concentrates along the adherent junction between emigrant Langerhans cells and CD4⁺ T cells conjugates from the human vaginal epithelium, supporting the formation of an infectious synapse (94, 95). Remarkably, individual Langerhans cells were heavily loaded with virions when viewed two hours after challenge by electron microscopy, but productive HIV-1 infection in these vaginal cells was not detected. Even if viral production occurred but was not detected, it must have been relatively inefficient in comparison to the great capacity of Langerhans cells to endocytose HIV-1 (95). These results favor a model in which viral transmission can occur efficiently in the absence of viral replication (138, 240, 243).

2.5 Role of DC maturation in HIV-1 transmission

Mature DCs are potent stimulators of naïve T cells concentrated in the secondary lymph nodes. Therefore, their preferential location at the key sites of viral replication and their continuous interaction with the HIV-1 main target cells renders mature DCs as one of the most compelling potential candidates to promote viral dissemination *in vivo*. However, the relevance of mature DC mediated *trans*-infection during acute and chronic phases of HIV-1 infection has not yet been evaluated, since most attention has been focused on early events of HIV infection and the role of immature DCs, as previously commented. Nevertheless, immune synapses established by mature DCs presenting HIV antigens to HIV specific CD4⁺ T cells can activate the proliferation of these cells within the T cell areas of the lymph nodes, thereby enhancing T cell susceptibility to viral infection. In this scenario, mature DCs would capture HIV and transmit the virus to HIV specific CD4⁺ T cells that would in turn become infected in *trans*, a process that could explain why HIV preferentially infects these specific CD4⁺ T cells (54).

Depending on the activating signals that immature DCs receive, they can develop into different subsets of mature DCs with differing capabilities of HIV-1 transmission. Immature DCs cultured with the CD40 ligand, interferon- γ (IFN γ), lipopolysaccharide (LPS) or polyinosinic–polycytidylic acid (polyI:C) have greater *trans*-infection capacity than immature DCs or DCs matured in the presence of prostaglandin E₂, or other maturation factors, such as IL-1 β and tumor-necrosis factor (241). Interestingly, it was also shown that circulating LPS is significantly increased in chronically infected HIV⁺ individuals (26). These authors suggest that during acute HIV infection, CD4⁺ T cells of the mucosal gut are depleted, compromising the integrity of the mucosal barrier and leading to increased translocation of bacteria from the intestinal lumen.

Bacteria and bacterial components stimulate innate immune cells like DCs systemically, creating the proinflammatory milieu associated with chronic HIV infection (25). Indeed, in this study, the median plasma LPS level in patients with disease progression was 75 pg/ml, five times the amount required to stimulate the systemic immune activation in non-infected volunteers (211).

This hypothesis could explain why in subjects with HIV-1 viremia, blood DCs have increased expression levels for costimulatory molecules (the hallmark of maturation status) that only diminish when HAART suppresses the viral load (13). Interestingly, a recent report shows that activated CD34-derived Langerhans cells mediate the *trans*-infection of HIV (63), suggesting a potential role for these mature cells during the establishment of HIV infection, particularly enhanced when sexually transmitted diseases cause inflammation of the genital lining.

Mature DCs could also act as viral reservoirs and maintain HIV-1 infection *in vivo*. However, the half-life of these cells is thought to be shorter than other cellular reservoirs, like memory T cells or macrophages. Indeed, mature DCs are estimated to live two to three days (115, 185). However, a recent report in mice has shown that in the spleen or the lymph nodes, migrating DCs persisted over a ten to fourteen-day period, being replenished from blood-borne precursors at a rate of nearly 4,300 cells per hour (123). Interestingly, these cells underwent a limited number of divisions and daughter DCs presented antigens captured by their progenitors, suggesting that DC division in peripheral lymphoid organs can prolong the duration of antigen presentation *in vivo* (123), perhaps through exosome exchange.

In vitro, it is well documented that the efficiency of HIV-1 transmission through *trans*-infection can be increased by maturation of DCs (81, 138, 191). This observation has led to the suggestion that more efficient interactions

between mature DCs and CD4⁺ T cells could contribute to the enhanced efficiency of HIV-1 transmission, possibly due to stronger DC–T cell interactions, owing to an increase expression of ICAM-1 that favors binding to T cell-expressed LFA-1 (138, 191). However, the mechanism or mechanisms that underlie this augment in viral transmission have not yet been defined properly (241).

Finally, differences in the membrane's attachment factors binding HIV-1, viral capture, endocytosis, intracellular trafficking and the recycling of HIV-1 within the diverse subsets of mature DCs could also contribute to the variation in their ability to transmit the virus. However, none of these mechanisms have been accurately characterized yet, though they could have major implications for disease progression.

According to this scenario, we believe that extensive work to reveal the unknown mechanisms associated with viral transmission mediated by mature DCs is needed to provide new insights into AIDS pathogenesis. This knowledge could accelerate the development of new therapeutic targets and aid in selecting the safer candidates to use in a DC-based therapeutic vaccine.

2.


Hypothesis
& Objectives.


Mature DCs have higher ability than immature DCs to transmit the virus to target T cells. Furthermore, mature DCs continuously interact with CD4⁺ T cells at the lymph nodes, the key site of viral replication during HIV pathogenesis.


Given the unique capability of mature DCs to enhance HIV-1 infection, we hypothesize that these cells could augment viral dissemination in the lymphoid tissue and contribute to disease progression *in vivo*. Therefore, elucidating the mechanisms underlying mature DC-enhanced HIV-1 transmission could be crucial for the design of effective therapeutic strategies aimed at blocking viral spread.


The **specific objectives** pursued in this thesis are outlined on the following page, and will be extensively presented in the next chapters.


Specific Aims:

 1. To compare the process of binding, endocytosis, intracellular trafficking and cell membrane recycling of HIV-1 in mature and immature DCs.

 2. To evaluate the role of DC-SIGN during viral capture, developing an *in vitro* assay to specifically assess the contribution of distinct DC-SIGN polymorphic variants during the *trans*-infection process.

 3. To explore the molecular determinant or determinants expressed on the membrane of mature DCs, responsible for the capture of HIV-1.

 4. To characterize the intracellular trafficking of the virus in mature DCs.

 5. To visualize and study the mechanisms of infectious synapse involved in the HIV-1 transmission from mature DCs to CD4⁺ T cells.

3.

Material & Methods

I. Cell culture

1. Primary cells

To obtain monocytes, heparin-treated venous blood from HIV-1-seronegative donors was diluted 1:2 (vol:vol) in phosphate buffer saline (PBS) and centrifuged for 15 minutes at 900 r.p.m., with the brake on during deceleration to easily discard the top phase containing the plasma and platelets. The blood was then diluted again in PBS and centrifuged for a second time as described above. Immediately after discarding the top phase, the blood was incubated for 20 minutes at room temperature with RosseteSep CD3 Depletion kit (Stem-Cell), adding 300 μ l anti-CD3-anti-glycophorin per 25 ml. The blood was then diluted 1:2 (vol:vol) in PBS and layered in a Ficoll-Hypaque density gradient. Peripheral blood mononuclear cells (PBMCs) lacking CD3⁺ cells were recovered after centrifugation for 30 minutes at 1,850 r.p.m. After washing three times with PBS, cells were counted with Perfectcount beads (Cytognos) using flow cytometry (Fig. 18). Isolation of highly purified monocyte populations was done with CD14 positive selection magnetic beads (Miltenyi Biotec) following the manufacturer's instructions. Monocytes were counted

with Perfectcount beads, and purity (>97% CD14⁺) was assessed by flow cytometry labeling CD14⁺ cells and analyzing forward and side-scatter parameters.

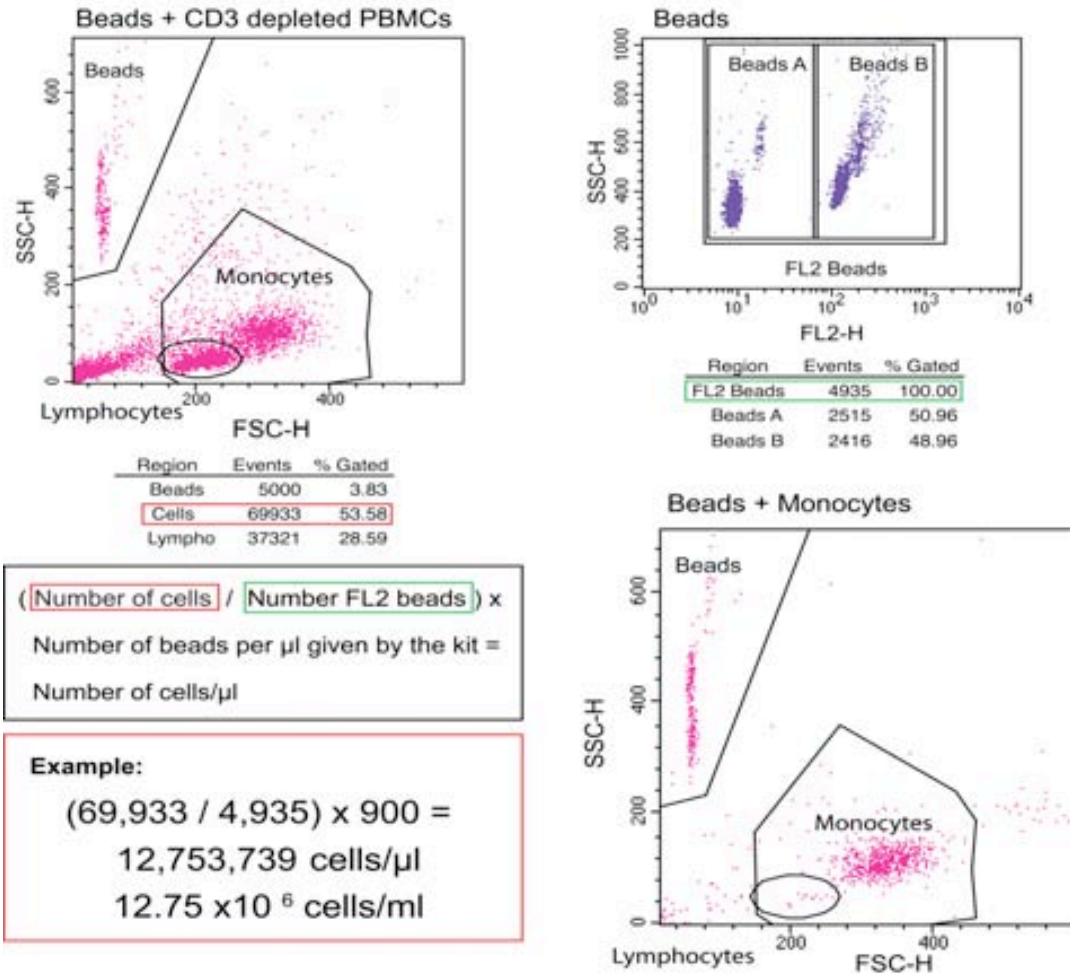
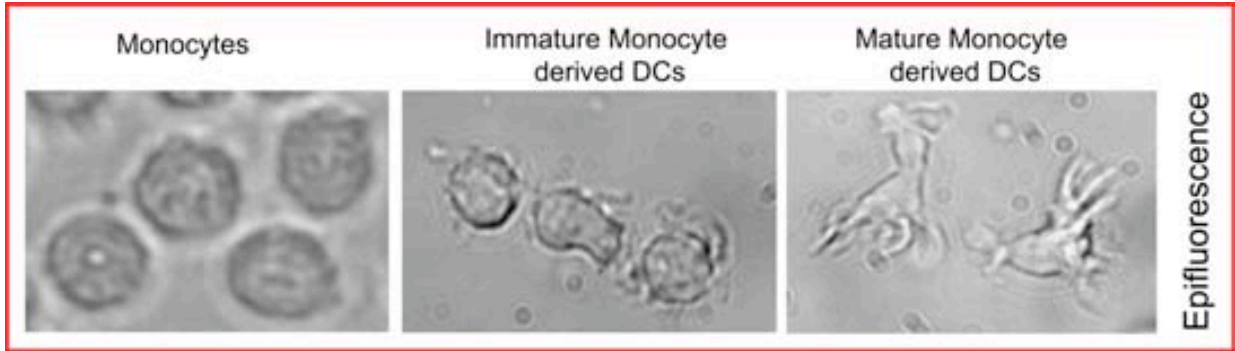


Figure 18. Cell count and monocyte isolation. Top dot plots are representative samples with Perfectcount beads and CD3 depleted PBMCs. The number of cells (highlighted in red) and the number of FL2-H fluorescent beads (highlighted in green) are indicated. The percentage of A and B Perfectcount beads (differentiated by their distinct fluorescent intensity) is also indicated because these parameters serve as an internal control to verify that the final number of beads per μl added to our sample is equal to the concentration specified in the kit. The formula employed to calculate absolute cell numbers is also shown in the marked box. The dot plot at the bottom shows a representative example of Perfectcount beads mixed with isolated monocytes.

The addition of 1,000 U/ml of granulocyte-macrophage colony-stimulating factor (GM-CSF) and 1,000 U/ml interleukin-4 (IL-4) – both from R&D – to 8×10^5 cells/ml cultured in RPMI containing 10% fetal bovine serum (FBS) from Invitrogen, differentiated monocytes into immature monocyte derived DCs (iDCs) after seven days. Culture medium containing IL-4 and GM-CSF was replaced every two to three days. DC maturation was achieved by culturing iDCs at day 5 for two more days in the presence of 100 ng/ml of lipopolysaccharides (LPS; Sigma). LPS treatment generated clustered cultures with mature monocyte derived DCs (mDCs) presenting more abundant and longer dendrites than in iDCs cultures (Fig. 19). Interestingly, the vertical culture of monocytes in T25 flasks (BD) yielded higher numbers of DCs in suspension after seven days of culture than the other systems tested. When we talked pleasantly to the cells (for instance, by wishing them good luck), DC recovery was routinely higher than 60% of the monocytes seeded.

Myeloid DCs were isolated from the PBMCs fraction of the HIV-1-seronegative donors by employing the CD1c⁺ (BDCA-1) isolation kit (Miltenyi Biotec) right after the depletion of CD3⁺ cells with the RosseteSep CD3 depletion kit. Enriched populations of Myeloid DCs were cultured at a final concentration of 8×10^5 cells/ml for two days in the presence of 20 U/ml of GM-CSF. After isolation, we obtained an average of 92% CD11c⁺ cells with traces of CD3⁺ cells (< 1%), where the main contaminants were monocytes and B lymphocytes (< 7%). However, plastic adherence after two days of culture in the presence of GM-CSF reduced the presence of CD14⁺ monocytes in suspension to 3% of the cells. Furthermore, when DCs and blood Myeloid DCs were obtained from the same donor, CD14⁺ cells were removed before BDCA-1 purification, resulting in reduced levels of contaminant CD14⁺ cells.

Mature Myeloid DCs were obtained by adding 100 ng/ml of LPS in parallel during those two days of culture.



64

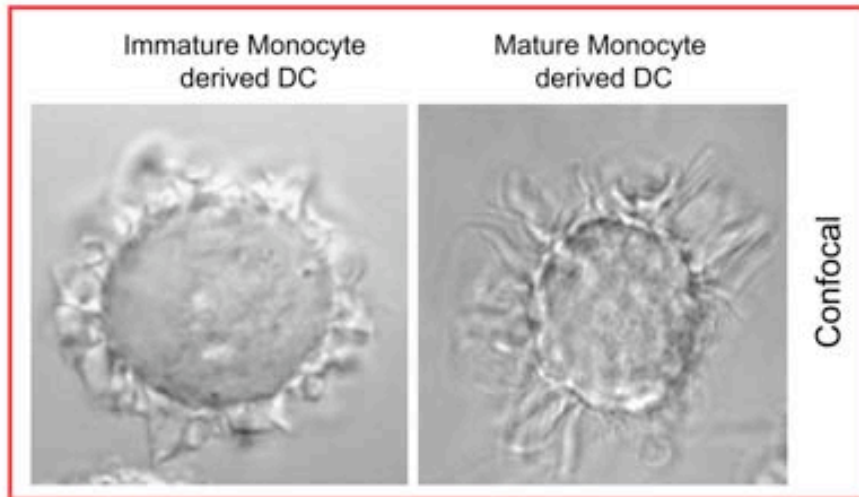


Figure 19. Comparative morphology of monocytes, iDCs and mDCs seen by epifluorescent microscopy. Rounded monocytes differentiate into iDCs that present dendrites or prolonged projections of the membrane. Maturation increases the length of dendrites, as can be seen by confocal microscopy.

2. Cell lines

Cells were kept at 37°C in 5% CO₂ incubators. All the cell lines were split three times a week until passage number 40. Cell lines were routinely tested for Mycoplasma using the Mycoalert™ detection assay (Lonza). All media contained 100 U/ml of penicillin, 10 µg/ml of streptomycin and 10% FBS (all from Invitrogen).

The cell lines employed during this thesis are characterized in Table 1.

| Cell type | Origin | Description | Media | Selection |
|---------------------------|--|--|-------|---|
| Raji ¹ | Human B cells | CD19 ⁺ | RPMI | None |
| Raji DC-SIGN ¹ | Human B cells | Raji cells stably transfected with DC-SIGN | RPMI | Geneticin, 1 mg/ml |
| Hut CXCR4 ² | Human T cells | CD4 ⁺ CXCR4 ⁺ | RPMI | None |
| Hut CCR5 ³ | Human T cells | Hut CXCR4 ⁺ stably transfected with CCR5 | RPMI | Geneticin, 300 µg/ml Puromycin, 1 µg/ml |
| Jurkat ² | Human T cells | CD4 ⁺ CXCR4 ⁺ | RPMI | None |
| MOLT NL43 ⁴ | Human T cells | Chronically infected with HIV _{NL43} provirus | RPMI | None |
| MT4 ² | Human T cells | CD4 ⁺ CXCR4 ⁺ | RPMI | None |
| GHOST P4R5 ² | Human HOS cell line derived from an osteosarcoma | Stably transfected with CD4, CXCR4, CCR5. Indicator: Contains an HIV-2 LTR linked to a green fluorescent protein (GFP) gene. | DMEM | Geneticin, 500 µg/ml Hygromycin, 100 µg/ml Puromycin, 1 µg/ml |
| HEK -293T ² | Human embryonic kidney cells | CD4 ⁻ CXCR4 ⁻ | DMEM | None |
| K562 DC-SIGN ⁵ | Human Monocytic cells | Stably transfected with DC-SIGN | RPMI | Geneticin, 300 µg/ml |
| TZM-bl ² | JC53-bl HeLa cell line (clone 13) | Stably transfected with CD4, CXCR4, CCR5. Indicator: Luciferase and β-galactosidase genes linked to the HIV-1 promoter. | DMEM | None |

Table 1. Cell lines. ¹ Kindly provided by Dr. Van-Kooyke; ² obtained through NIH AIDS Research and Reference Reagent Program, ³ kindly provided by Dr. KewalRamani, ⁴ characterized in the Fundació irsiCaixa by Dr. J. Blanco and ⁵ kindly provided by Dr. Corbi.

II. Immunophenotype

Monocytes were immunophenotyped immediately after isolation, while Myeloid DCs and DCs were stained at day 2 and at day 7 respectively. All cells were previously blocked with 1 mg/ml of human IgG (Baxter, Hyland Immuno) to prevent binding to Fc receptors through the Fc portion of the antibody. Rainbow calibration particles (BD) were used before labeling the cells to ensure the consistency of fluorescence intensity measurements throughout the experiments. All cells were stained at 4°C (to avoid antibody internalization) for 20 minutes, washed and resuspended in PBS containing 2% formaldehyde.

66
Samples were analyzed in a FACSCalibur flow cytometer (BD) using CellQuest software to evaluate the data collected. Forward-scatter and side-scatter light gating were used to exclude dead cells and debris from the analysis. Cells were stained using the previously titrated monoclonal antibodies (mAbs), listed in Table 2, using their matched isotype controls.

The basic immunophenotype of monocytes was evaluated before further culture (Fig. 20). Adequate differentiation from monocytes to iDCs was based on the loss of CD14 and the acquisition of DC-SIGN, while maturation upregulated the expression of CD83, CD86 and HLA-DR in DCs and Myeloid DCs (Fig. 20). The Raji B lymphoid cell line transfected with DC-SIGN (used as a control in several experiments) showed a similar surface marker pattern as mDCs, but lacked CD4 expression and displayed less CD86 (Fig. 20).

| Fluorophore | Antibody | Cell type identified | Brand |
|---|----------|----------------------------------|------------|
| FITC (Fluorescein isothiocyanate) | CD14 | Monocytes | Pharmingen |
| | CD11c | Blood Myeloid DCs | Serotec |
| | CD86 | Mature DCs | Pharmingen |
| PE (Phycoerythrin) | CD19 | B Lymphocytes | BD |
| | CD83 | Mature DCs | Pharmingen |
| | DC-SIGN | DCs | R&D |
| PerCP (Peridinin chlorophyll protein) | CD3 | T Lymphocytes | BD |
| | CD4 | T Lymphocytes; Monocytes; DCs | BD |
| | HLA-DR | Mature DCs | BD |

Table 2. Monoclonal antibodies (mAb) employed to phenotype membrane surface of monocytes, DCs, blood Myeloid DCs and cell lines.

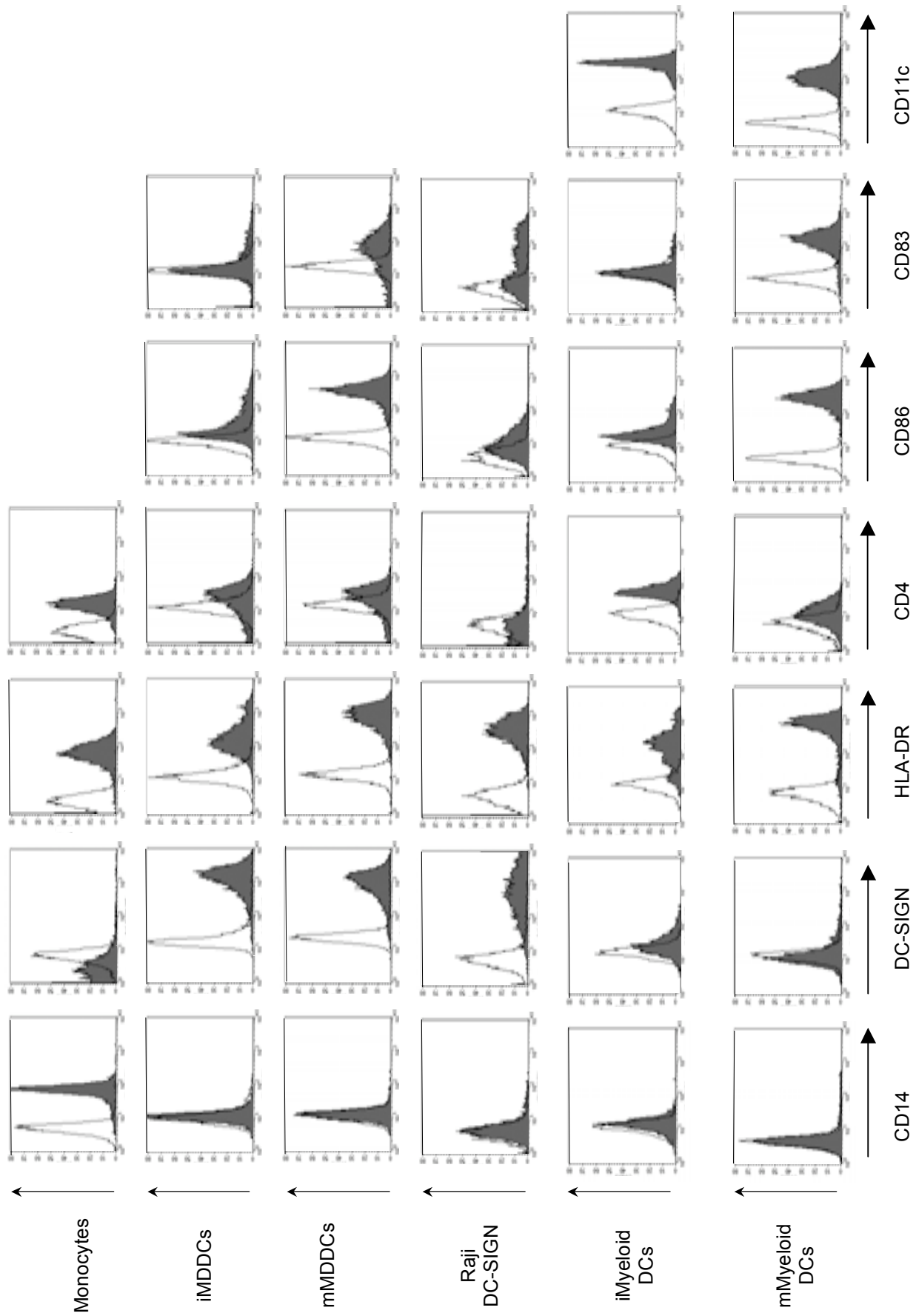


Figure 20. Expression of the cell surface markers CD14, DC-SIGN, HLA-DR, CD4, CD86, CD83 and CD11c in different cell types. Isotype-matched mouse IgG controls are also indicated (empty histograms).

1. DC-SIGN quantification

Quantibrite kit (BD) was routinely employed to obtain the mean number of DC-SIGN antibody binding sites (ABS) per cell.

The kit was used according to the manufacturer's instructions. However, to ensure the consistency of fluorescence intensity measurements throughout the experiments, Rainbow calibration particles (BD) were employed before each quantitation (Fig. 21).

The mean number of PE-labeled DC-SIGN ABS per cell (antibody-to-PE ratio of 1:1; R&D) was quantified by regressing the geometrical mean fluorescence intensity obtained in each sample to a standard linear regression curve built with four different precalibrated beads conjugated with fixed numbers of PE molecules per bead.

Geometrical mean fluorescence-obtained labeling with goat anti-mouse immunoglobulin G2b (IgG2b) PE was used as an isotype control (BD), and the ABS-per-cell values obtained were subtracted from the values of corresponding samples. Figure 21 summarizes this process.

All cells were previously blocked with 1 mg/ml of human IgG to prevent binding to Fc receptors through the Fc portion of the antibody. Cells were stained at 4°C for 20 minutes, washed and resuspended in PBS containing 2% formaldehyde. Samples were analyzed in a FACSCalibur flow cytometer (BD) using CellQuest software and the QuantiQuest function to evaluate the data collected.

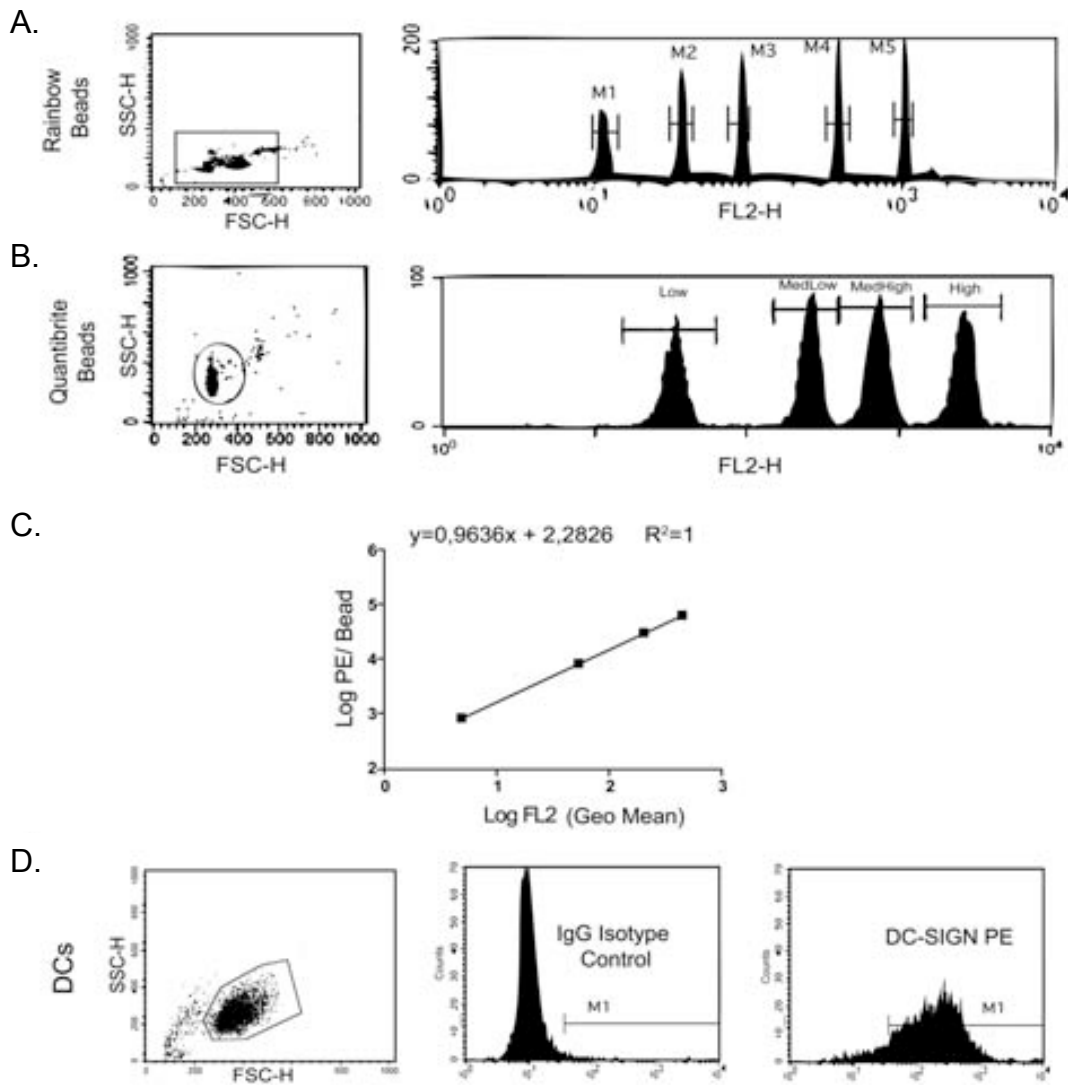


Figure 21. Diagram of the procedure followed to quantify DC-SIGN ABS. **(A)** Top dot plot and histogram show Rainbow beads forward-scatter and side-scatter parameters and the peaks of fluorescence in FL2. These beads were routinely employed to calibrate the cytometer laser. **(B)** The middle dot plot and histogram show Quantibrite beads morphology and fluorescence in FL2, corresponding to the four different precalibrated beads conjugated with fixed numbers of PE molecules. **(C)** These beads were employed to construct the regression line shown in the graph. **(D)** The bottom plots show mDCs forward and side-scatter, the fluorescence of the isotype control and the anti-DC-SIGN mAb labeling. Geometric mean fluorescence intensities obtained this way were extrapolated to the regression curve shown in the graph to obtain the mean number of DC-SIGN ABS per cell. Notably, the settings (detectors and amps) were kept constant throughout all the acquisitions of Rainbow beads, Quantibrite beads and the cells of interest.

III. Plasmids

Infectious single-round *pseudotyped* HIV-1 stocks ($\text{HIV}_{\text{JRFL/NL4-3-Luc}}$) were generated by cotransfecting the envelope-deficient proviral vector pNL4-3.Luc.R-E- containing the firefly luciferase reporter gene (obtained through the NIH AIDS Research and Reference Reagent Program from Dr. N. Landau) with the plasmid pJRFL expressing the envelope glycoprotein of the CCR5-tropic strain HIV-1_{JRFL} (kindly provided by Dr. V.N. KewalRamani). This process is depicted in Figure 22, where the single-round infectious assay is represented. The proviral constructs $\text{HIV}_{\Delta\text{env-NL4-3}}$ and $\text{HIV}_{\Delta\text{env-Bru}}$ (both lacking the envelope glycoprotein) were generated by transfecting the vector pNL4-3.Luc.R-E- alone or the proviral construct pBru engineered not to express the envelope gene (from Dr. S. Gummurulu).

Full-length replication-competent $\text{HIV}_{\text{NFN-SX}}$, $\text{HIV}_{\text{NL4-3}}$ and HIV_{Lai} were obtained by transfecting the proviral construct pNFN-SX (154), an HIV-1-NL4-3 provirus that expresses the HIV-1-JRFL envelope glycoprotein (kindly provided by Dr. W. O'Brien), the proviral construct pNL4-3 and the proviral construct pLai. $\text{HIV}_{\text{NL4-3/vpr-eGFP}}$ virus was generated by cotransfecting the vector pNL4-3 with a plasmid containing the vpr viral protein fused to eGFP, as previously described (247).

Viral-like particles $\text{VLP}_{\text{HIV-Gag-eGFP}}$ were generated by transfecting the molecular clone pGag-eGFP, obtained through the NIH AIDS Research and Reference Reagent Program, from Dr. Marilyn D. Resh (92, 122, 165, 196). The plasmid pHIV-Gag-Cherry was constructed by substituting the eGFP sequence for mCherry (derived from pmCherry-N1; Invitrogen) by swapping a BamHI-XbaI fragment. $\text{VLP}_{\text{MLV-Gag}}$ were produced by transfecting the molecular clone

pCL-Eco (ImGenex) that expresses all of the ecotropic murine leukemia virus (MLV) structural genes.

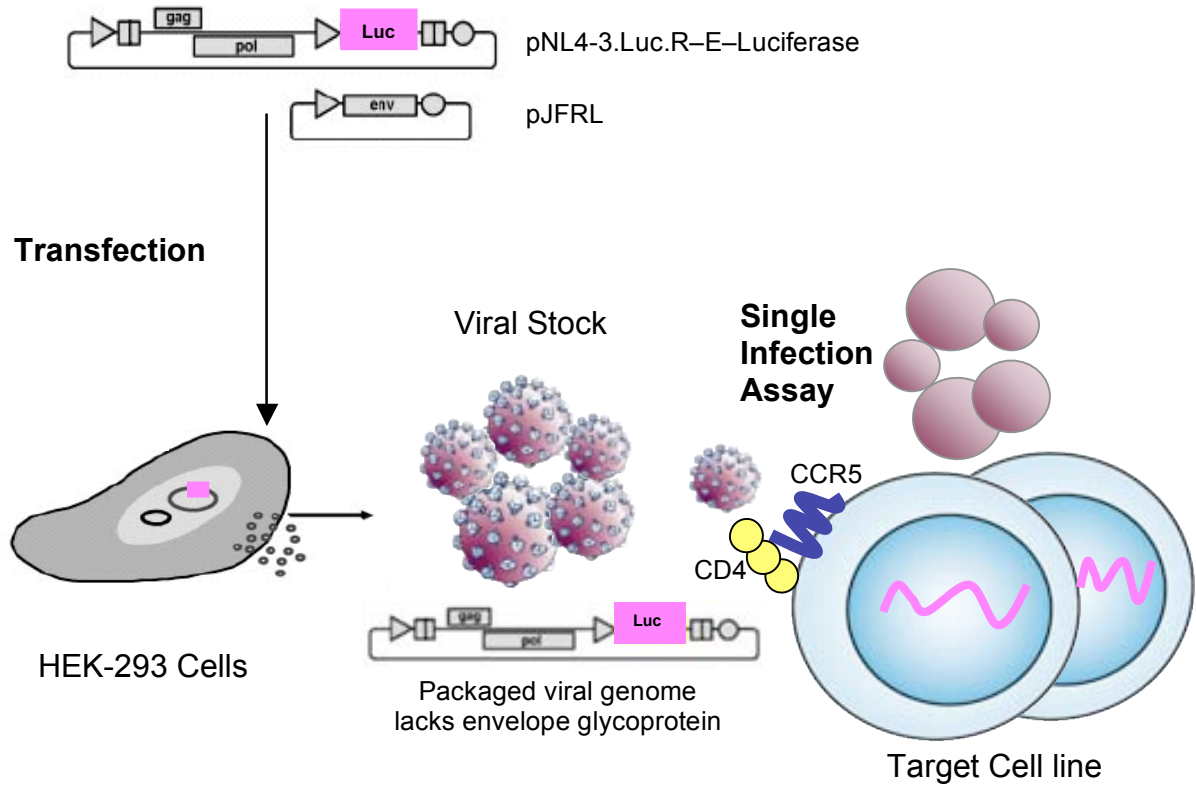


Figure 22. Schematic representation of single infection viral assay. An HIV-1 plasmid lacking the envelope glycoprotein and a construct containing it are cotransfected in HEK-293T cells. The viral stock produced has a viral genome lacking the envelope gene but bearing the intact envelope glycoprotein in the viral membrane. Once this stock infects the target cells, the viral genome integrated expresses the luciferase reporter gene that can be detected by luminometric techniques. These infected target cells produce viral particles that lack the envelope glycoprotein in their membrane and are therefore not able to infect new target cells.

IV. Transfections and viral stocks

All the previously described plasmids were used to transfect HEK-293T producer cells and obtain the different viral stocks. Briefly, HEK-293T cells were transfected with calcium phosphate (CalPhos, BD) in T75 flasks using up to 20–30 μg plasmid DNA. Viral stocks were also generated after HIV_{NL4-3} infection of phytohaemagglutinin (PHA) stimulated PBMCs or HIV_{NL4-3} electroporation of MT4. Supernatants containing virus and VLPs were filtered (Millex HV, 0.45 μm , Millipore) and frozen at -80°C until use.

To determine the p24^{Gag} content of viral stocks, an enzyme-linked immunosorbent assay (ELISA) was used (Alliance HIV-1 p24 antigen ELISA kit, Perkin-Elmer). Generally, viral stocks contained 1 to 2 μg of p24^{Gag} per ml. The p24^{Gag} content of VLP_{HIV-Gag-eGFP} stocks was measured with a sandwich p24^{Gag} ELISA using the anti-p24^{Gag} monoclonal antibody 183-H12-5C (AIDS Research and Reference Reagent Program) and HIV Ig (AIDS Research and Reference Reagent Program), as described previously (235).

HEK-293T cell derived VLP_{MLV-Gag} containing supernatants were tested for the presence of reverse transcriptase activity as described in (78). Briefly, 15 μl cell supernatant were incubated with 50 μl reverse transcriptase buffer (50 mM Tris pH 7.8, 75 mM KCl, 2 mM DTT, 5 mM MnCl₂, 0.05% NP40, 0.01 M EGTA, poly A-dT and [α -³²P]-TTP) for 90 minutes at 37°C. Ten μl of the reverse transcriptase reaction were spotted on DE81 cellulose paper, air-dried and washed five times with 1x SSC buffer and twice with 95% ethanol. The blots were exposed to autoradiography and the signals were quantified with a Phosphorimager (Molecular Dynamics).

To obtain the viral titers of HIV_{JRFL/NL4-3-Luc} used for *trans*-infection assays, we employed the Ghost CCR5⁺ indicator cell line containing an HIV-2

long terminal repeat linked to a GFP gene (146), resulting in a viral stock of 6.1 median 50% tissue culture infective doses/ml (TCID₅₀/ml).

The Indiana strain of the vesicular stomatitis virus (VSV) was grown on BHK cells according to established protocols (68). Briefly, cells at 70–80% confluence were infected with VSV (multiplicity of infection = 0.01). Twenty-four hours post-infection, the media was removed and centrifuged at 2,000 x g for five minutes to remove cell debris. Virions were then pelleted by high-speed centrifugation for one hour at 4°C (Sorvall Surespin rotor, 100,000 x g). Virus pellets were resuspended in 10 mM Tris pH 8.1. Aliquots of virus were checked for purity by SDS-PAGE and coomassie staining for viral proteins.

V. Virus binding and capture assays

Virus binding or attachment to the membrane's cell surface was assessed at 4°C to avoid endocytosis. Capture or endocytic assays were performed at 37°C. A total of 3 x 10⁵ Myeloid DCs, MDDCs, Raji DC-SIGN cells or Raji cells were incubated at 37°C for two hours with 80 ng of HIV_{NFN-SX} p24^{Gag} per 3 x 10⁵ cells at a final concentration of 1 x 10⁶ cells/ml, washed with PBS three times, and lysed with 0.5% Triton X-100 at a constant concentration of 5 x 10⁵ cells per ml. Lysates were cleared of cell debris by centrifugation (10,000 x g for five minutes) to measure p24^{Gag} antigen content by ELISA. Viral capture and the subsequent transfer to target cells were compared by pulsing MDDCs, Raji DC-SIGN cells and Raji cells at 37°C or 4°C for two hours with 300 ng HIV_{JRFL/NL4-3-Luc} p24^{Gag} per 3 x 10⁵ cells at a final concentration of 1 x 10⁶ cells/ml. Of note, we never observed in our experimental settings the maturation of DCs exposed to our viral stocks, as assessed by fluorescence-activated cell sorting (FACS) measuring CD86, CD83 and HLA-DR expression

levels. To further confirm these results, we used our highest viral input and increased the viral pulse to 48 hours to maximize the possible stimulation activity of our viral stocks (Fig. 23). A total of $0.3\text{--}0.5 \times 10^6$ iDCs and mDCs were exposed to 300 ng of HIV_{NFN-SX} and 20 μg of HIV plasmid DNA to compare them with non-pulsed cells.

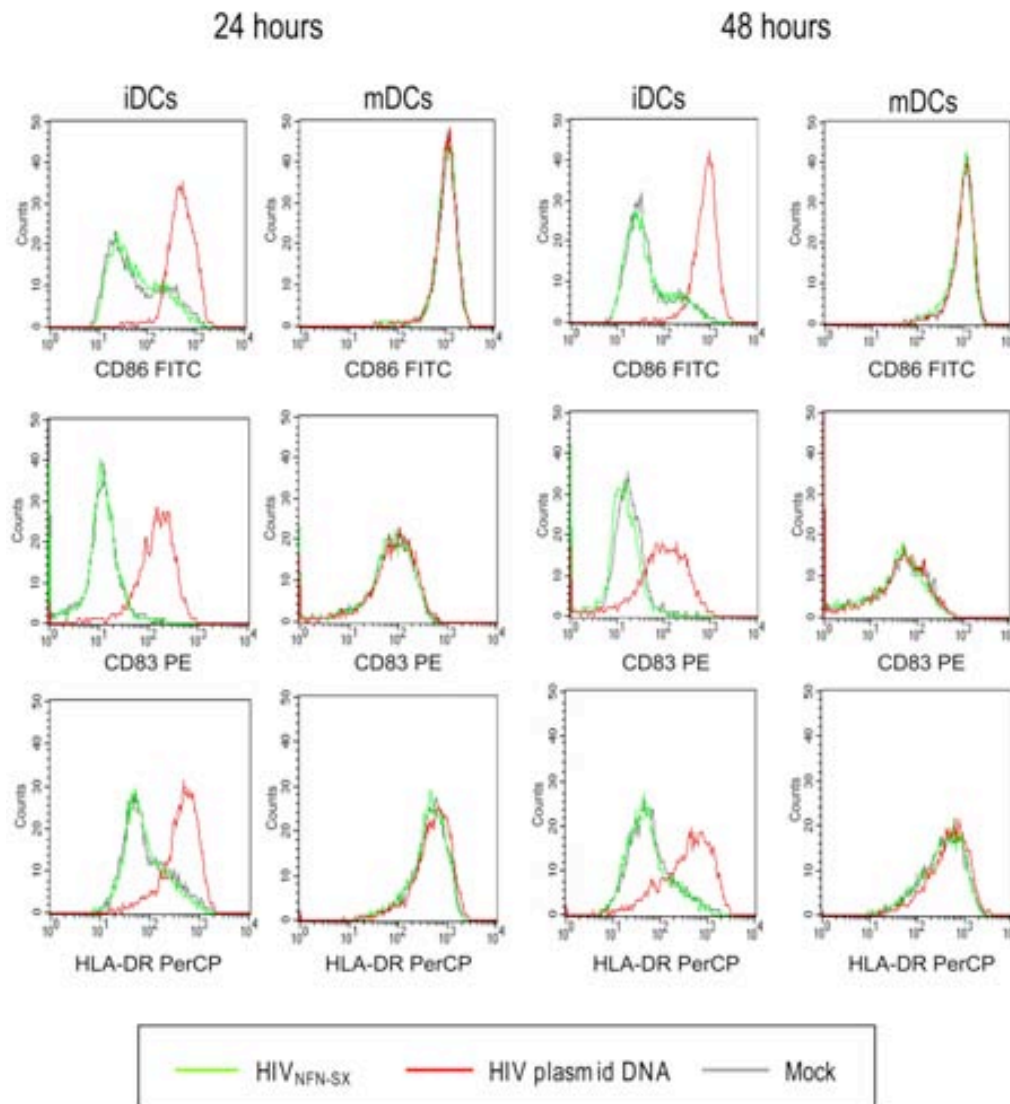


Figure 23. Lack of maturation of DCs exposed to viral stocks, assessed by FACS measuring CD86, CD83 and HLA-DR expression levels. Here, $0.3\text{--}0.5 \times 10^6$ iDCs and mDCs were exposed to 300 ng of HIV_{NFN-SX} p24^{Gag} and 20 μg of HIV plasmid DNA to compare them with non-pulsed cells. After 24 hours, the virus-exposed iDCs did not display any phenotypic changes, while the plasmid DNA did trigger their maturation. Identical results were obtained after 48 hours of viral and plasmid DNA exposition.

Virus-exposed iDCs did not display any phenotypic changes after 24 hours, while plasmid DNA did trigger their maturation. After 48 hours of viral pulsing, neither iDCs nor mDCs displayed phenotypic changes, excluding the presence of a latent maturation stimulus in the viral stocks, such as carryover plasmid DNA.

To potentially inhibit virus capture, cells were preincubated for 30 minutes at 4°C with mannan (500 µg/ml; Sigma) or the anti-DC-SIGN mAb MR-1 (kindly provided by Dr. A. Corbi) at saturating concentrations determined using Raji DC-SIGN. After preincubation, the cells were processed as described above.

To analyze the envelope glycoprotein requirement during viral capture, cells were pulsed with equal amounts of p24^{Gag} from HIV_{NFN-SX} and HIV_{Δenv-NL4.3}, as described above.

Kinetic analysis was performed by pulsing 2×10^6 to 4×10^6 DCs with 20 ng of p24^{Gag} per 5×10^5 cells at a final concentration of 2×10^6 cells/ml. To assess the viral capture time course, part of the cells was maintained in the presence of the virus at 37°C up to ten hours before they were lysed, right after an extensive wash. The remainder of the cells were used to monitor viral fate after capture: two hours after the pulse, free virus was washed out and the cells were kept in culture at 37°C for up to 48 hours before collecting the cell supernatants and lysing the cells at the indicated time points. HIV_{NL4.3/vpr-eGFP} was used to monitor viral capture with flow cytometry, pulsing 0.5×10^6 DCs with 150 ng of p24^{Gag} up to 12 hours before cell fixing. Analysis was performed on the living cell gate determined by forward and side-scatter light.

To analyze viral degradation pathways in iDCs and mDCs, cells were preincubated with 250 nM of bafilomycin A1 (an inhibitor of lysosomal degradation) or 10 µM of the proteasome inhibitor clasto-lactacystin-β-lactone

(both from Sigma) for 30 minutes at 37°C and then exposed to HIV_{NFN-SX} as previously described. After extensive washing, part of the cells were lysed and analyzed for p24^{Gag}. The rest of the cells were left for four more hours at 37°C in the presence of these blocking agents and in the absence of virus, before being lysed. Degradation was measured by subtracting cell-associated p24^{Gag} values obtained two hours immediately after the viral pulse from cell-associated p24^{Gag} values obtained four hours later. The percentage of degradation was calculated relative to the viral decay of p24^{Gag} values of untreated cells over four hours, normalized to 100%.

VI. Viral transmission assays

To characterize the viral transmission efficiencies of different DCs, immature and mature cells from the same seronegative donors were pulsed with HIV_{JRFL/NL4-3-Luc} as described in (240), with some modifications. Briefly, 3×10^5 to 5×10^5 DCs, Raji DC-SIGN cells and Raji B cells were counted with Perfectcount cytometer beads, pulsed with 180 to 300 ng of HIV_{JRFL/NL4-3-Luc} p24^{Gag} for three hours at 37°C or 4°C, washed five times with PBS and counted again with beads on the flow cytometer to ensure viability. In experiments done with Myeloid DCs, 2×10^5 cells were pulsed with 120 ng of HIV_{JRFL/NL4-3-Luc} p24^{Gag} for three hours at 37°C.

All pulsed cells were co-cultured in duplicate with the target Hut CCR5⁺ cell line at a ratio of 1:1 (up to 1×10^5 cells per well in a 96-well plate) in the presence of 10 µg/ml of polybrene (Sigma). Cells were assayed for luciferase activity 48 hours later (BrightGLO luciferase system; Promega) in a Fluoroskan Ascent FL luminometer. Notably, recombinant luciferase protein (Promega) was used each time to build a standard curve of seven logarithms to guarantee

the linearity of the relative light units (RLUs) obtained and the luminometer performance throughout the experiments.

It is worth mentioning that we also tested the monocytic cell line K562 as a control for DC-SIGN viral transmission efficiency while looking for a suitable DC-SIGN transfected cell line to use in our experiments. Despite the fact that this cell line had more than double the DC-SIGN ABS per cell of the Raji DC-SIGN cell line, viral transmission capacity was much lower in this monocytic cell line (Fig. 24).

To detect possible productive infection of pulsed DCs, the CCR5⁺ target cells in the co-cultures were substituted with CCR5⁻ target cells in all the experiments.

78

To potentially inhibit virus transfer, cells were preincubated for 30 minutes at 4°C with mannan (500 µg/ml; Sigma) or the anti-DC-SIGN mAb MR-1 and then processed as described above.

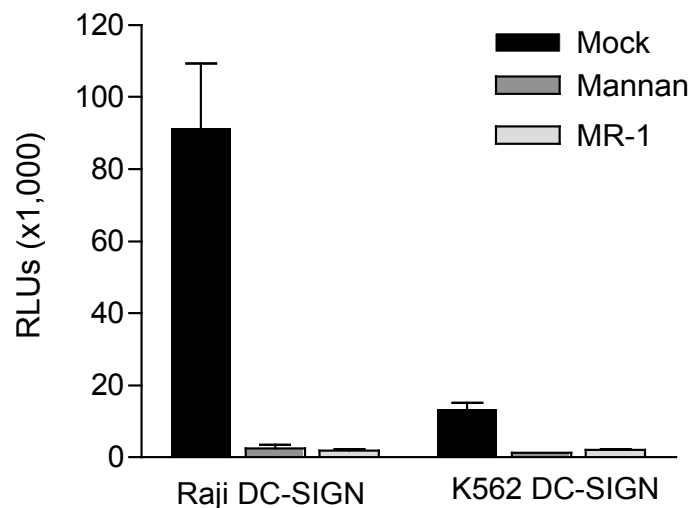


Figure 24. Raji DC-SIGN and K562 DC-SIGN transfer of HIV_{JRFL/NL4-3-Luc} to Hut CCR5⁺ target cells. Cells were preincubated with mannan and an anti-DC-SIGN mAb to verify DC-SIGN specific viral transfer. Co-cultures were assayed for luciferase activity 48 hours after viral pulse, measuring relative light units (RLUs).

VII. Exosome generation

Jurkat T cells were cultured in AIM-V serum-free medium (Invitrogen), free of contaminating vesicles and protein aggregates. Cells were labeled with Vybrant™ DiI cell-labeling solution (Molecular Probes) following the manufacturer's instructions. Supernatants were collected 24–48 hours after labeling. Exosome purification was performed as previously described (114) by three successive centrifugations at 300 x g (5 minutes), 1,200 x g (20 minutes) and 10,000 x g (30 minutes) to pellet cells and debris, followed by centrifugation of the resulting supernatants for one hour at 100,000 x g.

Western blot revealed that exosomes were positive for CD81, CD63 and flotillin (M.C. Puertas, unpublished results), as previously reported by (23).

To quantify exosome stocks for protein content, a Bradford Protein Assay kit (BioRad) was employed. To measure Exosome DiI fluorescence (545 nm of excitation and 565 nm of emission), a Fluoroskan Ascent FL fluorimeter was used. Notably, the DiI marker was used each time to build a standard curve to guarantee the linearity of the relative fluorescent units obtained and the fluorimeter performance throughout the experiments. Exosome pulse was performed with equal concentrations of exosomal proteins displaying equivalent fluorescence intensities.

VIII. VLP and exosome capture assays

A total of 1×10^5 mDCs and iDCs were incubated at 37°C for four hours with 2,500 pg of VLP_{HIV-Gag-eGFP} p24^{Gag} in a final volume of 0.1 ml. Exosome capture was performed the same way, by pulsing 1×10^5 DCs with

preparations at a final concentration of 150 µg of protein in 0.1 ml of Exosomes_{DII}. Positive DCs were analyzed by flow cytometry.

Competition experiments were performed by pre-incubating 1×10^5 mDCs at a final concentration of 1×10^6 cells/ml for 30 minutes with increasing amounts of Exosomes_{DII}, HIV_{Δenv-Bru}, VLP_{MLV-Gag}, and VSV particles previously treated with 400 µg/ml of the protease cocktail Pronase (Roche) to avoid viral fusion. The effectiveness of VSV-Pronase treatment was confirmed by infectious assays as detailed in the ‘Confirmation of Pronase activity’ section, below.

Alternatively, 200 ng of p24^{Gag} from HIV_{NL4-3} viral stocks produced in MOLT 4, MT4 and PHA stimulated PBMCs were preincubated with 1×10^5 mDCs at a final concentration of 1×10^6 cells/ml for 30 minutes. All mDCs were then pulsed with 2,500 pg of VLP_{HIV-Gag-eGFP} p24^{Gag} for one hour, washed with PBS and fixed to analyze the percentage of eGFP⁺ cells by FACS. Kinetic analysis of exosome capture was assessed by pulsing 2×10^5 mDCs with 150 µg or 75 µg of Exosomes_{DII} in a final volume of 0.1 ml. Cells were maintained at 37°C and aliquots were periodically harvested over a period of eight hours before being fixed and exosome capture being analyzed by FACS. Kinetic analysis of VLP_{HIV-Gag-eGFP} capture was assessed in a similar way, by pulsing cells with 2,500 pg of VLP_{HIV-Gag-eGFP} p24^{Gag} per 1×10^5 cells at a final volume of 0.1 ml. The fate of captured VLP_{HIV-Gag-eGFP} was determined by pulsing 0.5×10^6 mDCs with 12,500 pg of p24^{Gag} for two hours. Cells were extensively washed and kept in culture at 37°C for up to 48 hours before fixing the cells and analyzing the mDCs’ VLP retention capacity by FACS.

IX. Carboxylated beads assays

The yellow-green Carboxylated-Modified FluoSpheres® (Molecular Probes) of 0.1 μm diameter were sonicated before each use, and the homogenized suspension was briefly centrifuged at high speed to further remove aggregates. A total of 5×10^5 iDCs and mDCs were incubated at 4°C and 37°C for two hours with approximately 1.8×10^{10} beads at a final concentration of 2×10^6 cells/ml. Pulsed DCs were washed with PBS and fixed with 2% formaldehyde to analyze them by FACS.

The competition of carboxylated bead and HIV _{$\Delta\text{env-NL4-3}$} binding to mDCs was measured by preincubating 5×10^5 mDCs for 30 minutes with increasing numbers of beads, and then pulsing the cells additionally for one hour at 37°C with 130 ng of HIV _{$\Delta\text{env-NL4-3}$} p24^{Gag} in a final volume of 0.5 ml. Cells were washed extensively with PBS and each sample was divided in half. One half of the sample was fixed and analyzed by flow cytometry for carboxylated bead capture. The other half was lysed with 0.5% Triton X-100 (at a final concentration of 5×10^5 cells per ml), cleared of cell debris by centrifugation (10,000 x g for 5 minutes) and assayed for p24^{Gag} antigen content by an ELISA.

X. Capture and transmission followed by microscopy

1. Electron microscopy

Monocytes were negatively selected from PBMCs (Miltenyi Biotec) to avoid magnetic bead interference during electron microscopy observation. Subsequent differentiation to iDCs and mDCs was performed as stated above.

DCs were pulsed for 30 minutes or 24 hours with 200 ng of HIV_{JRFL/NL4-3-Luc} p24^{Gag} per 5 x 10⁵ cells. Alternatively, mDCs were pulsed for 12 hours with 150 ng of HIV_{NL4-3} p24^{Gag}, 12,500 pg of VLP_{HIV-Gag-eGFP} p24^{Gag} or 3 mg of Exosomes_{Dil} protein per 5 x 10⁵ cells. To perform co-localization analysis, mDCs were simultaneously pulsed for 12 hours with 150 ng of HIV_{NL4-3} p24^{Gag} and 3 mg of Exosomes_{Dil} per 5 x 10⁵ cells.

After extensive washes in PBS, all samples were fixed in 2.5% glutaraldehyde for one hour. The cells were processed as described elsewhere (24) for analysis of ultrathin sections using a Jeol JEM 1010 electron microscope. To monitor HIV_{JRFL/NL4-3-Luc} viral transmission, extensively washed DCs pulsed for 24 hours were co-cultured for an extra hour with Hut CCR5⁺ cells at a 1:1 ratio before being fixed.

2. Confocal microscopy and co-localization analysis

DCs and Myeloid DCs were pulsed with 50 ng of HIV_{NL4-3/vpr-eGFP} p24^{Gag} for three hours, washed with PBS, stained with DAPI (4,6-diamidino-2-phenylindole) from Sigma, fixed with 2% formaldehyde and cytospun onto glass slides.

Co-localization of particles with cellular markers was done by pulsing mature Myeloid DCs with equal amounts of HIV_{NFN-SX} and HIV_{Δenv-NL4-3} for four hours as described above. Cells were then fixed, permeabilized (Caltag), and stained with p24^{Gag}-RD1 mAb (Beckman Coulter), DAPI, and either CD81, CD63 or LAMP-1 (all conjugated with FITC; BD). Alternatively, mDCs were pulsed with VLP_{HIV-Gag-Cherry} and Exosomes_{Dil} in parallel for six hours as described in the capture assays section. Cells were then fixed, permeabilized and stained with DAPI, and CD81 or LAMP-1.

Co-localization among particles was done by pulsing mDCs simultaneously with VLP_{HIV-Gag-eGFP} and Exosomes_{Dil}, or with HIV_{NL4-3/vpr-eGFP} and Exosomes_{Dil} for six hours as described in the capture assays section.

The exosome transmission capacity of mDCs was assessed by confocal microscopy, analyzing DAPI labeled mDCs previously pulsed with Exosomes_{Dil} extensively washed and then co-cultured for four hours with Jurkat T cells labeled with the green-fluorescent cell tracker CMFDA (Molecular Probes).

All the samples were cytopun onto glass slides, mounted in Dako fluorescent medium and sealed with nail polish to be analyzed using a confocal microscope (Laser Optic Leica TCS SP2 AOBS). Alternatively, single sections were acquired with an Olympus FV1000 confocal microscope. Quantification of the co-localization was performed using the FV10-ASW 1.7 software (Olympus), analyzing 35 vesicles in mDCs from three different donors. The co-localization signals in percentages of the vesicle's area, and the Manders and Pearson coefficients (133) were calculated for each image. To obtain three-dimensional reconstructions, confocal Z stacks were acquired for some vesicles and imported into the three-dimensional visualization software Imaris 6.1.0 (Bitplane AG), employing the Imaris isosurface module.

3. Deconvolution microscopy

The VLP transmission capacity of mDCs was assessed by deconvolution microscopy analyzing DAPI labeled mDCs previously pulsed with VLP_{HIV-Gag-eGFP}, extensively washed and then co-cultured for four hours with Jurkat T cells labeled with the red-fluorescent cell tracker CMTMR (Molecular Probes). Co-cultures were cytopun and images were acquired on an Olympus IX70 microscope equipped for DeltaVision deconvolution (Applied Precision). Z

sections were acquired at 2- μm steps using a 60x, 1.4 NA Olympus PlanApo objective. The volume viewer function of the Softworx software (Applied Precision) was used to generate three-dimensional models from the Z stacks.

4. Epifluorescent microscopy

The viral kinetics of mDCs were analyzed with fluorescence microscopy (Nikon Eclipse TE200) by comparing HIV_{NL4-3/vpr-eGFP}-pulsed cells with the same cells left in culture in the absence of virus for four more hours.

All images generated were exported to Photoshop and Illustrator (Adobe).

XI. Capture assays after proteolytic treatments

mDCs were left untreated or incubated with 200 $\mu\text{g}/\text{ml}$ of Pronase for 30 minutes at 4°C. Part of the cells were stained with distinct mAb to monitor the efficiency of the protease treatment, as detailed below. VLP_{HIV-Gag-eGFP}, HIV_{NL4-3} and Exosomes_{Dil} were left untreated or pre-treated with 400 $\mu\text{g}/\text{ml}$ of Pronase for one hour at 4°C prior to incubation with Pronase or mock-treated mDCs. The effectiveness of the Pronase treatment on the VLPs and wild type virus particles was confirmed by Western blot and infectious assays, as detailed below.

Pronase or mock-treated mDCs were exposed to Pronase or mock-treated VLP_{HIV-Gag-eGFP}, HIV_{NL4-3} or Exosomes_{Dil} for 15 minutes at 37°C to avoid complete recycling of the surface-exposed cellular receptors digested by the proteases. The cells were washed, fixed and analyzed by FACS, or lysed to measure cell-associated p24^{Gag} with an ELISA. Alternatively, the binding of untreated VLP_{HIV-Gag-eGFP} was assessed by pulsing Pronase-treated or mock-

treated mDCs at 16°C for two hours and acquiring fixed cells with a flow cytometer.

1. Confocal microscopy of Pronase-treated mDCs

Pronase or mock-treated mDCs were exposed to VLP_{HIV-Gag-eGFP}, HIV_{NL4-3/vpr-eGFP} or Exosomes_{DII} for four hours at 37°C in the presence of 50 µg/ml of Pronase to avoid complete recycling of the surface-exposed cellular receptors previously digested by the proteases. Cells were then washed and fixed or allowed to recover for two hours before starting a four-hour co-culture with cell-tracker-labeled Jurkat T cells. All samples were analyzed in a confocal microscope (Laser Optic Leica TCS SP2 AOBS).

After pulse at 16°C, some mDCs were stained with DAPI and tetramethyl rhodamine isothiocyanate (TRITC) labeled wheat germ agglutinin to detect the cell membrane, fixed with 2% paraformaldehyde and cytospun onto glass slides to be analyzed in an Olympus IX70 microscope equipped for DeltaVision deconvolution.

2. Confirmation of Pronase activity

To assess protease activity on mDCs, mock-treated or Pronase-treated mDCs were stained with anti-DC-SIGN, anti-CD4 and anti-CD81 mAbs (BD). Mock-treated or Pronase-treated mDCs were also challenged with 5 ng of His-tagged soluble trimeric HIV-1 JRFL gp140 envelope glycoprotein (gracious gift of Dr. Joseph Sodroski, DFCD) for one hour at 4°C and then washed. Binding of gp140 to the cells was revealed by staining with serial incubations of biotin-conjugated anti-His mAb and streptavidin-FITC. The mean fluorescence intensity values of staining were used to calculate the efficiency of protease

treatment, which did not affect cell viability, as assessed by the percentage of positive cells labeled with propidium iodide (Sigma).

To evaluate protease activity on particles, VLP_{HIV-Gag-eGFP} *pseudotyped* with HIV-1 envelope glycoprotein gp120 were pelleted through 20% sucrose cushions (100,000 x g, two hours, 4°C), resuspended in Dulbecco-PBS containing Ca²⁺ and Mg²⁺, and then left untreated or treated with 400 µg/ml Pronase for one hour at 4°C. *Pseudotyped* VLPs were then diluted with DMEM media, containing protease inhibitors (Roche), layered over a 50% Optiprep cushion (0.85% NaCl, 60 mM HEPES, pH 7.4) and centrifuged for two hours at 100,000 x g. The VLPs present at the medium–50% optiprep interface were harvested, pelleted and analyzed for expression of gp120 with a murine anti-gp120 monoclonal antibody (Clone 1121; Immunodiagnostics, Woburn, MA) and for the presence of Gag-eGFP with a mouse anti-HIV p24^{Gag} mAb (Clone AG3.0, NIH AIDS Research and Reference Reagent Program) by Western blot.

The efficiency of Pronase activity on infectious virus particles (400 µg/ml of Pronase for one hour at 4°C) was confirmed by comparing the infectivity of untreated and Pronase-treated wild type HIV_{NL4-3} particles on TZM-bl cells (236). There was an 18-fold reduction in infectivity (94%) following Pronase treatment from a mean TCID₅₀/ml of 22,357 to 1,167 after Pronase treatment. Note that in these experiments the TZM-bl cells employed had the same final concentration of Pronase, regardless of whether viral stocks had been previously treated with Pronase.

Notably, Pronase-treated VSV particles used in competition binding assays with VLP_{HIV-Gag-eGFP} were also monitored to guarantee protease performance. VSV were either treated with 400 µg/ml of Pronase for one hour

at 4°C or mock digested. The number of infectious viruses remaining in each sample was then determined by dilution and plaque assay on BHK cells as described elsewhere (43). Infectivity was found to be reduced by >90% following proteases treatment.

XII. Capture of VLPs, HIV and exosomes produced from ceramide-deficient cells.

To produce sphingolipid deficient particles, HEK-293T or Jurkat cells were incubated for two or five days respectively, in the presence of 50 μ M Fumonisin B₁ (FB1; Cayman Chemical) or 500 μ M N-Butyldeoxynojirimycin, Hydrochloride (NB-DNJ; Calbiochem). HEK-293T cells were then transfected with pLai, pNL4-3 or pGag-eGFP plasmids using FuGENE[®] HD (Roche). Jurkat T cell line was labeled with DiI. HIV_{Lai}, HIV_{NL4-3}, VLP_{HIV-Gag-eGFP} and Exosomes_{DiI} were collected four or seven days after FB1 or NB-DNJ treatment (two days following transfection or DiI labeling). mDCs (1 x 10⁵ cells) were exposed to 2,500 pg of VLPs p24^{Gag}, 250 μ g of Exosomes_{DiI} (displaying equal fluorescent intensity) or 10 ng of HIV p24^{Gag} (produced from either FB1, NB-DNJ or mock-treated HEK-293T cells and Jurkat cells) for two hours at 37°C, then washed, fixed and analyzed by FACS to measure the percentage of positive cells, or washed thoroughly to remove unbound particles, lysed and assayed for cell-associated p24^{Gag} content by an ELISA.

To control for HIV_{NL4-3} functionality after FB-1 and NB-DNJ treatments, TCID₅₀/ml values were obtained with a TZM-bl reporter cell line and compared to mock-treated viral stocks, normalizing values obtained to the

p24^{Gag} levels released after transfections. Infectivity was also tested on a Ghost CXCR4⁺/CCR5⁺ cell line containing the GFP gene under the control of the HIV promoter, employing the viral dose used to pulse mDCs (10 ng of p24^{Gag} per 1 x 10⁵ cells) and analyzing the percentage of green cells 48 hours post-infection with FACS.

XIII. Characterization of macropinocytic activity and treatment of DCs with β -methyl-cyclodextrin, amantadine and chlorpromazine

iDCs and mDCs were incubated with Alexa 488-labeled dextran (Molecular Probes) for two hours at 4°C or 37°C and then fixed for FACS analysis. Mature DCs were treated with β -methyl-cyclodextrin (Sigma) at the concentrations indicated for 30 minutes at 37°C before being pulsed with HIV_{NFN-SX} and assayed for p24^{Gag} as described above. mDC viability in the presence of β -methyl-cyclodextrin was assessed with a flow cytometer by labeling cells with propidium iodide and DIOC-6 (Sigma and Molecular Probes respectively) as previously described (16). Cells were incubated with Alexa 555-conjugated transferrin (25 μ g/ml) from Molecular Probes for one hour at 4°C, washed and then shifted to 37°C for 30 minutes. Cells were then stained with DAPI, fixed with 2% formaldehyde and cytopun onto glass slides for analysis by confocal microscopy.

Cells were also treated with amantadine or chlorpromazine hydrochloride (both from Sigma) at the concentrations indicated for 30 minutes at 37°C before being pulsed with HIV_{NFN-SX}. Pulsed mDCs were

extensively washed and assayed for p24^{Gag} with an ELISA. Cell viability was assessed with FACS, as done previously. Amantadine-treated mDCs were also pulsed with VLP_{HIV-Gag-eGFP}, stained with DAPI and TRITC-wheat germ agglutinin, fixed with 2% formaldehyde and cytopun onto glass slides to be analyzed by deconvolution microscopy.

XIV. Statistical analysis

Statistical analysis was performed using GraphPad software Prism v.4 to assess paired t test and one sample t test.

4.

Results I:

Maturation of Blood-derived DCs
Enhances HIV-1 Capture
& Transmission

Dendritic cells (DCs) are specialized antigen-presenting cells. However, DCs exposed to human immunodeficiency virus type 1 (HIV-1) are also able to transmit a vigorous cytopathic infection to CD4⁺ T cells, a process that has been frequently related to the ability of DC-SIGN to bind HIV-1 envelope glycoproteins. The maturation of DCs can increase the efficiency of HIV-1 transmission through *trans*-infection. In this chapter, we aim to comparatively study the effect of maturation in monocyte-derived DCs (MDDCs) and blood-derived Myeloid DCs during the HIV-1 capture process. *In vitro* capture and transmission of envelope *pseudotyped* HIV-1 and its homologous replication-competent virus to susceptible target cells were assessed by p24^{Gag} detection, luciferase activity, and both confocal and electron microscopy.

Maturation of DCs or Myeloid DCs enhanced the active capture of HIV-1 in a DC-SIGN and viral envelope glycoprotein-independent manner, increasing the lifespan of trapped virus. Moreover, higher viral transmission of mature DCs to CD4⁺ T cells was highly dependent on active viral capture, a process mediated through cholesterol-enriched domains. Mature DCs concentrated captured virus in a single large vesicle staining for CD81 and

CD63 tetraspanins, while immature DCs lacked these structures, suggesting different intracellular trafficking processes.

These observations help explain the greater capacity of mature DCs to transfer HIV-1 to T lymphocytes, a process that could potentially contribute to the viral dissemination at lymph nodes *in vivo*, where viral replication takes place and there is a continuous interaction between susceptible T cells and mature DCs.

I. Results

1. mDCs capture larger amounts of HIV_{NFN-SX} than iDCs

To compare the viral capture abilities of mDCs and iDCs of the same seronegative donors, we pulsed both cell types with equal amounts of HIV_{NFN-SX} at 37°C for two hours. Raji B cells stably transfected with DC-SIGN were routinely employed to measure DC-SIGN viral capture efficiency, and the parental Raji cell line was used to determine the background viral capture. Interestingly, viral capture determined by p24^{Gag} ELISA was much more efficient in mDCs than in the rest of the cells tested, suggesting a differential active capture process of HIV_{NFN-SX} in this cell type ($P < 0.0001$, paired t test, Fig. 25A).

This enhanced mDC viral capture correlated with an increased viral transmission efficiency, as observed in 48-hour co-cultures of DCs pulsed with *pseudotyped* HIV_{JRFL/NL4-3-Luc} and target Hut CCR5⁺ T cells ($P = 0.048$, paired t test, Fig. 25B). Raji DC-SIGN cells were employed to confirm viral transfer efficiency and parental Raji cells were used as negative controls, showing the same relative light unit (RLU) values as those of non-pulsed cells (Fig. 25B,

dotted line). Notably, co-cultures with CCR5-negative target cells did not show any infection 48 hours post-pulse, indicating that neither Raji DC-SIGN cells nor DCs were productively infected during this experimental period (Fig. 25B, clear bars).

Results were analogous to using HIV_{NFN-SX} to pulse the cells and then measuring the viral transmission by intracellular staining of co-cultures with an anti-p24^{Gag} mAb (Fig. 25C). In this case, viral transfer, expressed as a percentage of p24^{Gag+} cells, was also more efficient when co-cultures were done with mDCs than when they were done with iDCs ($P < 0.0001$, paired t test). Of note, DCs were not infected in our co-culture system, as seen from the low percentage of DC-SIGN⁺/p24^{Gag+} double positive cells (<0.8%).

We then investigated whether Myeloid DCs expressing the CD1c (BDCA-1) antigen would behave similarly to MDDCs in terms of viral capture and *trans*-infection ability. We isolated the Myeloid dendritic CD1c subset from the PBMCs of seronegative donors. A fraction of these Myeloid DCs were subsequently LPS matured. We performed the same viral capture assay employed for MDDCs and, as reported above for mDCs, viral capture was more efficient in mature Myeloid DCs ($P = 0.039$, paired t test, Fig. 25D).

Regarding viral transmission, we tested the transfer capacity of HIV_{JRFL/NL4-3-Luc}-pulsed mature and immature Myeloid DCs from the same seronegative donors co-cultured with Hut CCR5⁺ cells. As observed for MDDCs, the mean viral transmission ability of mature Myeloid DCs was fifty times more efficient than that of immature Myeloid DCs ($P = 0.013$, paired t test, Fig. 25E).

Overall, these data show that mDCs and mature CD1c Myeloid DCs capture and transmit HIV-1 to a greater extent than iDCs and immature Myeloid DCs do.

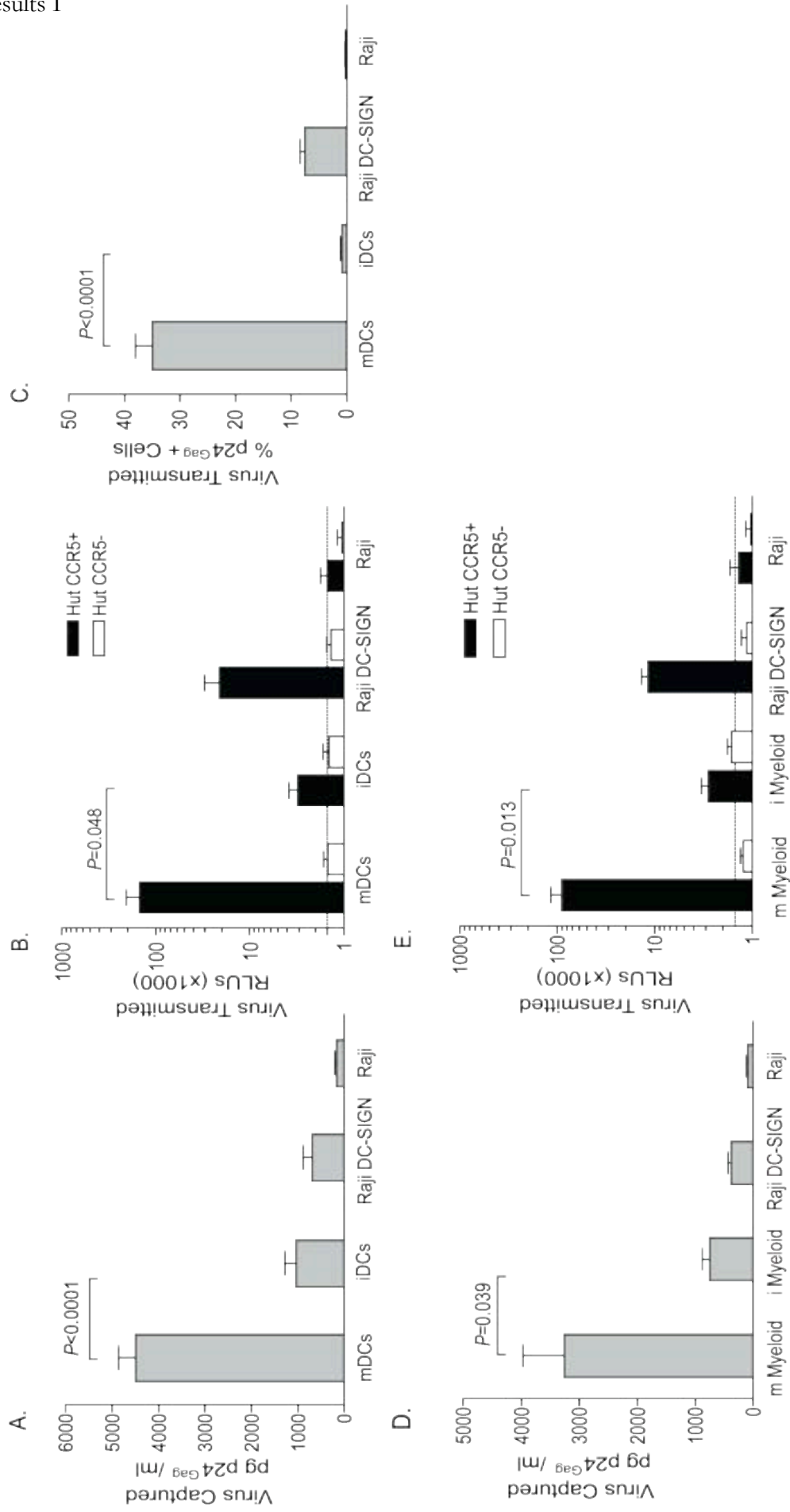


Figure 25. Caption overleaf.

Figure 25. (From previous page). Maturation of DCs and Myeloid DCs enhances HIV_{NFN-SX} capture and HIV_{JRFL/NL4-3-Luc} transmission. (A) Comparative capture of HIV_{NFN-SX} by distinct cell types. A total of 3×10^5 DCs, Raji DC-SIGN cells and Raji cells were pulsed for two hours at 37°C with 80 ng p24^{Gag} in 0.3 ml, washed with PBS and lysed with 0.5% Triton, at a final concentration of 5×10^5 cells per ml, to measure p24^{Gag} by ELISA. Results are expressed in pg of p24^{Gag} bound per ml of cell lysate. Data show the mean values and standard errors of the means (SEM) from six independent experiments. mDCs capture significantly larger amounts of virus than iDCs ($P < 0.0001$, paired t test, $n = 11$). **(B)** HIV_{JRFL/NL4-3-Luc} transmission from DCs, Raji DC-SIGN cells and Raji cells to Hut CCR5⁺ cells (dark bars). Co-cultures were assayed for luciferase activity 48 hours post-pulse. No productive infection of DCs or Raji DC-SIGN cells was detected, as shown when using Hut CCR5-negative target cells (clear bars). The dotted line shows background levels of RLUs observed when non-pulsed cells were lysed. mDCs transmit larger amounts of HIV_{JRFL/NL4-3-Luc} than iDCs derived from the same donors ($P = 0.048$, paired t test, $n = 6$). **(C)** HIV_{NFN-SX} transmission from iDCs, mDCs, Raji-DC-SIGN and Raji to Hut CCR5⁺ target cells. Co-cultures were assayed for p24^{Gag} intracellular staining 36 hours post-pulse. Co-cultures containing non-pulsed cells were used as a background control for p24^{Gag} FITC labeling. **(D)** Comparison of HIV_{NFN-SX} capture by Myeloid DCs as described above in (A). Mature Myeloid DCs (m Myeloid) capture significantly larger amounts of virus than immature Myeloid DCs (i Myeloid); ($P = 0.039$, paired t test, $n = 4$). **(E)** HIV_{JRFL/NL4-3-Luc} transmission from Myeloid DCs, Raji DC-SIGN cells and Raji cells to Hut CCR5⁺ cells and Hut CCR5⁻ cells as described above in (B). Mature Myeloid DCs transmit larger amounts of HIV_{JRFL/NL4-3-Luc} than immature Myeloid DCs derived from the same seronegative donors ($P = 0.013$, paired t test, $n = 6$).

2. Enhanced viral transmission of mDCs depends on the amount of virus actively captured

To test whether the higher viral capture of mDCs accounted for the increased HIV transmission observed, we pulsed both immature and mature DCs with high concentrations of HIV_{JRFL/NL4-3-Luc} at 4°C and 37°C (Fig. 26). After extensive washing, we lysed part of the cells and determined the cell-associated virus fraction by p24^{Gag} ELISA. The rest of the washed cells were co-cultured at 37°C with Hut CCR5⁺ target cells and assayed for luciferase activity.

Of note, the viral binding at 4°C in mDCs was similar to the viral capture at 37°C observed in iDCs (Fig. 26A). Interestingly, the subsequent viral transmission of these two cell subsets was analogous (Fig. 26B) regardless of the maturation status of the DCs. It is noteworthy that Raji DC-SIGN viral capture and transmission were also temperature sensitive, showing the same behavior at 4°C as for the Raji parental cell line. Again, the HIV_{JRFL/NL4-3-Luc} capture and transmission observed in mDCs pulsed at 37°C was the highest of all cell types tested.

In order to exclude the possibility that mDCs could better stimulate target cells in the co-cultures and thereby lead to a higher readout in RLUs, we also estimated the proliferation capacity of target cells in cultures with mDCs or iDCs. We found, however, no differences in Hut CCR5⁺ cell proliferation when cultured with any type of MDDCs (Fig. 26C). These results suggest that the higher viral transmission of mDCs is highly dependent on active viral capture.

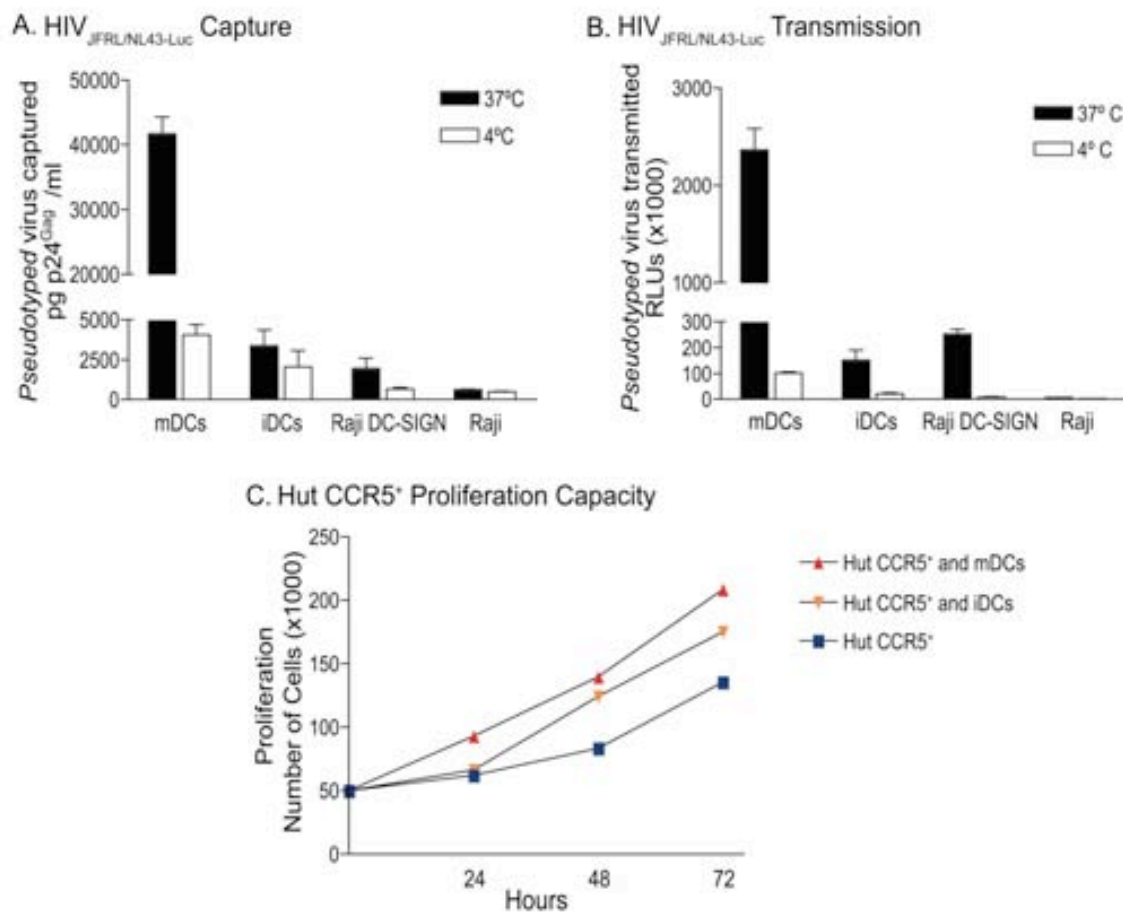


Figure 26. Enhanced viral transmission of mDCs depends on the amount of HIV_{JRFL/NL4-3-Luc} actively captured. (A) Comparative capture at 37°C and binding at 4°C of HIV_{JRFL/NL4-3-Luc} by distinct cell types. A total of 3×10^5 DCs, Raji DC-SIGN cells and Raji cells were incubated at 37°C (dark bars) or 4°C (clear bars) with 300 ng of HIV_{JRFL/NL4-3-Luc} p24^{Gag} in a final volume of 0.3 ml, washed five times with PBS and lysed with 0.5% Triton, at a final concentration of 5×10^5 cells per ml, to measure p24^{Gag} by ELISA. (B) HIV_{JRFL/NL4-3-Luc} transmission to Hut CCR5⁺ target cells of *pseudotyped* virus captured at 37°C (dark bars) or bound at 4°C (clear bars). Different cell types pulsed, as described above in (A), were co-cultured with target cells at 37°C and assayed for luciferase activity 48 hours post-pulse. (A) and (B) show a representative experiment including mean values and SEM for three different donors. (C) Proliferation capacity of CFSE labeled Hut CCR5⁺ cultured alone or with iDCs or mDCs and followed for three days. Hut CCR5⁺ cells were counted with FACS-counting beads and no significant differences were found in cell numbers, excluding the possibility that mDCs could better stimulate target cells leading to a higher readout in the RLUs.

3. mDC viral capture increases over time, and captured virus has a longer lifespan than in iDCs

To further characterize the viral capture process, we monitored mDCs and iDCs exposed to HIV_{NL4-3/vpr-eGFP} fluorescent virus or HIV_{NFN-SX} for ten to twelve hours at 37°C (Fig. 27A to D). After extensive washing, the percentage of GFP⁺ cells was analyzed by flow cytometry and the cell-associated virus fraction was determined by p24^{Gag} ELISA at each of the time points indicated. Interestingly, viral capture in mDCs increased over time (Fig. 27A and C) while remaining constant in iDCs (Fig. 27B and D). These data show that mDCs actively capture HIV-1 and that viral capture differences with respect to iDCs increase over time.

100

Next, we asked whether captured virus would follow different intracellular pathways in distinct MDDCs. Kinetic analyses of both the cell-associated and the cell-free virus fractions were longitudinally determined by p24^{Gag} in cultures of immature and mature DCs exposed to HIV_{NFN-SX} and extensively washed to remove unbound virus (Fig. 27E and F). Immediately following viral exposition and washing, cell-associated virus was approximately twenty-five times more abundant in mDCs than in iDCs. HIV_{NFN-SX} p24^{Gag} antigen associated with iDCs quickly became undetectable in the first four hours (Fig. 27F). Although these results suggest that iDCs may lead the virus to an intracellular lytic pathway, showing 50% ±10% viral degradation, the steady increase in soluble p24^{Gag} also indicated some degree of virus release to the culture supernatant (22% ±3% of captured virus). Conversely, mDCs degraded 30% ±10% of captured virus during the first four hours (Fig. 27E) without a substantial release of trapped virions (7% ±3%). p24^{Gag} associated with mDCs

decreased $50\% \pm 12\%$ in the first day of culture without a further increase in soluble antigen, indicating the persistence of detectable cell-associated p24^{Gag}.

Finally, to exclude that the greater viral degradation of iDCs as compared to mDCs ($P=0.024$, paired t test) could account for the viral capture differences observed, we treated cells with bafilomycin A1 (an inhibitor of lysosomic degradation) and clasto-lactacystin- β -lactone (an inhibitor of proteasome activity). We found no significant increase in viral capture of drug treated cells compared to mock treated cells over two hours, as previously reported (144). After four hours in the absence of virus but in the presence of these drugs, mDCs degraded a mean of $51\% \pm 19\%$ of the total lost virus (which was $30\% \pm 10\%$ of the captured virus) throughout the lysosomes and $55\% \pm 15\%$ through the proteasome machinery. Retained viral particles in iDCs were similarly processed. These data suggest that greater viral degradation in iDCs does not account for the viral capture differences observed between both cell types.

Overall, these observations support a more efficient capture process and a longer lifespan for captured HIV-1 in mDCs than in iDCs.

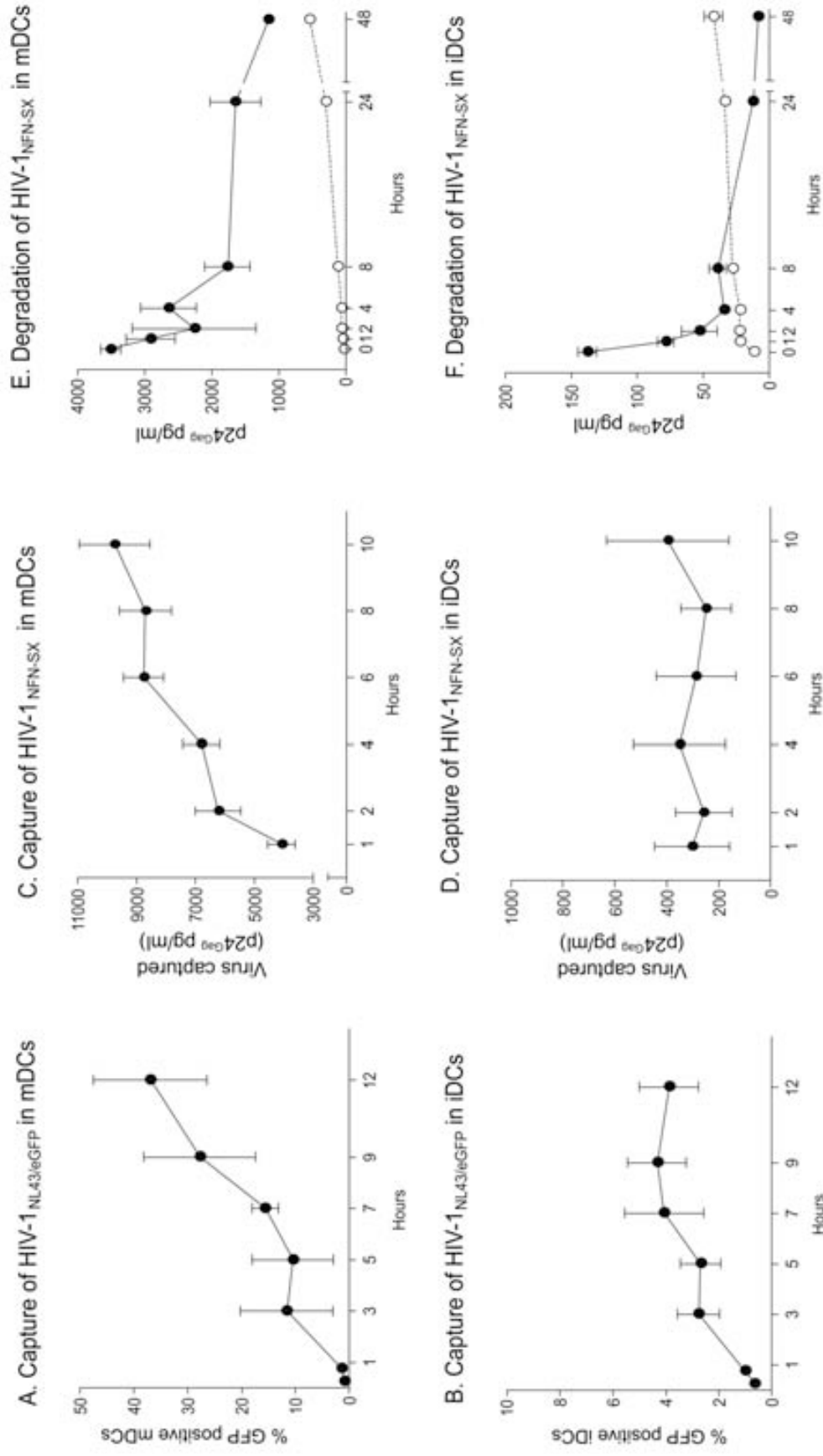


Figure 27. mDC viral capture increases over time, and captured virus has a longer lifespan than in iDCs. (A to D) Time course of HIV_{NL4-3/vpr-eGFP} or HIV_{NFN-SX} capture by mDCs and iDCs showed that mDC viral capture increases over time while remaining constant in iDCs. **(E and F)** Fate of HIV_{NFN-SX} captured for two hours by mDCs and iDCs respectively, monitored over two days. Cell-associated p24^{Gag} measured by ELISA is shown as closed symbols, while p24^{Gag} released to the cell culture medium is shown as open symbols. Captured virus showed a prolonged lifespan in mDCs. Data (means and SEM from two independent experiments) include cells from six different donors.

4. Higher viral capture in mDCs than in iDCs can occur independently of DC-SIGN and does not require viral envelope glycoprotein

Since the ability of DCs to bind and transmit HIV-1 has been previously related to DC-SIGN expression levels in the HEK-293T transfected cell line (172), we used a fluorescence quantitation method to obtain absolute numbers of DC-SIGN antibody binding sites (ABS) in DCs and Raji DC-SIGN cells (Fig. 28A). We focused on MDDCs because the immunophenotype of Myeloid DCs showed almost no expression of DC-SIGN (Fig. 28B). Monocytes from thirty HIV-1 seronegative donors were consecutively differentiated into immature and mature MDDCs and assayed in parallel for DC-SIGN expression. The mean number of DC-SIGN ABS per DC-SIGN⁺ cell in mDCs (4×10^4) was half that of iDCs (8×10^4); ($P < 0.0001$, paired t test; Fig. 28A). Raji DC-SIGN cells displayed a mean number of DC-SIGN ABS comparable to that of mDCs. Therefore, we found no correlation between DC-SIGN expression levels and the viral capture efficiency of mDCs and iDCs.

We decided to further address the impact of DC-SIGN on the viral capture process mediated by MDDCs and blood Myeloid DCs by testing mAb MR-1 against DC-SIGN or mannan (a C-type lectin competitive inhibitor) to see if they could impair HIV_{NFN-SX} capture at 37°C. Figure 28C shows the percentage of HIV_{NFN-SX} captured in the presence of different inhibitors relative to untreated cells normalized to 100% of viral capture. Pretreatment with these compounds efficiently inhibited Raji DC-SIGN viral capture to levels similar to those displayed by Raji cells (greater than 85% for any of the inhibitors; $P < 0.0001$, paired t test).

We also observed an inhibitory effect in iDCs, the DC subset displaying larger amounts of DC-SIGN, but this only reached 50% ($P=0.049$, paired t test, Fig. 28C). However, neither compound had any significant effect on viral capture mediated by mDCs (expressing DC-SIGN) or immature and mature Myeloid DCs (lacking DC-SIGN expression). Since DC-SIGN inhibitors had no blocking effect on mature DC viral capture and this C-type lectin is known to bind with high affinity to the gp120 viral envelope glycoprotein (46), we then analyzed the envelope requirement during the viral capture process.

We pulsed MDDCs and Myeloid DCs with equal amounts of a viral construct lacking the envelope glycoprotein ($\text{HIV}_{\Delta\text{env-NL4-3}}$) and its counterpart expressing the envelope protein ($\text{HIV}_{\text{NFN-SX}}$). Figure 28D shows the percentage of $\text{HIV}_{\Delta\text{env-NL4-3}}$ captured by each cell type relative to the cells pulsed with $\text{HIV}_{\text{NFN-SX}}$, normalized to 100% of viral capture. As expected, Raji DC-SIGN cell viral capture was totally dependent on the envelope glycoprotein, as apparent from the percentage of envelope-deficient virus captured compared to that of the wild type virus ($P= 0.0008$, paired t test, Fig. 28D). However, the envelope requirement for viral capture decreased in iDCs and was totally absent in Myeloid DCs and mDCs. These data are in agreement with the fact that preincubating $\text{HIV}_{\text{JFRL-NL4-3/Luc}}$ with the envelope glycoprotein-neutralizing antibody IgGb12 does not abrogate mDC viral capture (Fig. 29A), while efficiently blocking viral transfer to the U87 CCR5^+ cell line (Fig. 29B). Overall, these results suggest that Myeloid DC and mDC viral capture is independent of viral envelope glycoprotein, data which correlates with the lack of a blocking effect displayed by DC-SIGN inhibitors in these cell types.

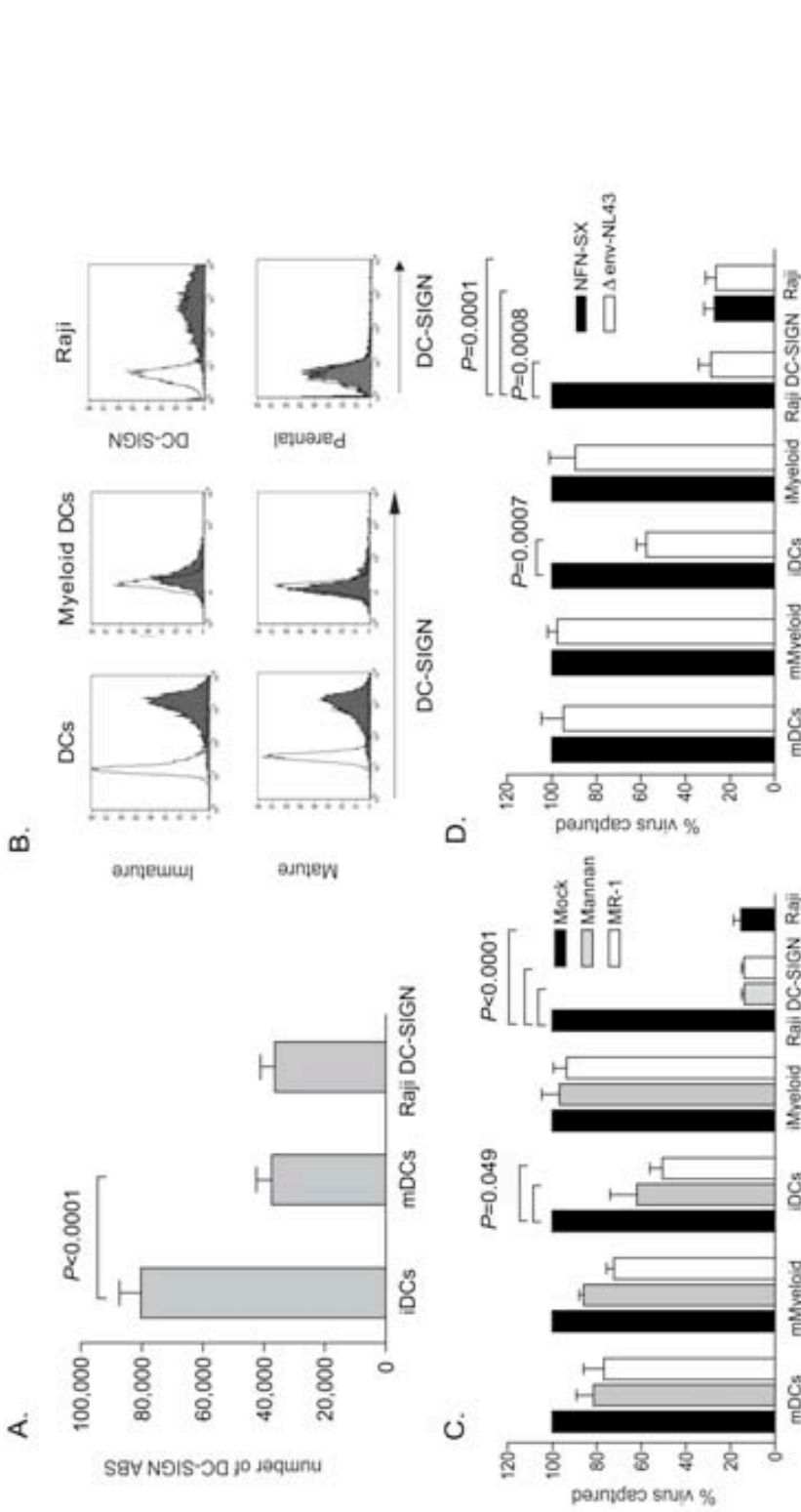


Figure 28. Higher viral capture in mDCs than in iDCs can occur independently of DC-SIGN and does not require viral envelope glycoprotein. (A) DCs of thirty seronegative donors were stained with anti-DC-SIGN mAb labeled with PE (1:1 ratio of mAb to PE) and analyzed for DC-SIGN surface expression using Quantibrite PE standard beads to calculate the number of DC-SIGN ABS displayed per PE-positive cell. Mean values and SEM are represented. iDCs had twice the mean number of DC-SIGN ABS per cell compared to mDCs and Raji DC-SIGN cells ($P < 0.0001$, paired t test). (B) Expression of DC-SIGN in DCs, Myeloid DCs, Raji DC-SIGN cells and Raji cells. Isotype-matched mouse IgG controls are also indicated (empty peaks). (C) Percentage of p24^{Gag} HIV_{NFN-SX} captured at 37°C in the presence of different DC-SIGN inhibitors relative to untreated cells normalized to 100% of viral capture. Raji cells were compared with untreated Raji DC-SIGN cells. Viral capture by cells with no inhibitor (dark bars) or preincubated with mannan (light gray bars) or MR-1 (white bars) is depicted. Significant inhibition in the Raji DC-SIGN cell line reached 85% ($P < 0.0001$, paired t test). Data show mean values and SEM from two independent experiments, including cells from six different donors. (D) Percentage of p24^{Gag} HIV_{Δenv-NL4.3} virus lacking the envelope glycoprotein captured by DCs, Myeloid DCs, Raji cells and Raji DC-SIGN cells relative to HIV_{NFN-SX} capture normalized to 100%. Cells were pulsed with equal amounts of both viruses and the Raji cell line was compared to the Raji DC-SIGN cells. The envelope requirement for mDC and Myeloid DC viral capture was not significant, while it reached significance in iDCs ($P = 0.0007$, paired t test). Raji DC-SIGN cells mainly captured HIV_{NFN-SX} enveloped virus and bound HIV_{Δenv-NL4.3} virus only to levels comparable to the background seen by employing the Raji cell line ($P < 0.0001$, paired t test). Data show mean values and SEM from two independent experiments, including cells from five different donors.

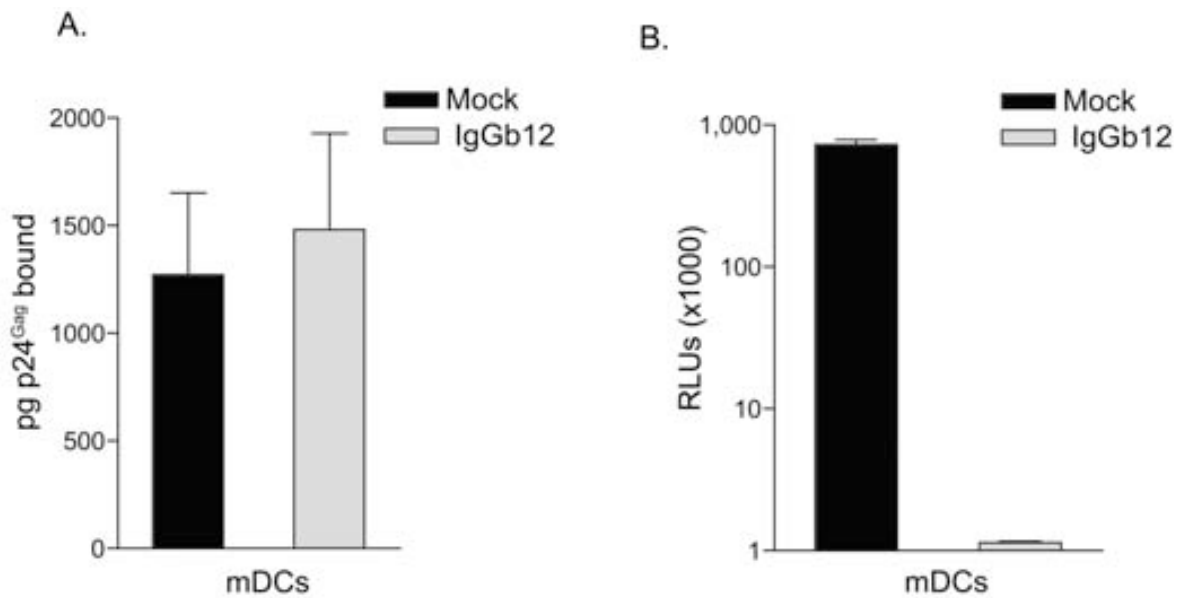


Figure 29. mDCs viral capture and transmission of *pseudotyped* HIV_{JRFL/NL4-3-Luc} preincubated with IgGb12 envelope-glycoprotein neutralizing-antibody or human IgGs as an isotype control. **(A)** mDC viral capture after treatment of *pseudotyped* HIV_{JRFL/NL4-3-Luc} stock with 20 µg/ml of IgGb12 or human IgGs over fifteen minutes. Capture is not affected by the blockade of viral envelope glycoprotein with IgGb12. **(B)** Transmission of mDC-captured virus to U87 CCR5⁺ cells. Luciferase activity was assayed 48 hours post-pulse. Preincubation of HIV_{JRFL/NL4-3-Luc} with IgGb12 inhibits viral transmission to U87 CCR5⁺ cells. The data in all panels show the means and SEM of two experiments.

5. Viral stocks produced in different cell lines are also captured with greater ability by mDCs than by iDCs

Since the viral envelope glycoprotein is not necessary for Myeloid DC and mDC viral uptake, host adhesion receptors dragged from the membrane of infected cells during viral budding have to be implicated in this viral capture process mediated by mature DCs. We decided to further address whether these host factors are ubiquitous, especially by focusing on T cell lines and stimulated PBMCs, given that these cells are natural producers of HIV-1. We

produced HIV-1_{NL4-3} in HEK-293T cells, MOLT 4 cells and stimulated PBMCs to pulse iDCs and mDCs with the same amount of each of the viral stocks. Figure 30 shows the percentage of HIV-1_{NL4-3} captured by each cell type relative to mDCs normalized to 100% of viral capture for each of the viral stocks produced. Notably, we observed an increased viral uptake pattern in mDCs compared to iDCs exposed to each of these viral stocks (Fig. 30, *P* values in the graph). Thus, viral stocks produced in T cell lines and primary lymphocytes are also captured with greater ease by mDCs than by iDCs.

These results highlight the need to analyze the role of host adhesion receptors dragged from the membrane of infected cells during viral budding, because this could aid in identifying the ubiquitous molecular determinants that lead to viral capture in mature DCs.

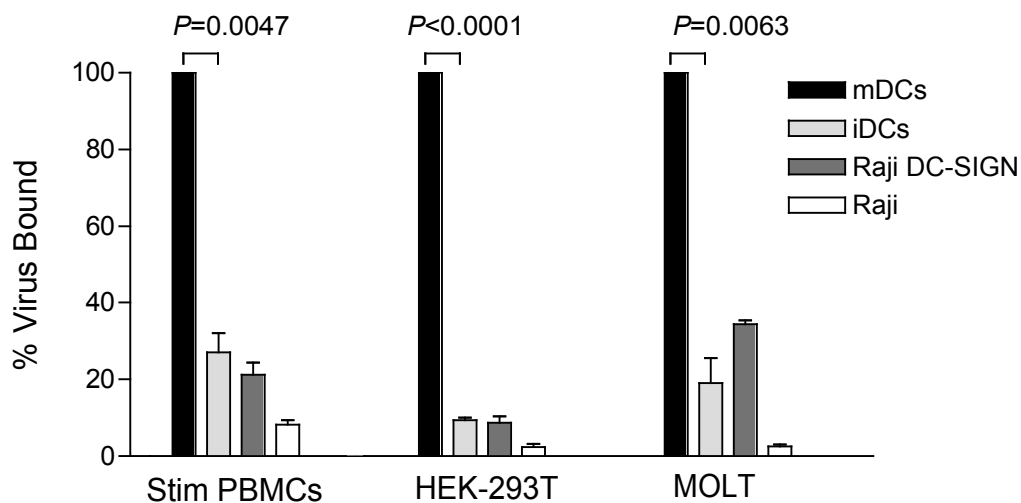


Figure 30. Relative capture of HIV_{NL4-3} produced in different cell types. Cells were pulsed with equal amounts of HIV_{NL4-3} generated by stimulated PBMCs, HEK-293T or MOLT 4 T cells and then assayed for p24^{Gag} ELISA. Results are expressed as the percentage of HIV_{NL4-3} captured by distinct cell types cells relative to mDCs, normalized to 100% of viral capture. Regardless of the virus-producing cell employed, there is an increased viral uptake pattern in mDCs compared to iDCs.

6. Greater viral transmission in mature DCs than in immature DCs can occur independently of DC-SIGN

Since no correlation was found between DC-SIGN expression levels and the viral capture capacity of iDCs and mDCs, we decided to further address the impact of DC-SIGN on the *trans*-infection process. We tested whether the mAb MR-1 against DC-SIGN or mannan could impair HIV_{JRFL/NL4-3-Luc} transmission mediated by DCs or Raji DC-SIGN cells. Figure 31A shows the percentage of HIV_{JRFL/NL4-3-Luc} transmitted to Hut CCR5⁺ by cells pulsed in the presence of different inhibitors, relative to untreated cells normalized to 100%. When Raji DC-SIGN were preincubated with MR-1 or mannan before pulsing, transfer was blocked up to a median of 95% ($P < 0.001$, paired t test, Fig. 31A). In contrast, iDCs pretreatment with any of the compounds could not prevent viral transmission beyond 50%. The same inhibitors only reduced HIV_{JRFL/NL4-3-Luc} transmission up to 40% in mDCs, suggesting even greater independence of DC-SIGN or other C-type lectin receptors than in iDCs.

Similar results were found in replication-competent HIV_{NFN-SX}, when we analyzed the percentage of p24^{Gag+} cells obtained by intracellular staining after 36 hours of co-culture with Hut CCR5⁺ target cells (Fig. 31B). We also tried to block viral transmission by pretreating mature and immature Myeloid DCs with MR-1 or mannan. As previously observed for DCs, despite complete inhibition of HIV_{JRFL/NL4-3-Luc} transfer mediated by Raji DC-SIGN (>94%; $P < 0.005$, paired t test), both mannan and MR-1 could only partially inhibit HIV transfer to CD4⁺ T cells by mature and immature Myeloid DCs (Fig. 31C).

Overall, these data suggest that mDCs and mature Myeloid DCs transmit HIV-1 independently of DC-SIGN.

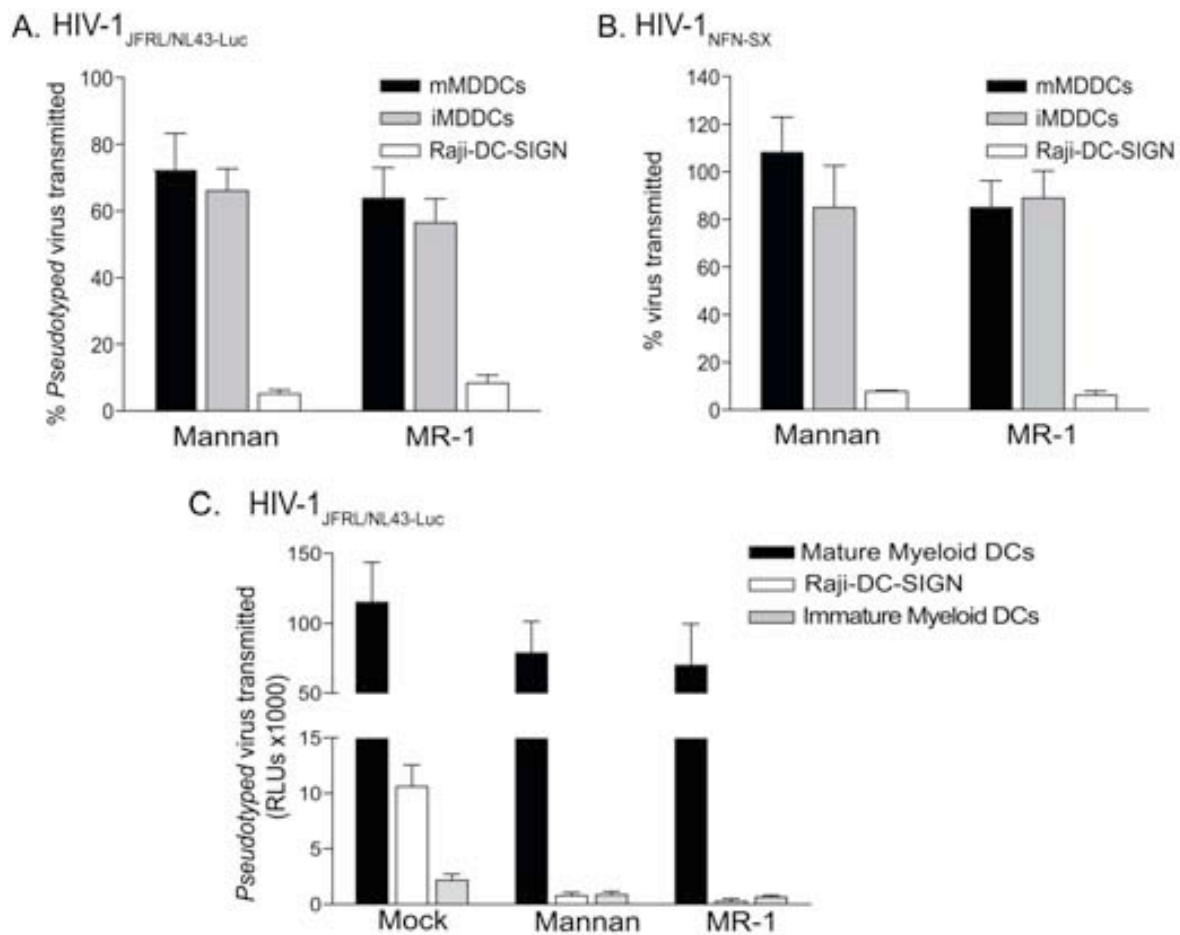


Figure 31. mDCs and mature Myeloid DCs viral transmission of *pseudotyped* HIV_{JFRL/NL4-3-Luc} and replication-competent HIV_{NFN-SX} is independent of DC-SIGN. (A) Percentage of HIV_{JFRL/NL4-3-Luc} transfer to Hut CCR5⁺ cells in the presence of different inhibitors relative to untreated cells normalized to 100% of viral transmission. Luciferase activity was assayed 48 hours post-pulse. Raji DC-SIGN (n=17), iDCs (n=33) and mDCs (n=10) were treated with mannan or MR-1. Inhibition in the Raji DC-SIGN cell line was statistically significant in all cases ($P=0.001$, paired t test). **(B)** Percentage of HIV_{NFN-SX} transferred to Hut CCR5⁺ in the presence of different inhibitors relative to untreated cells. Intracellular p24^{Gag} was determined by FACS 36 hours post-pulse. Non-pulsed cells co-cultured with target cells were used as a control for background p24^{Gag} FITC labeling. Raji DC-SIGN (n=2), iDCs (n=4) and mDCs (n=4) were treated with mannan or MR-1. The data in all the panels show means and SEM. **(C)** Net transmission from mature Myeloid DCs, immature Myeloid DCs and Raji DC-SIGN cells to Hut CCR5⁺ in the absence of DC-SIGN blocking agents, preincubated with mannan or MR-1. Inhibition in Raji DC SIGN was statistically significant ($P<0.005$, paired t test).

7. Confirmation of viral capture, turnover and transmission results by microscopy

To further address viral capture, HIV_{NL4-3/vpr-eGFP}-pulsed DCs and Myeloid DCs were monitored by confocal microscopy. In agreement with our capture observations, considerably larger amounts of viruses were found in mature DCs than in immature DCs after four hours of viral exposure (Fig. 32A and B). Many mDCs and mature Myeloid DCs showed a large single GFP⁺ vesicle-like structure, observed by reconstructing a series of x-y sections collected through the nucleus of the cells to project the z-x and z-y planes (Fig. 32C and D). Of note, iDCs and immature Myeloid DCs did not present any of these large vesicles (Fig. 32E and F), suggesting differential intracellular viral trafficking in mature DCs.

To better understand viral kinetics, HIV_{NL4-3/vpr-eGFP}-pulsed mDCs were analyzed by fluorescence microscopy. After four hours of viral capture, 97% \pm 3% of the pulsed mDCs were GFP⁺, presenting captured virus in a single vesicle (55% \pm 8%), polarized in the surface of the cell membrane (25% \pm 7%), and randomly distributed throughout the cell surface (14% \pm 9%); (Fig. 33). The same pulsed mDCs, washed and analyzed four hours later, presented a similar viral distribution pattern, although the mean percentage of captured virus in a single vesicle increased to 75% \pm 4% and the randomly distributed virus decreased to 4% \pm 6% (Fig. 33). These data indicate that viral vesicles represent a more stable compartment, as they contain most of the captured virus at the time when viral degradation reaches a plateau (Fig. 27E). However, the differences observed were not statistically significant, suggesting that viral turnover was comparable in each of the cell populations found.

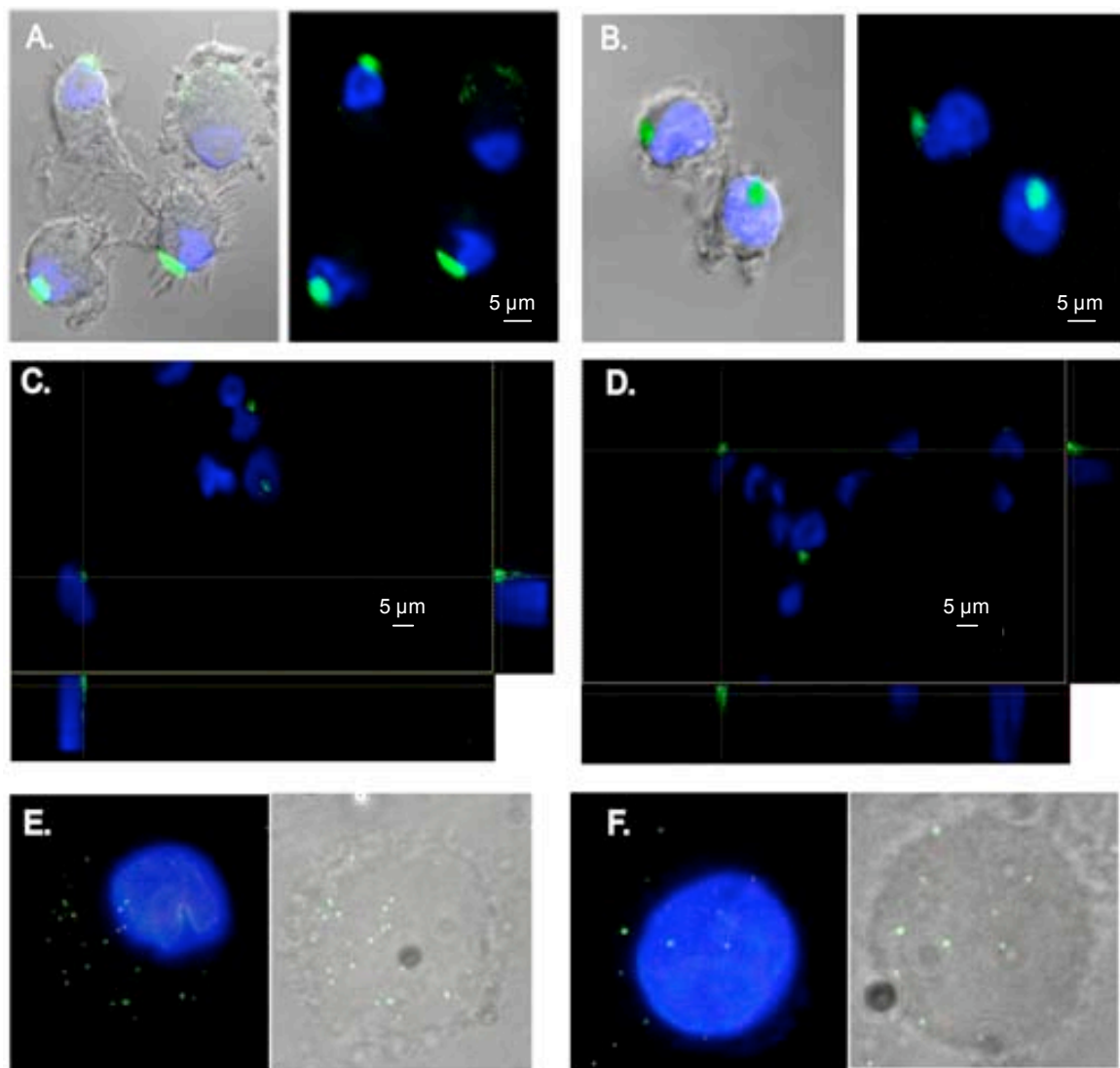


Figure 32. Confocal and epifluorescent microscopy of HIV-1 capture and transfer mediated by DCs. **(A)** Confocal images of a section of mDCs exposed to HIV_{NL4-3/vpr-eGFP} for four hours and stained with DAPI to reveal the nucleus. Merged images of the section showing the cells and the green and blue fluorescence are shown. **(B)** Composite of a series of x–y sections collected through the entire thickness of the cell nucleus of a mature Myeloid DC exposed to HIV_{NL4-3/vpr-eGFP} and projected onto a two-dimensional plane. A three-dimensional reconstruction of a series of x–y sections collected through part of the cell nucleus can be found as Video 1 in the supplementary CD. **(C)** Composition of a series of x–y sections of mDCs collected through part of the cell nucleus and projected onto a two-dimensional plane to show the x–z plane (bottom) and the y–z plane (right) at the points marked with the dotted white axes. **(D)** Confocal image composition of mature Myeloid DCs constructed as described above in (C). **(E and F)** Epifluorescent images of an iDC (E) or immature Myeloid DC (F) exposed to HIV_{NL4-3/vpr-eGFP} for four hours and stained with DAPI. Merged images show the cells and the green and blue fluorescence.

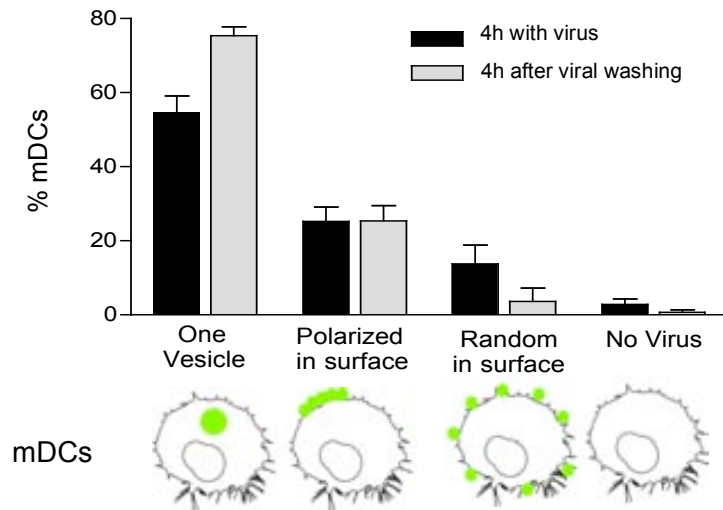


Figure 33. Percentage of mDCs analyzed by fluorescent microscopy after four hours in the presence of HIV_{NL4-3/vpr-eGFP}. Cells were washed and immediately analyzed (dark bars) or evaluated four hours later (light bars). Graph shows the means and SEM of cells from three different donors.

To gain further insight into the mechanism of viral capture and transmission, HIV_{JRFL/NL4-3-Luc}-pulsed DCs were monitored by electron microscopy. Viral particles in mDCs attached to the extracellular cell membrane proximal to the soma between dendrites (Fig. 34A and B). Initial endocytic events were also observed (Fig. 34C), and vacuoles containing numerous viral particles consistent with our previous confocal microscopy observation were found proximal to the plasma membrane or deep inside the cytoplasm (Fig. 34D and E). Quantitative differences between iDCs and mDCs confirmed our previous results: of 113 mDCs analyzed, 33% showed at least one virus in the cell surface and 28% had endocytosed virus. Conversely, of 90 iDCs analyzed, only 9% showed at least one virus in the cell surface and 6% had endocytosed virus. Virions were associated with dendrites in only two cases (one for mDCs and one for iDCs). Viral transmission was also monitored by using DCs co-cultured with Hut CCR5⁺ cells. mDCs filled with HIV_{JRFL/NL4-3-Luc} established associations with Hut CCR5⁺ cells, and virus could be found to be restricted to the site of the cell contact area (Fig. 34F and G). Polarization of viral particles at the cell-to-cell interface, where intimate contact between

mDCs and Hut CCR5⁺ cells takes place, suggested the formation of an infectious synapse.

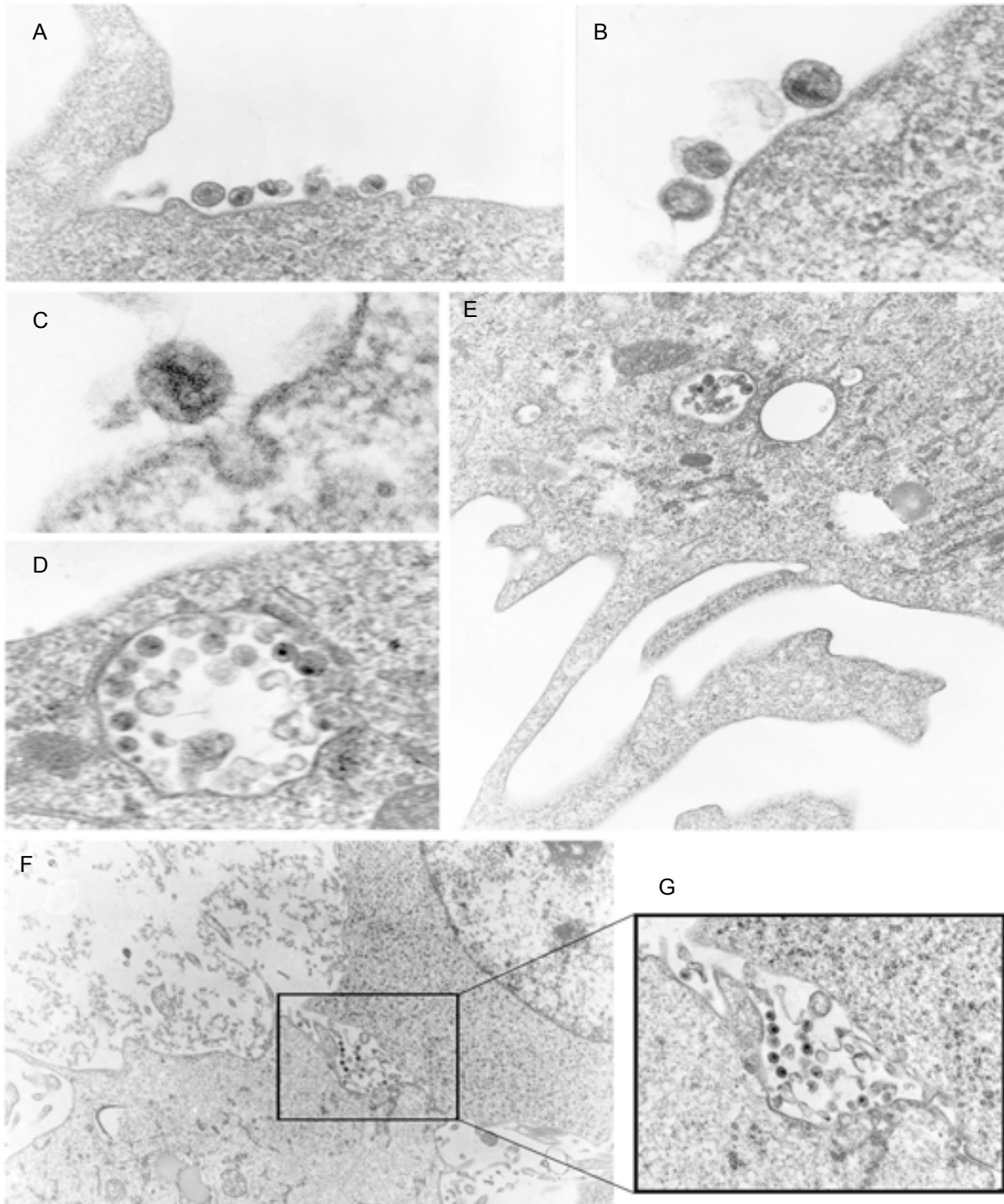


Figure 34. Caption overleaf.

Figure 34. (From previous page). Electron micrographs of pulsed mDCs. Cells presented large numbers of viral particles associated with the cell membrane outside dendrites (**A** and **B**) or initiating endocytosis (**C**). (**D** and **E**) Large vesicles containing numerous viral particles could be found proximal to the plasma membrane surface or deep inside the cellular cytoplasm. (**F**) Infectious synapse could also be observed in mDC and Hut CCR5⁺ cell co-cultures. The marked box on the picture shows the attachment of a mDC (with light cytoplasm at the bottom) to a Hut CCR5⁺ cell (with granulated cytoplasm and a large nucleus at the top). (**G**) Magnification of the marked box in F, where viral particles are polarized at the cell-to-cell contact area to form an infectious synapse.

8. Mature Myeloid DCs retain HIV_{NFN-SX} and HIV_{Δenv-NL4-3} in a compartment similar to that of mDCs

Previous work has demonstrated that in mDCs, HIV-1 accumulates in intracellular vacuoles containing CD81 and CD63 tetraspanins (74). We extended these observations to mature Myeloid DCs and found that HIV_{NFN-SX} co-localizes with CD81 and CD63 (Fig. 35, top) but not with the LAMP-1 lysosomal marker. Furthermore, by employing HIV_{Δenv-NL4-3}, we observed accumulation in the same intracellular compartments (Fig. 35, bottom).

Therefore, in mature Myeloid DCs, the process of viral accumulation in vesicles is not directed by the envelope glycoprotein, in agreement with our previous data (Fig. 28D). Furthermore, both types of captured viruses are retained in a single CD81 and CD63-positive compartment.

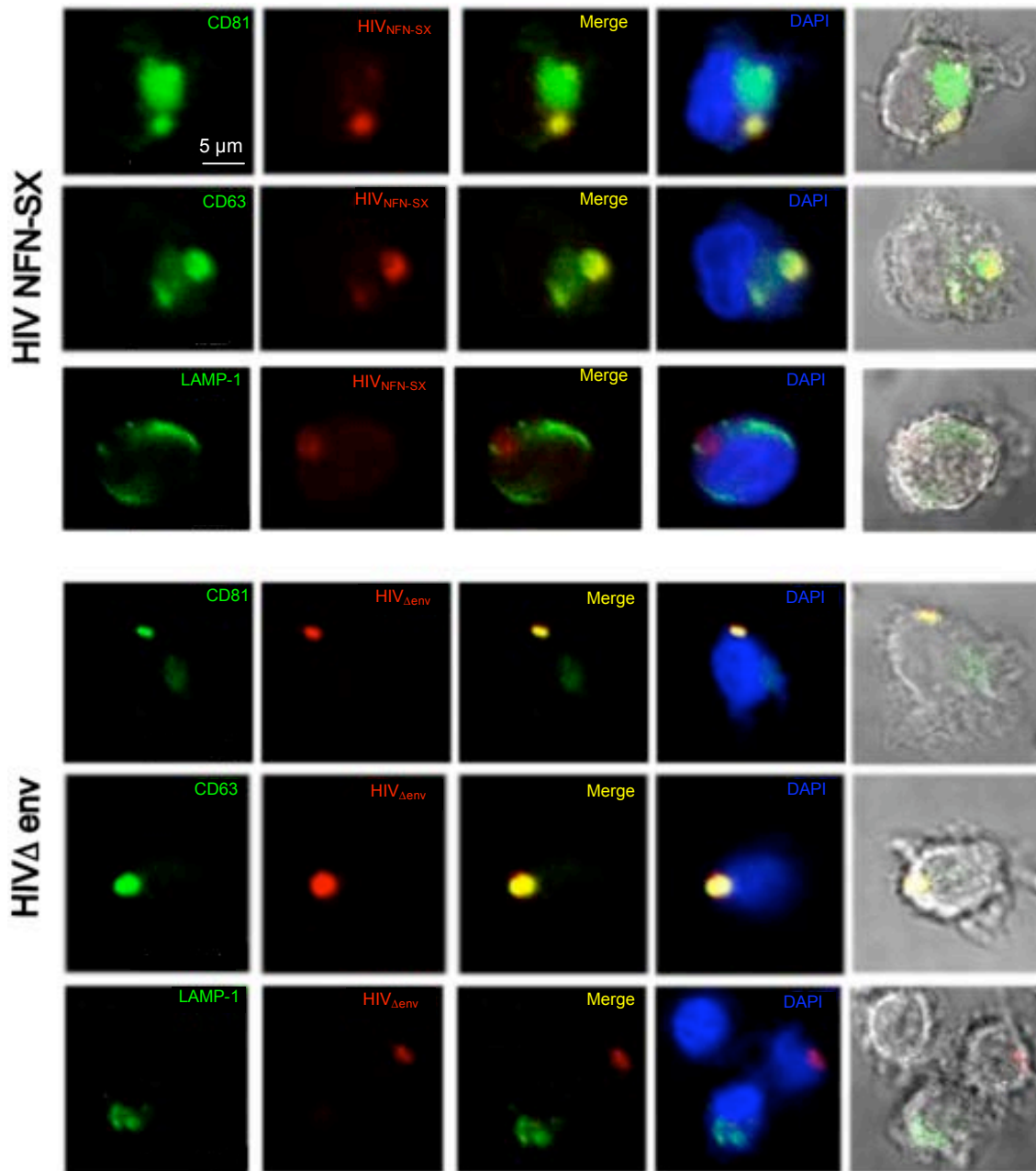


Figure 35. Mature Myeloid DCs retain HIV_{NFN-SX} and HIV_{Δenv-NL4-3} in a CD81⁺ and CD63⁺ compartment. Images show, from left to right, individual green and red fluorescence and the combination of both, either alone, merged with DAPI or with bright-field cellular shape. **(Top)** Confocal images of a section of mature Myeloid DCs exposed to HIV_{NFN-SX} for four hours, fixed and permeabilized to stain them with DAPI and p24^{Gag} (RD1). Cells were labeled in parallel for CD81, CD63 or LAMP-1 (all conjugated with FITC). **(Bottom)** Confocal images of a section of mature Myeloid DCs exposed to HIV_{Δenv-NL4-3} for four hours, fixed and permeabilized to stain them with DAPI and p24^{Gag} (RD1). Cells were labeled in parallel for CD81, CD63 or LAMP-1 (all conjugated with FITC).

9. mDC viral capture is not mediated through pinocytosis and requires cholesterol

We then asked whether pinocytosis events could determine the enhanced viral capture efficiency of mature DCs. We confirmed a greater macropinocytic capacity of iDCs compared to mDCs by analyzing the capture of dextran particles labeled with Alexa 488 (Fig. 36A). FACS analysis revealed that both cell types showed similar capacities to bind to dextran at 4°C. However, active dextran pinocytosis was higher at 37°C in iDCs. These preliminary data suggested that pinocytosis does not account for the enhanced viral capture observed in mature DCs. Previous work has shown that β -methyl-cyclodextrin (β MCD), a cholesterol-sequestering reagent, efficiently blocks iDC viral binding and capture (86). Therefore, we addressed whether cholesterol could also play a role during mDC viral capture.

We first checked mDC viability in the presence of β MCD with a flow cytometer, labeling cells with propidium iodide and DIOC-6 to analyze the drug induction of necrosis and apoptosis (Fig. 36B). We confirmed that mDCs were not affected by β MCD until we reached a concentration of 10 mM. We then measured the effect of β MCD on mDC viral capture at 37°C by employing nontoxic increasing concentrations of the drug. We found a dose-dependent inhibition of mDC active viral capture, reaching levels similar to those of viral binding observed at 4°C (Fig. 36C). Thus, mDC viral capture is a temperature-sensitive process that can be blocked by β MCD.

To assess the specificity of β MCD and exclude the possibility that it could be affecting other endocytic cellular pathways aside from lipid rafts, we analyzed the effect that this drug had on mDC pinocytosis by using dextran labeled with Alexa 488 (Fig. 36D). We found no significant effect of β MCD on

mDC macropinocytosis when we compared fluorescence intensities of pinocytosed dextran in mDCs exposed to increasing concentrations of the drug to those of mock-treated cells. This finding further supported our preliminary data indicating that mDC viral capture does not take place through pinocytosis.

Finally, to analyze β MCD activity for clathrin-mediated endocytosis, we employed transferrin labeled with Alexa 555, a control that is known to enter the cell through a clathrin mediated pathway. We pulsed mDCs previously exposed to β MCD or mock treated with transferrin at 4°C to allow binding to the cellular surface. We then washed away unbound transferrin, leaving part of the cells at 37°C to incorporate labeled ligands for thirty minutes and keeping the rest of the cells at 4°C to obtain binding controls. Cells were then fixed and analyzed by confocal microscopy (Fig. 36E). mDCs exposed to β MCD at 2.5 mM had almost no inhibition of transferrin uptake, which was absent for some of the donors tested and never exceeded 20% inhibition (Fig. 36E). However, cells exposed to β MCD at 5 mM showed inhibition of transferrin uptake, indicating that this drug has collateral effects on mDC clathrin-mediated endocytosis. Thus, we can conclude that β MCD at 2.5 mM blocks mDC viral capture by affecting cholesterol pathways to a higher extent than clathrin-mediated endocytosis.

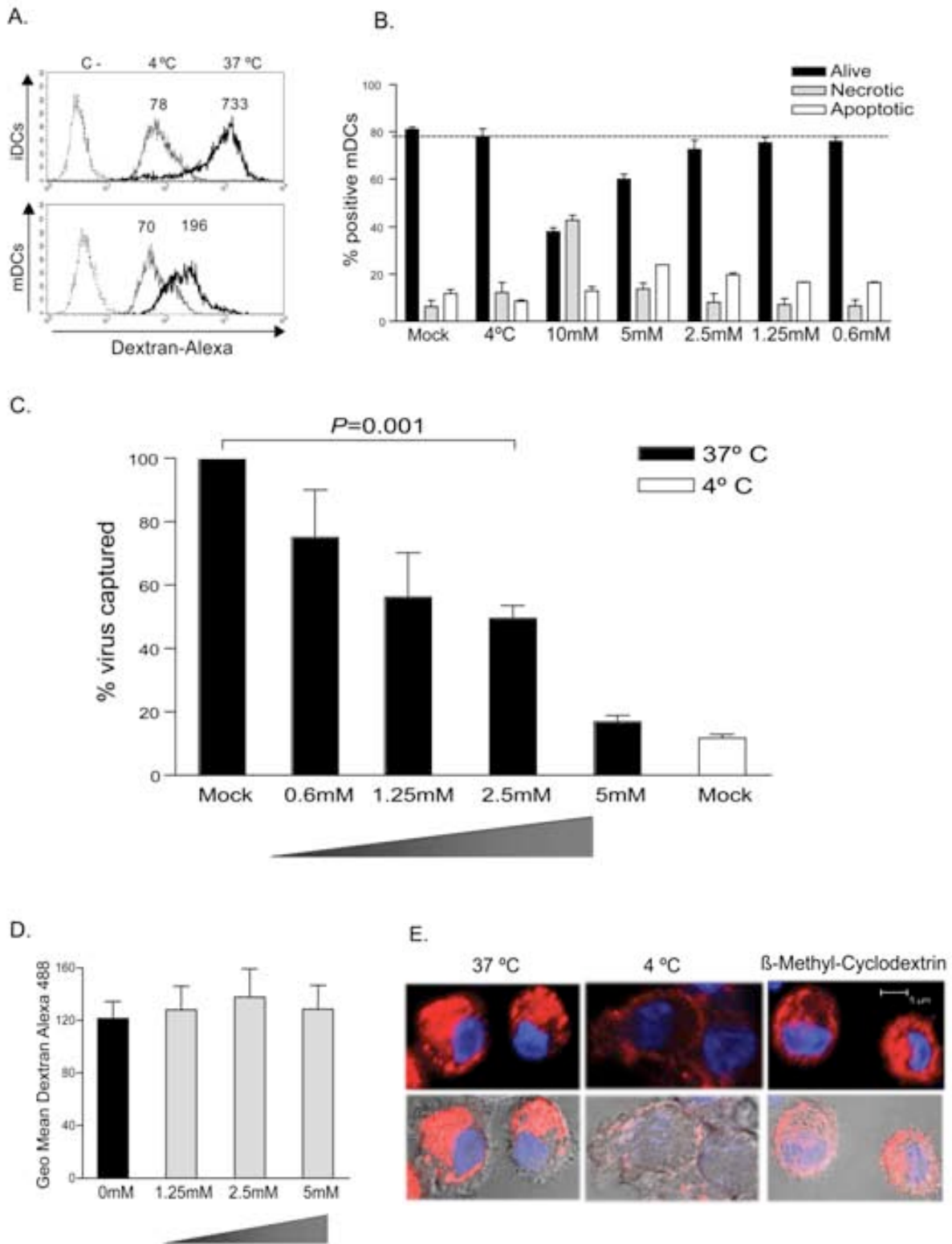


Figure 36. Caption overleaf.

Figure 36. (From previous page). mDC viral capture is not mediated through pinocytosis and depends on cholesterol-enriched domains. (A) Increased macropinocytosis of dextran labeled with Alexa 488 in iDCs *versus* mDCs. Thin histograms represent dextran binding at 4°C and thick histograms represent dextran capture at 37°C. Numbers above the peaks of the histograms indicate geometric mean (Geo mean) fluorescence intensities. The negative control was done in the absence of dextran (dotted histograms). **(B and C)** mDCs were preincubated with increasing concentrations of β -methylcyclodextrin (β MCD) below observed toxic concentrations (B). (C) Viral capture was inhibited in a dose-dependent manner, reaching statistical significance at 2.5 mM ($P=0.001$, paired t test). **(D)** mDCs were preincubated with increasing concentrations of β MCD for thirty minutes at 37°C and dextran was then added to measure macropinocytosis at 37°C. Geo mean fluorescence intensity for each condition is graphed, subtracting negative controls done in the absence of dextran but with the β MCD concentrations indicated. **(E)** Confocal images of a single plane of mDCs exposed to transferrin Alexa 555 at 4°C for one hour and then shifted to 37°C (where transferrin bound to its receptor is able to enter through clathrin-mediated endocytosis) or left at 4°C (as a control for transferrin external binding). Previous treatment of mDCs with 2.5 mM β MCD did not substantially affect transferrin clathrin-mediated endocytosis.

5.

Results II:

Capture & Transfer of HIV-1 Particles
by Mature DCs Converges with the
Exosome Dissemination Pathway

Exosomes are secreted cellular organelles that can be internalized by dendritic cells contributing to antigen-specific naïve CD4⁺ T cell activation. In this chapter, we demonstrate that HIV-1 can exploit this exosome antigen-dissemination pathway intrinsic to mature DCs to mediate *trans*-infection of T lymphocytes. Capture of HIV-1, HIV-1 Gag-eGFP viral-like particles (VLPs) and exosomes by DCs was upregulated upon maturation, resulting in localization within a CD81⁺ compartment. Uptake of VLPs or exosomes could be inhibited by a challenge with either particle, suggesting that the expression of common determinants in the VLP or exosome surface is necessary for internalization by mDCs. Capture by mDCs was insensitive to proteolysis but blocked when virus, VLPs or exosomes were produced from cells treated with sphingolipid biosynthesis inhibitors that modulate the lipid composition of the budding particles. Finally, VLPs and exosomes captured by mDCs were transmitted to T lymphocytes in a manner independent of the envelope glycoprotein, underscoring a new potential viral dissemination pathway in which HIV-1 and exosomes converge.

The present study suggests that HIV and other retroviruses might be exploiting a preexisting exosome dissemination pathway intrinsic to mature DCs, permitting viral transmission to CD4⁺ T cells.

I. Results

1. Maturation of DCs enhances VLP and exosome capture

In the previous chapter, we identified an HIV envelope glycoprotein-independent mechanism for viral binding and capture that does not rely on CD4 and C-type lectin receptors expressed on the DC surface. To characterize the molecular determinants required for this highly efficient viral capture mechanism that is upregulated upon DC maturation, we employed eGFP-expressing fluorescent virus-like particles (VLP_{HIV-Gag-eGFP}). Expression of the HIV Gag protein alone is sufficient for virus-like particle assembly and budding (71, 75, 155, 232), and GFP-tagged forms of HIV Gag have been previously used to follow virus particle biogenesis (189, 190).

We pulsed immature and mature monocyte-derived DCs (iDCs and mDCs respectively) with VLP_{HIV-Gag-eGFP} for four hours at 37°C, fixed the cells and determined the percentage of eGFP⁺ cells by FACS. Similar to our previously reported findings with infectious HIV-1 particles (Fig. 25A), VLP capture was enhanced in mDCs compared to iDCs derived from the same donors, suggesting a differential active virus capture process in mDCs ($P < 0.0001$, paired t test; Fig. 37A and B). We also confirmed equivalent upregulation of VLP capture with LPS-matured CD1c⁺ (BDCA-1) blood

Myeloid DCs (Fig. 37C). Furthermore, DCs matured in the presence of poly I:C (a TLR3 ligand) were comparable to LPS-matured DCs in their ability to capture $VLP_{HIV-Gag-eGFP}$, suggesting a maturation signal-independent upregulation of HIV-1 internalization in mDCs (Fig. 37D). To further determine whether mDC-mediated capture was not merely a size-regulated process, DCs were incubated with virus-size carboxylated fluorescent beads of 100 nm diameter. We employed a concentration of beads displaying similar binding profiles at 4°C in iDCs and mDCs (Fig. 38A). However, fluorescent bead capture was downregulated upon maturation, as the percentage of mDCs able to capture these beads at 37°C was lower than of iDCs ($P=0.0042$, paired t test; Fig. 38A and B).

In light of this result, we decided to determine whether exosomes that are also derived from cholesterol-enriched membrane microdomains (23, 65) can incorporate mDC-recognition determinants and be captured by mDCs through a mechanism similar to that exhibited by $VLP_{HIV-Gag-eGFP}$. Immature and mature DCs were pulsed with DiI-labeled exosomes released from Jurkat T cells ($Exosomes_{DiI}$) for four hours at 37°C, then fixed and analyzed by FACS to determine the percentage of DiI^+ cells. Similar to $VLP_{HIV-Gag-eGFP}$ capture, mDCs were much more efficient than iDCs at capturing exosomes ($P<0.0001$, paired t test; Fig. 39). Overall, these results demonstrate that the capture of $VLP_{HIV-Gag-eGFP}$ and $Exosomes_{DiI}$ is upregulated upon DC maturation, and that this uptake mechanism is not merely a size-regulated process, but rather requires the specific surface constituents of $VLP_{HIV-Gag-eGFP}$ and $Exosomes_{DiI}$.

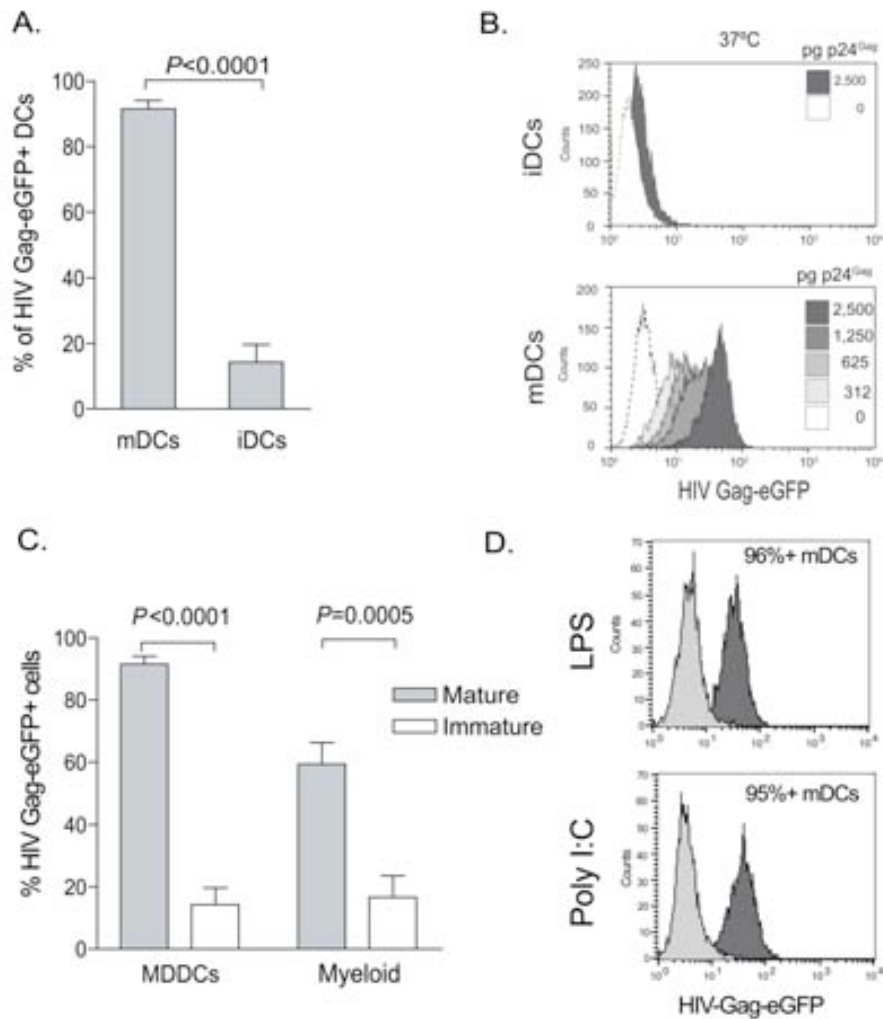


Figure 37. Maturation of DCs enhances VLP_{HIV-Gag-eGFP} capture. **(A)** Comparative capture of VLP_{HIV-Gag-eGFP} by DCs. A total of 1×10^5 DCs were pulsed for four hours at 37°C with 2,500 pg p24^{Gag} in 0.1 ml, washed with PBS and fixed, to analyze the percentage of eGFP⁺ cells by FACS. Data show the mean values and SEM from five independent experiments. Mature MDDCs (mDCs) capture significantly larger amounts of VLPs compared to immature MDDCs (iDCs), ($P < 0.0001$, paired t test, $n=6$). **(B)** Capture profile of increasing numbers of VLPs_{HIV-Gag-eGFP} by iDCs and mDCs over two hours at 37°C. Maturation of DCs resulted in increased VLP capture at 37°C compared to iDCs, and this capture was dose-dependent. Histograms show a representative capture profile of iDCs (top) and mDCs (bottom) at 37°C. **(C)** Comparative capture of VLP_{HIV-Gag-eGFP} by MDDCs and blood Myeloid DCs. Cells were pulsed as in (A). Data show the mean values and SEM from six independent experiments. Mature DCs capture significantly larger quantities of VLPs compared to immature DCs (P values on the graph, paired t test, $n=6$). **(D)** Capture profile of VLP_{HIV-Gag-eGFP} by mDCs matured in the presence of LPS and Poly I:C is similar at 37°C. Histograms show a representative capture profile of mDCs from the same seronegative donor matured in parallel.

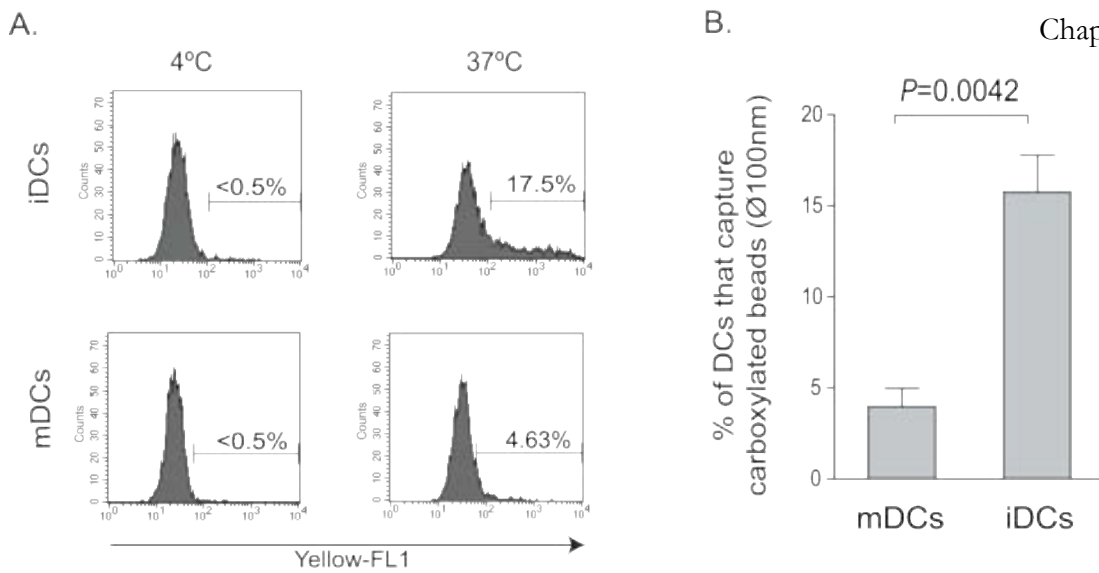


Figure 38. Maturation of DCs diminishes carboxylated bead capture. (A) Binding profile of carboxylated yellow fluorescent beads (comparable in size to HIV-1 particles – approximately 100 nm diameter) by iDCs and mDCs is similar at 4°C. However, maturation of DCs resulted in diminished bead capture at 37°C. Histograms show a representative binding and capture profile for iDCs and mDCs at 4°C and 37°C, respectively. (B) Comparative capture of carboxylated yellow fluorescent beads by DCs. A total of 5×10^5 iDCs and mDCs were incubated at 4°C and 37°C for two hours with approximately 1.8×10^{10} beads. Cells were washed, fixed and analyzed by FACS. The graph displays the percentage of DCs capturing beads at 37°C, after subtracting binding percentages at 4°C. Data show the mean values and SEM from four independent experiments including cells from seven donors. iDCs capture significantly larger quantities of beads than mDCs ($P=0.0042$, paired t test).

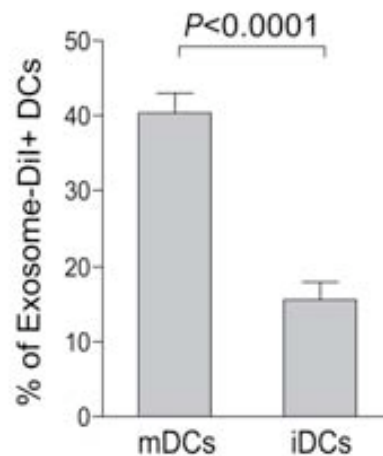


Figure 39. Maturation of DCs enhances Exosome_{Dil} capture. Comparative capture of Jurkat derived Exosomes_{Dil} by DCs. A total of 1×10^5 DCs were pulsed for eight hours at 37°C with 150 μg exosomes, washed with PBS and fixed to analyze the percentage of Dil⁺ cells by FACS. Data show the mean values and SEM from four independent experiments including cells from eleven donors. mDCs capture significantly larger amounts of exosomes than iDCs ($P<0.0001$, paired t test).

2. Competition experiments suggest that different particles derived from cholesterol-enriched domains use the same entry pathway into mDCs

To determine whether $\text{VLP}_{\text{HIV-Gag-eGFP}}$ and $\text{Exosomes}_{\text{DiI}}$ share a common entry mechanism, we performed different competition experiments. Mature DCs were preincubated with increasing quantities of $\text{Exosomes}_{\text{DiI}}$ and subsequently pulsed with a constant amount of $\text{VLP}_{\text{HIV-Gag-eGFP}}$ for one hour at 37°C. Cells were then washed and we determined the percentage of eGFP and DiI-positive cells by FACS. Pre-incubation of mDCs with increasing amounts of $\text{Exosomes}_{\text{DiI}}$ resulted in a dose-dependent decrease in the percentage of $\text{VLP}_{\text{HIV-Gag-eGFP}}$ positive cells (Fig. 40A, $P=0.0078$, paired t test). In contrast, pre-incubating cells with increasing numbers of virus-size fluorescent carboxylated beads resulted in no reduction in the ability of mDCs to capture envelope-glycoprotein-deficient $\text{HIV}_{\Delta\text{env-NL4-3}}$ (Fig. 40B). Hence, the competition observed between $\text{Exosomes}_{\text{DiI}}$ and $\text{VLP}_{\text{HIV-Gag-eGFP}}$ suggests that both particles use a common saturable entry mechanism to gain access to mDCs.

Since most retroviruses, including ecotropic murine leukemia virus (MLV) also bud from lipid raft-like plasma membrane domains (37), binding of $\text{VLP}_{\text{HIV-Gag-eGFP}}$ to mDCs was competed by incubation either with non-fluorescent HIV-1 particles lacking the envelope glycoprotein ($\text{HIV}_{\Delta\text{env-Bru}}$) or with ecotropic envelope glycoprotein expressing MLV Gag VLPs ($\text{VLP}_{\text{MLV-Gag}}$). Pre-incubation of mDCs with unlabeled $\text{HIV}_{\Delta\text{env-Bru}}$ or $\text{VLP}_{\text{MLV-Gag}}$ significantly reduced the percentage of mDCs able to capture $\text{VLP}_{\text{HIV-Gag-eGFP}}$ in a dose-dependent manner (Fig. 40C and D, P values on the graphs, paired t test). Notably, unlabeled $\text{HIV}_{\text{NL4-3}}$ particles derived from different T cell lines and

stimulated PBMCs were also able to reduce the percentage of mDCs capturing VLP_{HIV-Gag-eGFP} (Fig. 40E). In contrast, pre-incubating mDCs with increasing concentrations of Pronase-treated G protein-deficient VSV particles – known to bud from non-raft membrane microdomains (37) – showed no reduction in the ability of mDCs to capture VLP_{HIV-Gag-eGFP} (Fig. 40F). These results suggest that virus particles or exosomes derived from lipid raft-like plasma membrane domains have a common entry mechanism into mDCs.

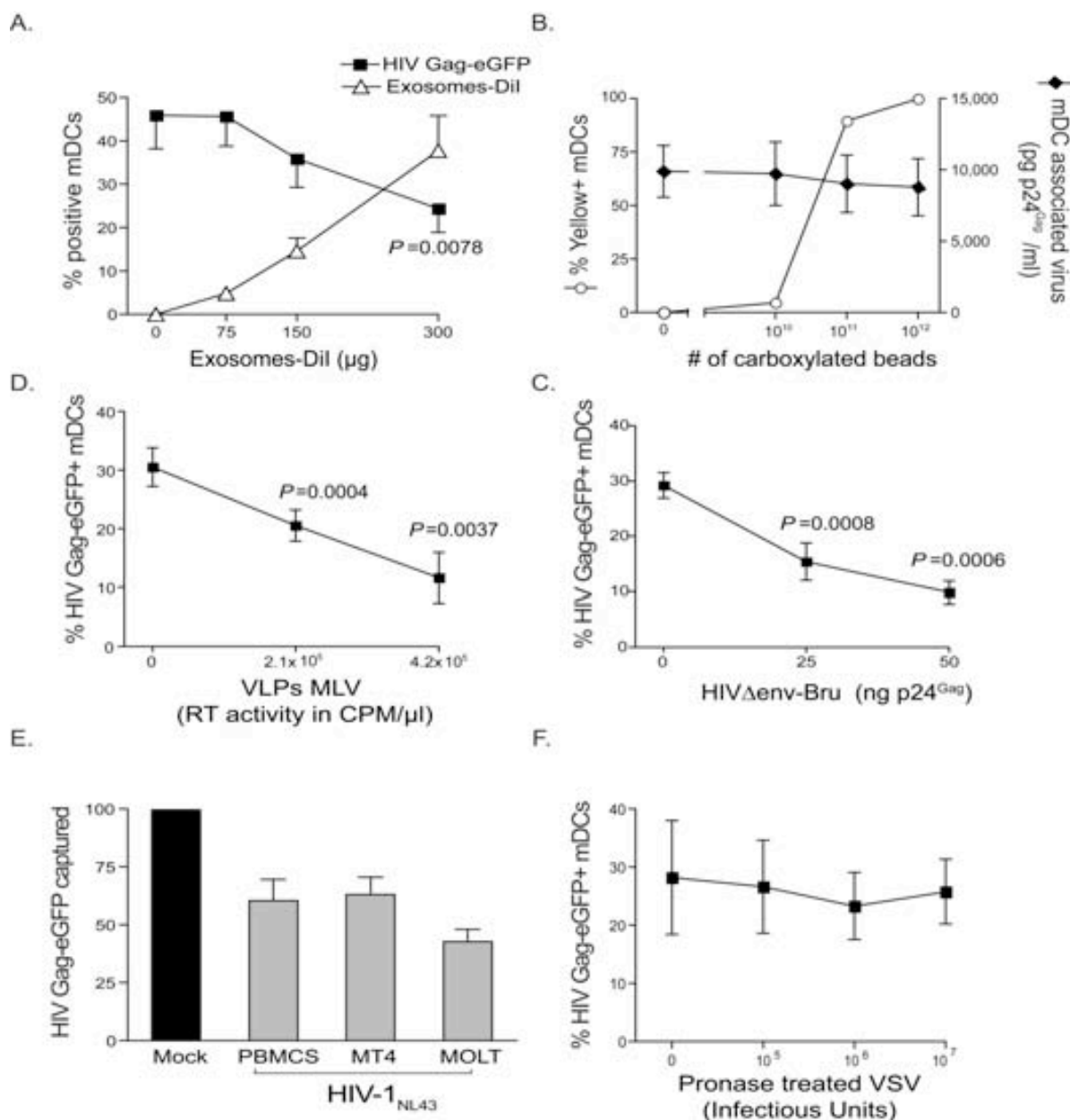


Figure 40. Caption overleaf.

Figure 40. (From previous page). Competition experiments suggest that different particles derived from cholesterol-enriched domains use the same entry pathway into mDCs. (A) Capture of VLP_{HIV-Gag-eGFP} by mDCs previously exposed to increasing quantities of Jurkat derived Exosomes_{DiI}. Cells were preincubated for thirty minutes with increasing amounts of Exosomes_{DiI} and then pulsed with 625 pg of VLP_{HIV-Gag-eGFP} p24^{Gag} for one hour at 37°C, washed with PBS, fixed and analyzed by FACS to determine the percentage of eGFP and DiI positive cells. mDCs capture fewer VLP_{HIV-Gag-eGFP} in the presence of increasing quantities of Exosomes_{DiI} ($P=0.0078$, paired t test). **(B)** Capture of HIV_{Δenv-NL4-3} by mDCs previously exposed to increasing numbers of yellow carboxylated 100 nm beads. A total of 5×10^5 mDCs were preincubated thirty minutes with the beads, pulsed for one hour at 37°C with 130 ng of HIV_{Δenv-NL4-3} p24^{Gag} in 0.5 ml and then extensively washed with PBS. Each sample was then divided and either fixed for analysis by FACS for bead capture or lysed with 0.5% Triton (at a final concentration of 5×10^5 cells per ml) to measure p24^{Gag} content in the cell lysate by ELISA. Results represent the percentage of yellow positive mDCs (circles) and the quantity of pg of p24^{Gag} bound per ml of cell lysate (diamonds). **(C–D)** Capture of VLP_{HIV-Gag-eGFP} by mDCs previously exposed to increasing amounts of HIV_{Δenv-Bru} (C) and VLP_{MLV-Gag} (D). Cells were preincubated for thirty minutes with increasing amounts of HIV_{Δenv-Bru} or VLP_{MLV-Gag} and then pulsed with 625 pg of VLP_{HIV-Gag-eGFP} p24^{Gag} for one hour at 37°C, washed with PBS and fixed to analyze the percentage of eGFP positive cells by FACS. mDCs capture less VLP_{HIV-Gag-eGFP} in the presence of increasing concentrations of particles derived from cholesterol-enriched membrane microdomains (P values on the graphs, paired t test). **(E)** The data represent the relative VLP_{HIV-Gag-eGFP} capture by mDCs that had been preincubated with 200 ng of HIV_{NL4-3} p24^{Gag} obtained from either MT4, MOLT 4 or PHA-stimulated PBMCs, and normalized to the level of VLP_{HIV-Gag-eGFP} capture by mock-treated mDCs (set at 100%). mDCs capture less VLP_{HIV-Gag-eGFP} in the presence of these different viral stocks. **(F)** Capture of VLP_{HIV-Gag-eGFP} by mDCs that had been preincubated with increasing amounts of Pronase-treated VSV particles. Cells were preincubated for thirty minutes in the presence of Pronase-treated VSV particles and then pulsed with the 625 pg of VLP_{HIV-Gag-eGFP} p24^{Gag} for one hour at 37°C, washed with PBS, and fixed to analyze the percentage of eGFP⁺ cells by FACS. mDCs capture similar amounts of VLP_{HIV-Gag-eGFP} in the presence of Pronase-treated VSV particles. Panels A through F show mean values and SEM from three independent experiments including cells from at least four different donors.

3. Mature DCs retain HIV-1, VLPs and exosomes within the same CD81⁺ intracellular compartment

To gain further insight into this capture mechanism, we monitored mDCs pulsed in parallel with HIV_{NL4-3}, VLP_{HIV-Gag-eGFP} and Exosomes_{DII} by electron microscopy (Fig. 41A–D). Most of the mDC-associated particles were found in similar intracellular compartments. Furthermore, when mDCs pulsed simultaneously with HIV_{NL4-3} and Exosomes_{DII} were analyzed, particles displaying viral and exosomal morphology could be found within the same compartment (Fig. 42A–C).

Confocal microscopy of mDCs pulsed simultaneously with Exosomes_{DII} and the vpr-eGFP containing fluorescent wild type virus HIV-1_{NL4-3/vpr-eGFP} or VLP_{HIV-Gag-eGFP} also revealed that both virus and VLPs co-localized with exosomes in the same intracellular compartment (Figs. 41E and F, 42D–G and Videos 2 and 3, which can be found in the supplementary CD). Similar to HIV-1 trafficking in DCs – (74) and Fig. 35 – VLP_{HIV-Gag-Cherry} and Exosomes_{DII} also accumulated in intracellular vesicular compartments co-localizing with the CD81 tetraspanin but not with the LAMP-1 lysosomal marker (Fig. 41G and H).

Previously, other researchers and we have characterized that β -methylcyclodextrin, a cholesterol-sequestering reagent, can block DC viral capture by affecting cellular lipid raft endocytic pathways – (86) and (Fig. 36). Interestingly, pretreatment of mDCs with amantadine and chlorpromazine, classical clathrin-mediated endocytosis inhibitors, also blocked VLP_{HIV-Gag-eGFP} uptake (Fig. 43 and Video 4 in the supplementary CD). Therefore, HIV and exosome trafficking within mDCs relies on active endocytosis that leads captured particles to the same CD81⁺ compartments.

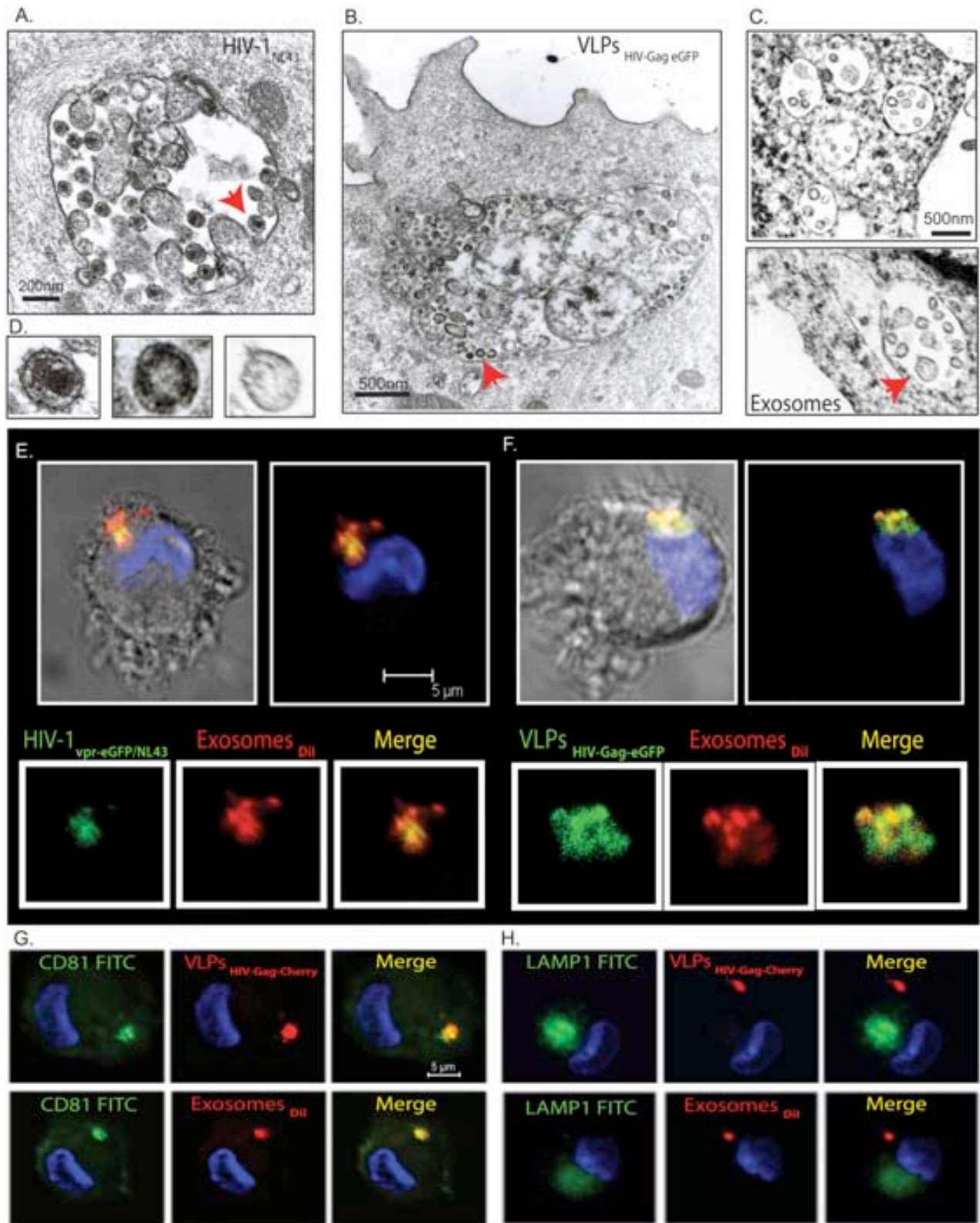


Figure 41. Caption overleaf.

Figure 41. (From previous page) mDCs retain HIV-1, VLPs and exosomes in the same CD81⁺ intracellular compartment (A–C) Electron micrographs of mDC sections exposed in parallel to HIV_{NL4-3}, VLP_{HIV-Gag-eGFP} and Exosomes_{Dil}, showing similar large vesicles containing these particles. Arrows indicate captured particles magnified in **(D)**, where comparative micrographs show, from left to right: HIV_{NL4-3}, VLP_{HIV-Gag-eGFP} and a Jurkat derived exosome. **(E)** Confocal images of a section of a mDC exposed to HIV_{NL4-3/vpr-eGFP} and Exosomes_{Dil} for four hours and stained with DAPI. The top images show the mDC red and green fluorescence merged with DAPI, either with or without the bright field cellular shape. The bottom images show magnification of vesicles containing these particles and depict individual green and red fluorescence and the combination of the two. **(F)** Confocal images of a section of a mDC exposed to VLP_{HIV-Gag-eGFP} and Exosomes_{Dil} as described in **(E)**. **(G)** Confocal images of a section of a mDC exposed to red fluorescent VLP_{HIV-Gag-Cherry} (top) or Exosomes_{Dil} (bottom) in parallel for four hours, fixed and then permeabilized to stain with DAPI and FITC-CD81. Images shown, from left to right, depict individual green and red fluorescence channels and the combination of both merged with DAPI. **(H)** Confocal images obtained as in **(G)**, except that cells were stained with DAPI and FITC-LAMP-1. mDCs retain VLP_{HIV-Gag-eGFP} and Exosomes_{Dil} in a CD81⁺ LAMP1⁻ compartment.

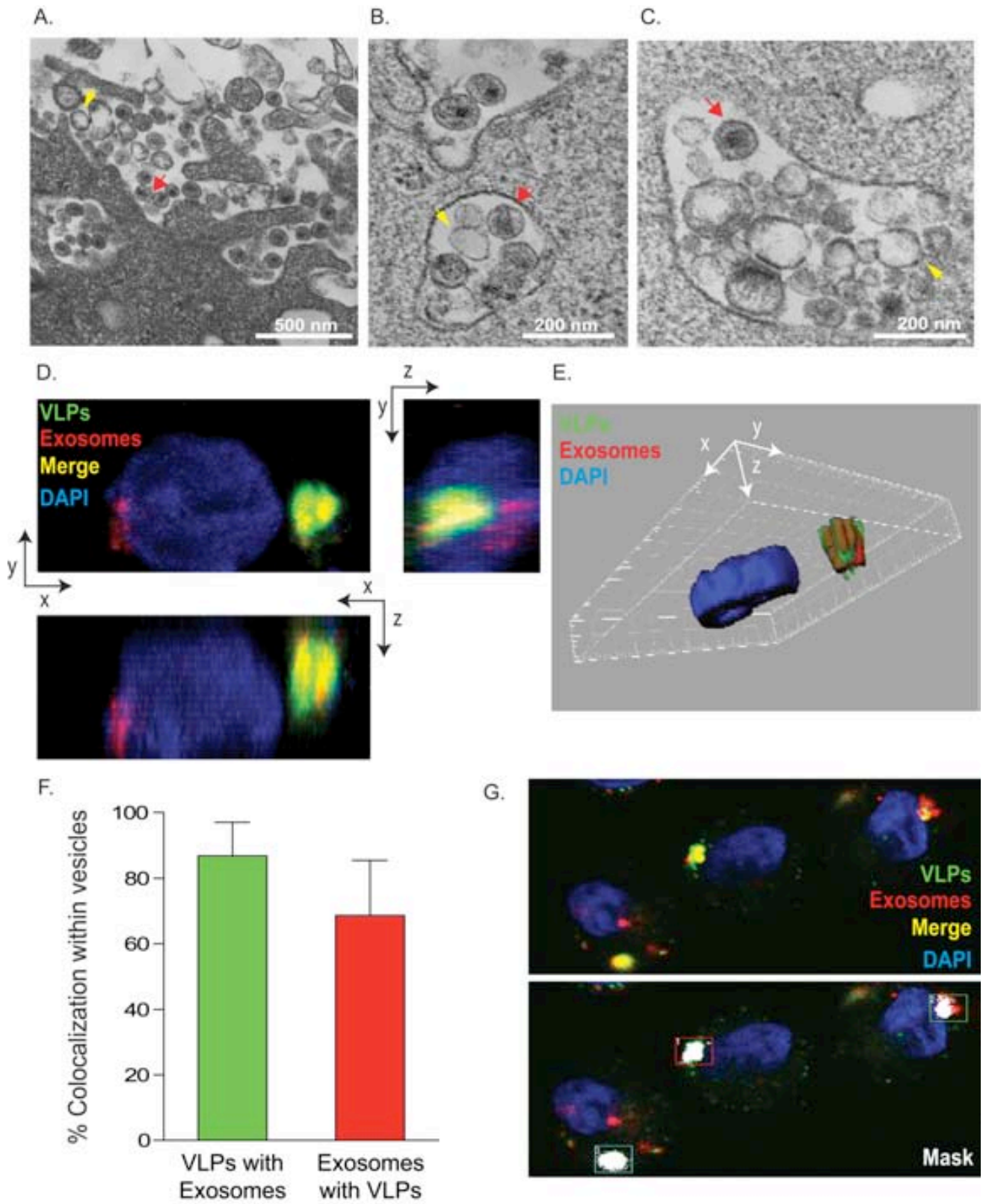
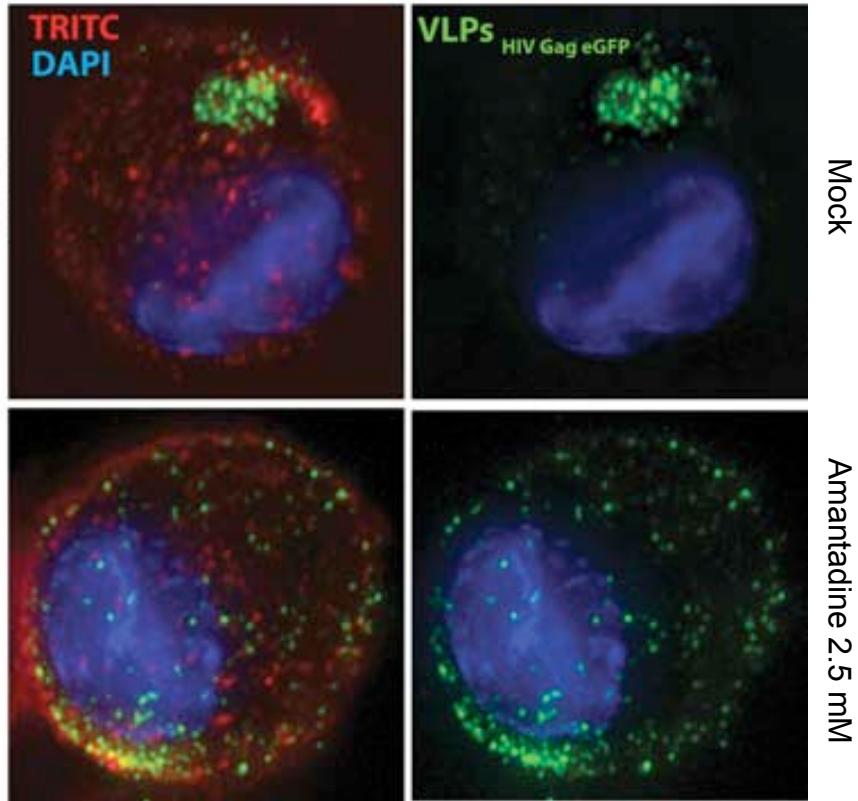


Figure 42. Caption overleaf.

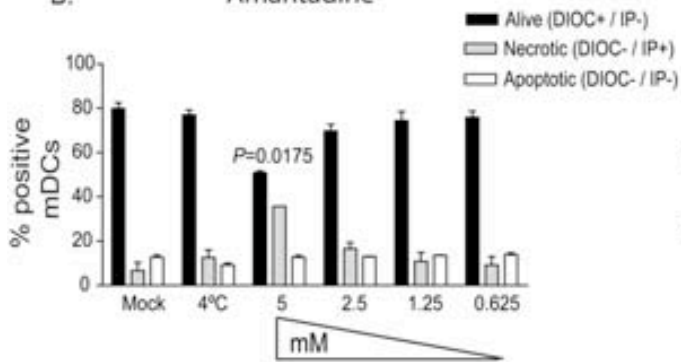
Figure 42. (From previous page). (A–C) mDCs accumulate HIV, VLPs and exosomes within the same intracellular compartment. Electron microscopy images of mDCs simultaneously pulsed with HIV_{NI4.3} and Exosomes_{DII}. Particles displaying viral morphology (with an electro-dense core: red arrows) or exosome morphology (with lighter core: yellow arrows) accumulated in the same area of the membrane (A) or within the same vesicles (B and C). **(D–G) Confocal microscopy analysis of mDCs pulsed simultaneously with VLP_{HIV-Gag-eGFP} and Exosomes_{DII}, then stained with DAPI. (D)** Composition of a series of x–y sections of a mDC collected through part of the cell nucleus and projected onto a two-dimensional plane to show the x–z plane (bottom) and the y–z plane (right). VLP_{HIV-Gag-eGFP} and Exosomes_{DII} accumulated within the same compartment. **(E)** Isosurface representation of the cell shown in (D), computing the nucleus and vesicle surfaces within a three-dimensional volumetric x–y–z data field. **(F)** Quantification of the percentage of VLP_{HIV-Gag-eGFP} co-localizing with Exosomes_{DII} and *vice versa*, obtained by analyzing 35 mDC vesicles from three different donors. The mean and SD of the Manders and Pearson correlation coefficients (obtained considering all the images) were 0.84 ± 0.08 and 0.75 ± 0.1 respectively, indicating co-localization. **(G)** Confocal images depicting vesicles analyzed in (F), where the green, red and blue fluorescences are merged (top), or with the vesicles marked in regions of interest (squares) showing the white mask of overlapping fluorescence signals (bottom).

A.



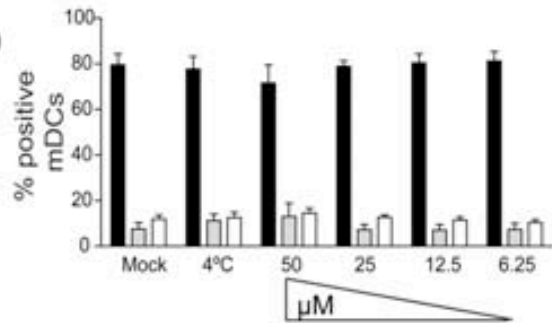
B.

Amantadine



C.

Chlorpromazine



D.

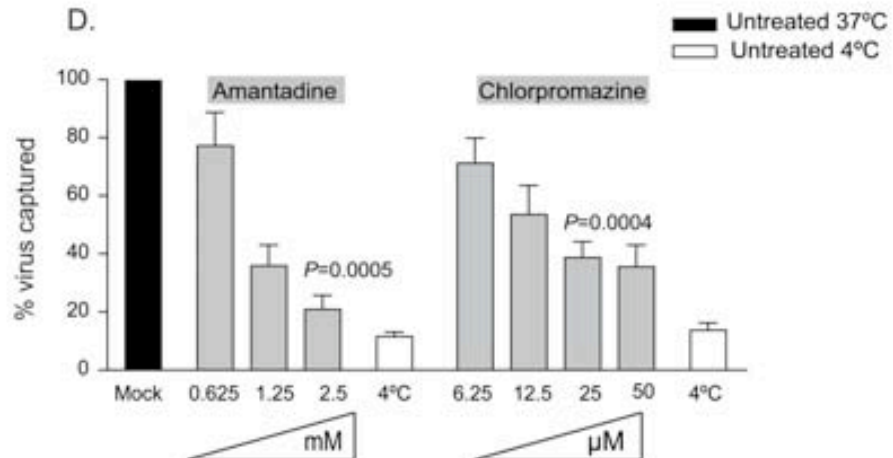


Figure 43. Caption overleaf.

Figure 43. (From previous page) Effect of amantadine and chlorpromazine treatment in viral capture mediated by mDCs. (A) Fluorescent microscopy images of control mDCs compared to mDCs treated with 2.5 mM amantadine. The left panels show a projection of stacked images obtained by merging the red, blue and green fluorescence of mDCs exposed to VLPs_{HIV-Gag-eGFP} for two hours at 37°C and then labeled with DAPI and TRITC-wheat germ agglutinin (to stain the cell membrane). Video 4 in the supplementary CD compares control cells to amantadine treated mDCs. The right panels show a projection of stacked images obtained by merging only the blue and green fluorescence. **(B)** mDC viability in the presence of increasing concentrations of amantadine was not compromised until cells were incubated with 5 mM amantadine ($P=0.0175$, one sample t test). Cells were labeled with propidium iodide and DIOC-6 to analyze the drug induction of necrosis and apoptosis with FACS. **(C)** Viability in the presence of increasing concentrations of chlorpromazine assessed as in panel (B). **(D)** Percentage of HIV_{NFN-SX} captured by amantadine and chlorpromazine treated mDCs relative to untreated cells normalized to 100% of viral capture at 37°C. mDCs were pre-incubated with increasing concentrations of amantadine and chlorpromazine, exposed to the virus and lysed in 0.5% Triton to measure the cell-associated p24^{Gag} by ELISA. Viral capture was inhibited in a dose-dependent manner, reaching statistical significance at 2.5 mM of amantadine and 25 μ M of chlorpromazine (P values on the graph, paired t test). Data show the mean values and SEM from six donors and two independent experiments for each compound.

4. Mechanism of VLP and exosome uptake in mDCs is dose-dependent and increases over time, allowing efficient transfer to target CD4⁺ T cells

To further characterize the kinetics of this specific exosome, HIV and VLP uptake process that is enhanced upon DC maturation, we monitored mDCs exposed to varying amounts of Exosomes_{Dil} and VLP_{HIV-Gag-eGFP} for four to eight hours at 37°C (Fig. 44A and B). Similar to HIV_{NL4-3/vpr-eGFP} capture by mDCs (Fig. 27A), the capture of Exosomes_{Dil} (Fig. 44A) and VLP_{HIV-Gag-eGFP} (Fig. 44B) by mDCs took place in a dose-dependent manner and increased over time. Although the percentage of eGFP⁺ mDCs exposed to VLP_{HIV-Gag-eGFP} reached a plateau during the first four hours of culture (Fig. 44B), we have previously seen that the mDC-associated virus fraction increases over time when viral capture of HIV_{NFN-SX} was assayed by a p24^{Gag} ELISA (Fig. 27C). Therefore, while particle binding to the mDC-surface is a saturable process that can be outcompeted, active endocytosis continues over time.

A number of studies have argued for long-term retention of HIV-1 infectivity within DCs that can be transmitted to CD4⁺ T cells upon contact (144, 226). Accordingly, we decided to address the ability of mDCs to retain captured particles by taking advantage of the fluorescence intensity of the VLP_{HIV-Gag-eGFP}. Mature DCs were pulsed with VLP_{HIV-Gag-eGFP}, washed and then cultured for two days. Cells were periodically harvested and assayed for retention of VLP_{HIV-Gag-eGFP}, as measured by the percentage of eGFP⁺ cells left in the culture (Fig. 44C; *P* values on the graph, one sample t test). Though there is a steady decline in the percentage of eGFP⁺ cells over time, the results in Fig. 44C suggest that a significant percentage of mDCs retain VLP_{HIV-Gag-eGFP} for at least two days.

Since mDCs are extremely efficient at transmitting captured HIV-1 particles to CD4⁺ T cells (81, 138, 191), we wanted to determine if internalized envelope-glycoprotein-deficient VLP_{HIV-Gag-eGFP} or Exosomes_{DII} could also be transferred to CD4⁺ T cells. We assessed transmission of VLP_{HIV-Gag-eGFP} and Exosomes_{DII} by mDCs to CD4⁺ T cells by fluorescent microscopy. Mature DCs were pulsed with VLP_{HIV-Gag-eGFP} and then co-cultured with Jurkat T cells labeled with a red cell tracker dye. Fluorescent microscopy analysis of projections of stacked images of unconjugated red Jurkat T cells revealed a few VLP_{HIV-Gag-eGFP} per T cell (Fig. 44D). Analysis of conjugated Jurkat T cells with mDCs also revealed VLP_{HIV-Gag-eGFP} polarization at the site of cell-to-cell contact, showing the dramatic rearrangement of VLPs contained in the mDC vesicular compartments to the site of viral synapse upon contact with Jurkat T cells (Fig. 44E and Video 5, which can be found in the supplementary CD).

Similar results were found when analyzing mDCs pulsed with Exosomes_{DII} co-cultured with Jurkat T cells, pre-stained with a green cell tracker dye. We observed unconjugated green Jurkat T cells bearing Exosomes_{DII} (Fig. 44F) and Exosome_{DII} polarization to the site of the DC–T cell contact zone (Fig. 44G). Most of the VLPs or exosomes captured by mDCs were recruited to the DC–T cell contact zone (Fig. 44H) as previously reported for HIV-1 (74, 138).

Overall, these results suggest that VLPs and Exosomes_{DII} captured by mDCs can be transferred to CD4⁺ T cells, mimicking HIV-1 transmission to CD4⁺ T cells during *trans*-infection.

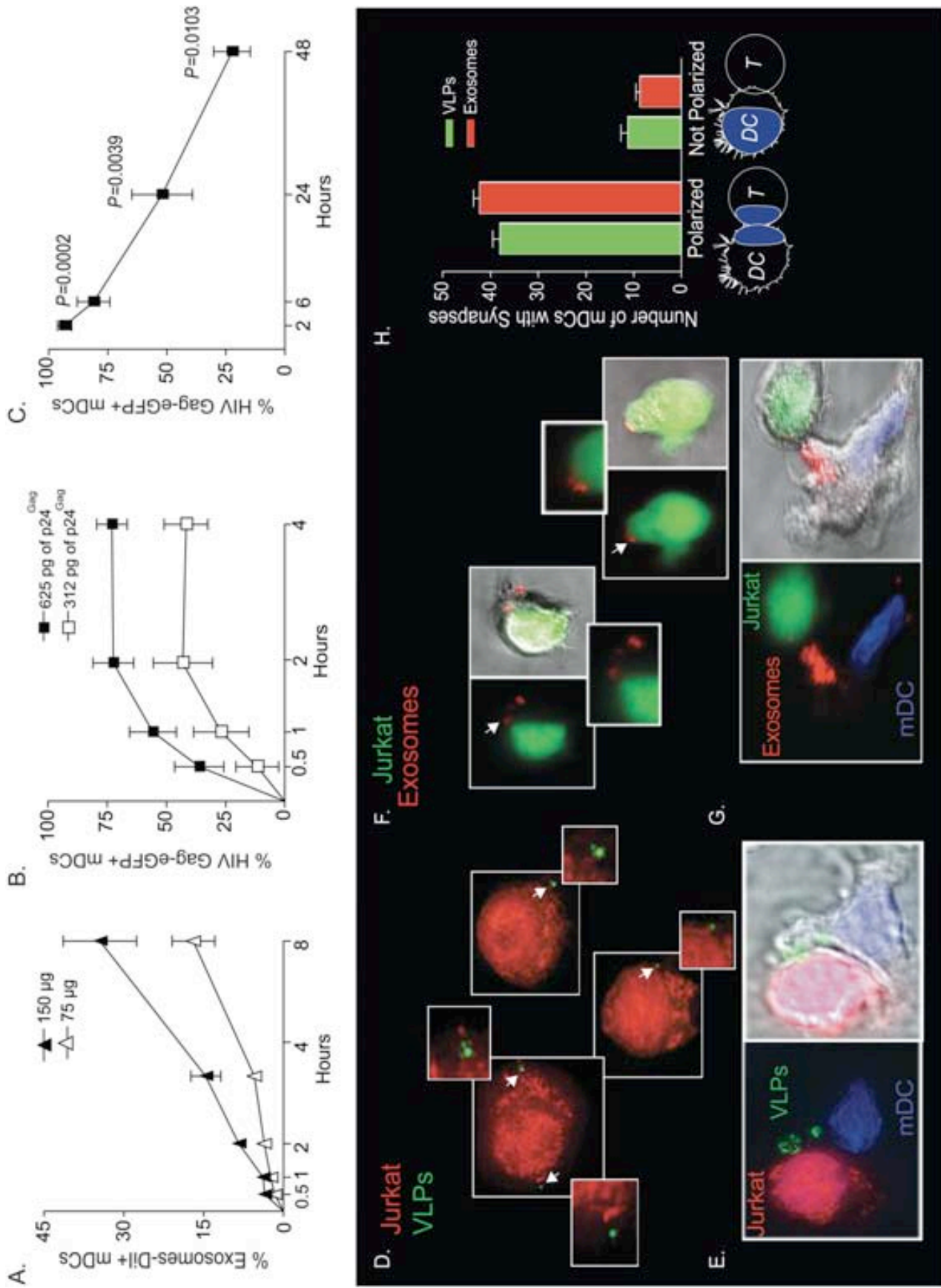


Figure 44. Caption overleaf.

Figure 44. (From previous page) VLP and exosome uptake in mDCs is a dose-dependent mechanism that increases over time, allowing efficient transfer to target CD4+ T cells. (A) Time course of mDCs (n=4) exposed to two different concentrations of Exosomes_{DiI} and fixed at each of the indicated time points and analyzed by FACS. Exosome capture by mDCs increases over time in a dose-dependent manner. **(B)** Time course of mDCs (n=4) exposed to two different concentrations of VLP_{HIV-Gag-eGFP} and fixed at each of the indicated time points and analyzed by FACS. VLP_{HIV-Gag-eGFP} capture by mDCs increases over time in a dose-dependent manner. **(C)** Fate of VLP_{HIV-Gag-eGFP} captured by mDCs and followed by flow cytometry for two days. Graph shows the percentage of Gag-eGFP⁺ cells measured by FACS at the indicated time points. *P* values on the graph reveal that 48 hours after pulse with VLP_{HIV-Gag-eGFP}, a significant percentage of mDCs still retained VLPs (one sample t test). Data (mean and SEM from three independent experiments) include cells from four different donors. **(D)** Red cell tracker dye-labeled Jurkat T cells were analyzed by deconvolution microscopy after four hours of co-culture with mDCs previously pulsed with VLP_{HIV-Gag-eGFP} and extensively washed before co-culture. The cells shown in the panels are projections of stacked images obtained by merging the red and green fluorescence. Arrows indicate Gag-eGFP dots associated with Jurkat T cells, magnified in the nearby marked boxes **(E)**. Viral synapses could also be observed in these co-cultures, where mDCs pulsed with VLP_{HIV-Gag-eGFP} were stained with DAPI. Images shown, from left to right, depict the red and green fluorescence channels merged with DAPI, the bright field cellular shape and the combination of both. **(F)** Jurkat T cells labeled with a green cell tracker dye were analyzed by confocal microscopy after four hours of co-culture with mDCs previously pulsed with Exosomes_{DiI} and extensively washed. Images were obtained by merging the red and green fluorescence. Arrows indicate DiI dots associated with Jurkat T cells, magnified in the nearby marked boxes. Bright field cellular shape merged with the red and green fluorescence is also shown. **(G)** Exosome polarization to the site of DC-T cell contact, where mDCs pulsed with Exosomes_{DiI} were stained with DAPI. Images shown, from left to right, depict the red and green fluorescence channels merged with DAPI, the bright field cellular shape and the combination of both. **(H)** Quantification of mDCs forming synapses like those shown in (E) and (G). Polarization of particles towards the synapse was considered when VLP_{HIV-Gag-eGFP} (green) or Exosomes_{DiI} (red) were found within one-third of the cell proximal to the contact zone (as represented in the illustration by the blue colored area). Mean values and SEM of fifty synapses from two donors counted by three distinct observers.

5. VLPs, HIV-1 and exosomes enter mDCs through a mechanism resistant to proteolysis

Our data suggest that common molecular determinants expressed on the surfaces of HIV, VLPs and exosomes govern entry into mDCs, allowing particle storage and transmission to CD4⁺ T cells. To further gain insight into the nature of these components, we analyzed the role of host proteins incorporated during viral and exosomal budding and the putative role of cellular protein-receptors expressed on the mDC surface.

We employed Pronase, a cocktail of proteases that displays high proteolytic activity (149), to treat VLPs, infectious virus particles, exosomes and cells prior to particle challenge of mDCs. The efficiency of Pronase treatment was confirmed by the lack of expression of gp120 in Pronase-treated VLP_{HIV-Gag-eGFP} co-transfected with a viral envelope glycoprotein plasmid (Fig. 45A). We also observed an eighteen-fold reduction on the infectivity of a wild type HIV_{NL4-3}, following equal Pronase treatment (Fig. 45B).

Similarly, Pronase treatment of mDCs resulted in an 80%, 100%, 84% and 85% reduction in the cell-surface expression of DC-SIGN, CD4, CD81 and binding of trimeric HIV envelope glycoprotein, respectively (Fig. 45C).

After pulsing Pronase-treated or mock-treated mDCs at 37°C (for fifteen minutes, to avoid complete recycling of the cellular receptors cut by the proteases) with either Pronase-treated or mock-treated VLP_{HIV-Gag-eGFP}, we measured the percentage of eGFP⁺ mDCs by FACS (Fig. 46A). Surprisingly, neither the protease pretreatment of the mDCs nor the VLPs diminished the percentage of eGFP⁺ cells. Similar results were obtained when HIV_{NL4-3} or Exosomes_{Dil} were treated with Pronase (Fig. 46B and C). Furthermore, no differences in intracellular localization of VLP_{HIV-Gag-eGFP}, Exosomes_{Dil} and

HIV_{NL4-3/vpr-eGFP} were found when we compared mock-treated or Pronase-treated mDCs (Fig. 45D).

Additional experiments performed with Pronase-treated mDCs pulsed with VLPs at 16°C to arrest endocytosis, also confirmed the lack of effect of Pronase treatment on VLP binding to mDCs (Fig. 45E and F). Consistently, VLPs, exosomes and HIV particles captured by Pronase-treated mDCs (which were allowed to recover before starting a co-culture with Jurkat T cells) were also recruited to the site of DC–T cell contact (Fig. 45G). Thus, broad proteolytic pretreatment of cells or VLPs, HIV-1 or exosomes was not sufficient to prevent particle capture by mDCs.

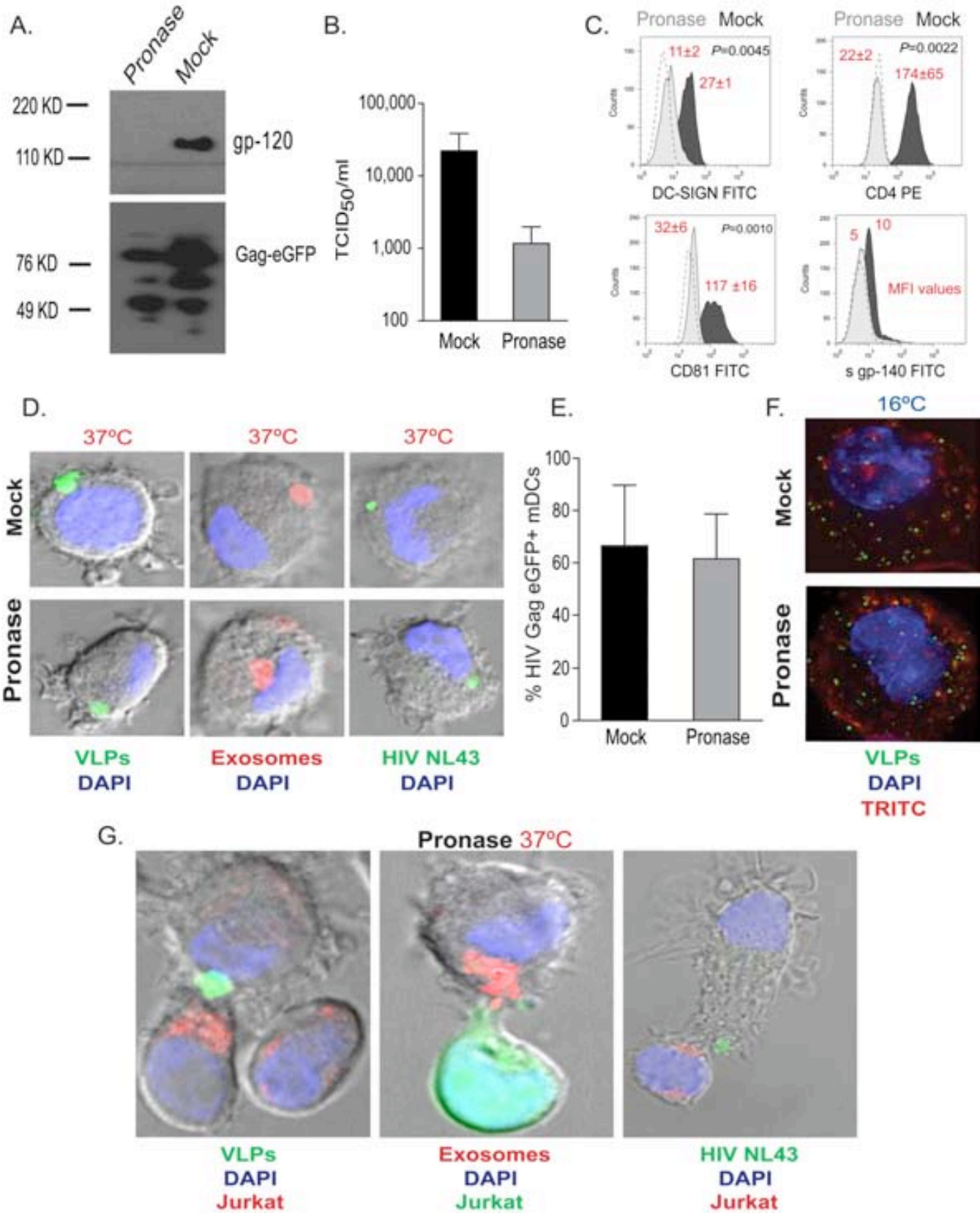


Figure 45. Caption overleaf.

Figure 45. (From previous page). Effect of Pronase treatment on mDCs. (A) Western blot of VLP_{HIV-Gag-eGFP} co-transfected with an HIV-1 envelope glycoprotein plasmid to express gp120. Particles were treated with 400 µg/ml of Pronase or left untreated for one hour at 4°C. Pronase treatment efficiently diminished gp120 detection levels when compared to the mock-treated VLPs. mAb against p24^{Gag} was used for detection of Gag-eGFP expression in both VLPs. **(B)** TCID₅₀/ml of untreated and Pronase-treated wild type HIV_{NL4.3} particles on TZM-bl cells containing the luciferase reporter gene. Upon Pronase treatment, there was an eighteen-fold reduction in infectivity (from a mean of 22,357 to 1,167). **(C)** Representative histograms of untreated mDCs and those treated with 200 µg/ml of Pronase for thirty minutes at 4°C and stained with an anti-DC-SIGN, CD4, CD81 and trimeric HIV-1 envelope glycoprotein gp140 detecting mAbs. Pronase treatment (light grey histogram) efficiently diminished DC-SIGN, CD4 and CD81 expression levels, or binding of gp140, as compared to mock-treated cells (dark grey histogram), seen by the reduction in geometric mean fluorescence intensity (MFI); (*P* values on the graphs, paired t test, n=6). Unlabeled cells are shown in blank dotted histograms. **(D)** When untreated (top panels) or Pronase-treated mDCs (bottom panels) were pulsed at 37°C for four hours (in the absence or in the presence of Pronase, respectively) with VLP_{HIV-Gag-eGFP}, Exosomes_{Dil} or HIV_{NL4.3/vpr-eGFP}, no differences in trafficking of the particles were observed by confocal microscopy, confirming our previous FACS results. **(E)** Binding of VLP_{HIV-Gag-eGFP} at 16°C for two hours was assessed by FACS employing mDCs previously exposed to 200 µg/ml of Pronase or mock-treated. Notably, by adding Pronase we were not able to block viral binding when pulsing treated mDCs with VLP_{HIV-Gag-eGFP}. **(F)** After pulse at 16°C, some cells were stained with DAPI and TRITC-labeled wheat germ agglutinin (to label the cell membrane), fixed with 2% paraformaldehyde and cytospun onto glass slides to be analyzed by deconvolution microscopy. Analysis of the projection of stacked images revealed that at 16°C, most of the bound VLPs were not endocytosed but remained on the cell surface in both untreated (top panel) and Pronase-treated mDCs (bottom panel). **(G)** After pulse at 37°C, as in panel (D), Pronase-treated mDCs were extensively washed, allowed to recover and then co-cultured with cell tracker-labeled Jurkat T cells. Confocal sections show VLP_{HIV-Gag-eGFP}, Exosomes_{Dil} and HIV_{NL4.3/vpr-eGFP} polarization at the site of DC–T cell contact. Images depict the red and green fluorescence channels merged with DAPI and the bright field cellular shape.

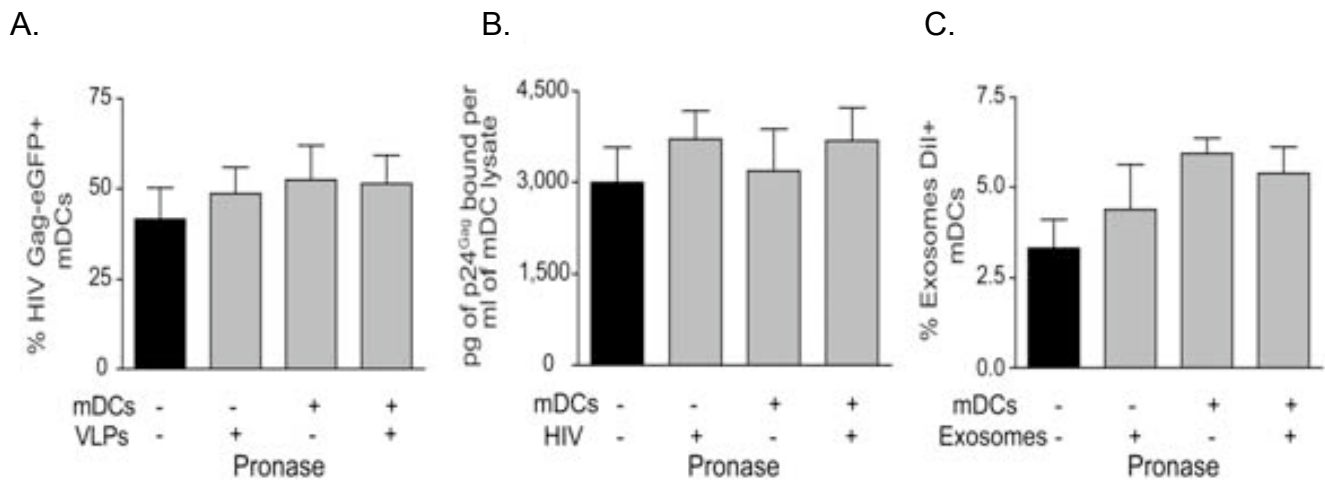


Figure 46. VLPs, HIV-1 and exosomes enter mDCs through a mechanism resistant to proteolysis. mDC capture of **(A)** VLP_{HIV-Gag-eGFP}, **(B)** HIV_{NL4-3} or **(C)** Exosomes_{Dil}. Pronase treated or untreated mDCs were pulsed for fifteen minutes at 37°C with Pronase or mock-treated VLP_{HIV-Gag-eGFP}, HIV_{NL4-3} and Exosomes_{Dil}. Neither the protease pre-treatment of the cells nor the particles was sufficient to prevent the capture of VLP_{HIV-Gag-eGFP}, Exosomes_{Dil} or HIV_{NL4-3} by mDCs. Panels (A) to (C) show the mean values and SEM from six independent experiments including cells from at least four different donors.

6. VLP, HIV-1 and exosome capture can be inhibited when particles are produced from ceramide-deficient cells

Virus particle budding or exosome biogenesis not only results in selective incorporation of host proteins in the particle membrane, but also selects for expression of unusual sphingolipids in the virus particle or exosome membranes (28, 37, 151, 216). Furthermore, it has been previously shown that the lipids of enveloped viruses play a critical role in viral infectivity (28, 186). However, the impact of viral lipid composition on the mDC viral capture process has never been evaluated. We decided to address this issue by pre-treating HEK-293T producer cells with FB1, an agent that blocks both the *de*

novo synthesis of sphingolipids (by inhibiting the synthesis of dihydroceramide, which serves as precursor to all sphingolipid species including glycosphingolipids and sphingomyelin) and the salvage pathway (233). To inhibit a different step of the metabolism of dihydroceramide species, we also employed NB-DNJ, a reagent that only blocks the synthesis of glycosphingolipids (171).

Treatment of HEK-293T cells with FB1 or NB-DNJ had no significant effect on cell viability or VLP release after HIV Gag-eGFP transfection, as measured by p24^{Gag} ELISA or western blot analysis (Fig. 47A and B). Interestingly, challenging mDCs with VLP_{HIV-Gag-eGFP} released from FB1-treated HEK-293T cells resulted in negligible VLP capture ($1.2 \pm 0.6\%$ Gag-eGFP⁺ cells, Fig. 48A), compared to mDCs challenged with VLPs generated from mock-treated cells ($79.4 \pm 14.4\%$ Gag-eGFP⁺ cells; $P=0.0003$; paired t test; Fig. 48A). Equivalent results were obtained when VLPs were produced from NB-DNJ-treated HEK-293T cells ($P=0.0062$; paired t test, Fig. 48A).

Similarly, wild type HIV-1 particles derived from FB1 or NB-DNJ-treated HEK-293T cells were deficient in binding to mDCs compared to the mDC-capture observed with HIV particles produced from untreated HEK-293T cells (Fig. 48B). Although HIV-1 particles derived from HEK-293T cells treated with FB1 had reduced infectivity relative to untreated controls (Fig. 47C), as previously reported (28), we found that NB-DNJ treatment of virus producer cells had no significant impact on viral infectivity when compared to untreated stocks (Fig. 47C). Furthermore, at the viral dose employed to pulse mDCs, the infectivity of FB1 treated virus was only $20\% \pm 10\%$ lower than the wild type virus (Fig. 47D). Analogously, FB1 or NB-DNJ-treated Jurkat T cells released similar amounts of Exosomes_{Dil} to mock-treated Jurkat T cells, measured both by fluorimetry assays and protein determination (Bradford)

assays (Fig. 47E and F). Again, after two hours at 37°C, mDCs were able to capture greater quantities of exosomes released from the mock-treated Jurkat T cells than the exosomes derived from FB1 or NB-DNJ-treated Jurkat T cells (Fig. 48C; $P=0.0042$ and $P=0.0062$; paired t test). Overall, these results suggest that sphingolipids facing the outer layer of VLP, HIV-1 and exosome membranes could be implicated in the initial particle attachment at the surface of mDCs.

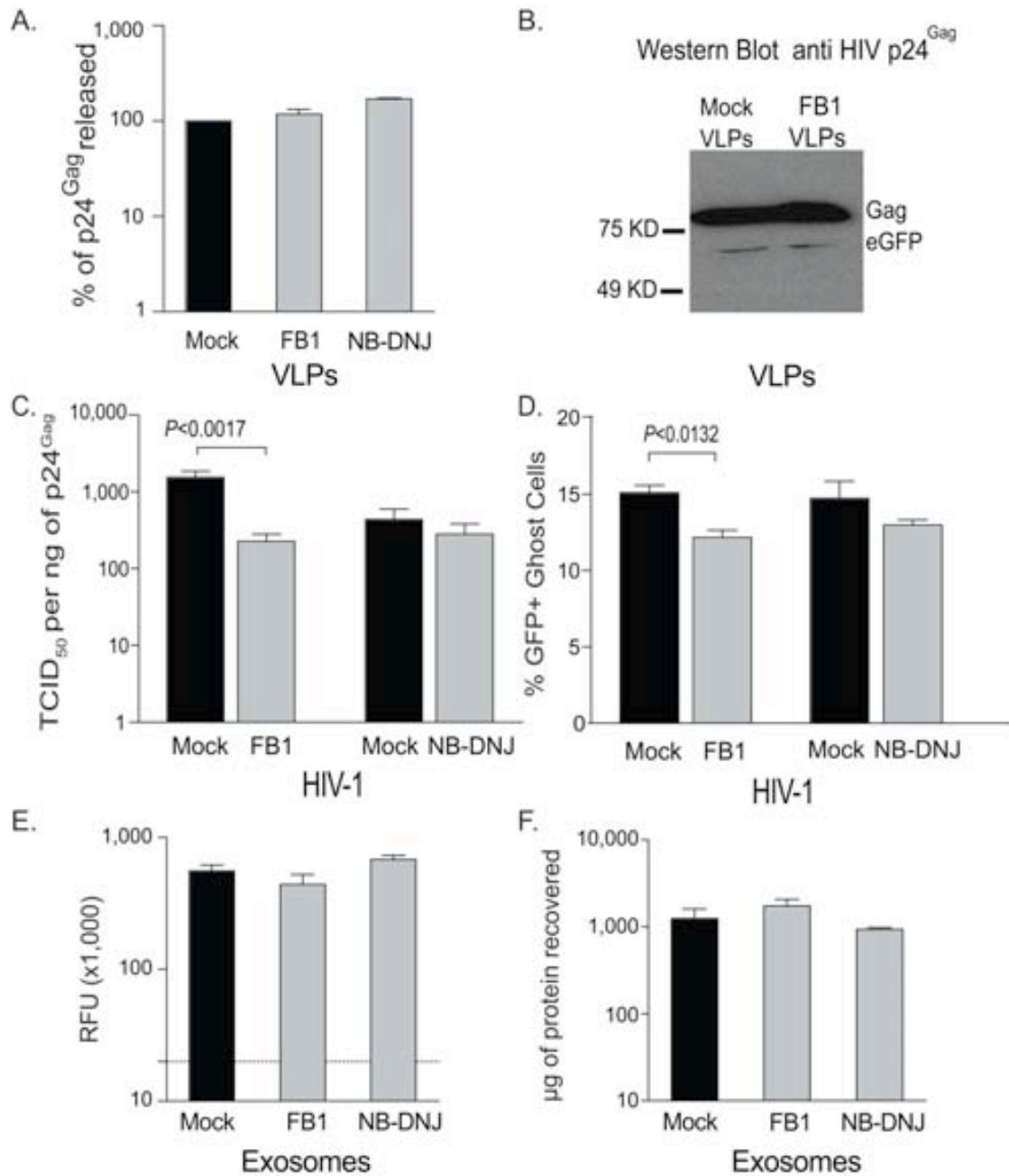


Figure 47. Caption overlesaf.

Figure 47. (From previous page). Effect of sphingolipid inhibitors in VLP, HIV and exosome release. (A–B) HEK-293T cell treatment with inhibitors of sphingolipid biosynthesis (50 μM of FB1 or 500 μM of NB-DNJ) for four days does not impact on VLP release after HIV Gag-eGFP transfection, measured both by (A) p24^{Gag} ELISA or (B) p24^{Gag} western blot. **(C)** HEK-293T cell treatment with 500 μM of NB-DNJ for four days does not impact on HIV_{NL4-3} infectivity, while affecting virus produced from FB1-treated HEK-293T cells ($P < 0.0017$, unpaired t test). TCID₅₀ values were obtained with a TZM-bl reporter cell line and are normalized to the p24^{Gag} levels released after transfection. Data show the mean and SEM of viral stocks obtained in five different transfections. **(D)** At the viral dose employed to pulse mDCs (10 ng of p24^{Gag} per 1×10^5 cells), HIV_{NL4-3} derived from FB1-treated HEK-293T cells only reduces its infectivity 20% \pm 10% compared to untreated HIV_{NL4-3}. Ghost CXCR4⁺/CCR5⁺ cells containing the GFP gene under the control of the HIV promoter were acquired with FACS 48 hours post-infection. Data show the mean and SEM of viral stocks obtained in three different transfections. **(E–F)** Jurkat treatment with FB1 (50 μM) or NB-DNJ (500 μM) for seven days does not affect exosome release after DiI labeling, measured both by (E) fluorescence assay or (F) protein quantification by Bradford assay. Dotted line in (E) indicates background levels of media assayed for relative fluorescence units (RFUs).

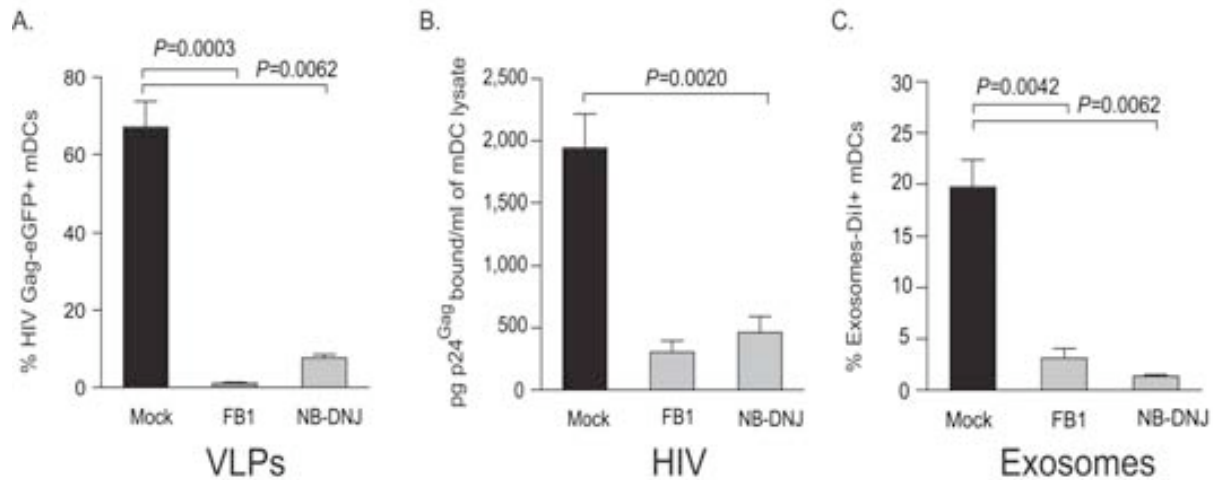


Figure 48. VLP, HIV-1 and exosome capture can be inhibited when particles are produced from ceramide deficient cells. (A) A total of 1×10^5 mDCs were exposed to 2,500 pg of VLP_{HIV-Gag-eGFP} p24^{Gag} produced from either FB1, NB-DNJ or mock-treated HEK-293T cells, fixed and analyzed by FACS to measure the percentage of eGFP⁺ cells. mDCs capture significantly larger amounts of VLP_{HIV-Gag-eGFP} produced from mock-treated HEK-293T cell ($P=0.0003$, paired t test). Mean values and SEM from three independent experiments including cells from five donors are plotted. **(B)** mDCs were exposed to 10 ng of HIV-1_{Lai} or HIV-1_{NL4-3} p24^{Gag} produced from either FB1, NB-DNJ or mock-treated HEK-293T cells, washed thoroughly to remove unbound particles, lysed, then assayed to measure the cell-associated p24^{Gag} content by an ELISA. mDCs capture larger amounts of HIV-1 produced from mock-treated HEK-293T cells. Mean values and SEM from two independent experiments and cells from three donors are plotted. **(C)** 1×10^5 mDCs were exposed to 250 μ g of Exosomes_{DiI} produced either from FB1, NB-DNJ or mock-treated Jurkat cells, fixed and analyzed by FACS to measure the percentage of DiI⁺ cells. mDCs capture significantly larger amounts of Exosomes_{DiI} produced from mock-treated Jurkat cells ($P=0.0042$, paired t test). The mean values and SEM from three independent experiments and cells from six donors are plotted.

6.

Discussion &
Future directions.

I. mDCs *versus* iDCs: Two evil sides for Mr. Hyde

Soon after HIV-1 exposure, both mature and immature DCs are able to transfer the virus preferentially to antigen-specific CD4⁺ T cells in the absence of productive infection (126, 145). This viral transmission process, known as *trans*-infection, is enhanced when DCs are matured in the presence of lipopolysaccharide (LPS), gamma interferon, poly (I:C) and CD40 ligand (191, 241). The first part of this thesis compares the effect of LPS maturation on monocyte-derived DCs and blood Myeloid DCs during viral capture, underscoring new insights into a mechanism that might have relevant implications for HIV-1 pathogenesis, given the interaction of mature DCs with CD4⁺ T cells at the lymph nodes.

Previous research has shown that iDCs capture virus to a greater or similar extent compared to mDCs (70, 191). When we performed binding experiments at 4°C, no major differences between these cell types were observed (Fig. 26). Strikingly, when cells were exposed to virus at 37°C, larger amounts of virus were found in mDCs, and this difference increased over time (Figs. 25 to 27). We extended our observations to blood-derived DCs of

Myeloid lineage and found that mature Myeloid DCs also capture larger amounts of virus than immature Myeloid DCs (Fig. 25). Therefore, contrary to previous studies (70, 191), our cell culture system and the viral isolates that we employed underscore a viral capture mechanism that is dramatically enhanced upon DC maturation. Interestingly enough, another different group has now independently reproduced these results (234).

Early research also proposed that iDC viral capture protects virions against degradation (76, 112), but others and we have demonstrated that iDCs show rapid degradation of captured viral particles – (144, 226) and (Fig. 27F). It is notable that we found still greater amounts of virus 48 hours post-pulse in mDCs than in iDCs immediately after pulsing (Fig. 27). Therefore, the possible explanations for enhanced viral transmission in mDCs as compared to iDCs include an increased ability to capture the virus and a longer lifespan for the trapped virions. If this is indeed the physiological case, strategies directed to augment viral degradation through the proteasome and lysosome machinery could diminish *trans*-infection while favoring HIV-specific antigen presentation. However, further research is needed to provide the therapeutic tools required to redirect captured virus into the cellular lytic pathways.

The initial Trojan horse hypothesis relied on the iDCs' *trans*-infection ability – reviewed in (227). However, several results (138, 234) – reviewed in (241) – including our own (Fig. 25B, C and E), indicate that iDCs have reduced *trans*-infection ability. Furthermore, a number of reports highlight that long-term transfer of HIV to susceptible T cells relies on the iDCs' productive infection rather than on *trans*-infection (30, 226).

Conversely, mDCs are much less vulnerable to viral fusion events and productive HIV infection than iDCs (34, 81), while displaying a greater ability to capture incoming virions and transmit them to target T cells through *trans*-

infection (Fig. 25). Even though endocytosis-mediated HIV-1 entry can generate productive infection in certain cell types, including human monocyte-derived macrophages (47, 62, 134), endocytosed HIV-1 cannot initiate productive infection in DCs, as has been recently established (104). Therefore, productive HIV-1 infection in DCs is dependent on fusion-mediated viral entry events (30, 34, 152, 153, 169).

Our results using confocal and electron microscopy corroborate this hypothesis, revealing a totally distinct uptake pattern in iDCs compared to mDCs (Figs. 32 and 34). The lack of viral accumulation within iDCs favors a model in which viral interactions lead to fusion events and productive infection. In marked contrast, maturation increases the DCs' ability to endocytose virus in large intracellular vesicles that co-localize with CD81 and CD63 tetraspanins in blood Myeloid DCs (Fig. 35), as previously reported for mDCs (74).

Collectively, these results favor a model in which both direct infection and *trans*-infection abilities coexist to a different extent in immature and mature DC subsets. Maturation of DCs enhances viral capture activity and *trans*-infection capacity, while diminishing the viral fusion events and the productive infection that characterizes iDCs. Under these circumstances, iDCs would preferentially transmit *de novo* synthesized virus upon productive infection (226), and the mDCs' enhanced *trans*-infection ability would play a key role in the mucosa and lymph nodes, mediating viral transmission to new target naïve CD4⁺ T cells (Fig. 49). Our results reveal that HIV works as a different kind of evil potion depending on the DCs' maturation status, promoting two distinct viral dispersion mechanisms that define two evil sides for Mr. Hyde.

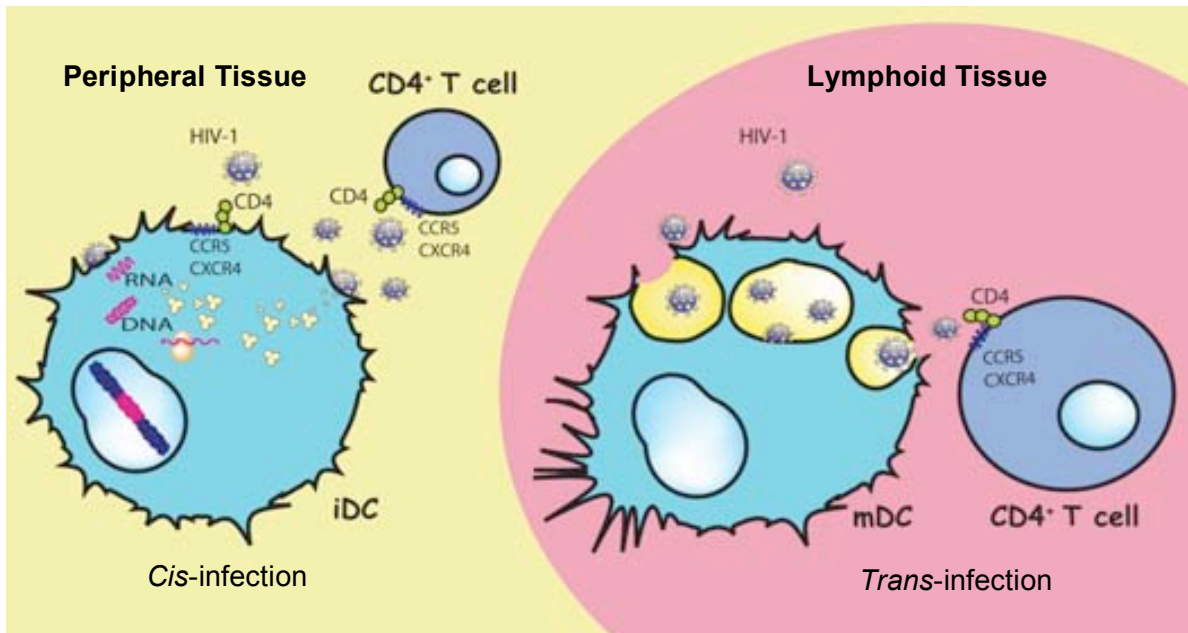


Figure 49. Proposed major roles of iDCs and mDCs during HIV disease progression. Productive infection of iDCs allows viral transmission in the peripheral tissues, while mDC viral capture leads to *trans*-infection in the lymphoid tissues.

II. mDC *trans*-infection

Which of these two viral dispersion mechanisms has the most profound effect in HIV pathogenesis? Given the unique capability of mDCs to enhance HIV-1 infection, we hypothesize that *in vivo*, mDC *trans*-infection could augment viral dissemination in the lymphoid tissue and significantly contribute to HIV disease progression. That is why in this thesis we have tried to underscore the processes behind mDC functional metamorphosis into Mr. Hyde, focusing on HIV binding and capture, intracellular trafficking and the final transmission of captured virus to CD4⁺ T cells.

1. *In vivo* evidence of Mr. Hyde's criminal activity

mDCs continuously interact with CD4⁺ T cells at the lymph nodes, the key site of viral replication. Therefore, mDCs find themselves in the right place and at the right time to play a prominent role in HIV pathogenesis. We should not forget that mDCs have a greater ability to stimulate CD4⁺ T cell proliferation than iDCs. Accordingly, upon infection, mDCs presenting viral antigens could activate HIV-specific naïve CD4⁺ T cells in the course of their first encounters in the lymph node. As a result, HIV-specific naïve CD4⁺ T cells would undergo several rounds of division during their initial expansion and differentiation into effector CD4⁺ T cells, turning highly susceptible to actual HIV infection (54).

Once infected, these activated CD4⁺ T cells are known to have short half-lives *in vivo*, lasting less than two days (164). Therefore, under rapid T cell turnover, DCs could be indispensable to permitting continuous infection of new CD4⁺ T cells (85). Recently, it has also been suggested that simultaneous priming and infection of T cells by DCs is the main driving force behind the early infection dynamics, when activated CD4⁺ T cell numbers are low (97). However, the viral dissemination process mediated by mDCs in the mucosa could take place at all the stages of HIV infection, influencing the viral load fluctuations throughout the whole course of disease. Consequently, mDCs located in the lymphoid tissue could also facilitate viral persistence and continuous replenishment of cellular viral reservoirs. Unfortunately, even when HAART is successfully introduced and the viral load is controlled, HIV replication might not be totally suppressed, and low levels of viral replication could take place 'cryptically' below the limits of clinical detection (52, 53). Recent works have demonstrated that HIV persists in the GALT of infected individuals who received effective antiviral therapy for prolonged periods (41),

underscoring a potential situation where mDC *trans*-infection could mediate the replenishment of cellular reservoirs. Nevertheless, the mDC contribution to HIV pathogenesis in these physiological settings needs further investigation.

Notably, the viral dissemination that mDCs can potentially mediate *in vivo* is enormous: T cells approach mDCs randomly and make exploratory contacts that last only minutes, enabling DCs to contact thousands of T cells per hour (141). Thus, since viral transmission through *trans*-infection does not rely on antigen presentation, many CD4⁺ T cells could capture mDC-transmitted virus; however, only after antigen presentation through immunological synapses would naïve CD4⁺ T cells be activated and their subsequent proliferation render these cells more susceptible to HIV infection.

Accordingly, we propose that this mDC *trans*-infection model could be intimately related to the course of infection, helping explaining why viral replication occurs mainly in the paracortical regions of the peripheral lymphoid organs (57, 161, 164) where DCs and CD4⁺ T cells mostly concentrate (90).

Interestingly, it has been previously shown that circulating LPS, the stimulus used to mature DCs in this thesis, is significantly augmented in chronically infected HIV individuals, due to the increased translocation of bacteria from the intestinal lumen upon infection (26). This means that the bacterial components released could stimulate DCs systemically, contributing to their maturation and therefore enhancing viral spread in the mucosa, while creating the pro-inflammatory milieu associated with chronic HIV infection. This hypothesis is further supported by another report showing that in subjects with HIV-1 viremia, DCs from blood have increased expression levels for costimulatory molecules (the hallmark of maturation status) that only diminish when HAART suppresses the viral load (13). The median LPS plasma levels

found in patients with disease progression was 75 pg/ml (26), five times the amount required to stimulate the systemic immune activation in non-infected volunteers (211). Although this LPS concentration is much lower than the one we have used to mature DCs *in vitro*, it is conceivable that *in vivo*, higher amounts of LPS could accumulate in the most compartmentalized areas of the mucosa or in the adjacent tissues. Therefore, future experiments should measure LPS tissue levels *in vivo* and address whether the physiological amounts of LPS found can trigger the same DC maturation status and viral transmission efficacy described in this thesis.

In contraposition to the mDC *trans*-infection model we propose, initial studies emphasized iDCs' role in the establishment of HIV infection (76, 112). However, the strongest correlate associated with the sexual transmission of HIV is prior infection with other sexually transmitted pathogens (198). This implies that the probability of a person acquiring HIV infection is increased when there is a preexisting infection or inflammation of the genital epithelium. Under these circumstances, it is quite likely that mucosal inflammation arising from other sexually transmitted pathogens could directly activate and mature DCs *in vivo*, promoting HIV settlement and favoring the subsequent spread of the viral infection. Therefore, mDCs' enhanced *trans*-infection capacity could also play a role during primo-infection. Notably, recent experiments performed in tissue culture models *ex vivo* showed that individual Langerhans cells from the human vaginal epithelium were heavily loaded with virions a few hours after HIV challenge (95). Although in this study the productive infection of Langerhans cells was not detected, HIV was easily found along the contact zone of emigrant Langerhans cells and T cells conjugates, forming infectious synapses (94, 95).

Unfortunately, recent failures in HIV prophylactic vaccine trials stand as an additional corroboration of the prominent role mDCs could be playing during HIV primoinfection *in vivo*. The STEP HIV vaccine trial evaluated a replication-defective adenovirus type 5 (Ad5) vector, which is a weakened form of a common cold virus, modified to carry HIV genes into the body to induce HIV-specific immune responses. One reasonable worry about the Ad5 vector was that the widespread immunity to adenoviruses could cause vaccine recipients with circulating antibodies against Ad5 to contract HIV more readily than vaccinated individuals without prior antibodies or the non-vaccinated controls. Indeed, this Merck clinical trial was recently stopped due to the vaccine's lack of efficacy and the twofold increase in the incidence of HIV acquisition among vaccinated recipients with increased Ad5-neutralizing antibody titers compared with placebo recipients (HIV vaccine trials network, http://www.hvtn.org/science/step_buch.html). Of note, a recent report demonstrates that the Ad5 vector, with its neutralizing antiserum (present in people with prior immunity), induced a more marked DC maturation than the vector alone, as indicated by increased CD86 expression levels, decreased endocytosis and production of tumor necrosis factor and type I interferons (166). Furthermore, when the Ad5 vector and the neutralizing antiserum were added to DCs, significantly enhanced HIV infection was observed in DC-T cell co-cultures. That is why these authors argue that mDCs from people with prior immunity to Ad5 virus could have activated CD4⁺ T cells *in vivo*, augmenting their susceptibility to HIV infection (166). Furthermore, Ad5 infected mDCs could have been killed by Ad5-specific CD8⁺ T cells, thereby reducing the pool of DCs presenting HIV antigens. Indeed, weaker HIV-specific CD8 responses were seen in Ad5-seropositive individuals in response to vaccination. Overall, these results highlight the functional relevance that DC

maturation could possess under physiological settings, providing the basis for a chronic permissive environment for HIV-1 infection.

2. Viral binding and capture: No sign of DC-SIGN

Owing to its implications for HIV pathogenesis *in vivo*, we believe that elucidating the mechanisms underlying the enhanced HIV-1 transmission by mDCs is crucial to designing effective therapeutic strategies to block viral spread. In order to address this issue, we first focused on DC-SIGN's role in the viral capture process, as it is proposed to be the most important HIV-1 attachment factor concentrating virus particles on the surface of DCs (12, 58, 76, 89, 112, 172, 203, 219, 227). However, as we performed our experiments, an increasing number of studies started to suggest that HIV-1 binding, uptake and transfer from DCs to CD4⁺ T lymphocytes may involve alternative pathways such as C-type lectin receptors (CLRs) – including the mannose binding receptor, DCIR and trypsin-sensitive CLRs – CD4-independent receptors, and glycosphingolipids such as galactosyl-ceramide expressed on the DC surface (22, 82, 86, 113, 132, 223, 225, 240). These studies and the results presented in this thesis demonstrate that a single receptor is not responsible for HIV-1 binding to all DC subsets (100, 225), highlighting that additional HIV-1 receptors and their respective endocytic routes remain to be identified.

Here, we show that despite the fact that DC-SIGN expression is almost absent from Myeloid DCs and that mDCs display half the number of DC-SIGN antibody binding sites compared to iDCs (Fig. 28), HIV-1 capture and transfer to target T cells are augmented upon maturation in both DC types (Figs. 25 and 26). These results are in agreement with other reports showing HIV *trans*-infection mediated by cells that do not express DC-SIGN, such as blood Myeloid DCs and Langerhans cells (63, 82). Therefore, even though the

efficiency of DC-SIGN-transfected cell lines in transmitting HIV-1 has been previously related to DC-SIGN expression levels (12, 172), we confirm that the cellular context in which DC-SIGN is expressed determines viral capture and transmission ability (219, 241–243). It would be of great interest to further confirm DC-SIGN's contribution to HIV-1 transmission in other primary cells, such as B lymphocytes or macrophages (179, 192).

We also found that DC-SIGN blocking agents such as mannan or anti-DC-SIGN antibodies had minimal effects on mDC viral capture and transfer, while completely abrogating Raji DC-SIGN cell viral capture and transfer (Figs. 28 and 31). Therefore, conclusions drawn from employing transfected cell lines should be extrapolated to primary cells with care, because effective blocking concentrations of DC-SIGN-inhibitory compounds in these model cell lines do not prevent viral capture or transmission by mDCs and Myeloid DCs.

Our results also show that only iDCs, the DC subset displaying larger amounts of DC-SIGN, partially rely on DC-SIGN activity to promote viral capture, confirming the extensive literature that has showed a variable contribution by DC-SIGN in HIV capture and its subsequent transfer to CD4⁺ T cells, as reviewed in (168). These data nicely correlate with a previous report showing that in iDCs, the HIV envelope and DC-SIGN-dependent pathways account for about 50% of antigen presentation through MHC-II (145), and with a recent work showing that HIV targeting of the CD81 compartment is dependent on the viral envelope glycoprotein in iDCs (73). Therefore, it would be interesting to address whether the remaining 50% of viral capture in iDCs that does not rely on the viral envelope glycoprotein is taking place through the same mechanism as in mDCs.

DC-SIGN affinity for the gp120 envelope glycoprotein is five times greater than that displayed by the receptor CD4 (46). That is why it was first

suggested that DC-SIGN could efficiently capture low numbers of HIV-1 particles in the periphery, facilitating HIV transport to secondary lymphoid organs rich in CD4⁺ T cells, where infection of target cells would take place (76). This DC-SIGN high affinity interaction could play a prominent role in situations where the number of free viral particles is limited. However, as other groups (138) and we (Figs. 17 and 44E, Video 5) have shown, the infectious synapse polarizes large amounts of virus, efficiently concentrating viral particles at the site of CD4⁺ T cell contact. Therefore, in cell-to-cell viral transmission, where large amounts of virus are concentrated, DC-SIGN's role could be dispensable. Previous studies have calculated that only ~10% of the infections in lymphoid tissue are transmitted by cell-free virions and that ~90% are transmitted by infected cells (51). This could be due to the short half-life of the cell-free virus, less than two hours in plasma (164, 176), further limiting the opportunity for viral particles to directly infect CD4⁺ T cells. In fact, cell-associated transfer of HIV-1 is estimated to be 92 to 18,600-fold more efficient than that of cell-free virus (38), due to the increased numbers of contacting virus (64, 234) and their higher infectivity through cell-to-cell synapse formation (50).

Since DC-SIGN binds specifically to gp120, we decided to further address DC-SIGN's role in DC viral capture by employing viral particles lacking the envelope glycoprotein. Notably, Raji DC-SIGN cell viral capture was totally dependent on this glycoprotein (Fig. 28D), further confirming the specificity of this C-type lectin receptor for gp120 (46). However, the envelope requirement in iDCs decreased by a similar extent to that observed in the presence of DC-SIGN inhibitory agents (Fig. 28C), verifying that other molecules are implicated in the viral capture process as well in this cell type (22,

82, 86, 113, 132, 223, 225, 240), despite the high expression of this C-type lectin receptor (Fig. 28A).

Strikingly, we found that the envelope glycoprotein is not necessary for Myeloid DC and mDC viral uptake (Fig. 28D). Therefore, in these primary cells, viral capture has to take place independently of fusion events. Interestingly, these results are in agreement with a previous report showing a decreased viral fusion with the plasma membrane of mDCs when compared to iDCs (34). Hence, although the cell-associated p24^{Gag} values provided in Figures 25 to 27 do not distinguish between the net viral capture and the fusion events, the uptake of virus lacking the envelope glycoprotein (Figs. 28D and 35, bottom) helps to discriminate this non-fusogenic viral entry pathway. This mechanism could explain why mDCs, having limited antigen capture activity, sequester significantly larger numbers of intact whole viral particles than iDCs (Fig. 34), as previously reported (70). Furthermore, these results clearly highlight the need to find viral envelope-independent binding receptors in mDCs. Accordingly, analyzing the role of adhesion molecules dragged from the membrane of infected cells during viral budding could aid in identifying the molecular determinants that lead to viral capture in mDCs. These factors could be ubiquitous because we observed an increased viral uptake pattern in mDCs when compared to iDCs exposed to viral stocks produced in HEK-293T cells, MOLT 4 cells, and stimulated PBMCs (Fig. 30).

3. Hiding Dr. Jeckyll's evil potion: Intracellular viral trafficking

Regardless the nature of the initial receptors implicated in the viral binding process, once the virus is attached to the surface of the DCs, it is internalized in endosomes or multivesicular bodies (74, 111). Our results confirm that in mDCs, virus accumulates in vesicles enriched in proteins distinctive of multivesicular bodies (Fig. 35), such as CD81 and CD63 tetraspanins. A recent study challenges this internalization view and suggests that cell-surface-bound HIV is the predominant pathway for viral transmission mediated by MDDCs (35). Remarkably, these authors performed experiments pulsing DCs at 4°C, and then allowed the endocytosis of bound virions at 37°C. Under these experimental conditions it is possible that the initial viral binding process is restrained; at lower temperatures, the average speed of particles in suspension decreases and the probability of interactions is thus reduced, introducing a bias that could obscure the more relevant interactions taking place at physiological temperatures.

In contrast to the results obtained by this group (Fig. 16A), several other publications have reported that HIV associated with DCs at 37°C is protected from trypsin treatment (19, 76, 238) and from Pronase treatment (22, 63, 234). Therefore, the most extended view proposes that virus is endocytosed and accumulated into a non-conventional, non-lysosomal, endocytic compartment resistant to protease treatment (Fig. 16B). Despite this, the latest report on the topic tries to reconcile these two models by demonstrating that the intracellular, apparently endocytosed HIV remains fully accessible to surface-applied viral inhibitors and other membrane-impermeable probes (245). Therefore, this group argues that HIV resides in an invaginated domain within DCs that is both contiguous with the plasma membrane and distinct from classical

endocytic vesicles (Fig. 16C). These results are not discarded by our confocal and electron microscopy observations. It is therefore conceivable that the multivesicular bodies we refer to could be connected to the plasma membrane throughout the whole process, while virus is being endocytosed and even before it is released to mediate *trans*-infection of CD4⁺ T cells. Further research is needed to clarify this issue, but if viral inhibitors can gain access to the compartment where virus accumulates, already available therapeutic options could efficiently block this mechanism of viral spread.

Apart from the physical connection of the multivesicular body with the plasma membrane, our results clearly highlight that HIV trafficking within mDCs relies on active endocytic mechanisms. The first evidence we obtained came from the viral capture experiments performed at different temperatures, where we found that mDC viral uptake increased over time at 37°C, the optimal temperature for endocytosis to occur (Fig. 26). However, it is well established that DC maturation induces a rapid decrease in macropinocytic activity of fluid-phase markers such as dextran particles (166, 187, 207). Therefore, mDC-enhanced viral capture through a pinocytic pathway is highly unlikely, since this transportation system is less active in mDCs than in iDCs (Fig. 36A). Recent studies have shown brief co-localization of HIV with transferrin (112), the archetypical cargo of clathrin-mediated endocytosis. Interestingly, pretreatment of mDCs with amantadine and chlorpromazine, the classical clathrin-mediated endocytosis inhibitors, also blocked HIV uptake (Fig. 43). Further work should address whether the inhibitory doses of amantadine and chlorpromazine employed in our assays do not affect other endocytic mechanisms, such as those mediated by cholesterol-enriched lipid raft domains.

Notably, virus-containing compartments in mDCs colabel with lipid raft-associated tetraspanins CD81, CD82 and CD9 (74). In addition, it has been previously shown that depleting cholesterol from membranes with agents such as β -methyl-cyclodextrin inhibits iDC viral capture (86). That is why we also focused on cholesterol-mediated internalization pathways, further confirming their role during viral capture (Fig. 36). Although we found β -methyl-cyclodextrin concentrations that blocked mDC viral capture without affecting transferrin clathrin-mediated endocytosis, higher concentrations did affect this process. We have seen, however, that β -methyl-cyclodextrin does not affect dextran pinocytosis. It is thus likely that both clathrin-mediated endocytosis and cholesterol-enriched lipid rafts mechanisms coexist or cooperate during mDC viral capture, although the specific contribution of each of these pathways remains to be clarified. These data correlate with previous results showing that other retroviruses such as the avian sarcoma and leukosis virus (ASLV) use both clathrin and cholesterol-dependent internalization routes to gain access to intracellular endosomes (150). Interestingly, the binding of ASLV to a transmembrane form of its receptor results in a rapid internalization via clathrin-coated pits, while binding to a GPI-anchored form of the same receptor leads to a slow lipid raft mediated internalization (163). Overall, these results highlight the complexity that governs HIV-1 endocytosis in mDCs.

4. Mr. Hyde's murder weapon: The infectious synapse

How is the endocytosed virus released and transferred to CD4⁺ T cells? This is a key issue that still lacks a molecular explanation. mDC and T cell conjugates form quite efficiently and virions concentrate at the conjugate contact zone, while CD4 receptors and coreceptors appear to be partially enriched in the T cell at the point of contact with the DC (138). Therefore, receptor recruitment

and virus polarization at the synapse site explains, at least in part, why mDC transmission of HIV-1 to CD4⁺ T cells is such an efficient process (168).

Interestingly, it has been previously suggested that the structure of the infectious synapse is maintained by adhesion molecules such as ICAM-1 and 3, upregulated upon DC maturation (83, 143, 191). However, our results correlate net viral capture with final viral transmission, regardless the DC maturation status (Fig. 26). Therefore, in our experimental settings, mDC differences in ICAM-1 expression or viral distribution during the infectious synapse, as previously suggested by other works (138, 191), cannot exclusively account for the enhanced HIV-1 transmission to a T cell line displayed by this cell type. *In vivo*, however, viral capture would need to be considered along with the DCs' ability to contact primary CD4⁺ T cells, including any subsequent stimulation arriving from this interaction.

Intriguingly, the infectious synapse appears to share structural similarities with the immunological synapse that allows the initiation of immune responses (Fig. 50). However, the infectious synapse does not require antigen presentation and thus needs less time to be formed. We have seen how structures similar to infectious synapses can be formed independently of the envelope glycoprotein (Fig. 44 and Video 5) as previously demonstrated in macrophages (80), contrasting in this way with the virological synapses established between productively infected cells and uninfected target cells that rely on gp120 (173, 222).

Notably, the set of cell-surface molecules that contributes to the formation of infectious synapses, potentially supporting the transfer of HIV-1 from DCs to CD4⁺ T cells, has not been fully identified, although DC-SIGN involvement has been highlighted (6). Hence, defining the mechanisms of infectious synapse formation and underscoring the role of immune adhesion

molecules implicated in mDC *trans*-infection is a key issue in finding new potential therapeutic targets. By blocking the formation of infectious synapses we could prevent DC mediated HIV-1 transmission to CD4⁺ T cells. However, if we want to maintain the integrity of the anti-HIV immune responses, this strategy should not impair immunological synapse formation.

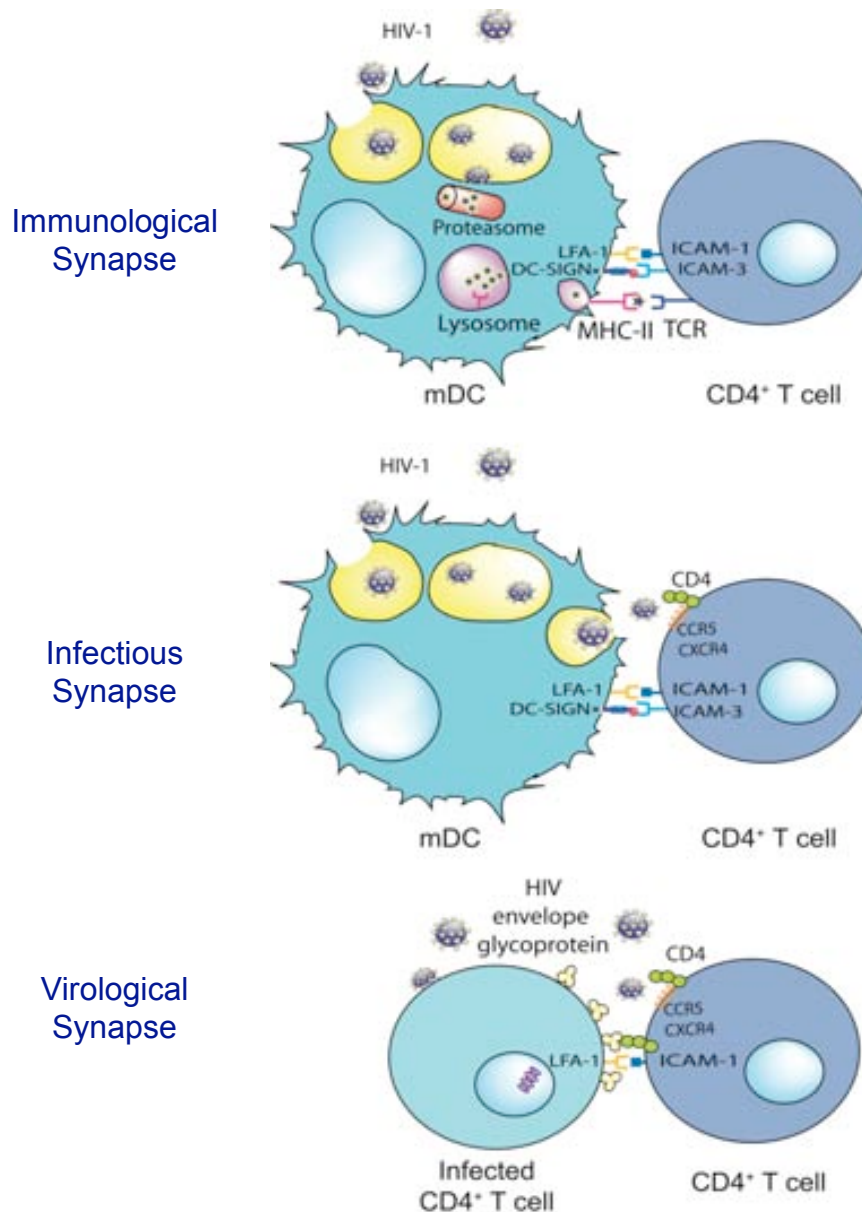


Figure 50. Comparison between the formation of immunological, infectious and virological synapses. Several molecules are implicated in the formation of these synapses, although each of them involves specific pathways represented in this illustration.

In addition, the topological disposition of the infectious synapse could facilitate infection of CD4⁺ T cells by viral populations with low affinity for the CD4 receptor or the CCR5/CXCR4 coreceptor. This implies that the differences observed between viral particles with high and low affinities for CD4, CCR5 or CXCR4 could disappear with this mechanism of viral transmission, modulating the establishment of certain viral populations *in vivo* and directly influencing pathogenesis. mDCs could play a prominent role in this scenario, selecting viral populations during disease progression.

III. Convergence with the exosome dissemination pathway

Taken as a whole, the first part of this thesis reveals that there is an HIV gp120-independent mechanism of viral binding and endocytosis that is upregulated upon DC maturation, suggesting that HIV-1 could be exploiting a preexisting cellular pathway of antigen uptake and transmission.

Why would DCs accumulate viral particles instead of degrade them? What could be the physiological relevance of the mechanism we describe? In mDCs, increased viral uptake and longer retention of intact viral particles within an intracellular compartment could permit the retention of a source of antigen to present to T cells in the absence of surrounding viral particles, aiding immunological surveillance through MHC-II antigen presentation and MHC-I cross-presentation pathways. Intriguingly enough, DCs have an inherent mechanism to control endosomal acidification to preserve antigen cross-presentation over long periods (193).

Interestingly, several lines of evidence suggest that viral envelope-independent capture by DCs can allow antigen presentation to CD4⁺ and CD8⁺ T cells. In iDCs, HIV envelope and DC-SIGN-dispensable pathways account for about 50% of the antigen presentation through MHC-II molecules (145). DCs are also able to capture envelope-*pseudotyped* VLP_{HIV-Gag} through a DC-SIGN-independent pathway, activating autologous naïve CD4⁺ T cells that are then able to induce primary and secondary responses in an *ex vivo* immunization assay (29). In addition, it has been previously shown that DCs can endocytose VLPs and induce immune responses through an endosome-to-cytosol cross-presentation pathway (147). These VLPs do not have the envelope glycoprotein, meaning that the uptake mechanism could be the same as the one we have shown for virus lacking the envelope glycoprotein (Figs. 28D and 35). Overall, these findings reinforce the idea that envelope-independent capture pathways allow viral antigen presentation, favoring immune responses.

Likewise, exosomes can induce humoral and cytotoxic immune responses. These small-secreted cellular vesicles are also internalized and stored in endocytic compartments by DCs, as with viral particles, stimulating antigen specific naïve CD4⁺ T cell responses *in vivo* (213, 215). Notably, exosomes do not induce naïve T cell proliferation *in vitro* unless mDCs are also present, indicating that exosomes do not overcome the need for a competent APC to stimulate naïve CD4⁺ T cells. In addition, exosomes from cultured DCs loaded with tumor-derived peptides on MHC-I are also able to stimulate cytotoxic T lymphocyte-mediated anti-tumor responses *in vivo* (249). Moreover, it has been demonstrated that tumor cells secrete exosomes carrying tumor antigens, which, after transfer to DCs, also mediate CD8⁺ T cell-dependent anti-tumor effects (239). Therefore, exosomes carrying tumor peptides provide a source of antigen for cross-presentation by DCs.

In summary, distinct works have shown that both exosomes and virus can be internalized in DCs, allowing final antigen presentation. Interestingly, it has been suggested that in addition to carrying antigens, exosomes can promote the exchange of functional peptide–MHC complexes between DCs (213, 215). Such a mechanism could increase the number of DCs bearing a particular peptide, thus amplifying the initiation of primary adaptive immune responses (215). It is then reasonably conceivable that, as suggested for exosomes (215), virus could also be exchanged between DCs, increasing the number of DCs bearing viral antigens and amplifying the antiviral immune responses or contributing to viral dissemination. However, further studies are needed to confirm these ideas.

In the second part of this thesis, we suggest that HIV and other retroviruses could be exploiting an exosome antigen dissemination pathway intrinsic to mDCs, allowing the final *trans*-infection of T cells (Fig. 51). In particular, HIV hijacks a pathway that exosomes produced by DCs can follow, mediating the indirect activation of CD4⁺ T cells by presenting functional peptide–MHC complexes through a *trans*-dissemination mechanism (213, 215). Our data supports the Trojan exosome hypothesis that proposes that retroviruses take advantage of a cell-encoded intercellular vesicle traffic and exosome exchange pathway, moving between cells in the absence of fusion events (79).

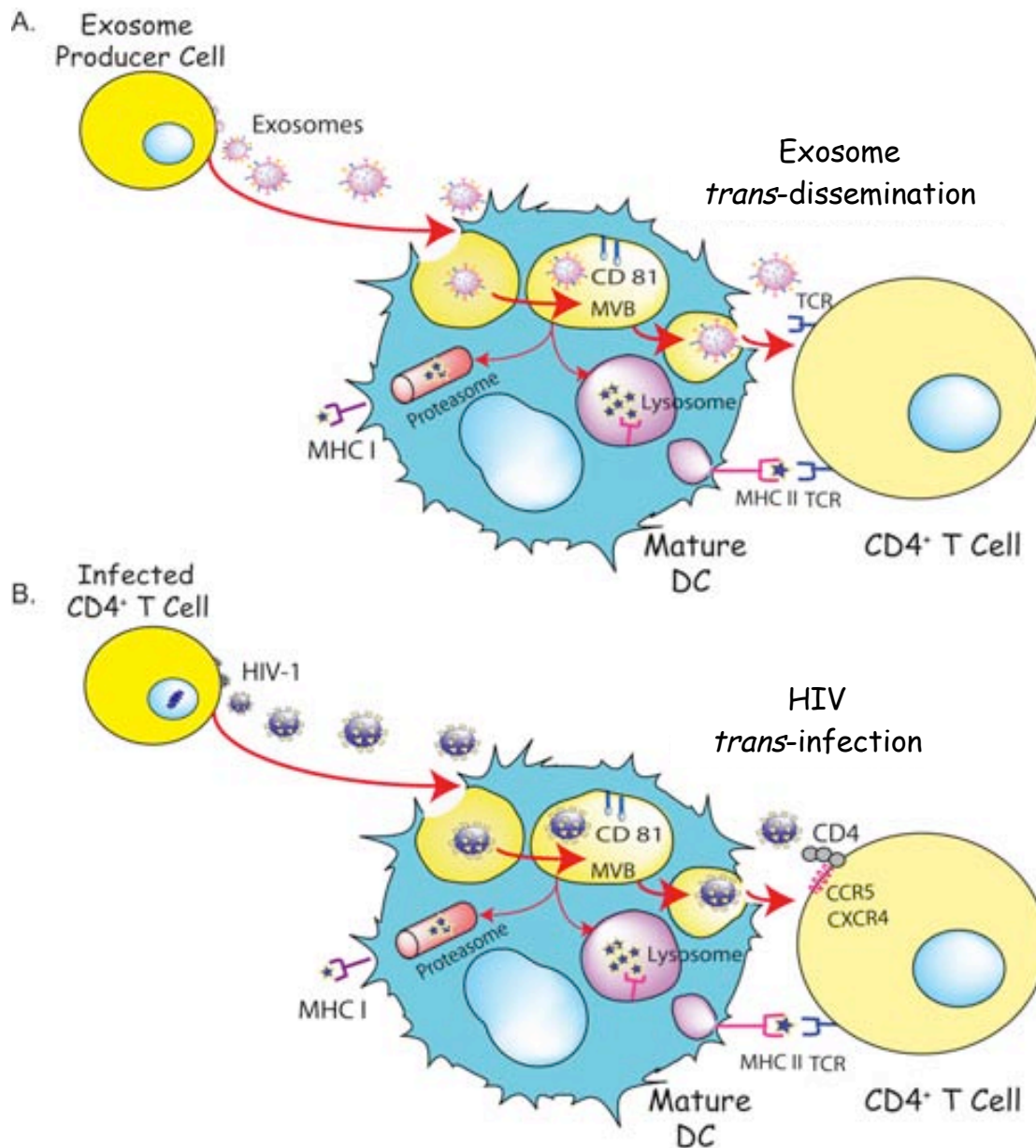


Figure 51. HIV can exploit a pre-existing exosome *trans*-dissemination pathway intrinsic to mature DCs, allowing the final *trans*-infection of CD4⁺ T cells. **(A)** Exosomes can transfer antigens from infected, tumoral or antigen-presenting cells to mDCs, increasing the number of DCs bearing a particular antigen and amplifying the initiation of primary adaptive immune responses through the MHC II pathway, cross-presentation, or the release of intact exosomes, a mechanism described here as *trans*-dissemination. **(B)** HIV gains access into mDCs by hijacking this exosome *trans*-dissemination pathway, thus allowing the final *trans*-infection of CD4⁺ T cells.

Here we show how, upon maturation, DCs captured larger amounts of VLP_{HIV-Gag-eGFP} and Jurkat-derived Exosomes_{Dil}, accumulating both particles in the same large CD81⁺ intracellular compartment (Figs. 37 to 39 and 41 to 42). These data nicely correlate with our previous findings regarding internalization of virus lacking envelope glycoprotein in mDCs and mature Myeloid DCs (Figs. 28D and 35). Therefore, if exosomes use the same trafficking pathway in mDCs as HIV, the receptors dragged from the membrane of infected cells during viral budding (that ultimately lead to viral capture) should also be present in the membrane of exosomes. Interestingly, both exosomes and HIV can bud from particular cholesterol-enriched microdomains in the T cell plasma membrane (23, 65, 151), sharing glycosphingolipids and tetraspanin proteins previously used as *bona fide* lipid raft markers (23, 244). These similarities in composition and size are a strong argument for the Trojan exosomes hypothesis, which suggests that retroviruses are, at their most fundamental level, exosomes (79).

We have further confirmed the specificity of the mDC entry mechanism by observing direct competition between different particles (exosomes, VLP_{HIV-Gag-eGFP}, HIV-1 and VLP_{MLV-Gag}) derived from similar cholesterol-enriched membrane microdomains (Fig. 40), which could not be inhibited by 100 nm carboxylated beads or Pronase-treated VSV particles budding from non-raft membrane locations (37). Therefore, budding from lipid raft domains is essential to include specific mature DC-recognition determinants that allow viral and exosome capture.

Interestingly, a previous study revealed an association between endocytosed HIV-1 particles and intraluminal vesicle-containing compartments within iDCs (238). However, the mechanism described here differs from this previous paper in two fundamental aspects. First, the earlier work focuses on

iDCs and second, in their case, virus was endocytosed into the compartment where iDCs typically produce exosomes by reverse budding (Fig. 11), thus contrasting with the gather mechanism of exosome and HIV uptake that we describe here for mDCs. However, our findings concur because HIV-1 particles captured by iDCs were exocytosed in association with exosomes and could mediate *trans*-infection of CD4⁺ T cells (238). Analogously, we found that mDC capture of HIV-1, VLPs and exosomes allowed efficient transmission of captured particles to target T cells (Figs. 25, 27 and 44). Furthermore, we describe that entry of HIV-1, VLPs and exosomes into mDCs is a dose-dependent mechanism that increases over time (Figs. 27, 38 and 44).

Our data also revealed that internalization of HIV-1, VLPs or exosomes could not be abrogated with an effective protease pretreatment of either of these particles or mDCs (Figs. 45 and 46). Nevertheless, this observation does not exclude the potential role of proteins during viral or exosome capture, and might just reflect that the molecular determinants involved in capture were not fully processed by the proteases employed. However, treatment of virus, VLP or exosome producing cells with inhibitors of sphingolipid biosynthesis extensively reduced particle entry into mDCs (Fig. 48) without interfering with the net release from producer cells (Fig. 47). Although it has previously been shown that FB1 treatment of virus-producer cells diminishes the infectivity of released HIV-1 particles (28) and blocks HCV replication *in vitro* (186), differences in infectivity were moderate at the viral input used in this study. Moreover, treatment with NB-DNJ did not affect viral infectivity at all (Fig. 47). Therefore, our findings establish a critical role for sphingolipids during mDC binding and endocytosis of particles derived from cholesterol-enriched domains such as HIV and exosomes. These data could imply a direct interaction of the sphingolipids with the plasma membrane of mDCs.

Alternatively, the sphingolipids could maintain the structural entities required for viral and exosome binding to mDCs, allowing the interaction of Pronase-resistant proteins with the mDC membrane surface. Further studies will help clarify which of the two models our data support actually accounts for particle endocytosis.

In conclusion, we have shown that the capture of retroviruses and exosomes is upregulated upon DC maturation, leading internalized particles into the same CD81⁺ intracellular compartment and allowing efficient transmission to T cells. This novel capture pathway, where retroviruses and exosomes converge, has clear implications for the design of effective HIV therapeutic vaccines. Although mDCs pulsed with inactivated virus could stimulate specific CD8⁺ T cell immune responses in infected patients, as reviewed in (4), these injected mDCs could also mediate *trans*-infection of new CD4⁺ T target cells, amplifying viral dissemination. Therefore, the safety of these strategies should be carefully evaluated, preferentially in patients with undetectable viral load. Regarding prophylactic HIV vaccines, the proposed exosomal origin of retrovirus predicts that HIV poses an unsolvable paradox for adaptive immune responses (79). Even more challenging from this perspective, retroviral-based vaccines are unlikely to provide any protection. Further work should address the specific differences between retroviral particles and exosomes to overcome these difficulties.

Taken as a whole, our results suggest that mDCs, which have a greater ability than iDCs to transmit the virus to target cells, and interact continuously with CD4⁺ T cells at the lymph nodes – the key site of viral replication – could play a prominent role in augmenting viral dissemination. Underscoring the molecular determinants of this highly efficient viral capture process, where retroviruses mimic exosomes to evade the host immune system, could lead to


new therapeutic strategies for infectious diseases caused by retroviruses, such as HIV-1 and other T-lymphotropic agents such as HTLV-1. Furthermore, this knowledge can help in the design of safer candidates for use in a DC-based vaccine.

Our ultimate goal is to find a new therapeutic potion to turn Mr. Hyde back into Dr. Jekyll once and for all, hoping that by limiting DC functionality to immune responses during HIV disease progression, we can rewrite the end of Robert Louis Stevenson's book and get closer to finally winning the war against the HIV pandemic.

7.

Conclusions


The most remarkable conclusions obtained in the studies performed during this thesis can be summarized as follows:

 **1.1** Mature Myeloid DCs and mDCs are able to capture HIV-1 with greater ability than immature Myeloid DCs and iDCs, contributing to their higher viral transmission to CD4⁺ T cells.


1.2 Maturation of DCs also enhances VLP and exosome capture.

1.3 Confocal and electron microscopy reveal the lack of viral accumulation within iDCs. In marked contrast, maturation increases DCs' ability to endocytose HIV-1, VLPs and exosomes in large intracellular vesicles.


1.4 In mDCs, HIV-1, VLP and exosome capture increases over time and the lifespan of trapped particles is longer than in iDCs.

 **2.1** Mature Myeloid DC and mDC increased viral uptake does not correlate with DC-SIGN expression levels, cannot be blocked by DC-SIGN-specific inhibitors and is not mediated by the envelope glycoprotein, indicating that alternative mechanisms are implicated in HIV capture other than C-type lectin receptors.


2.2 Studying polymorphic variants of the DC-SIGN gene might not improve our understanding of the *trans*-infection process.

 **3.1** Competition experiments suggest that different particles derived from cholesterol-enriched domains use the same entry pathway into mDCs. Therefore, budding from lipid raft domains is essential to include specific mature DC-recognition determinants that allow viral and exosome capture.

3.2 HIV-1, VLPs and exosomes enter mDCs through a mechanism resistant to proteolysis. However, HIV-1, VLP and exosome capture can be inhibited when particles are produced from ceramide-deficient cells.

 **4.1** Viral capture by mDCs is an active process most likely dependent on cholesterol-enriched lipid rafts and clathrin-mediated endocytic mechanisms.

4.2 Mature Myeloid DCs retain viral particles in a CD81⁺ and CD63⁺ compartment. Analogously, mDCs retain HIV-1, VLPs and exosomes in the same CD81⁺ intracellular compartment.

 **5.** Most of the virus captured by mDCs is recruited to the DC–T cell contact zone, allowing viral *trans*-infection. Likewise, VLPs and exosomes captured by mDCs can be transferred to CD4⁺ T cells, mimicking HIV-1 transmission. Therefore, infectious synapses and similar structures can be formed independently of the viral envelope glycoprotein.

8.

Bibliography.

A

1. **Akira, S., K. Takeda, and T. Kaisho.** 2001. Toll-like receptors: critical proteins linking innate and acquired immunity. *Nat Immunol* **2**:675-80.
2. **Albert, M. L., B. Sauter, and N. Bhardwaj.** 1998. Dendritic cells acquire antigen from apoptotic cells and induce class I-restricted CTLs. *Nature* **392**:86-9.
3. **Aloia, R. C., H. Tian, and F. C. Jensen.** 1993. Lipid composition and fluidity of the human immunodeficiency virus envelope and host cell plasma membranes. *Proc Natl Acad Sci U S A* **90**:5181-5.
4. **Andrieu, J. M., and W. Lu.** 2007. A dendritic cell-based vaccine for treating HIV infection: background and preliminary results. *J Intern Med* **261**:123-31.
5. **Ardavin, C., G. Martinez del Hoyo, P. Martin, F. Anjuere, C. F. Arias, A. R. Marin, S. Ruiz, V. Parrillas, and H. Hernandez.** 2001. Origin and differentiation of dendritic cells. *Trends Immunol* **22**:691-700.
6. **Arrighi, J. F., M. Pion, E. Garcia, J. M. Escola, Y. van Kooyk, T. B. Geijtenbeek, and V. Piguet.** 2004. DC-SIGN-mediated infectious synapse formation enhances X4 HIV-1 transmission from dendritic cells to T cells. *J Exp Med* **200**:1279-88.
7. **Arthur, L. O., J. W. Bess, Jr., R. C. Sowder, 2nd, R. E. Benveniste, D. L. Mann, J. C. Chermann, and L. E. Henderson.** 1992. Cellular proteins bound to immunodeficiency viruses: implications for pathogenesis and vaccines. *Science* **258**:1935-8.

B

8. **Badovinac, V. P., K. A. Messingham, A. Jabbari, J. S. Haring, and J. T. Harty.** 2005. Accelerated CD8+ T-cell memory and prime-boost response after dendritic-cell vaccination. *Nat Med* **11**:748-56.
9. **Bakri, Y., C. Schiffer, V. Zennou, P. Charneau, E. Kahn, A. Benjouad, J. C. Gluckman, and B. Canque.** 2001. The maturation of dendritic cells results in postintegration inhibition of HIV-1 replication. *J Immunol* **166**:3780-8.
10. **Banchereau, J., F. Briere, C. Caux, J. Davoust, S. Lebecque, Y. J. Liu, B. Pulendran, and K. Palucka.** 2000. Immunobiology of dendritic cells. *Annu Rev Immunol* **18**:767-811.
11. **Banchereau, J., and R. M. Steinman.** 1998. Dendritic cells and the control of immunity. *Nature* **392**:245-52.
12. **Baribaud, F., S. Pohlmann, G. Leslie, F. Mortari, and R. W. Doms.** 2002. Quantitative expression and virus transmission analysis of DC-SIGN on monocyte-derived dendritic cells. *J Virol* **76**:9135-42.
13. **Barron, M. A., N. Blyveis, B. E. Palmer, S. MaWhinney, and C. C. Wilson.** 2003. Influence of plasma viremia on defects in number and immunophenotype of blood dendritic cell subsets in human immunodeficiency virus 1-infected individuals. *J Infect Dis* **187**:26-37.
14. **Bennett, L., A. K. Palucka, E. Arce, V. Cantrell, J. Borvak, J. Banchereau, and V. Pascual.** 2003. Interferon and granulopoiesis signatures in systemic lupus erythematosus blood. *J Exp Med* **197**:711-23.
15. **Bess, J. W., Jr., R. J. Gorelick, W. J. Bosche, L. E. Henderson, and L. O. Arthur.** 1997. Microvesicles are a source of contaminating cellular proteins found in purified HIV-1 preparations. *Virology* **230**:134-44.
16. **Blanco, J., J. Barretina, B. Clotet, and J. A. Este.** 2004. R5 HIV gp120-mediated cellular contacts induce the death of single CCR5-expressing CD4 T cells by a gp41-dependent mechanism. *J Leukoc Biol* **76**:804-11.

17. **Blanco, J., B. Bosch, M. T. Fernandez-Figueras, J. Barretina, B. Clotet, and J. A. Este.** 2004. High level of coreceptor-independent HIV transfer induced by contacts between primary CD4 T cells. *J Biol Chem* **279**:51305-14.
18. **Blanco, P., A. K. Palucka, M. Gill, V. Pascual, and J. Banchereau.** 2001. Induction of dendritic cell differentiation by IFN-alpha in systemic lupus erythematosus. *Science* **294**:1540-3.
19. **Blauvelt, A., H. Asada, M. W. Saville, V. Klaus-Kovtun, D. J. Altman, R. Yarchoan, and S. I. Katz.** 1997. Productive infection of dendritic cells by HIV-1 and their ability to capture virus are mediated through separate pathways. *J Clin Invest* **100**:2043-53.
20. **Blom, J., C. Nielsen, and J. M. Rhodes.** 1993. An ultrastructural study of HIV-infected human dendritic cells and monocytes/macrophages. *Apmis* **101**:672-80.
21. **Boehme, K. W., and T. Compton.** 2004. Innate sensing of viruses by toll-like receptors. *J Virol* **78**:7867-73.
22. **Boggiano, C., N. Manel, and D. R. Littman.** 2007. Dendritic cell-mediated trans-enhancement of human immunodeficiency virus type 1 infectivity is independent of DC-SIGN. *J Virol* **81**:2519-23.
23. **Booth, A. M., Y. Fang, J. K. Fallon, J. M. Yang, J. E. Hildreth, and S. J. Gould.** 2006. Exosomes and HIV Gag bud from endosome-like domains of the T cell plasma membrane. *J Cell Biol* **172**:923-35.
24. **Bosch, B., J. Blanco, E. Pauls, I. Clotet-Codina, M. Armand-Ugon, B. Grigorov, D. Muriaux, B. Clotet, J. L. Darlix, and J. A. Este.** 2005. Inhibition of coreceptor-independent cell-to-cell human immunodeficiency virus type 1 transmission by a CD4-immunoglobulin G2 fusion protein. *Antimicrob Agents Chemother* **49**:4296-304.
25. **Brenchley, J. M., D. A. Price, and D. C. Douek.** 2006. HIV disease: fallout from a mucosal catastrophe? *Nat Immunol* **7**:235-9.
26. **Brenchley, J. M., D. A. Price, T. W. Schacker, T. E. Asher, G. Silvestri, S. Rao, Z. Kazzaz, E. Bornstein, O. Lambotte, D. Altmann, B. R. Blazar, B. Rodriguez, L. Teixeira-Johnson, A. Landay, J. N. Martin, F. M. Hecht, L. J. Picker, M. M. Lederman, S. G. Deeks, and D. C. Douek.** 2006. Microbial

- translocation is a cause of systemic immune activation in chronic HIV infection. *Nat Med* **12**:1365-71.
27. **Briggs, J. A., K. Grunewald, B. Glass, F. Forster, H. G. Krausslich, and S. D. Fuller.** 2006. The mechanism of HIV-1 core assembly: insights from three-dimensional reconstructions of authentic virions. *Structure* **14**:15-20.
28. **Brugger, B., B. Glass, P. Haberkant, I. Leibrecht, F. T. Wieland, and H. G. Krausslich.** 2006. The HIV lipidome: a raft with an unusual composition. *Proc Natl Acad Sci U S A* **103**:2641-6.
29. **Buonaguro, L., M. L. Tornesello, M. Tagliamonte, R. C. Gallo, L. X. Wang, R. Kamin-Lewis, S. Abdelwahab, G. K. Lewis, and F. M. Buonaguro.** 2006. Baculovirus-derived human immunodeficiency virus type 1 virus-like particles activate dendritic cells and induce ex vivo T-cell responses. *J Virol* **80**:9134-43.
30. **Burleigh, L., P. Y. Lozach, C. Schiffer, I. Staropoli, V. Pezo, F. Porrot, B. Canque, J. L. Virelizier, F. Arenzana-Seisdedos, and A. Amara.** 2006. Infection of dendritic cells (DCs), not DC-SIGN-mediated internalization of human immunodeficiency virus, is required for long-term transfer of virus to T cells. *J Virol* **80**:2949-57.
31. **Buseyne, F., S. Le Gall, C. Boccaccio, J. P. Abastado, J. D. Lifson, L. O. Arthur, Y. Riviere, J. M. Heard, and O. Schwartz.** 2001. MHC-I-restricted presentation of HIV-1 virion antigens without viral replication. *Nat Med* **7**:344-9.

C

32. **Cameron, P. U., P. S. Freudenthal, J. M. Barker, S. Gezelter, K. Inaba, and R. M. Steinman.** 1992. Dendritic cells exposed to human immunodeficiency virus type-1 transmit a vigorous cytopathic infection to CD4+ T cells. *Science* **257**:383-7.
33. **Canque, B., Y. Bakri, S. Camus, M. Yagello, A. Benjouad, and J. C. Gluckman.** 1999. The susceptibility to X4 and R5 human immunodeficiency virus-1 strains of dendritic cells derived in vitro from CD34(+) hematopoietic progenitor cells is primarily determined by their maturation stage. *Blood* **93**:3866-75.

34. **Cavrois, M., J. Neidleman, J. F. Kreisberg, D. Fenard, C. Callebaut, and W. C. Greene.** 2006. Human immunodeficiency virus fusion to dendritic cells declines as cells mature. *J Virol* **80**:1992-9.
35. **Cavrois, M., J. Neidleman, J. F. Kreisberg, and W. C. Greene.** 2007. In vitro derived dendritic cells trans-infect CD4 T cells primarily with surface-bound HIV-1 virions. *PLoS Pathog* **3**:e4.
36. **Cella, M., A. Engering, V. Pinet, J. Pieters, and A. Lanzavecchia.** 1997. Inflammatory stimuli induce accumulation of MHC class II complexes on dendritic cells. *Nature* **388**:782-7.
37. **Chazal, N., and D. Gerlier.** 2003. Virus entry, assembly, budding, and membrane rafts. *Microbiol Mol Biol Rev* **67**:226-37.
38. **Chen, P., W. Hubner, M. A. Spinelli, and B. K. Chen.** 2007. Predominant mode of human immunodeficiency virus transfer between T cells is mediated by sustained Env-dependent neutralization-resistant virological synapses. *J Virol* **81**:12582-95.
39. **Chiu, Y. L., V. B. Soros, J. F. Kreisberg, K. Stopak, W. Yonemoto, and W. C. Greene.** 2005. Cellular APOBEC3G restricts HIV-1 infection in resting CD4+ T cells. *Nature* **435**:108-14.
40. **Chow, Y. H., D. Yu, J. Y. Zhang, Y. Xie, O. L. Wei, C. Chiu, M. Foroohar, O. O. Yang, N. H. Park, I. S. Chen, and S. Pang.** 2002. gp120-Independent infection of CD4(-) epithelial cells and CD4(+) T-cells by HIV-1. *J Acquir Immune Defic Syndr* **30**:1-8.
41. **Chun, T. W., D. C. Nickle, J. S. Justement, J. H. Meyers, G. Roby, C. W. Hallahan, S. Kottlil, S. Moir, J. M. Mican, J. I. Mullins, D. J. Ward, J. A. Kovacs, P. J. Mannon, and A. S. Fauci.** 2008. Persistence of HIV in gut-associated lymphoid tissue despite long-term antiretroviral therapy. *J Infect Dis* **197**:714-20.
42. **Colonna, M., G. Trinchieri, and Y. J. Liu.** 2004. Plasmacytoid dendritic cells in immunity. *Nat Immunol* **5**:1219-26.
43. **Connor, J. H., M. O. McKenzie, and D. S. Lyles.** 2006. Role of residues 121 to 124 of vesicular stomatitis virus matrix protein in virus assembly and virus-host interaction. *J Virol* **80**:3701-11.

44. **Connor, R. I., K. E. Sheridan, D. Ceradini, S. Choe, and N. R. Landau.** 1997. Change in coreceptor use correlates with disease progression in HIV-1-infected individuals. *J Exp Med* **185**:621-8.
45. **Coren, L. V., T. Shatzer, and D. E. Ott.** 2008. CD45 immunoaffinity depletion of vesicles from Jurkat T cells demonstrates that exosomes contain CD45: no evidence for a distinct exosome/HIV-1 budding pathway. *Retrovirology* **5**:64.
46. **Curtis, B. M., S. Scharnowske, and A. J. Watson.** 1992. Sequence and expression of a membrane-associated C-type lectin that exhibits CD4-independent binding of human immunodeficiency virus envelope glycoprotein gp120. *Proc Natl Acad Sci U S A* **89**:8356-60.

D

47. **Daecke, J., O. T. Fackler, M. T. Dittmar, and H. G. Krausslich.** 2005. Involvement of clathrin-mediated endocytosis in human immunodeficiency virus type 1 entry. *J Virol* **79**:1581-94.
48. **de Witte, L., M. Bobardt, U. Chatterji, G. Degeest, G. David, T. B. Geijtenbeek, and P. Gallay.** 2007. Syndecan-3 is a dendritic cell-specific attachment receptor for HIV-1. *Proc Natl Acad Sci U S A* **104**:19464-9.
49. **Denzer, K., M. J. Kleijmeer, H. F. Heijnen, W. Stoorvogel, and H. J. Geuze.** 2000. Exosome: from internal vesicle of the multivesicular body to intercellular signaling device. *J Cell Sci* **113 Pt 19**:3365-74.
50. **Dimitrov, D. S., R. L. Willey, H. Sato, L. J. Chang, R. Blumenthal, and M. A. Martin.** 1993. Quantitation of human immunodeficiency virus type 1 infection kinetics. *J Virol* **67**:2182-90.
51. **Dixit, N. M., and A. S. Perelson.** 2004. Multiplicity of human immunodeficiency virus infections in lymphoid tissue. *J Virol* **78**:8942-5.
52. **Dornadula, G., G. Nunnari, M. Vanella, J. Roman, T. Babinchak, J. DeSimone, J. Stern, M. Braffman, H. Zhang, and R. J. Pomerantz.** 2001. Human immunodeficiency virus type 1-infected persons with residual disease and

- virus reservoirs on suppressive highly active antiretroviral therapy can be stratified into relevant virologic and immunologic subgroups. *J Infect Dis* **183**:1682-7.
53. **Dornadula, G., H. Zhang, B. VanUitert, J. Stern, L. Livornese, Jr., M. J. Ingerman, J. Witek, R. J. Kedanis, J. Natkin, J. DeSimone, and R. J. Pomerantz.** 1999. Residual HIV-1 RNA in blood plasma of patients taking suppressive highly active antiretroviral therapy. *Jama* **282**:1627-32.
 54. **Douek, D. C., J. M. Brenchley, M. R. Betts, D. R. Ambrozak, B. J. Hill, Y. Okamoto, J. P. Casazza, J. Kuruppu, K. Kunstman, S. Wolinsky, Z. Grossman, M. Dybul, A. Oxenius, D. A. Price, M. Connors, and R. A. Koup.** 2002. HIV preferentially infects HIV-specific CD4+ T cells. *Nature* **417**:95-8.
 55. **Dustin, M. L., S. Y. Tseng, R. Varma, and G. Campi.** 2006. T cell-dendritic cell immunological synapses. *Curr Opin Immunol* **18**:512-6.
 56. **Dzionic, A., A. Fuchs, P. Schmidt, S. Cremer, M. Zysk, S. Miltenyi, D. W. Buck, and J. Schmitz.** 2000. BDCA-2, BDCA-3, and BDCA-4: three markers for distinct subsets of dendritic cells in human peripheral blood. *J Immunol* **165**:6037-46.

E

57. **Embretson, J., M. Zupancic, J. L. Ribas, A. Burke, P. Racz, K. Tenner-Racz, and A. T. Haase.** 1993. Massive covert infection of helper T lymphocytes and macrophages by HIV during the incubation period of AIDS. *Nature* **362**:359-62.
58. **Engering, A., S. J. Van Vliet, T. B. Geijtenbeek, and Y. Van Kooyk.** 2002. Subset of DC-SIGN(+) dendritic cells in human blood transmits HIV-1 to T lymphocytes. *Blood* **100**:1780-6.
59. **Engering, A., S. J. van Vliet, K. Hebeda, D. G. Jackson, R. Prevo, S. K. Singh, T. B. Geijtenbeek, H. van Krieken, and Y. van Kooyk.** 2004. Dynamic populations of dendritic cell-specific ICAM-3 grabbing nonintegrin-positive immature dendritic cells and liver/lymph node-specific ICAM-3 grabbing nonintegrin-positive endothelial cells in the outer zones of the paracortex of human lymph nodes. *Am J Pathol* **164**:1587-95.

60. **Escola, J. M., M. J. Kleijmeer, W. Stoorvogel, J. M. Griffith, O. Yoshie, and H. J. Geuze.** 1998. Selective enrichment of tetraspan proteins on the internal vesicles of multivesicular endosomes and on exosomes secreted by human B-lymphocytes. *J Biol Chem* **273**:20121-7.
61. **Esser, M. T., D. R. Graham, L. V. Coren, C. M. Trubey, J. W. Bess, Jr., L. O. Arthur, D. E. Ott, and J. D. Lifson.** 2001. Differential incorporation of CD45, CD80 (B7-1), CD86 (B7-2), and major histocompatibility complex class I and II molecules into human immunodeficiency virus type 1 virions and microvesicles: implications for viral pathogenesis and immune regulation. *J Virol* **75**:6173-82.

F

62. **Fackler, O. T., and B. M. Peterlin.** 2000. Endocytic entry of HIV-1. *Curr Biol* **10**:1005-8.
63. **Fahrbach, K. M., S. M. Barry, S. Ayeahunie, S. Lamore, M. Klausner, and T. J. Hope.** 2007. Activated CD34-derived Langerhans cells mediate transinfection with human immunodeficiency virus. *J Virol* **81**:6858-68.
64. **Fais, S., M. R. Capobianchi, I. Abbate, C. Castilletti, M. Gentile, P. Cordiali Fei, F. Ameglio, and F. Dianzani.** 1995. Unidirectional budding of HIV-1 at the site of cell-to-cell contact is associated with co-polarization of intercellular adhesion molecules and HIV-1 viral matrix protein. *Aids* **9**:329-35.
65. **Fang, Y., N. Wu, X. Gan, W. Yan, J. C. Morrell, and S. J. Gould.** 2007. Higher-order oligomerization targets plasma membrane proteins and HIV gag to exosomes. *PLoS Biol.* **5**:e158.
66. **Fellay, J., K. V. Shianna, D. Ge, S. Colombo, B. Ledergerber, M. Weale, K. Zhang, C. Gumbs, A. Castagna, A. Cossarizza, A. Cozzi-Lepri, A. De Luca, P. Easterbrook, P. Francioli, S. Mallal, J. Martinez-Picado, J. M. Miro, N. Obel, J. P. Smith, J. Wyniger, P. Descombes, S. E. Antonarakis, N. L. Letvin, A. J. McMichael, B. F. Haynes, A. Telenti, and D. B. Goldstein.** 2007. A whole-

- genome association study of major determinants for host control of HIV-1. *Science* **317**:944-7.
67. **Figdor, C. G., Y. van Kooyk, and G. J. Adema.** 2002. C-type lectin receptors on dendritic cells and Langerhans cells. *Nat Rev Immunol* **2**:77-84.
68. **Flood, E. A., and D. S. Lyles.** 1999. Assembly of nucleocapsids with cytosolic and membrane-derived matrix proteins of vesicular stomatitis virus. *Virology* **261**:295-308.
69. **Fox, C. H., K. Tenner-Racz, P. Racz, A. Firpo, P. A. Pizzo, and A. S. Fauci.** 1991. Lymphoid germinal centers are reservoirs of human immunodeficiency virus type 1 RNA. *J Infect Dis* **164**:1051-7.
70. **Frank, I., M. Piatak, Jr., H. Stoessel, N. Romani, D. Bonnyay, J. D. Lifson, and M. Pope.** 2002. Infectious and whole inactivated simian immunodeficiency viruses interact similarly with primate dendritic cells (DCs): differential intracellular fate of virions in mature and immature DCs. *J Virol* **76**:2936-51.
71. **Freed, E. O.** 1998. HIV-1 gag proteins: diverse functions in the virus life cycle. *Virology* **251**:1-15.

G

72. **Galibert, L., C. R. Maliszewski, and S. Vandenabeele.** 2001. Plasmacytoid monocytes/T cells: a dendritic cell lineage? *Semin Immunol* **13**:283-9.
73. **Garcia, E., D. S. Nikolic, and V. Piguet.** 2008. HIV-1 replication in dendritic cells occurs through a tetraspanin-containing compartment enriched in AP-3. *Traffic* **9**:200-14.
74. **Garcia, E., M. Pion, A. Pelchen-Matthews, L. Collinson, J. F. Arrighi, G. Blot, F. Leuba, J. M. Escola, N. Demaurex, M. Marsh, and V. Piguet.** 2005. HIV-1 trafficking to the dendritic cell-T-cell infectious synapse uses a pathway of tetraspanin sorting to the immunological synapse. *Traffic* **6**:488-501.
75. **Garrus, J. E., U. K. von Schwedler, O. W. Pornillos, S. G. Morham, K. H. Zavitz, H. E. Wang, D. A. Wettstein, K. M. Stray, M. Cote, R. L. Rich, D. G.**

- Myszka, and W. I. Sundquist.** 2001. Tsg101 and the vacuolar protein sorting pathway are essential for HIV-1 budding. *Cell* **107**:55-65.
76. **Geijtenbeek, T. B., D. S. Kwon, R. Torensma, S. J. van Vliet, G. C. van Duijnhoven, J. Middel, I. L. Cornelissen, H. S. Nottet, V. N. KewalRamani, D. R. Littman, C. G. Figdor, and Y. van Kooyk.** 2000. DC-SIGN, a dendritic cell-specific HIV-1-binding protein that enhances trans-infection of T cells. *Cell* **100**:587-97.
77. **Gilliet, M., W. Cao, and Y. J. Liu.** 2008. Plasmacytoid dendritic cells: sensing nucleic acids in viral infection and autoimmune diseases. *Nat Rev Immunol* **8**:594-606.
78. **Goff, S., P. Traktman, and D. Baltimore.** 1981. Isolation and properties of Moloney murine leukemia virus mutants: use of a rapid assay for release of virion reverse transcriptase. *J Virol* **38**:239-48.
79. **Gould, S. J., A. M. Booth, and J. E. Hildreth.** 2003. The Trojan exosome hypothesis. *Proc Natl Acad Sci U S A* **100**:10592-7.
80. **Gousset, K., S. D. Ablan, L. V. Coren, A. Ono, F. Soheilian, K. Nagashima, D. E. Ott, and E. O. Freed.** 2008. Real-time visualization of HIV-1 GAG trafficking in infected macrophages. *PLoS Pathog* **4**:e1000015.
81. **Granelli-Piperno, A., E. Delgado, V. Finkel, W. Paxton, and R. M. Steinman.** 1998. Immature dendritic cells selectively replicate macrophagetropic (M-tropic) human immunodeficiency virus type 1, while mature cells efficiently transmit both M- and T-tropic virus to T cells. *J Virol* **72**:2733-7.
82. **Granelli-Piperno, A., A. Pritsker, M. Pack, I. Shimeliovich, J. F. Arrighi, C. G. Park, C. Trumpfheller, V. Piguet, T. M. Moran, and R. M. Steinman.** 2005. Dendritic cell-specific intercellular adhesion molecule 3-grabbing nonintegrin/CD209 is abundant on macrophages in the normal human lymph node and is not required for dendritic cell stimulation of the mixed leukocyte reaction. *J Immunol* **175**:4265-73.
83. **Groot, F., T. W. Kuijpers, B. Berkhout, and E. C. de Jong.** 2006. Dendritic cell-mediated HIV-1 transmission to T cells of LAD-1 patients is impaired due to the defect in LFA-1. *Retrovirology* **3**:75.

84. **Groot, F., T. M. van Capel, J. Schuitemaker, B. Berkhout, and E. C. de Jong.** 2006. Differential susceptibility of naive, central memory and effector memory T cells to dendritic cell-mediated HIV-1 transmission. *Retrovirology* **3**:52.
85. **Gummuluru, S., V. N. KewalRamani, and M. Emerman.** 2002. Dendritic cell-mediated viral transfer to T cells is required for human immunodeficiency virus type 1 persistence in the face of rapid cell turnover. *J Virol* **76**:10692-701.
86. **Gummuluru, S., M. Rogel, L. Stamatatos, and M. Emerman.** 2003. Binding of human immunodeficiency virus type 1 to immature dendritic cells can occur independently of DC-SIGN and mannose binding C-type lectin receptors via a cholesterol-dependent pathway. *J Virol* **77**:12865-74.
87. **Guo, M. M., and J. E. Hildreth.** 1995. HIV acquires functional adhesion receptors from host cells. *AIDS Res Hum Retroviruses* **11**:1007-13.
88. **Gurer, C., A. Cimorelli, and J. Luban.** 2002. Specific incorporation of heat shock protein 70 family members into primate lentiviral virions. *J Virol* **76**:4666-70.
89. **Gurney, K. B., J. Elliott, H. Nassanian, C. Song, E. Soilleux, I. McGowan, P. A. Anton, and B. Lee.** 2005. Binding and transfer of human immunodeficiency virus by DC-SIGN+ cells in human rectal mucosa. *J Virol* **79**:5762-73.

H

90. **Haase, A. T.** 1999. Population biology of HIV-1 infection: viral and CD4+ T cell demographics and dynamics in lymphatic tissues. *Annu Rev Immunol* **17**:625-56.
91. **Heath, W. R., G. T. Belz, G. M. Behrens, C. M. Smith, S. P. Forehan, I. A. Parish, G. M. Davey, N. S. Wilson, F. R. Carbone, and J. A. Villadangos.** 2004. Cross-presentation, dendritic cell subsets, and the generation of immunity to cellular antigens. *Immunol Rev* **199**:9-26.
92. **Hermida-Matsumoto, L., and M. D. Resh.** 2000. Localization of human immunodeficiency virus type 1 Gag and Env at the plasma membrane by confocal imaging. *J Virol* **74**:8670-9.

93. **Hildreth, J. E., and R. J. Orentas.** 1989. Involvement of a leukocyte adhesion receptor (LFA-1) in HIV-induced syncytium formation. *Science* **244**:1075-8.
94. **Hladik, F., and M. J. McElrath.** 2008. Setting the stage: host invasion by HIV. *Nat Rev Immunol* **8**:447-57.
95. **Hladik, F., P. Sakchalathorn, L. Ballweber, G. Lentz, M. Fialkow, D. Eschenbach, and M. J. McElrath.** 2007. Initial events in establishing vaginal entry and infection by human immunodeficiency virus type-1. *Immunity* **26**:257-70.
96. **Hodges, A., K. Sharrocks, M. Edelmann, D. Baban, A. Moris, O. Schwartz, H. Drakesmith, K. Davies, B. Kessler, A. McMichael, and A. Simmons.** 2007. Activation of the lectin DC-SIGN induces an immature dendritic cell phenotype triggering Rho-GTPase activity required for HIV-1 replication. *Nat Immunol* **8**:569-77.
97. **Hogue, I. B., S. H. Bajaria, B. A. Fallert, S. Qin, T. A. Reinhart, and D. E. Kirschner.** 2008. The dual role of dendritic cells in the immune response to human immunodeficiency virus type 1 infection. *J Gen Virol* **89**:2228-39.
98. **Hong, P. W., K. B. Flummerfelt, A. de Parseval, K. Gurney, J. H. Elder, and B. Lee.** 2002. Human immunodeficiency virus envelope (gp120) binding to DC-SIGN and primary dendritic cells is carbohydrate dependent but does not involve 2G12 or cyanovirin binding sites: implications for structural analyses of gp120-DC-SIGN binding. *J Virol* **76**:12855-65.
99. **Hu, J., M. B. Gardner, and C. J. Miller.** 2000. Simian immunodeficiency virus rapidly penetrates the cervicovaginal mucosa after intravaginal inoculation and infects intraepithelial dendritic cells. *J Virol* **74**:6087-95.
100. **Hu, Q., I. Frank, V. Williams, J. J. Santos, P. Watts, G. E. Griffin, J. P. Moore, M. Pope, and R. J. Shattock.** 2004. Blockade of attachment and fusion receptors inhibits HIV-1 infection of human cervical tissue. *J Exp Med* **199**:1065-75.
101. **Huppa, J. B., and M. M. Davis.** 2003. T-cell-antigen recognition and the immunological synapse. *Nat Rev Immunol* **3**:973-83.

I

102. **Inaba, K., S. Turley, F. Yamaide, T. Iyoda, K. Mahnke, M. Inaba, M. Pack, M. Subklewe, B. Sauter, D. Sheff, M. Albert, N. Bhardwaj, I. Mellman, and R. M. Steinman.** 1998. Efficient presentation of phagocytosed cellular fragments on the major histocompatibility complex class II products of dendritic cells. *J Exp Med* **188**:2163-73.

J

103. **Jameson, B., F. Baribaud, S. Pohlmann, D. Ghavimi, F. Mortari, R. W. Doms, and A. Iwasaki.** 2002. Expression of DC-SIGN by dendritic cells of intestinal and genital mucosae in humans and rhesus macaques. *J Virol* **76**:1866-75.
104. **Janas, A. M., C. Dong, J. H. Wang, and L. Wu.** 2008. Productive infection of human immunodeficiency virus type 1 in dendritic cells requires fusion-mediated viral entry. *Virology* **375**:442-51.
105. **Jung, S., D. Unutmaz, P. Wong, G. Sano, K. De los Santos, T. Sparwasser, S. Wu, S. Vuthoori, K. Ko, F. Zavala, E. G. Pamer, D. R. Littman, and R. A. Lang.** 2002. In vivo depletion of CD11c(+) dendritic cells abrogates priming of CD8(+) T cells by exogenous cell-associated antigens. *Immunity* **17**:211-20.

K

106. **Kadowaki, N., S. Ho, S. Antonenko, R. W. Malefyt, R. A. Kastelein, F. Bazan, and Y. J. Liu.** 2001. Subsets of human dendritic cell precursors express different toll-like receptors and respond to different microbial antigens. *J Exp Med* **194**:863-9.
107. **Kapsenberg, M. L.** 2003. Dendritic-cell control of pathogen-driven T-cell polarization. *Nat Rev Immunol* **3**:984-93.

108. **Kawamura, T., S. S. Cohen, D. L. Borris, E. A. Aquilino, S. Glushakova, L. B. Margolis, J. M. Orenstein, R. E. Offord, A. R. Neurath, and A. Blauvelt.** 2000. Candidate microbicides block HIV-1 infection of human immature Langerhans cells within epithelial tissue explants. *J Exp Med* **192**:1491-500.
109. **Kawamura, T., F. O. Gulden, M. Sugaya, D. T. McNamara, D. L. Borris, M. M. Lederman, J. M. Orenstein, P. A. Zimmerman, and A. Blauvelt.** 2003. R5 HIV productively infects Langerhans cells, and infection levels are regulated by compound CCR5 polymorphisms. *Proc Natl Acad Sci U S A* **100**:8401-6.
110. **Kawamura, T., M. Qualbani, E. K. Thomas, J. M. Orenstein, and A. Blauvelt.** 2001. Low levels of productive HIV infection in Langerhans cell-like dendritic cells differentiated in the presence of TGF-beta1 and increased viral replication with CD40 ligand-induced maturation. *Eur J Immunol* **31**:360-8.
111. **Kramer, B., A. Pelchen-Matthews, M. Deneka, E. Garcia, V. Piguet, and M. Marsh.** 2005. HIV interaction with endosomes in macrophages and dendritic cells. *Blood Cells Mol Dis* **35**:136-42.
112. **Kwon, D. S., G. Gregorio, N. Bitton, W. A. Hendrickson, and D. R. Littman.** 2002. DC-SIGN-mediated internalization of HIV is required for trans-enhancement of T cell infection. *Immunity* **16**:135-44.

L

113. **Lambert, A. A., C. Gilbert, M. Richard, A. D. Beaulieu, and M. J. Tremblay.** 2008. The C-type lectin surface receptor DCIR acts as a new attachment factor for HIV-1 in dendritic cells and contributes to trans- and cis-infection pathways. *Blood* **12**:1299-307.
114. **Lamparski, H. G., A. Metha-Damani, J. Y. Yao, S. Patel, D. H. Hsu, C. Ruegg, and J. B. Le Pecq.** 2002. Production and characterization of clinical grade exosomes derived from dendritic cells. *J Immunol Methods* **270**:211-26.
115. **Lanzavecchia, A., and F. Sallusto.** 2001. Regulation of T cell immunity by dendritic cells. *Cell* **106**:263-6.

116. **Laulagnier, K., C. Motta, S. Hamdi, S. Roy, F. Fauvelle, J. F. Pageaux, T. Kobayashi, J. P. Salles, B. Perret, C. Bonnerot, and M. Record.** 2004. Mast cell- and dendritic cell-derived exosomes display a specific lipid composition and an unusual membrane organization. *Biochem J* **380**:161-71.
117. **Lee, B., G. Leslie, E. Soilleux, U. O'Doherty, S. Baik, E. Levroney, K. Flummerfelt, W. Swiggard, N. Coleman, M. Malim, and R. W. Doms.** 2001. cis Expression of DC-SIGN allows for more efficient entry of human and simian immunodeficiency viruses via CD4 and a coreceptor. *J Virol* **75**:12028-38.
118. **Leon, B., M. Lopez-Bravo, and C. Ardavin.** 2007. Monocyte-derived dendritic cells formed at the infection site control the induction of protective T helper 1 responses against *Leishmania*. *Immunity* **26**:519-31.
119. **Levy, J. A.** 2007. *HIV and the Pathogenesis of AIDS*, Third ed. ASM press.
120. **Levy, J. A.** 1993. HIV pathogenesis and long-term survival. *Aids* **7**:1401-10.
121. **Li, Q., L. Duan, J. D. Estes, Z. M. Ma, T. Rourke, Y. Wang, C. Reilly, J. Carlis, C. J. Miller, and A. T. Haase.** 2005. Peak SIV replication in resting memory CD4⁺ T cells depletes gut lamina propria CD4⁺ T cells. *Nature* **434**:1148-52.
122. **Lindwasser, O. W., and M. D. Resh.** 2002. Myristoylation as a target for inhibiting HIV assembly: unsaturated fatty acids block viral budding. *Proc Natl Acad Sci U S A* **99**:13037-42.
123. **Liu, K., C. Waskow, X. Liu, K. Yao, J. Hoh, and M. Nussenzweig.** 2007. Origin of dendritic cells in peripheral lymphoid organs of mice. *Nat Immunol* **8**:578-83.
124. **Liu, Y. J.** 2001. Dendritic cell subsets and lineages, and their functions in innate and adaptive immunity. *Cell* **106**:259-62.
125. **Liu, Y. J.** 2005. IPC: professional type 1 interferon-producing cells and plasmacytoid dendritic cell precursors. *Annu Rev Immunol* **23**:275-306.
126. **Lore, K., A. Smed-Sorensen, J. Vasudevan, J. R. Mascola, and R. A. Koup.** 2005. Myeloid and plasmacytoid dendritic cells transfer HIV-1 preferentially to antigen-specific CD4⁺ T cells. *J Exp Med* **201**:2023-33.
127. **Lore, K., A. Sonnerborg, C. Brostrom, L. E. Goh, L. Perrin, H. McDade, H. J. Stellbrink, B. Gazzard, R. Weber, L. A. Napolitano, Y. van Kooyk, and J. Andersson.** 2002. Accumulation of DC-SIGN⁺CD40⁺ dendritic cells with reduced

- CD80 and CD86 expression in lymphoid tissue during acute HIV-1 infection. *Aids* **16**:683-92.
128. **Lu, X., Y. Xiong, and J. Silver.** 2002. Asymmetric requirement for cholesterol in receptor-bearing but not envelope-bearing membranes for fusion mediated by ecotropic murine leukemia virus. *J Virol* **76**:6701-9.
129. **Luban, J., K. L. Bossolt, E. K. Franke, G. V. Kalpana, and S. P. Goff.** 1993. Human immunodeficiency virus type 1 Gag protein binds to cyclophilins A and B. *Cell* **73**:1067-78.
130. **Lusso, P.** 2006. HIV and the chemokine system: 10 years later. *Embo J* **25**:447-56.

M

131. **MacDonald, K. P., D. J. Munster, G. J. Clark, A. Dzionek, J. Schmitz, and D. N. Hart.** 2002. Characterization of human blood dendritic cell subsets. *Blood* **100**:4512-20.
132. **Magerus-Chatinet, A., H. Yu, S. Garcia, E. Ducloux, B. Terris, and M. Bomsel.** 2007. Galactosyl ceramide expressed on dendritic cells can mediate HIV-1 transfer from monocyte derived dendritic cells to autologous T cells. *Virology* **362**:67-74.
133. **Manders, E. M. M., F. J. Verbeek, and J. A. Aten.** 1993. Measurement of co-localization of object in dual-color confocal images. *J Microsc* **169**:375-382.
134. **Marechal, V., F. Clavel, J. M. Heard, and O. Schwartz.** 1998. Cytosolic Gag p24 as an index of productive entry of human immunodeficiency virus type 1. *J Virol* **72**:2208-12.
135. **Marschang, P., J. Sodroski, R. Wurzner, and M. P. Dierich.** 1995. Decay-accelerating factor (CD55) protects human immunodeficiency virus type 1 from inactivation by human complement. *Eur J Immunol* **25**:285-90.
136. **Mathew, A., A. Bell, and R. M. Johnstone.** 1995. Hsp-70 is closely associated with the transferrin receptor in exosomes from maturing reticulocytes. *Biochem J* **308 (Pt 3)**:823-30.

137. **McCoombe, S. G., and R. V. Short.** 2006. Potential HIV-1 target cells in the human penis. *Aids* **20**:1491-5.
138. **McDonald, D., L. Wu, S. M. Bohks, V. N. KewalRamani, D. Unutmaz, and T. J. Hope.** 2003. Recruitment of HIV and its receptors to dendritic cell-T cell junctions. *Science* **300**:1295-7.
139. **McIlroy, D., B. Autran, R. Cheynier, S. Wain-Hobson, J. P. Clauvel, E. Oksenhendler, P. Debre, and A. Hosmalin.** 1995. Infection frequency of dendritic cells and CD4+ T lymphocytes in spleens of human immunodeficiency virus-positive patients. *J Virol* **69**:4737-45.
140. **Mellman, I., and R. M. Steinman.** 2001. Dendritic cells: specialized and regulated antigen processing machines. *Cell* **106**:255-8.
141. **Miller, M. J., O. Safrina, I. Parker, and M. D. Cahalan.** 2004. Imaging the single cell dynamics of CD4+ T cell activation by dendritic cells in lymph nodes. *J Exp Med.* **200**:847-56.
142. **Mobius, W., E. van Donselaar, Y. Ohno-Iwashita, Y. Shimada, H. F. Heijnen, J. W. Slot, and H. J. Geuze.** 2003. Recycling compartments and the internal vesicles of multivesicular bodies harbor most of the cholesterol found in the endocytic pathway. *Traffic* **4**:222-31.
143. **Montoya, M. C., D. Sancho, G. Bonello, Y. Collette, C. Langlet, H. T. He, P. Aparicio, A. Alcover, D. Olive, and F. Sanchez-Madrid.** 2002. Role of ICAM-3 in the initial interaction of T lymphocytes and APCs. *Nat Immunol* **3**:159-68.
144. **Moris, A., C. Nobile, F. Buseyne, F. Porrot, J. P. Abastado, and O. Schwartz.** 2004. DC-SIGN promotes exogenous MHC-I-restricted HIV-1 antigen presentation. *Blood* **103**:2648-54.
145. **Moris, A., A. Pajot, F. Blanchet, F. Guivel-Benhassine, M. Salcedo, and O. Schwartz.** 2006. Dendritic cells and HIV-specific CD4+ T cells: HIV antigen presentation, T-cell activation, and viral transfer. *Blood* **108**:1643-51.
146. **Morner, A., A. Bjorndal, J. Albert, V. N. KewalRamani, D. R. Littman, R. Inoue, R. Thorstensson, E. M. Fenyo, and E. Bjorling.** 1999. Primary human immunodeficiency virus type 2 (HIV-2) isolates, like HIV-1 isolates, frequently use CCR5 but show promiscuity in coreceptor usage. *J Virol* **73**:2343-9.

147. **Moron, V. G., P. Rueda, C. Sedlik, and C. Leclerc.** 2003. In vivo, dendritic cells can cross-present virus-like particles using an endosome-to-cytosol pathway. *J Immunol* **171**:2242-50.

N

148. **Napolitani, G., A. Rinaldi, F. Bertoni, F. Sallusto, and A. Lanzavecchia.** 2005. Selected Toll-like receptor agonist combinations synergistically trigger a T helper type 1-polarizing program in dendritic cells. *Nat Immunol* **6**:769-76.
149. **Narahashi, Y., and J. Fukunaga.** 1969. Complete separation of three alkaline proteinases a, b, and c from pronase and some characteristics of alkaline proteinase b. *J Biochem* **66**:743-5.
150. **Narayan, S., R. J. Barnard, and J. A. Young.** 2003. Two retroviral entry pathways distinguished by lipid raft association of the viral receptor and differences in viral infectivity. *J Virol* **77**:1977-83.
151. **Nguyen, D. H., and J. E. Hildreth.** 2000. Evidence for budding of human immunodeficiency virus type 1 selectively from glycolipid-enriched membrane lipid rafts. *J Virol* **74**:3264-72.
152. **Nobile, C., A. Moris, F. Porrot, N. Sol-Foulon, and O. Schwartz.** 2003. Inhibition of human immunodeficiency virus type 1 Env-mediated fusion by DC-SIGN. *J Virol* **77**:5313-23.
153. **Nobile, C., C. Petit, A. Moris, K. Skrabal, J. P. Abastado, F. Mammano, and O. Schwartz.** 2005. Covert human immunodeficiency virus replication in dendritic cells and in DC-SIGN-expressing cells promotes long-term transmission to lymphocytes. *J Virol* **79**:5386-99.

O

154. **O'Brien, W. A., Y. Koyanagi, A. Namazie, J. Q. Zhao, A. Diagne, K. Idler, J. A. Zack, and I. S. Chen.** 1990. HIV-1 tropism for mononuclear phagocytes can be determined by regions of gp120 outside the CD4-binding domain. *Nature* **348**:69-73.
155. **Ono, A., S. D. Ablan, S. J. Lockett, K. Nagashima, and E. O. Freed.** 2004. Phosphatidylinositol (4,5) bisphosphate regulates HIV-1 Gag targeting to the plasma membrane. *Proc Natl Acad Sci U S A* **101**:14889-94.
156. **Orentas, R. J., and J. E. Hildreth.** 1993. Association of host cell surface adhesion receptors and other membrane proteins with HIV and SIV. *AIDS Res Hum Retroviruses* **9**:1157-65.
157. **Ostrowski, M. A., T. W. Chun, S. J. Justement, I. Motola, M. A. Spinelli, J. Adelsberger, L. A. Ehler, S. B. Mizell, C. W. Hallahan, and A. S. Fauci.** 1999. Both memory and CD45RA+/CD62L+ naive CD4(+) T cells are infected in human immunodeficiency virus type 1-infected individuals. *J Virol* **73**:6430-5.
158. **Ott, D. E.** 1997. Cellular proteins in HIV virions. *Rev Med Virol* **7**:167-180.

P

159. **Pang, S., D. Yu, D. S. An, G. C. Baldwin, Y. Xie, B. Poon, Y. H. Chow, N. H. Park, and I. S. Chen.** 2000. Human immunodeficiency virus Env-independent infection of human CD4(-) cells. *J Virol* **74**:10994-1000.
160. **Pantaleo, G., C. Graziosi, L. Butini, P. A. Pizzo, S. M. Schnittman, D. P. Kotler, and A. S. Fauci.** 1991. Lymphoid organs function as major reservoirs for human immunodeficiency virus. *Proc Natl Acad Sci U S A* **88**:9838-42.
161. **Pantaleo, G., C. Graziosi, J. F. Demarest, L. Butini, M. Montroni, C. H. Fox, J. M. Orenstein, D. P. Kotler, and A. S. Fauci.** 1993. HIV infection is active and progressive in lymphoid tissue during the clinically latent stage of disease. *Nature* **362**:355-8.

162. **Pashine, A., N. M. Valiante, and J. B. Ulmer.** 2005. Targeting the innate immune response with improved vaccine adjuvants. *Nat Med* **11**:S63-8.
163. **Pelkmans, L., and A. Helenius.** 2003. Insider information: what viruses tell us about endocytosis. *Curr Opin Cell Biol* **15**:414-22.
164. **Perelson, A. S., A. U. Neumann, M. Markowitz, J. M. Leonard, and D. D. Ho.** 1996. HIV-1 dynamics in vivo: virion clearance rate, infected cell life-span, and viral generation time. *Science* **271**:1582-6.
165. **Perlman, M., and M. D. Resh.** 2006. Identification of an intracellular trafficking and assembly pathway for HIV-1 gag. *Traffic* **7**:731-45.
166. **Perreau, M., G. Pantaleo, and E. J. Kremer.** 2008. Activation of a dendritic cell-T cell axis by Ad5 immune complexes creates an improved environment for replication of HIV in T cells. *J Exp Med* **205**:2717-25.
167. **Piguet, V., and Q. Sattentau.** 2004. Dangerous liaisons at the virological synapse. *J Clin Invest* **114**:605-10.
168. **Piguet, V., and R. M. Steinman.** 2007. The interaction of HIV with dendritic cells: outcomes and pathways. *Trends Immunol* **28**:503-10.
169. **Pion, M., J. F. Arrighi, J. Jiang, C. A. Lundquist, O. Hartley, C. Aiken, and V. Piguet.** 2007. Analysis of HIV-1-X4 fusion with immature dendritic cells identifies a specific restriction that is independent of CXCR4 levels. *J Invest Dermatol* **127**:319-23.
170. **Pion, M., A. Granelli-Piperno, B. Mangeat, R. Stalder, R. Correa, R. M. Steinman, and V. Piguet.** 2006. APOBEC3G/3F mediates intrinsic resistance of monocyte-derived dendritic cells to HIV-1 infection. *J Exp Med* **203**:2887-93.
171. **Platt, F. M., G. R. Neises, R. A. Dwek, and T. D. Butters.** 1994. N-butyldeoxynojirimycin is a novel inhibitor of glycolipid biosynthesis. *J Biol Chem* **269**:8362-5.
172. **Pohlmann, S., F. Baribaud, B. Lee, G. J. Leslie, M. D. Sanchez, K. Hiebenthal-Millow, J. Munch, F. Kirchhoff, and R. W. Doms.** 2001. DC-SIGN interactions with human immunodeficiency virus type 1 and 2 and simian immunodeficiency virus. *J Virol* **75**:4664-72.
173. **Puigdomenech, I., M. Massanella, N. Izquierdo-Useros, R. Ruiz-Hernandez, M. Curriu, M. Bofill, J. Martinez-Picado, M. Juan, B. Clotet, and J. Blanco.**

2008. HIV transfer between CD4 T cells does not require LFA-1 binding to ICAM-1 and is governed by the interaction of HIV envelope glycoprotein with CD4. *Retrovirology* **5**:32.
174. **Pulendran, B., J. L. Smith, G. Caspary, K. Brasel, D. Pettit, E. Maraskovsky, and C. R. Maliszewski.** 1999. Distinct dendritic cell subsets differentially regulate the class of immune response in vivo. *Proc Natl Acad Sci U S A* **96**:1036-41.

R

175. **Rabesandratana, H., J. P. Toutant, H. Reggio, and M. Vidal.** 1998. Decay-accelerating factor (CD55) and membrane inhibitor of reactive lysis (CD59) are released within exosomes during In vitro maturation of reticulocytes. *Blood* **91**:2573-80.
176. **Ramratnam, B., S. Bonhoeffer, J. Binley, A. Hurley, L. Zhang, J. E. Mittler, M. Markowitz, J. P. Moore, A. S. Perelson, and D. D. Ho.** 1999. Rapid production and clearance of HIV-1 and hepatitis C virus assessed by large volume plasma apheresis. *Lancet* **354**:1782-5.
177. **Raposo, G., M. Moore, D. Innes, R. Leijendekker, A. Leigh-Brown, P. Benaroch, and H. Geuze.** 2002. Human macrophages accumulate HIV-1 particles in MHC II compartments. *Traffic* **3**:718-29.
178. **Raposo, G., H. W. Nijman, W. Stoorvogel, R. Liejendekker, C. V. Harding, C. J. Melief, and H. J. Geuze.** 1996. B lymphocytes secrete antigen-presenting vesicles. *J Exp Med* **183**:1161-72.
179. **Rappocciolo, G., P. Piazza, C. L. Fuller, T. A. Reinhart, S. C. Watkins, D. T. Rowe, M. Jais, P. Gupta, and C. R. Rinaldo.** 2006. DC-SIGN on B lymphocytes is required for transmission of HIV-1 to T lymphocytes. *PLoS Pathog* **2**:e70.
180. **Reece, J. C., A. J. Handley, E. J. Anstee, W. A. Morrison, S. M. Crowe, and P. U. Cameron.** 1998. HIV-1 selection by epidermal dendritic cells during transmission across human skin. *J Exp Med* **187**:1623-31.

181. **Revy, P., M. Sospedra, B. Barbour, and A. Trautmann.** 2001. Functional antigen-independent synapses formed between T cells and dendritic cells. *Nat Immunol* **2**:925-31.
182. **Rissoan, M. C., V. Soumelis, N. Kadowaki, G. Grouard, F. Briere, R. de Waal Malefyt, and Y. J. Liu.** 1999. Reciprocal control of T helper cell and dendritic cell differentiation. *Science* **283**:1183-6.
183. **Robinson, S. P., S. Patterson, N. English, D. Davies, S. C. Knight, and C. D. Reid.** 1999. Human peripheral blood contains two distinct lineages of dendritic cells. *Eur J Immunol* **29**:2769-78.
184. **Rowland-Jones, S. L.** 2003. Timeline: AIDS pathogenesis: what have two decades of HIV research taught us? *Nat Rev Immunol* **3**:343-8.
185. **Ruedl, C., P. Koebel, M. Bachmann, M. Hess, and K. Karjalainen.** 2000. Anatomical origin of dendritic cells determines their life span in peripheral lymph nodes. *J Immunol* **165**:4910-6.

S

186. **Sakamoto, H., K. Okamoto, M. Aoki, H. Kato, A. Katsume, A. Ohta, T. Tsukuda, N. Shimma, Y. Aoki, M. Arisawa, M. Kohara, and M. Sudoh.** 2005. Host sphingolipid biosynthesis as a target for hepatitis C virus therapy. *Nat Chem Biol* **1**:333-7.
187. **Sallusto, F., M. Cella, C. Danieli, and A. Lanzavecchia.** 1995. Dendritic cells use macropinocytosis and the mannose receptor to concentrate macromolecules in the major histocompatibility complex class II compartment: downregulation by cytokines and bacterial products. *J Exp Med* **182**:389-400.
188. **Sallusto, F., P. Schaerli, P. Loetscher, C. Schaniel, D. Lenig, C. R. Mackay, S. Qin, and A. Lanzavecchia.** 1998. Rapid and coordinated switch in chemokine receptor expression during dendritic cell maturation. *Eur J Immunol* **28**:2760-9.

189. **Sandefur, S., R. M. Smith, V. Varthakavi, and P. Spearman.** 2000. Mapping and characterization of the N-terminal I domain of human immunodeficiency virus type 1 Pr55(Gag). *J Virol* **74**:7238-49.
190. **Sandefur, S., V. Varthakavi, and P. Spearman.** 1998. The I domain is required for efficient plasma membrane binding of human immunodeficiency virus type 1 Pr55Gag. *J Virol* **72**:2723-32.
191. **Sanders, R. W., E. C. de Jong, C. E. Baldwin, J. H. Schuitemaker, M. L. Kapsenberg, and B. Berkhout.** 2002. Differential transmission of human immunodeficiency virus type 1 by distinct subsets of effector dendritic cells. *J Virol* **76**:7812-21.
192. **Satomi, M., M. Shimizu, E. Shinya, E. Watari, A. Owaki, C. Hidaka, M. Ichikawa, T. Takeshita, and H. Takahashi.** 2005. Transmission of macrophage-tropic HIV-1 by breast-milk macrophages via DC-SIGN. *J Infect Dis* **191**:174-81.
193. **Savina, A., C. Jancic, S. Hugues, P. Guermonprez, P. Vargas, I. C. Moura, A. M. Lennon-Dumenil, M. C. Seabra, G. Raposo, and S. Amigorena.** 2006. NOX2 controls phagosomal pH to regulate antigen processing during crosspresentation by dendritic cells. *Cell* **126**:205-18.
194. **Scarlatti, G., E. Tresoldi, A. Bjorndal, R. Fredriksson, C. Colognesi, H. K. Deng, M. S. Malnati, A. Plebani, A. G. Siccardi, D. R. Littman, E. M. Fenyo, and P. Lusso.** 1997. In vivo evolution of HIV-1 co-receptor usage and sensitivity to chemokine-mediated suppression. *Nat Med* **3**:1259-65.
195. **Schnare, M., G. M. Barton, A. C. Holt, K. Takeda, S. Akira, and R. Medzhitov.** 2001. Toll-like receptors control activation of adaptive immune responses. *Nat Immunol* **2**:947-50.
196. **Schwartz, S., M. Campbell, G. Nasioulas, J. Harrison, B. K. Felber, and G. N. Pavlakis.** 1992. Mutational inactivation of an inhibitory sequence in human immunodeficiency virus type 1 results in Rev-independent gag expression. *J Virol* **66**:7176-82.
197. **Seder, R. A., W. E. Paul, M. M. Davis, and B. Fazekas de St Groth.** 1992. The presence of interleukin 4 during in vitro priming determines the lymphokine-producing potential of CD4+ T cells from T cell receptor transgenic mice. *J Exp Med* **176**:1091-8.

198. **Shattock, R. J., and J. P. Moore.** 2003. Inhibiting sexual transmission of HIV-1 infection. *Nat Rev Microbiol* **1**:25-34.
199. **Shortman, K., and Y. J. Liu.** 2002. Mouse and human dendritic cell subtypes. *Nat Rev Immunol* **2**:151-61.
200. **Shortman, K., and S. H. Naik.** 2007. Steady-state and inflammatory dendritic-cell development. *Nat Rev Immunol* **7**:19-30.
201. **Smed-Sorensen, A., K. Lore, J. Vasudevan, M. K. Louder, J. Andersson, J. R. Mascola, A. L. Spetz, and R. A. Koup.** 2005. Differential susceptibility to human immunodeficiency virus type 1 infection of myeloid and plasmacytoid dendritic cells. *J Virol* **79**:8861-9.
202. **Snyder, G. A., J. Ford, P. Torabi-Parizi, J. A. Arthos, P. Schuck, M. Colonna, and P. D. Sun.** 2005. Characterization of DC-SIGN/R interaction with human immunodeficiency virus type 1 gp120 and ICAM molecules favors the receptor's role as an antigen-capturing rather than an adhesion receptor. *J Virol* **79**:4589-98.
203. **Soilleux, E. J., and N. Coleman.** 2004. Expression of DC-SIGN in human foreskin may facilitate sexual transmission of HIV. *J Clin Pathol* **57**:77-8.
204. **Soto-Ramirez, L. E., B. Renjifo, M. F. McLane, R. Marlink, C. O'Hara, R. Sutthent, C. Wasi, P. Vithayasai, V. Vithayasai, C. Apichartpiyakul, P. Auewarakul, V. Pena Cruz, D. S. Chui, R. Osathanondh, K. Mayer, T. H. Lee, and M. Essex.** 1996. HIV-1 Langerhans' cell tropism associated with heterosexual transmission of HIV. *Science* **271**:1291-3.
205. **Stahl-Hennig, C., R. M. Steinman, K. Tenner-Racz, M. Pope, N. Stolte, K. Matz-Rensing, G. Grobschupff, B. Raschdorff, G. Hunsmann, and P. Racz.** 1999. Rapid infection of oral mucosal-associated lymphoid tissue with simian immunodeficiency virus. *Science* **285**:1261-5.
206. **Steinman, R. M.** 1991. The dendritic cell system and its role in immunogenicity. *Annu Rev Immunol* **9**:271-96.
207. **Steinman, R. M., and J. Banchereau.** 2007. Taking dendritic cells into medicine. *Nature* **449**:419-26.
208. **Steinman, R. M., and Z. A. Cohn.** 1973. Identification of a novel cell type in peripheral lymphoid organs of mice. I. Morphology, quantitation, tissue distribution. *J Exp Med* **137**:1142-62.

209. **Steinman, R. M., A. Granelli-Piperno, M. Pope, C. Trumpfheller, R. Ignatius, G. Arrode, P. Racz, and K. Tenner-Racz.** 2003. The interaction of immunodeficiency viruses with dendritic cells. *Curr Top Microbiol Immunol* **276**:1-30.
210. **Stoorvogel, W., M. J. Kleijmeer, H. J. Geuze, and G. Raposo.** 2002. The biogenesis and functions of exosomes. *Traffic* **3**:321-30.
211. **Suffredini, A. F., H. D. Hochstein, and F. G. McMahon.** 1999. Dose-related inflammatory effects of intravenous endotoxin in humans: evaluation of a new clinical lot of Escherichia coli O:113 endotoxin. *J Infect Dis* **179**:1278-82.

T

212. **Thery, C., M. Boussac, P. Veron, P. Ricciardi-Castagnoli, G. Raposo, J. Garin, and S. Amigorena.** 2001. Proteomic analysis of dendritic cell-derived exosomes: a secreted subcellular compartment distinct from apoptotic vesicles. *J Immunol* **166**:7309-18.
213. **Thery, C., L. Duban, E. Segura, P. Veron, O. Lantz, and S. Amigorena.** 2002. Indirect activation of naive CD4⁺ T cells by dendritic cell-derived exosomes. *Nat Immunol* **3**:1156-62.
214. **Thery, C., A. Regnault, J. Garin, J. Wolfers, L. Zitvogel, P. Ricciardi-Castagnoli, G. Raposo, and S. Amigorena.** 1999. Molecular characterization of dendritic cell-derived exosomes. Selective accumulation of the heat shock protein hsc73. *J Cell Biol* **147**:599-610.
215. **Thery, C., L. Zitvogel, and S. Amigorena.** 2002. Exosomes: composition, biogenesis and function. *Nat Rev Immunol* **2**:569-79.
216. **Trajkovic, K., C. Hsu, S. Chiantia, L. Rajendran, D. Wenzel, F. Wieland, P. Schwille, B. Brugger, and M. Simons.** 2008. Ceramide triggers budding of exosome vesicles into multivesicular endosomes. *Science* **319**:1244-7.
217. **Trombetta, E. S., and I. Mellman.** 2005. Cell biology of antigen processing in vitro and in vivo. *Annu Rev Immunol* **23**:975-1028.

218. **Trumpfheller, C., J. S. Finke, C. B. Lopez, T. M. Moran, B. Moltedo, H. Soares, Y. Huang, S. J. Schlesinger, C. G. Park, M. C. Nussenzweig, A. Granelli-Piperno, and R. M. Steinman.** 2006. Intensified and protective CD4⁺ T cell immunity in mice with anti-dendritic cell HIV gag fusion antibody vaccine. *J Exp Med* **203**:607-17.
219. **Trumpfheller, C., C. G. Park, J. Finke, R. M. Steinman, and A. Granelli-Piperno.** 2003. Cell type-dependent retention and transmission of HIV-1 by DC-SIGN. *Int Immunol* **15**:289-98.
220. **Tsunetsugu-Yokota, Y., S. Yasuda, A. Sugimoto, T. Yagi, M. Azuma, H. Yagita, K. Akagawa, and T. Takemori.** 1997. Efficient virus transmission from dendritic cells to CD4⁺ T cells in response to antigen depends on close contact through adhesion molecules. *Virology* **239**:259-68.
221. **Turner, B. G., and M. F. Summers.** 1999. Structural biology of HIV. *J Mol Biol* **285**:1-32.
222. **Turville, S. G., M. Aravantinou, H. Stossel, N. Romani, and M. Robbiani.** 2008. Resolution of de novo HIV production and trafficking in immature dendritic cells. *Nat Methods* **5**:75-85.
223. **Turville, S. G., J. Arthos, K. M. Donald, G. Lynch, H. Naif, G. Clark, D. Hart, and A. L. Cunningham.** 2001. HIV gp120 receptors on human dendritic cells. *Blood* **98**:2482-8.
224. **Turville, S. G., P. U. Cameron, J. Arthos, K. MacDonald, G. Clark, D. Hart, and A. L. Cunningham.** 2001. Bitter-sweet symphony: defining the role of dendritic cell gp120 receptors in HIV infection. *J Clin Virol* **22**:229-39.
225. **Turville, S. G., P. U. Cameron, A. Handley, G. Lin, S. Pohlmann, R. W. Doms, and A. L. Cunningham.** 2002. Diversity of receptors binding HIV on dendritic cell subsets. *Nat Immunol* **3**:975-83.
226. **Turville, S. G., J. J. Santos, I. Frank, P. U. Cameron, J. Wilkinson, M. Miranda-Saksena, J. Dable, H. Stossel, N. Romani, M. Piatak, Jr., J. D. Lifson, M. Pope, and A. L. Cunningham.** 2004. Immunodeficiency virus uptake, turnover, and 2-phase transfer in human dendritic cells. *Blood* **103**:2170-9.

V

227. **van Kooyk, Y., and T. B. Geijtenbeek.** 2003. DC-SIGN: escape mechanism for pathogens. *Nat Rev Immunol* **3**:697-709.
228. **van Montfort, T., A. A. Thomas, G. Pollakis, and W. A. Paxton.** 2008. Dendritic Cells Preferentially Transfer CXCR4 using Human Immunodeficiency Virus Type 1 Variants to CD4+ T Lymphocytes in trans. *J Virol* **82**:7886-96.
229. **van Vliet, S. J., J. den Dunnen, S. I. Gringhuis, T. B. Geijtenbeek, and Y. van Kooyk.** 2007. Innate signaling and regulation of Dendritic cell immunity. *Curr Opin Immunol* **19**:435-40.
230. **Varol, C., L. Landsman, D. K. Fogg, L. Greenshtein, B. Gildor, R. Margalit, V. Kalchenko, F. Geissmann, and S. Jung.** 2007. Monocytes give rise to mucosal, but not splenic, conventional dendritic cells. *J Exp Med* **204**:171-80.
231. **Villadangos, J. A., and P. Schnorrer.** 2007. Intrinsic and cooperative antigen-presenting functions of dendritic-cell subsets in vivo. *Nat Rev Immunol* **7**:543-55.
232. **von Schwedler, U. K., M. Stuchell, B. Muller, D. M. Ward, H. Y. Chung, E. Morita, H. E. Wang, T. Davis, G. P. He, D. M. Cimbora, A. Scott, H. G. Krausslich, J. Kaplan, S. G. Morham, and W. I. Sundquist.** 2003. The protein network of HIV budding. *Cell* **114**:701-13.

W

233. **Wang, E., W. P. Norred, C. W. Bacon, R. T. Riley, and A. H. Merrill, Jr.** 1991. Inhibition of sphingolipid biosynthesis by fumonisins. Implications for diseases associated with *Fusarium moniliforme*. *J Biol Chem* **266**:14486-90.
234. **Wang, J. H., A. M. Janas, W. J. Olson, and L. Wu.** 2007. Functionally distinct transmission of human immunodeficiency virus type 1 mediated by immature and mature dendritic cells. *J Virol* **81**:8933-43.

235. **Wehrly, K., and B. Chesebro.** 1997. p24 antigen capture assay for quantification of human immunodeficiency virus using readily available inexpensive reagents. *Methods* **12**:288-93.
236. **Wei, X., J. M. Decker, H. Liu, Z. Zhang, R. B. Arani, J. M. Kilby, M. S. Saag, X. Wu, G. M. Shaw, and J. C. Kappes.** 2002. Emergence of resistant human immunodeficiency virus type 1 in patients receiving fusion inhibitor (T-20) monotherapy. *Antimicrob Agents Chemother* **46**:1896-905.
237. **Welsch, S., O. T. Keppler, A. Habermann, I. Allespach, J. Krijnse-Locker, and H. G. Krausslich.** 2007. HIV-1 buds predominantly at the plasma membrane of primary human macrophages. *PLoS Pathog* **3**:e36.
238. **Wiley, R. D., and S. Gummuluru.** 2006. Immature dendritic cell-derived exosomes can mediate HIV-1 trans infection. *Proc Natl Acad Sci U S A* **103**:738-43.
239. **Wolfers, J., A. Lozier, G. Raposo, A. Regnault, C. Thery, C. Masurier, C. Flament, S. Pouzieux, F. Faure, T. Tursz, E. Angevin, S. Amigorena, and L. Zitvogel.** 2001. Tumor-derived exosomes are a source of shared tumor rejection antigens for CTL cross-priming. *Nat Med* **7**:297-303.
240. **Wu, L., A. A. Bashirova, T. D. Martin, L. Villamide, E. Mehlhop, A. O. Chertov, D. Unutmaz, M. Pope, M. Carrington, and V. N. KewalRamani.** 2002. Rhesus macaque dendritic cells efficiently transmit primate lentiviruses independently of DC-SIGN. *Proc Natl Acad Sci U S A* **99**:1568-73.
241. **Wu, L., and V. N. KewalRamani.** 2006. Dendritic-cell interactions with HIV: infection and viral dissemination. *Nat Rev Immunol* **6**:859-68.
242. **Wu, L., T. D. Martin, M. Carrington, and V. N. KewalRamani.** 2004. Raji B cells, misidentified as THP-1 cells, stimulate DC-SIGN-mediated HIV transmission. *Virology* **318**:17-23.
243. **Wu, L., T. D. Martin, Y. C. Han, S. K. Breun, and V. N. KewalRamani.** 2004. Trans-dominant cellular inhibition of DC-SIGN-mediated HIV-1 transmission. *Retrovirology* **1**:14.
244. **Wubbolts, R., R. S. Leckie, P. T. Veenhuizen, G. Schwarzmann, W. Mobius, J. Hoernschemeyer, J. W. Slot, H. J. Geuze, and W. Stoorvogel.** 2003. Proteomic and biochemical analyses of human B cell-derived exosomes. Potential implications for their function and multivesicular body formation. *J Biol Chem* **278**:10963-72.

Y

245. **Yu, H. J., M. A. Reuter, and D. McDonald.** 2008. HIV traffics through a specialized, surface-accessible intracellular compartment during trans-infection of T cells by mature dendritic cells. *PLoS Pathog* **4**:e1000134.

Z

246. **Zaitseva, M., A. Blauvelt, S. Lee, C. K. Lapham, V. Klaus-Kovtun, H. Mostowski, J. Manischewitz, and H. Golding.** 1997. Expression and function of CCR5 and CXCR4 on human Langerhans cells and macrophages: implications for HIV primary infection. *Nat Med* **3**:1369-75.
247. **Zhang, Y. J., T. Hatzioannou, T. Zang, D. Braaten, J. Luban, S. P. Goff, and P. D. Bieniasz.** 2002. Envelope-dependent, cyclophilin-independent effects of glycosaminoglycans on human immunodeficiency virus type 1 attachment and infection. *J Virol* **76**:6332-43.
248. **Zhang, Z., T. Schuler, M. Zupancic, S. Wietgreffe, K. A. Staskus, K. A. Reimann, T. A. Reinhart, M. Rogan, W. Cavert, C. J. Miller, R. S. Veazey, D. Notermans, S. Little, S. A. Danner, D. D. Richman, D. Havlir, J. Wong, H. L. Jordan, T. W. Schacker, P. Racz, K. Tenner-Racz, N. L. Letvin, S. Wolinsky, and A. T. Haase.** 1999. Sexual transmission and propagation of SIV and HIV in resting and activated CD4+ T cells. *Science* **286**:1353-7.
249. **Zitvogel, L., A. Regnault, A. Lozier, J. Wolfers, C. Flament, D. Tenza, P. Ricciardi-Castagnoli, G. Raposo, and S. Amigorena.** 1998. Eradication of established murine tumors using a novel cell-free vaccine: dendritic cell-derived exosomes. *Nat Med* **4**:594-600.

9.

Publications

1. **Dalmau, J., M. C. Puertas, M. Azuara, A. Marino, N. Frahm, B. Mothe, N. Izquierdo-Useros, M. J. Buzon, R. Paredes, L. Matas, T. M. Allen, C. Brander, C. Rodrigo, B. Clotet, and J. Martinez-Picado.** 2009. Contribution of immunological and virological factors to extremely severe primary HIV type 1 infection. *Clin Infect Dis* **48**:229-38.
2. **Izquierdo-Useros*, N., M. Naranjo-Gomez*, J. Archer, S. C. Hatch, I. Erkizia, J. Blanco, F. E. Borrás, M. C. Puertas, J. H. Connor, M. T. Fernandez-Figueras, L. Moore, B. Clotet, S. Gummuluru, and J. Martinez-Picado.** 2008. *First authorship shared. Capture and transfer of HIV-1 particles by mature dendritic cells converge with the exosome-dissemination pathway. *Blood*: Oct 22. [Epub ahead of print]
3. **Puigdomenech, I., M. Massanella, N. Izquierdo-Useros, R. Ruiz-Hernandez, M. Curriu, M. Bofill, J. Martinez-Picado, M. Juan, B. Clotet, and J. Blanco.** 2008. HIV transfer between CD4 T cells does not require LFA-1 binding to ICAM-1 and is governed by the interaction of HIV envelope glycoprotein with CD4. *Retrovirology* **5**:32.
4. **Minuesa, G., S. Purcet, I. Erkizia, M. Molina-Arcas, M. Bofill, N. Izquierdo-Useros, F. J. Casado, B. Clotet, M. Pastor-Anglada, and J. Martinez-Picado.** 2008. Expression and functionality of anti-human immunodeficiency virus and anticancer drug uptake transporters in immune cells. *J Pharmacol Exp Ther* **324**:558-67.
5. **Izquierdo-Useros, N., J. Blanco, I. Erkizia, M. T. Fernandez-Figueras, F. E. Borrás, M. Naranjo-Gomez, M. Bofill, L. Ruiz, B. Clotet, and J. Martinez-Picado.** 2007. Maturation of blood-derived dendritic cells enhances human immunodeficiency virus type 1 capture and transmission. *J Virol* **81**:7559-70.

6. **Serrano-Gomez, D., R. T. Martinez-Nunez, E. Sierra-Filardi, N. Izquierdo, M. Colmenares, J. Pla, L. Rivas, J. Martinez-Picado, J. Jimenez-Barbero, J. L. Alonso-Lebrero, S. Gonzalez, and A. L. Corbi.** 2007. AM3 modulates dendritic cell pathogen recognition capabilities by targeting DC-SIGN. *Antimicrob Agents Chemother* **51**:2313-23.
7. **Martinez-Picado, J., K. Morales-Lopetegi, C. Villena, C. Gutierrez, N. Izquierdo, S. Marfil, B. Clotet, and L. Ruiz.** 2005. Evidence for preferential genotyping of a minority human immunodeficiency virus population due to primer-template mismatching during PCR-based amplification. *J Clin Microbiol* **43**:436-8.
8. **Izquierdo, N.*, M. Naranjo*, A. Fernández M, J. Cos , L. Massuet , J. Martínez-Picado, F. Borràs.** *First authorship shared. 2003. Leukocyte Reduction Filters: an alternative source of Peripheral Blood Mononuclear Cells. *Inmunología* **22 (3)**: 255-262.
9. **Martinez-Picado, J., S. D. Frost, N. Izquierdo, K. Morales-Lopetegi, S. Marfil, T. Puig, C. Cabrera, B. Clotet, and L. Ruiz.** 2002. Viral evolution during structured treatment interruptions in chronically human immunodeficiency virus-infected individuals. *J Virol* **76**:12344-8.

10.

Acknowledgments

Resulta difícil no cogerle cariño a unas células maduras, tragonas y desmelenadas. Por eso quisiera dedicar este trabajo a las dendríticas, mis eternas compañeras, porque hemos ido madurando juntas a lo largo de esta tesis y porque cuanto más nos conocemos más cerca estamos de contribuir al avance científico, el único motor que debería mover la investigación. Y aunque quizás alguno este tentado en pensar que esta observación es un tanto “inmadura”, otra ciencia es posible.

Citando a uno de los grandes poetas de mi pueblo “Tengo tantas cosas que decir, y tú como si no fuera contigo, la historia se repite y aun así, prometo estarte agradecido”. Por eso, llegados a este punto y aún a riesgo de extenderme más de la cuenta, voy a tomarme mi tiempo para agradecerle a todas las personas que han hecho posible este trabajo su contribución y su apoyo. A todos ellos les debo el haber llegado hasta aquí y seguir con ganas de adentrarme por nuevas rutas, con su ayuda como única brújula.

Gracias, Javier, por confiar en mi desde el principio, incluso sabiendo que no era capaz de formular. Siempre has dicho que hacer la tesis es como correr

una maratón. Teniendo en cuenta que ya en el colegio me escondía para no tener que dar vueltas a la pista de atletismo, parece imposible que hoy esté a punto de llegar a la meta. Pero la verdad es que con tu apoyo incondicional he superado incluso las cuestas más escarpadas, y me siguen quedando fuerzas para continuar corriendo. Te agradezco que no hayas tirado la toalla en los momentos de más incertidumbre y que hayas mantenido la motivación siempre tan alta.

Gracias, Julià, por “adoptarme” por el camino y por estar siempre ahí dispuesto a resolver cualquier duda. Tú eres más de la opinión de que el doctorado es como montar en bicicleta. Tampoco soy una gran ciclista, pero gracias a tus consejos aquí sigo pedaleando. Te agradezco mucho que te hayas implicado tanto en este proyecto y espero seguir teniendo muchas oportunidades para colaborar contigo.

Esta tesis no habría sido posible sin el apoyo ilimitado de a la gente del grupo. Gracias, Itziar, por haberte liado la manta a la cabeza y por haberte convertido en una auténtica bióloga celular para ayudarme. Ha sido un lujo formar equipo contigo, y quiero que sepas que sin tu dedicación, tu esfuerzo y tu formaldehído jamás habría podido sacar esta tesis adelante. Julis, ya no estás en el labo, pero no puedo dejar de agradecerte todos tus sabios consejos. Gracias por enseñarme las palabras mágicas que hacen que los cultivos celulares funcionen y por facilitarme tanto las cosas en los comienzos. Kristina, gracias a ti también por tu entusiasmo vital, compromiso y compañerismo. El mundo será un lugar mejor cuando seas Secretaria General de la ONU. Gerard, la alegría de la huerta, tu llegada fue un soplo de aire fresco del que seguimos disfrutando. Eres el mejor compañero de ordenador que se puede desear. Gracias también a Mari Carmen, cuya aparición en un momento decisivo salvó el proyecto. Te agradezco muchísimo todo tu trabajo y esfuerzo para poner a

punto la técnica de purificación de exosomas, más conocida hoy por todos nosotros como la técnica del millón de dólares. Y por supuesto, gracias a Maria José y Judith, por hacer piña y por ser tan buena gente, porque así da gusto ir a trabajar. Maria Teresa, espero que esta tesis sea un buen punto de partida para que consigas todo lo que te propongas.

Gracias también a toda la gente de Irsi, por los buenos momentos, las risas y porque al final, aunque no sepamos muy bien cómo, siempre triunfa el buen rollo. Después de tantos años solo puedo decir que ha sido un auténtico placer trabajar a vuestro lado. Y ya que estamos, aprovecho para agradecer a todos mis amigos invisibles (a los que nunca he llegado a ver) sus estupendos regalos navideños. Lidia, me diste la primera oportunidad. Margarita, para contestar a tus preguntas me leí todos los papers del mundo. Rafi, Eulalia, Rocío y ahora Tania, durante mucho tiempo habéis sido mi única compañía segura en P3. Eli, aunque no te acordarás, tu me enseñaste a procesar los buffys. En múltiples ocasiones, la organización del laboratorio de Silvia, Mariona y Susana me ha facilitado un montón las cosas. Teresa, sin tu sentido del humor, muchos días no habrían sido tan memorables. Charo, tú demostraste que un cotilleo tarda 5 minutos en dar la vuelta al ruedo en Irsi. Mireia y Edu, con vosotros conocí las Vegas, aunque no jugáramos ni a una tragaperras. Jordi B, mi vecino en South End, fuiste un anfitrión perfecto. Christian B, gracias por acogerme tan bien los meses que estuve en Boston. Jordi S, sin tus gags los retrovirus no tendrían tanta gracia. Raúl, Ruth, Gemma C, Esther J, Sandra, Isa, Marta M, Marta C, Emmanuel, Imma, Ceci, Ferdinand y Francesc, os agradezco vuestra compañía en la biblioteca durante estos años, os echaré de menos! Mer, Ester A, Samandhy y Moncu, sois las Paquitas de P3. Esther B, Anuska, Christian P, Elena, Glòria, Maria, las Cristinas, Lucia y todas las nuevas adquisiciones: vosotros también habéis aportado vuestro granito de arena. Y por supuesto, no

puedo olvidarme de Natalia, Gerau, Berta y Arantxa, a los que seguimos echando de menos.

También he tenido la fortuna de colaborar con personas de otros grupos y laboratorios que han sabido ilusionarse y participar en nuestro proyecto con un grado de compromiso altísimo. Gracias, Mar, por haber estado siempre ahí, dispuesta a echar una mano, a enseñarme un protocolo y a discutir cualquier cosa sobre nuestras niñas. Quiero que sepas que tu alegría e ilusión por la investigación me han devuelto las ganas de seguir en esto en numerosas ocasiones. Gracias también por animarme a seguir buscando becas debajo de la tapa de los yogures (al final hubo premio), por ser mi compi infatigable en los cursos de doctorado y por los buenos ratos en P3, ¡aunque menudos programas de radio te pongo! Me siento muy afortunada por haber compartido estos años contigo y estoy deseando que volvamos a cacharrear juntas. Francesc, a ti también te agradezco muchísimo todas tus ganas. Y aunque son muchas las anécdotas, en especial quería agradecerte que en su momento me explicaras que los monocitos se desenganchan una vez que empiezan a diferenciarse a dendríticas, aclarándome que mis protocolos no eran “asesinatos” celulares involuntarios.

Marco, muchas gracias por ayudarnos a poner a punto la técnica de cuantificación de moléculas por citometría de flujo. Sin tu interés y tu tiempo jamás lo habríamos conseguido, y yo tampoco me habría interesado tanto por la citometría, una herramienta que ha resultado decisiva para sacar adelante esta tesis.

Gracias también a Maite y Purificación de Anatomía Patológica. A pesar de los múltiples problemas técnicos que ha tenido el microscopio electrónico y la gran presión asistencial a la que estáis sometidas siempre habéis encontrado un

huequito para buscar nuestros virus y exosomas. Sin vuestra aportación y buen ojo jamás habríamos obtenido las micrografías decisivas para convencer a los revisores de nuestros artículos. Muchísimas gracias por vuestra colaboración durante todos estos años.

Quisiera también agradecer a Gemma y Fina el haber sabido acercarme al difícil pero apasionante mundo de la biosíntesis de los esfingolípidos. Nunca antes había discutido sobre una ruta bioquímica con tanto entusiasmo como con vosotras. Sólo espero que este sea el comienzo de una colaboración muy fructífera.

Muchas de las fotos de microscopia confocal de esta tesis se han realizado en el servicio de Microscopia de la UAB, gracias al soporte técnico y al apoyo moral de Mónica Roldán, Andrea Carvalho y Helena Montón. Gracias a todas por vuestras ganas y por esas películas que no hacen ni en Hollywood.

Some of the results presented in this thesis were generated in Boston University School of Medicine, while I was in the laboratory of Dr. Rahm Gummurulu. I would like to thank Rahm for all the helpful discussions we shared while I was in Boston. I learned a lot and really enjoyed it! I would also like to express my gratitude to Becca, Estelle, Jacob and Steve for their warm welcome and for sharing their group feeling with me. It was great to be part of your team for a while and share meetings with Tim and Greg. Many thanks to John and Landon, terrific VSV and deconvolution experts.

Thank you, Harry, for your incredible effort rewriting this thesis in proper English! But overall, thanks for your amazing friendship.

Pedro, Elena, Eugenio y Angelines fueron los maestros que me enseñaron a imaginar, escribir, razonar y seguir adelante. Muchas veces me acuerdo de lo que aprendí con vosotros en el Ágora y me siento tremendamente afortunada.

También agradezco a Carlos y Jaime, profesores de citogenética de la UAM, que me iniciaran en esto de la investigación, aunque fuera a base de karaokes y saltamontes. Ángel, mi profesor de citología, me dio la primera oportunidad, y los tiempos en su laboratorio los recuerdo con especial cariño. También quisiera agradecer a todo el laboratorio de citogenética de la Clínica de la Concepción el tiempo que me dedicaron durante las prácticas que hice allí.

De la llegada a Barcelona, suscribo lo dicho por Don Quijote: “ Barcelona, archivo de la cortesía, albergue de los extranjeros, hospital de los pobres, patria de los valientes, venganza de los ofendidos y correspondencia grata de firmes amistades, y en sitio y belleza única”. Eso si, de tirar cañas no saben tanto como en mi pueblo ...Gracias, Zara, por acogerme en tu casa recién llegada. Vanesa y Luana, en vuestra compañía me fui sintiendo parte de una ciudad extraña durante esos primeros meses en la residencia de Badalona. Luego encontré a la Fauna de Barna, a la que no habría conocido sin la intervención providencial de Aitana. Cristian, Sylvie, Espe y Mónica fueron los primeros en acogerme y hacerme sentir parte del grupo. Gracias también a Javi, mi compañero de piso durante todos estos años, por haber sacado Lepanto adelante, por las paellitas y por fregar los platos cuando estaba encerrada escribiendo un paper, por dejarme hablar del p24 y los esfígolípidos y por tu amistad incondicional. Sin los martes de la champanería, con Svatia, Katka, Guillermo, Caro, Alexis, Paola, Javi, Cristian, Sylvie, Espe y Mónica los primeros tiempos no habrían sido tan memorables. Y por supuesto no puedo olvidarme de los que se hicieron derogar: Julia, Roger, Kristina, Mer y Juanito. Tampoco habría sido lo mismo sin las visitas de Amagoia y Katixa ni los jueves harumaki, con Itziar, Laura, Nagore, Caro, Alexis, Paola, Isaac, Juan, Yaiza, Euri, Kiko, Vivian, Eva y Aurora. Todos vosotros habéis sido mi familia en Barcelona y me habéis hecho sentir tan a gusto como en el salón de mi propia casa...¡¡millones de gracias!!

Me gustaría añadir que sin la contribución de Laura, que me ha sacado de más de un apuro informático, Alexis, el mago del photoshop y Yaiza, que me enseñó como funciona el illustrator, no habría podido hacer gran parte de este trabajo.

Thanks, Christine, for your extraordinary friendship throughout the years, for coming to visit me and cook those amazing cakes every May, and for always believing in me.

Micky, mi sorellina, aunque aumenten los kilómetros de distancia entre nosotras, tú siempre estás ahí. ¡Gracias por ser tú!

Azu, Elena, Isa e Inés también forman parte de todo esto, por sus visitas a Barna (¡y hasta a Boston!) y por ser tan genuinas y auténticas.

Lo mismo puedo decir de las incombustibles Ayelén y Clara, que siguen a mi lado desde siempre y cuya amistad ni se crea ni se destruye, sino que simplemente se transforma.

Hay un grupo de personas con las que comparto mi día a día desde los tiempos de la universidad, primero en la cafetería, las clases, las excursiones y los baretos y después en Internet, y ¡sin necesidad del Facebook! Formar parte de este foro de personas tan sabias, integras y maravillosas hace que recibir el correo sea como mirar un calidoscopio, lleno de hermosos colores y formas distintas que admiro y respeto profundamente. Sois mi punto de referencia y os quiero un montón, gracias por estar siempre ahí. Aitana, tu sagacidad mordaz y tu gran corazón son una mezcla explosiva que hacen de tu amistad algo único y muy divertido. Mario, mi niño, espero que sepas que mi visión de las terapias tiene otra dimensión gracias a ti, eres un valiente. Ana, tu forma de cuestionar las cosas en clase, el laboratorio, Picón y en la vida en general siempre han sido una fuente de inspiración para mí, eres un auténtico diamante, bruta. Maria,

siempre estoy tan a gusto a tu lado, que sólo siento que Montejo no esté en Badalona. Marta, cuando se acabe el petróleo salvarás el planeta, tu energía es una fuente inacabable y contagiosa. Elena, eres la persona más emprendedora que conozco, ojalá todo el mundo buscara con tanto ahínco su camino como tú lo haces. Patricia S, sigues luchando por una ciencia más humana contra viento y marea, y saber que tú estás en el barco hace que confíe en que algún día llegaremos a buen puerto. Patricia del B, ¡Qué habría hecho yo sin tus apuntes! contigo comencé en esto de la investigación y creo que si no hubiera aprendido algo de tu increíble capacidad de organización ahora no estaría aquí, quiero que sepas que eres la mejor compañera que se puede desear. Raúl, espero que puedas volver pronto por aquí, echo de menos nuestras cenitas entre semana. Paloma, eres un amor, y sin tu visitas a Boston y a Barcelona todo esto habría sido mucho más aburrido. Laura, eres la persona con mayor entereza que conozco, espero que muy pronto puedas tomarte el descanso que te mereces, por ejemplo en Barcelona. Nacho, me encantan tus apariciones estelares en el foro.

Por último, quisiera dar las gracias a mi familia, por haberme dado todas las oportunidades del mundo y por haber estado siempre ahí. Se que mi abuelo Jesús se estará atusando el lazo el día que defienda esta tesis, y yo me tomaré el aperitivo de después a su salud. Todos estos años sin calefacción, mi abuela Angelita me ha mantenido abrigada gracias a sus jerseys, bufandas, gorros y todo su cariño. Papá, has sido un ejemplo de dedicación al trabajo y espíritu de superación, te agradezco muchísimo que siempre hayas intentado ayudarme en todo.

Me falta hablar de las mujeres del mundo a las que más admiro, las Useros-Serrano. Mi abuela Teresa es abogado, feminista y segoviana, una combinación irrepetible. Te agradezco muchísimo que lucharas por allanarnos el camino a

todas y solo espero que aunque esta tesis no sea de derecho, te alegres de tener por fin una doctora en la familia. Mi madre es ingeniero, informática y la persona más brillante que conozco. Pero por encima de su extraordinaria inteligencia, mi madre es un ejemplo de integridad, fortaleza y amor. Siempre has creído tanto en mí que me ha resultado prácticamente imposible no dejar de intentar alcanzar mis sueños una y otra vez hasta conseguirlos. Esta tesis demuestra un vez más que tenías razón, pero sobre todo demuestra tu gran sabiduría vital. Y aunque resulte imposible traducir mi gratitud en palabras, quiero que sepas lo mucho que te quiero.

Y ahora sí termino, espero no haberme olvidado de nadie...

¡Muchísimas gracias a todos!

